U.S. Department
of Commerce

Volume 113
Number 4
October 2015

Fishery Bulletin

The *Fishery Bulletin* (ISSN 0090-0656) is published quarterly by the Scientific Publications Office, National Marine Fisheries Service, NOAA, 7600 Sand Point Way NE, Seattle, WA 98115-0070.

The Secretary of Commerce has determined that the publication of this periodical is necessary according to law for the transaction of public business of this Department. Use of funds for printing of this periodical has been approved by the Director of the Office of Management and Budget.

For Sale by the Superintendent of Documents, U.S. Government Printing Office, Washington, DC 20402. Subscription price per year: $32.00 domestic and $44.80 foreign. Cost per single issue: $19.00 domestic and $26.60 foreign. **See back for order form.**

Fishery Bulletin

***Fishery Bulletin* web site: www.fisherybulletin.noaa.gov**

The *Fishery Bulletin* carries original research reports on investigations in fishery science, engineering, and economics. It began as the Bulletin of the United States Fish Commission in 1881; it became the Bulletin of the Bureau of Fisheries in 1904 and the *Fishery Bulletin* of the Fish and Wildlife Service in 1941. Separates were issued as documents through volume 46; the last document was no. 1103. Beginning with volume 47 in 1931 and continuing through volume 62 in 1963, each separate appeared as a numbered bulletin. A new system began in 1963 with volume 63 in which papers are bound together in a single issue. Beginning with volume 70, number 1, January 1972, *Fishery Bulletin* became a periodical, issued quarterly. In this form, it is available by subscription from the Superintendent of Documents, U.S. Government Printing Office, Washington, DC 20402. It is also available free in limited numbers to libraries, research institutions, state and federal agencies, and in exchange for other scientific publications.

U.S. Department of Commerce
Seattle, Washington

Volume 113
Number 4
October 2015

Fishery Bulletin

Contents

Articles

NOAA
National Marine
Fisheries Service

Fishery Bulletin
established 1881

Spencer F. Baird
First U.S. Commissioner
of Fisheries and founder
of *Fishery Bulletin*

A new species of *Sebastes* (Scorpaeniformes: Sebastidae) from the northeastern Pacific, with a redescription of the blue rockfish, *S. mystinus* (Jordan and Gilbert, 1881)

Benjamin W. Frable (contact author)[1, 2]
D. Wolfe Wagman[2]
Taylor N. Frierson[2]
Andres Aguilar[3]
Brian L. Sidlauskas[1]

Email address for contact author: ben.frable@oregonstate.edu

[1] Department of Fisheries and Wildlife
Oregon State University
104 Nash Hall
Corvallis, Oregon 97331

[2] Oregon Department of Fish and Wildlife
Marine Resources Program
2040 SE Marine Science Drive
Newport, Oregon 97365

[3] Department of Biological Sciences
California State University, Los Angeles
5151 State University Drive
Los Angeles, California 90032

Abstract—The diverse predatory rockfishes (*Sebastes* spp.) support extensive commercial fisheries in the northeastern Pacific. Although 106 species of *Sebastes* are considered valid, many of the ecological, geographical, and morphological boundaries separating them lack clarity. We clarify one such boundary by separating the blue rockfish *Sebastes mystinus* (Jordan and Gilbert, 1881) into 2 species on the basis of molecular and morphological data. We redescribe *S. mystinus*, designate a lectotype, and describe the deacon rockfish, *Sebastes diaconus* n. sp. Aside from its unambiguous distinction at 6 microsatellite loci, the new species is most easily differentiated from *S. mystinus* by its possession of a solid in contrast with a blotched color pattern. *Sebastes diaconus* also possesses a prominent symphyseal knob versus a reduced or absent knob, a flat rather than rounded ventrum, and longer first and second anal-fin spines. *Sebastes diaconus* occurs from central California northward to British Columbia, Canada, and *S. mystinus* occurs from northern Oregon south to Baja California Sur, Mexico, indicating a broad region of sympatry in Oregon and northern California. Further collection and study are necessary to clarify distributional boundaries and to understand the ecology and mechanisms of segregation for this species. Additionally, fisheries assessments will need revision to account for the longstanding conflation of these 2 species.

Manuscript submitted 30 May 2014.
Manuscript accepted 10 June 2015.
Fish. Bull. 113:355–377 (2015)
Online publication date: 9 July 2015.
doi: 10.7755/FB.113.4.1
http://zoobank.org/References/297E1E76-94C2-49B2-9520-A519B80BC99B

The rockfish genus *Sebastes* is one of the most diverse and abundant genera along the Pacific coast of North America (Love et al., 2002). Rockfish biology and ecology have been well studied because of their commercial importance, yet some taxonomic limits, population boundaries, and phylogenetic relationships within *Sebastes* remain unclear (Hyde and Vetter, 2007; Orr and Hawkins, 2008) because many species are very similar and overlap in meristic counts and morphometrics. As a result, fishery managers struggle to correctly identify *Sebastes* species and sometimes lack accurate species diagnoses to determine proper management.

Several clusters of similar species within *Sebastes* merit increased taxonomic attention. For example, the uniformly dark-colored species of *Sebastes*, such as the blue rockfish *S. mystinus* (Jordan and Gilbert, 1881), black rockfish *S. melanops* Girard, 1856, light dusky rockfish *S. variabilis* (Pallas, 1814), and dusky rockfish *S. ciliatus* (Tilesius, 1813), are among the most frequently conflated and confused when landed in the same fishery (Kramer and O'Connell, 1995; Orr and Blackburn, 2004). Even among brightly colored rockfishes, increased study has revealed cryptic species. Gharrett et al. (2005) found 2 genetically distinct forms within the rougheye rockfish *S. aleutianus* (Jordan and Evermann, 1898), and those forms were later designated as the rougheye rockfish *S. aleutianus* and blackspotted rockfish *S. melanostictus* (Matsubara, 1934) (Orr and Hawkins, 2008). The historical concept of the vermilion rockfish *S. miniatus* (Jordan and Gilbert, 1880a) was also shown relatively recently to

include 2 reproductively isolated entities (Hyde, et al., 2008).

In this study, we focus taxonomic attention on *S. mystinus,* a common nearshore species found from northern Mexico to British Columbia, Canada. In the 19th century, *S. mystinus* was the most commercially important species in California; now it is mainly targeted recreationally (Love et al., 2002). Over the last decade, multiple studies have identified 2 genetically distinct groups of *S. mystinus* along the Pacific coast (Cope, 2004; Burford and Larson, 2007; Burford and Bernardi, 2008; Burford, 2009; Burford et al., 2011a, 2011b), and in several studies the presence of 2 morphologically unrecognized species have been hypothesized (Burford and Bernardi, 2008; Burford, 2009; Burford et al., 2011a, 2011b).

Cope (2004) first identified genetic distinctions between northern and southern populations of blue rockfish while studying their stock structure. His analysis revealed numerous fixed differences in the sequence of the mitochondrial control region between samples from the Oregon–Washington region and samples from California waters. These data indicate that the genetic break occurred in the vicinity of Cape Mendocino, California.

Burford and colleagues then applied additional molecular and phylogeographic analyses to these 2 populations (Burford and Larson, 2007; Burford and Bernardi, 2008; Burford, 2009; Burford et al., 2011a, 2011b). In a combined analysis of mitochondrial (control region) and nuclear (recombination-activating gene 1 [RAG1]) markers and microsatellites for the subgenus *Sebastosomus*, Burford and Bernardi (2008) were the first to propose that the 2 populations might represent different species. Within *S. mystinus*, Burford and Bernardi (2008) identified 2 clades with higher genetic divergence (F_{ST}=0.120) than that found between 2 well-established species (Narum et al., 2004), the gopher rockfish *Sebastes carnatus* (Jordan and Gilbert, 1880b) and the black-and-yellow rockfish *S. chrysomelas* (Jordan and Gilbert, 1881), and with much higher genetic divergence than that among populations of *S. melanops* (F_{ST}=0.032) (Miller et al., 2005). They estimated the divergence time of the 2 lineages to be between 780,000 and 920,000 years ago, far preceding the Last Glacial Maximum (LGM) and, therefore, refuting Burford and Larsons's (2007) hypothesis that the LGM caused allopatric speciation within *S. mystinus*.

Burford and Bernardi (2008) concluded that the 2 genetically distinct groups of *S. mystinus* are incipient species on the basis of the evidence presented here previously and the lack of evidence for introgression or hybridization. Burford (2009) expanded on this conclusion by directly testing hypotheses of demographic history and speciation scenarios with an expanded sampling of 6 microsatellites and the control region marker. They found evidence for a demographic contraction and rapid expansion near the time of genetic coalescence and far earlier than the LGM (Burford, 2009). Burford (2009) concluded that the 2 lineages speciated allopatrically much earlier than the LGM and that they have subsequently expanded ranges to form an area of sympatry from central Oregon to northern California.

Finally, Burford et al. (2011a, 2011b) examined microsatellite data from 466 type-1 (northern group) and 1752 type-2 (southern group) specimens collected from Fort Bragg, California, south to Santa Cruz Island, California, to determine rates of hybridization (Burford et al., 2011a) and year-class compositional and ecological differences (Burford et al., 2011b). Burford et al. (2011a) found no hybridization in northern localities with higher co-occurrence, but they identified low levels in Southern California (highest rate of hybridization=4.1%). This finding, combined with the identification of a Wahlund Effect (i.e., lower heterozygosity than expected at random between the 2 populations), indicates that reproductive isolation helps maintain the segregation, especially in areas of overlap (Burford et al., 2011a). Burford et al. (2011a, 2011b) considered their results to provide sufficient evidence that the 2 genetic lineages are cryptic rather than incipient species.

Despite the accumulating detail on genetic differentiation, no study provided a complementary physical description of the 2 types. Because of the lack of physical descriptions or defining characteristics, precise field identification of Burford's genetic lineages (type 1 and type 2) has eluded biologists and fishermen alike.

Meanwhile, fisheries biologists acknowledged 2 different trunk pigmentation patterns in *S. mystinus* from near the Oregon, Washington, and California shores: the "blue-sided" (Fig. 1, A and C) and "blue-blotched" rockfishes (Fig. 1, B and D) (Love, 2011), which, as the authors of the earlier genetic studies have indicated, match the type-1 and type-2 genetic lineages, respectively (Burford[1]). That difference in color pattern indicates that these lineages may be more morphologically distinguishable than originally thought.

The wealth of recent genetic work on *S. mystinus* and the discovery of a color polymorphism that is congruent with the major genetic break indicate that a formal taxonomic revaluation is overdue. In this study, we 1) test whether the morphotypes correspond with the types of Burford and Bernardi (2008), 2) characterize the morphological features of the 2 genetic types, 3) use genetic and morphological data to evaluate species status, and 4) clarify the geographic ranges of the 2 forms. In doing so, we confirm the genetic separation of the 2 color morphs and provide a formal description of the type-1 or blue-sided form as a new species, *S. diaconus,* the deacon rockfish. The type-2 or blue-blotched form matches most of the original syntype series of *S. mystinus*, from which we designate a lectotype and redescribe the species. This study provides information essential to proper population monitoring and management of these species in Oregon and the northeastern Pacific.

[1] Burford, M. 2012. Personal commun. Department of Applied Ecology, North Carolina State Univ., Raleigh, NC 27695.

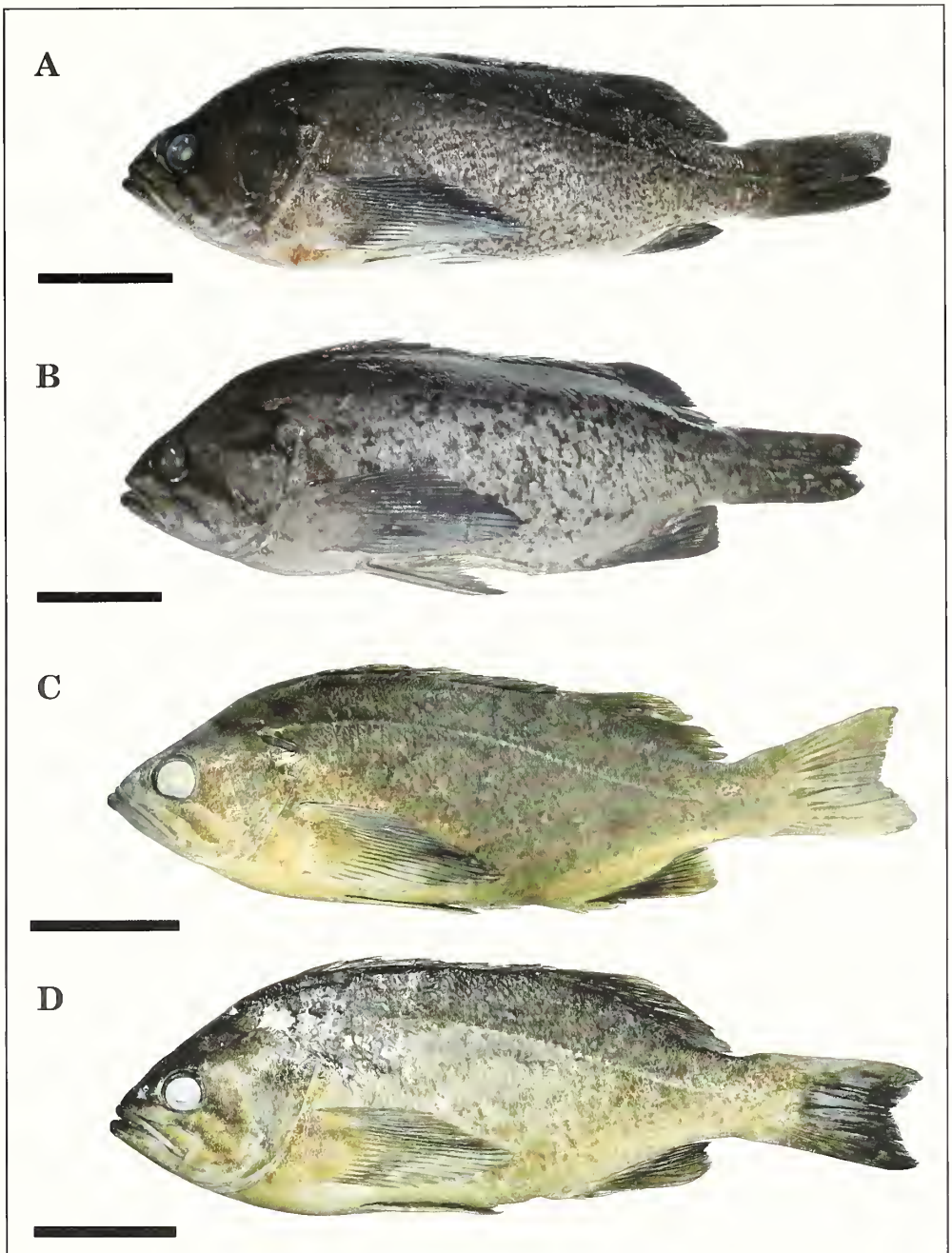

Figure 1

(**A**) Holotype of *Sebastes diaconus*, deacon rockfish, OS 18901, 260 mm SL, recently deceased. (**B**) *S. mystinus*, blue rockfish, OS 18900, 264 mm SL, recently deceased. (**C**) holotype of *S. diaconus*, OS 18901, 260 mm SL, after 1 year in preservation. (**D**) *S. mystinus*, OS 18900, 264 mm SL, after 1 year in preservation. Scale bars indicate 50 mm.

Materials and methods

Samples

Type material and preserved specimens were examined from 6 ichthyology collections containing major holdings from the northeastern Pacific: CAS, UBC, LACM, UWFC, OS, and USNM (collection abbreviations sensu Sabaj Peréz, 2013). Fresh specimens were collected by DWW and TNF with hook and line from nearshore reefs (13–29 m deep) off the central Oregon coast (44°44′12.30″N, 124°4′33.59″W to 44°24′11.74″N,

124°13′55.56″W) from 9 April to 25 June 2012 under the annual scientific collecting permit issued by the Oregon Department of Fish and Wildlife (ODFW) for the collection of samples by their employees (DWW and TNF). Specimens were frozen for transport, thawed, and photographed. Samples of tissue from the trunk musculature were removed and archived, and 35 of these freshly collected samples (*S. mystinus* [*n*=15], *S. diaconus* [*n*=20]) were genotyped during microsatellite analysis. Voucher specimens were fixed in 10% formalin, preserved in 50% isopropanol, cataloged, and deposited in the Oregon State Ichthyology Collection (OS). More detailed information on catalog number, collection locality, and size of each examined specimen appears in the species descriptions that follow. We examined 134 specimens for comparisons of meristic and linear morphometric data: *S. mystinus* (*n*=68), *S. diaconus* (*n*=58), *S. ciliatus* (*n*=6), and *S. variabilis* (*n*=2).

Genetic sampling

Muscle tissue was used to extract DNA from 15 blue-blotched and 20 blue-sided individuals with DNeasy[2] blood and tissue kits (Qiagen, Valencia, CA). Microsatellite loci were amplified by a 3-primer polymerase chain reaction (PCR) protocol (Schuelke, 2000). To test the assignment of the color morphotypes with the previously described genetic groups, 16 type-1 and type-2 individuals previously identified and analyzed by Burford and Bernardi (2008) were included in microsatellite amplification and analysis.

Amplification of microsatellite markers and DNA sequences

We amplified 6 anonymous microsatellite markers (*Seb37*, Roques et al., 1999; *Spi4*, Gomez-Uchida et al., 2003; *Sra7–7*, *Sra15–8*, Westerman et al., 2005; *Ssc69*, Yoshida et al., 2005; and *KSs18A*, An et al., 2009). Two microsatellite loci (*Sra7–7* and *Sra15–8*) were used by Burford and Bernardi (2008) in the original description of the 2 lineages. The 3-primer amplification protocol was used to run in 15-µL volumes with the following reaction concentrations: 1× AmpliTaq PCR Buffer (Thermo Fisher Scientific, Inc., Waltham, MA) buffer, 2.5 mM $MgCl_2$, 0.4 mM of each dNTP, 2.7×10^{-4} mg/mL BSA, 0.3 µM reverse primer, 0.3 µM fluorescently labeled M13 sequence (5′CACGACGTTGTAAAACGAC3′) with dye labels (FAM, VIC, NED, PET; Thermo Fisher Scientific, Inc.), 0.07 µM M13 5′-end labeled forward primer, 0.2 units of AmpliTaq DNA polymerase, and 5µL DNA (5–20 ng/µL). We used the following thermal profile: initial denaturing step at 94°C for 5 min, followed by 30 cycles of 94°C for 30 s, 52°C for 30 s, and 72°C for 45 s. The incorporation of the M13 primer required 15 cycles of 94°C for 30 s, 48°C for 30 s, and 72°C for 45 s. A 7-min extension after the final cycle completed the thermal profile. Amplified products were run on an Applied Biosystems 3100 automated sequencer with GeneScan 500 LIZ Size Standard and genotyped with GeneMapper, vers. 3.7 (Thermo Fisher Scientific, Inc.).

Analysis of microsatellite markers and DNA sequence

We used the software program Structure, vers. 2.3 (Falush et al., 2003; Pritchard et al., 2000) to determine the correspondence of blue-sided and blue-blotched morphotypes with the type-1 and type-2 genetic groups described by Burford and Bernardi (2008). Parameters in Structure were set to produce posterior probabilities with 500,000 replicates recorded after a burn-in period of 50,000 steps that were discarded. Default settings were used with the admixture option in Structure. Because the optimal K value was previously identified as 2 (Burford and Bernardi, 2008), we ran simulations according to these parameters to identify the corresponding genetic groups of each morphotype. We also simulated structure runs with K values within a range of 2–4 and identified optimal K value with the online program Structure Harvester, vers. 6.92 (Earl and vonHoldt, 2012).

Measurements and meristics

Measurements were taken to the nearest 0.01 mm with digital calipers. Morphometrics (32 measurements) and meristics (17 counts) followed Orr and Hawkins (2008), except as follows. Symphyseal knob length was measured on the ventral side of the lower jaw from the posterior margin of the symphysis to the anterior tip of the knob. Head depth was measured along the vertical bisecting the eye. An additional point-to-point measurement was taken from the dorsal-fin origin to anal-fin origin. We augmented the meristics used by previous authors with counts of dorsal-fin spines, of branched and unbranched pectoral-fin rays on both sides of the fish, of transverse lateral scale rows, and of posterior and anterior gill rakers from the left side of the fish. Dorsal-, anal-, pectoral- and pelvic-fin rays and spines were counted from preserved specimens. Vertebrae and caudal-fin rays were counted from a subsample of specimens (*n*=68) via film radiographs.

Morphometric analysis

We created a size-standardized morphospace for 120 specimens (6 specimens were excluded because of damage) with the Allometric Burnaby technique (Burnaby, 1966) implemented in the software PAST, vers. 2.17 (Hammer et al., 2001), which log transforms the 32 linear measurements and projects them orthogonally to the first principal component. These data were then used in a principal components analysis (PCA). For statistical analyses, putative species membership

[2] Mention of trade names or commercial companies is for identification purposes only and does not imply endorsement by the National Marine Fisheries Service, NOAA.

was assigned a priori on the basis of trunk color pattern (blotched versus solid). To allow for the inclusion of juveniles, which lack distinguishing color patterns, and for faded long-preserved specimens in the morphometric analysis, we assigned specimens from extreme ends of the known geographic ranges to the only species known to occur in such regions. No ambiguous juveniles or faded specimens from the known region of geographic overlap were included in morphometric analysis.

The overall morphometric distinctiveness of the 2 putative species was tested by inputting the eigenvectors that explained the greatest percent variance from the PCA into a multivariate analysis of variance (MANOVA) implemented in PAST software. The significances of differences between the means of putative species ($P \leq 0.05$) on each axis were tested with pairwise post-hoc comparisons, by using Tukey's honestly significant difference (HSD) test. A discriminant function analysis (DFA, also implemented in PAST) was used to further determine which morphometric measurements best separated the species. The robustness of the DFA to assign the data to a priori groupings was evaluated with a leave-one-out cross-validation in PAST. Results of this procedure are reported in percentages assigned to the same a priori grouping. The untransformed versions of the 32 variables that explained the highest proportion of variance in the DFA were regressed against length (standard length [SL]) for each species to determine whether the traits differed allometrically or isometrically. This comparison of allometric trajectories was performed in the smatr package (Warton et al., 2012) in R, vers. 3.0.1 (R Core Team, 2013). Linear regressions were plotted with the ggplot2 package in R (Wickham, 2009). Some individual linear morphometric measurements were compared to determine statistical significance with a 2-tailed Student's *t*-test for unequal frequencies implemented in R.

Results

Genetic analysis

When K was 2, all of the individuals genotyped from this study were assigned high ancestry (>90%) with 1 of the 2 clusters (Fig. 2). The specimens identified as *S. diaconus* or blue-sided sensu Love (2011) clustered unambiguously with the type-1 blue rockfish and the *S. mystinus* or blue-blotched individuals clustered with the type-2 blue rockfish of Burford and Bernardi (2008) (Fig. 2), thereby confirming that the color polymorphism reliably separates the genetic types.

Morphometric analysis

Principal component analysis of size-standardized linear morphometric variables for specimens with clear a priori classification (see the *Materials and methods* section) revealed overlap between the 2 putative species (Fig. 3) but a clear difference in mean phenotype ($P<0.0001$, MANOVA on first 4 axes explaining 51.0% of total variance). Percent variance explained dropped after PC4 (Fig. 4A). The most discrimination was offered by PC1 (17.1% of variance; Table 1), with blue-sided individuals, or *S. diaconus*, having on average more positive scores than members of *S. mystinus*, or the blue-blotched phenotype (Fig. 3). The variables with the highest loadings along PC1 were symphyseal knob length, the lengths of the first 2 anal-fin spines, and the length of the first dorsal-fin spine (Table 1). Explaining 12.1% of variance, PC2 primarily indexes variation in suborbital depth, anal-fin spine I length, and the dorsal and ventral lengths of the caudal peduncle (Table 1). Pairwise Tukey's HSD tests recovered significant differences between the 2 species on PC1 ($P=0.0001$) but not on the subsequent axes.

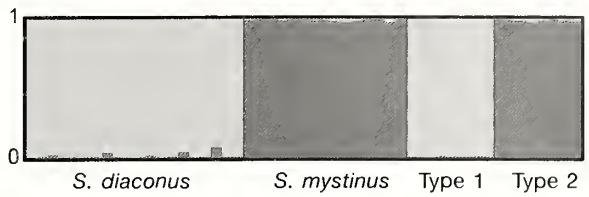

Figure 2

Structure plot derived from microsatellite data showing genetic group assignments of specimens of *Sebastes diaconus* (deacon rockfish; $n=20$) and *S. mystinus* (blue rockfish; $n=15$) from this study (on left) compared with specimens previously genotyped by Burford and Bernardi (2008) (on right), type 1 ($n=8$) and type 2 ($n=8$) with a K value of 2. Each bar represents one individual with color corresponding to population assignment.

When individuals under 150 mm SL were removed from the data set, the percent variance explained by the first 2 principal components (PCs) increased (Fig. 4B). For PC1 (23.1% of total variance), the main measurements of variation were symphyseal knob length, anal-fin spines I and II lengths, and ventral caudal peduncle length (Table 1), and, for PC2 (13.4% of total variance), the largest loadings were for symphyseal knob length and lengths of anal-fin spines I, II and III (Table 1). As with the analysis of the complete data set, the multivariate means of the 2 species differed significantly (MANOVA, $P<0.001$): only the analysis of PC1 revealed a significant morphometric difference in the pairwise Tukey's HSD tests ($P=0.001$).

The depth at dorsal-fin origin, pelvic-fin ray length, preanal fin length, and dorsal-fin origin to anal-fin origin received the highest weight in the linear discriminant equation of the variation between the 2 species (Table 2) in the size-standardized morphospace. This discriminant function correctly reclassified all but 2 individuals in a leave-one-out cross-validation (98.3% correct reclassification; Fig. 5A). The exclusion of juveniles under 150 mm SL improved the performance of

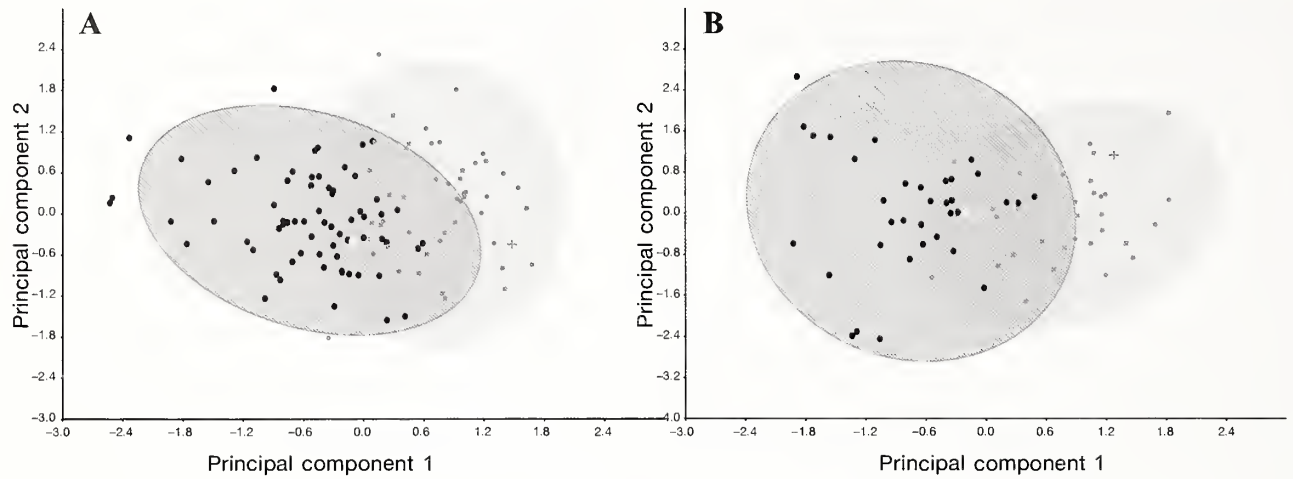

Figure 3

Scatterplot of principal components 1 and 2 from principal component analysis of 32 linear morphometric measurements (**A**) for all specimens of *Sebastes mystinus*, blue rockfish (black circles), and *S. diaconus* new species, deacon rockfish (gray squares), examined for this study (n=120) and (**B**) for only specimens over 150 mm SL (*S. mystinus*, n=37, and *S. diaconus*, n=36). Ellipses represent 95% confidence intervals. The white circle indicates the lectotype of *S. mystinus*, USNM 27085, and the gray cross indicates the holotype of *S. diaconus*, CAS 236653.

the DFA and yielded a linear equation permitting 100% correct reclassification of 73 adult specimens (Fig 5B). The coefficients for head length (HL) and prepelvic fin length increased substantially in the discriminant function that was restricted to individuals over 150 mm SL, in comparison with the function including specimens of all sizes (Table 2).

Between-group comparison of type-II regressions of the untransformed measurements with the highest loadings on size-standardized PC1 against SL indicated significantly different slopes for the lengths of anal-fin spine I (P<0.001) and anal-fin spine II (P=0.002), for symphyseal knob length (P<0.001), and for ventral caudal peduncle length (P=0.003). Linear regressions of these 4 variables against SL illustrate the differences in slope (Fig. 6, A–D). It appears that the 2 species are morphometrically similar at smaller sizes yet differentiate interspecifically as they age, with the symphyseal knob length (Fig. 6A) and the lengths of the anal-fin spines (Fig. 6, B and C) diverging substantially in specimens over 150 mm SL. Ventral caudal peduncle length diverges less pronouncedly (Fig 6D).

On the basis of the morphometric differences discovered in this study, the differences in body coloration, and the correspondence of the morphotypes with previously identified genetic groups, we recognize the 2 genetic lineages within the previous concept of *S. mystinus* as full species. We describe *S. diaconus*, or the type-1 or blue-sided form, as new; we restrict *S. mystinus* to the type-2 or blue-blotched form; and we redescribe the latter species and designate a lectotype and paralectotypes.

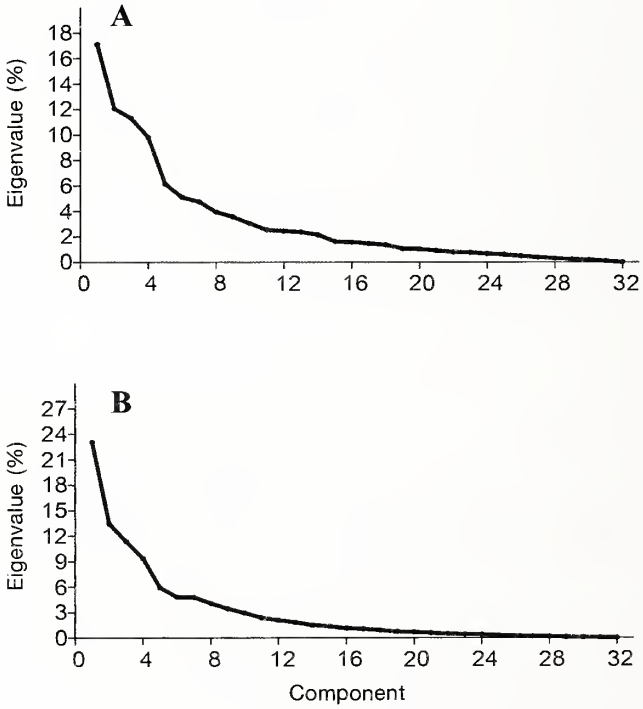

Figure 4

Scree plot of percent variance explained by principal components of morphometric measurements (**A**) for all specimens of *Sebastes mystinus* (blue rockfish) and *S. diaconus* (deacon rockfish) combined (n=120) and (**B**) for only specimens over 150 mm SL (*S. mystinus*, n=37, and *S. diaconus*, n=36).

Table 1

Variable loadings and percent variance explained for the first 4 principal component axes of a principal component analysis for morphometric measurements of all specimens examined for this study, *Sebastes mystinus* (blue rockfish; n=68) and *S. diaconus* (deacon rockfish; n=52) combined, and of specimens over 150 mm SL, *S. mystinus* (n=37) and *S. diaconus* (n=36) combined. Highest loadings are indicated in bold.

	All specimens				Specimens over 150 mm SL			
Measurement	Axis 1	Axis 2	Axis 3	Axis 4	Axis 1	Axis 2	Axis 3	Axis 4
Percent variance explained	17.113	12.066	11.313	9.813	23.055	13.443	11.373	9.362
Head length	0.061	0.017	−0.031	0.126	0.110	−0.003	−0.007	0.165
Orbit length	0.094	0.046	−0.003	0.106	0.115	0.003	−0.081	0.153
Snout length	0.036	−0.027	0.123	**−0.370**	−0.041	0.040	0.249	**−0.347**
Interorbital width	−0.081	−0.023	−0.072	−0.010	−0.107	0.001	−0.040	0.029
Suborbital depth	**−0.194**	**−0.586**	**0.564**	−0.285	−0.181	0.061	**−0.531**	**−0.700**
Head depth	−0.086	−0.049	−0.207	0.162	−0.140	−0.133	−0.214	0.174
Upper jaw length	0.010	−0.024	−0.019	−0.018	−0.026	−0.008	0.084	0.027
Lower jaw length	0.098	0.018	0.019	0.083	0.132	−0.021	−0.002	0.011
First gill arch length	−0.017	0.033	−0.072	**0.359**	0.051	0.031	**−0.313**	0.392
Symphyseal knob length	**0.818**	−0.273	**−0.267**	−0.242	**0.637**	**−0.625**	0.099	**−0.193**
Predorsal fin length	0.040	0.000	0.026	−0.031	0.035	−0.017	0.036	0.001
Prepelvic fin length	0.009	−0.097	0.000	0.119	0.023	−0.067	−0.136	0.057
Preanal fin length	−0.035	−0.056	−0.034	0.105	−0.019	−0.045	−0.068	0.112
Depth at dorsal fin origin	−0.114	−0.051	−0.065	0.129	−0.101	−0.021	−0.074	0.091
Depth at pelvic fin origin	−0.094	−0.049	−0.084	0.179	−0.078	−0.039	−0.118	0.137
Depth at anal fin origin	−0.049	−0.053	−0.114	0.096	−0.051	−0.060	−0.017	0.043
Dorsal-fin spine I length	0.073	0.160	0.038	−0.144	0.009	0.130	0.115	0.074
Dorsal-fin spine IV length	0.083	0.066	−0.006	0.048	0.099	0.074	0.082	0.072
Spinous dorsal-fin base length	−0.044	−0.136	−0.072	0.175	−0.036	−0.059	−0.144	0.147
Soft rayed dorsal-fin base length	−0.084	0.011	−0.056	−0.044	−0.078	−0.109	−0.033	−0.017
Pectoral-fin base depth	−0.125	−0.067	−0.052	0.001	−0.138	−0.020	0.084	−0.028
Pectoral fin length	−0.100	−0.088	−0.020	−0.020	−0.116	−0.040	0.049	0.012
Pelvic-fin ray length	−0.109	0.030	−0.015	−0.109	−0.144	0.007	0.115	−0.027
Pelvic-fin spine length	−0.058	0.136	0.145	−0.032	−0.040	0.149	0.144	0.074
Anal-fin base length	0.005	0.030	−0.015	0.034	0.028	0.045	0.060	−0.010
Anal-fin spine I length	**0.273**	**0.450**	**0.574**	0.152	**0.477**	**0.628**	−0.016	−0.044
Anal-fin spine II length	0.147	0.146	0.193	0.203	**0.251**	**0.237**	−0.049	−0.066
Anal-fin spine III length	0.085	0.109	0.222	0.033	0.083	0.202	0.125	−0.062
Dorsal fin origin to anal fin origin	−0.066	−0.051	−0.044	0.108	−0.058	0.002	−0.060	0.122
Caudal peduncle depth	−0.093	0.003	−0.063	0.007	−0.125	−0.009	0.035	−0.021
Caudal peduncle dorsal length	−0.173	**0.444**	−0.222	**−0.479**	−0.180	−0.066	**0.531**	−0.072
Caudal peduncle ventral length	−0.132	0.189	−0.096	−0.270	−0.200	0.115	0.221	−0.016

***Sebastes diaconus*, new species**
Proposed English common name: deacon rockfish
Figures 1, A and C, 2–6, 7A, 8A, 9, and 10; Tables 1–3.

Sebastichthys mystinus Jordan and Gilbert, 1881: Bean, 1882:26 (presence in Puget Sound, Washington]; Goode, 1884:266 (in part, mention of fishes from Vancouver Island, Canada, and Puget Sound; having affinity with *Sebastes melanops* in Puget Sound).

Sebastodes mystinus (Jordan and Gilbert, 1881): Whiteaves, 1887:135 (first record of capture in Canada); Jordan and Evermann, 1898:1785 (in part, presence in Puget Sound); Phillips, 1957:52–53 (in part); Clemens and Wilby, 1961:252–253.

Sebastes mystinus (Jordan and Gilbert, 1881): Hart, 1973:429; Eschmeyer and Herald, 1983:144 (in part); Kramer and O'Connell, 1995:45 (in part); Mecklenburg et al., 2002:360; Love et al., 2002:215 (in part); Love, 2011:250–251 (in part).

Holotype

OS 18901, 260 mm SL, 1.8 km west of Seal Rock, OR, 44°29′49.38″N, 124°6′30.48″W, 20.9 m depth, 20 April 2012, D. W. Wagman and T. N. Frierson.

Paratypes

CAS 25336, 1, 153 mm SL, off Point Diablo, San Francisco, CA, 2 August 1947, W. I. Follett, C. O. Garrels, and C. F. Maertins; LACM 31942.008, 6, 240–266 mm SL, northeast of Redding Rock, Humboldt County, CA,

Table 2

Discriminant functions for morphometric measurements determined by a discriminant function analysis for all individuals, *Sebastes mystinus* (blue rockfish; n=68) and *S. diaconus* (deacon rockfish; n=52) combined, and for individuals over 150 mm SL, *S. mystinus* (n=37) and *S. diaconus* (n=36). Most extreme coefficients are indicated in bold.

Measurement	All individuals	Individuals over 150 mm SL
Head length	36.018	**-448.42**
Orbit length	27.157	-219.98
Snout length	44.661	-214.68
Interorbital width	30.4	-289.5
Suborbital depth	43.81	-275.26
Head depth	37.254	-235.15
Upper jaw length	30.458	-275.91
Lower jaw length	31.126	-206.71
First gill arch length	36.431	-138.46
Symphyseal knob	0.88836	**-321.07**
Predorsal fin length	33.422	-261.83
Prepelvic fin length	34.419	**-487.52**
Preanal fin length	**88.378**	28.582
Depth at dorsal fin origin	**89.738**	-125.6
Depth at pelvic fin origin	34.136	-276.5
Depth at anal fin origin	13.885	-241.26
Dorsal-fin spine I length	57.141	-129.78
Dorsal-fin spine IV length	31.63	-213.65
Spinous dorsal-fin base length	60.405	9.4878
Soft rayed dorsal-fin base length	44.333	-171.56
Pectoral-fin base depth	55.919	**-367.57**
Pectoral fin length	48.979	-248.9
Pelvic-fin ray length	**85.235**	-150.96
Pelvic-fin spine length	49.767	-64.665
Anal-fin base length	27.607	-242.01
Anal-fin spine I length	15.63	-175.03
Anal-fin spine II length	-8.2368	**-367.43**
Anal-fin spine III length	12.647	-235.56
Dorsal fin origin to anal fin origin	**110.32**	-270.45
Caudal peduncle depth	42.199	-218.95
Caudal peduncle dorsal length	23.46	-243.75
Caudal peduncle ventral length	45.236	-152.4

15.4 m depth, 4 August 1971, McBean et al.; OS 18882, 1, 160 mm SL, 1.4 km west of Tokatee Kloochman State Natural Site, OR, 44°12′26.28″N, 124°8′2.04″W, 19.2 m depth, 24 April 2012, D. W. Wagman and T. N. Frierson; OS 18883, 1, 218 mm SL, 1.8 km southeast of Seal Rock, OR, 44°29′4.20″N, 124°6′14.62″W, 17.9 m depth, 7 May 2012, D. W. Wagman and T. N. Frierson; OS 18884, 4, 190–272 mm SL, 2.9 km west of Ona Beach State Park, OR, 44°31′8.94″N, 124°7′2.96″W, 15.2 m depth, 7 May 2012, D. W. Wagman and T. N. Frierson; OS 18885, 2, 125 and 235 mm SL, 1.8 km west Ona Beach State Park, OR, 44°31′27.98″N, 124°6′6.55″W, 16.5 m depth, 8 May 2012, D. W. Wagman and T. N. Frierson; OS 18888, 1, 125 mm SL, 2.1 km west of Lost Creek State Park, OR, 44°33′14.83″N, 124°6′1.94″W, 8 May 2012, 13.2 m depth, D. W. Wagman and T. N. Frierson; OS 18889, 3, 140–188 mm SL, 2.0 km west of Lost Creek State Park, OR, 44°33′16.34″N, 124°6′0.04″W, 13.2 m depth, 15 May 2012, D. W. Wagman and T. N. Frierson; OS 18890, 3, 164–292 mm SL, 1.1 km west of Lost Creek State Park, OR, 44°33′21.96″N, 124°5′20.36″W, 14.5 m depth, 20 April 2012, D. W. Wagman and T. N. Frierson; OS 18893, 1, 225 mm SL, 1.8 km west of north end of Lost Creek State Park, OR, 44°33′37.51″N, 124°5′45.82″W, 18.8 m depth, 8 May 2012, D. W. Wagman and T. N. Frierson; OS 18895, 2, 230 and 270 mm SL, 1.8 km northwest of Lost Creek State Park, OR, 44°33′57.17″N, 124°5′43.26″W, 14.3 m depth, 8 May 2012, D. W. Wagman and T. N. Frierson; OS 18897, 1, 259 mm SL, 3.2 km southwest of South Beach State Park, OR, 44°34′49.98″N, 124°6′18.94″W, 19.0 m depth, 7 May 2012, D. W. Wagman and T. N. Frierson; UW 44179, 1, 330 mm SL, off Ozette Island, WA, 9.1 m depth, collector and date unknown; UW 44330, 1, 246 mm SL, off Neah Bay, WA, 29 January 1993, Seattle Aquarium.

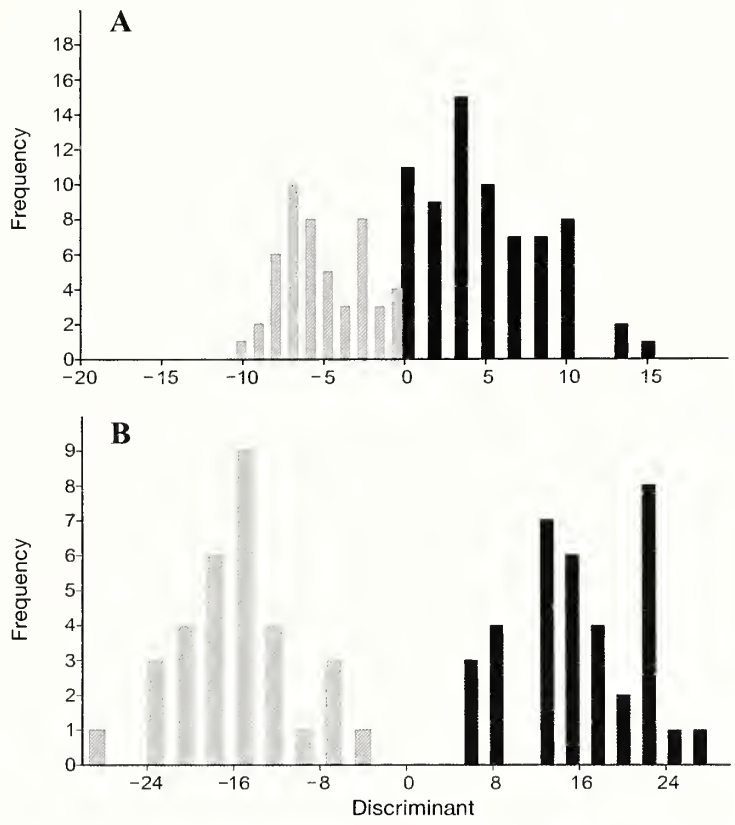

Figure 5

Results of a discriminant function from analysis of 32 linear measurements (**A**) for all specimens of *Sebastes mystinus* (blue rockfish) and *S. diaconus* (deacon rockfish) combined (n=120), showing 98.3% discrimination, and (**B**) only specimens over 150 mm SL (*S. mystinus*, n=37, and *S. diaconus*, n=36), showing 100% discrimination. Black bars represent *Sebastes mystinus*, and light gray bars represent *S. diaconus*.

Additional nontype material

CAS 18799, 1, 128 mm SL, Off Santa Cruz Island, CA, 29 August 1954, E. Hunter; CAS 25976, 1, 104 mm SL, Southeast Farallon Island, CA, 8 May 1949, G. D. Hanna and A. G. Smith; CAS 27910, 2, 67–93 mm SL, Arena Cove, Mendocino, CA, 38°54′51″N, 123°42′55″W, 8.5–9.1 m depth, 8 April 1973, R. N. Lea et al.; CAS 28487, 1, 65 mm SL, Arena Cove, Mendocino, CA, 8 April 1973, R. N. Lea et al.; SU 11776, 1, 228 mm SL, Monterey, CA, December 1895, D. S. Jordan; SU 15112, 3, 63–117 mm SL, Pacific Grove, pier at far end of city beach, CA, 3 August 1948, C. Limbaugh, A. Flechzig, and E. Walker; LACM 31938.002, 6 of 27, 52–120 mm SL, St. Georges Reef, Whale Rock, Del Norte, CA, 10.7–13.7 m depth, 2 August 1971, D. Gotshall, D. Odenweiler, C. Swift, and D. Clifton; OS 1252, 2, 130–140 mm SL, beyond Yaquina Bay Bridge, OR, 27 May 1962, H. Murray; OS 4162, 1, 250 mm SL, Pacific Ocean off mouth of Columbia River, OR, 9 May 1961, P. Wolf; OS 7466, 107 mm SL, Pacific Ocean off Tillamook County, OR, 45°15.7′N, 124°0.6′W, 36.6 m depth, RV *Cayuse*, cruise C-7805-D, station 8, haul SBMT 224, 16 May 1978, E. E. Krygier; OS 11176, 1, 48 mm SL, off Oregon, 43°37′N, 124°15′W, 36.6 m depth, 28 June 1978, collector unknown; UW 1559, 1, 168 mm SL, Farallon Islands, CA, 26 October 1922, C. L. Hubbs; UW 40703, 3 of 6, 71–111 mm SL, Monterey Bay, CA, 7 October 1953, W. I. Follett.

Diagnosis

A species of *Sebastes* differentiated from all congeners, except *S. ciliatus, S. melanops*, and *S. mystinus*, by possession of dark gray, blue, brown, or black body coloration, scales that cover the mandible, and weak or absent head spination. *Sebastes diaconus* can be distinguished from *S. ciliatus* and *S. melanops* by the maxilla not extending beyond the posterior margin of the pupil when the mouth is closed. It is further distinguished from *S. ciliatus* by 4 bars of dark pigmentation that extend across the head and nape, versus the almost uniformly dark head coloration with 2 faint bars below the orbit in *S. ciliatus*, and by 26–27 vertebrae versus 28–29 vertebrae in *S. ciliatus*. *Sebastes diaconus* is further distinguished from *S. melanops* by having a uniform, light blue-gray, speckled pattern on the trunk, versus the darker black-gray coloration with irregular areas of dark pigmentation ranging from speckling to blotches in *S. melanops*, and by having dark dorsal-fin membranes without dark spots. *Sebastes diaconus* is most easily distinguished from *S. mystinus* by a brownish-blue to blue-gray trunk with distinct lighter blue-gray speckles versus the steel-blue to greenish-blue body coloration and large, dark blotches (also apparent in preserved specimens) of *S. mystinus*; this character is indistinct in many individuals under 100 mm SL. In specimens over 150 mm SL, *S. diaconus* can be further distinguished from *S. mystinus* by having the ventral margin of head and ventrum generally flat versus rounded and by the allometric development of the symphyseal knob (length of dentary symphysis 4.0–7.0% HL vs. 2.6–5.7% HL in *S. mystinus*). Although these ratios overlap, the symphyseal knob length differs diagnostically among specimens of equal size over 150 mm SL. This measurement can be diagnosed by comparison with allometric plots (Fig. 6A).

Description

Description based on 58 specimens, 48.2–344.0 mm SL. Counts and measurements of holotype and ranges, av-

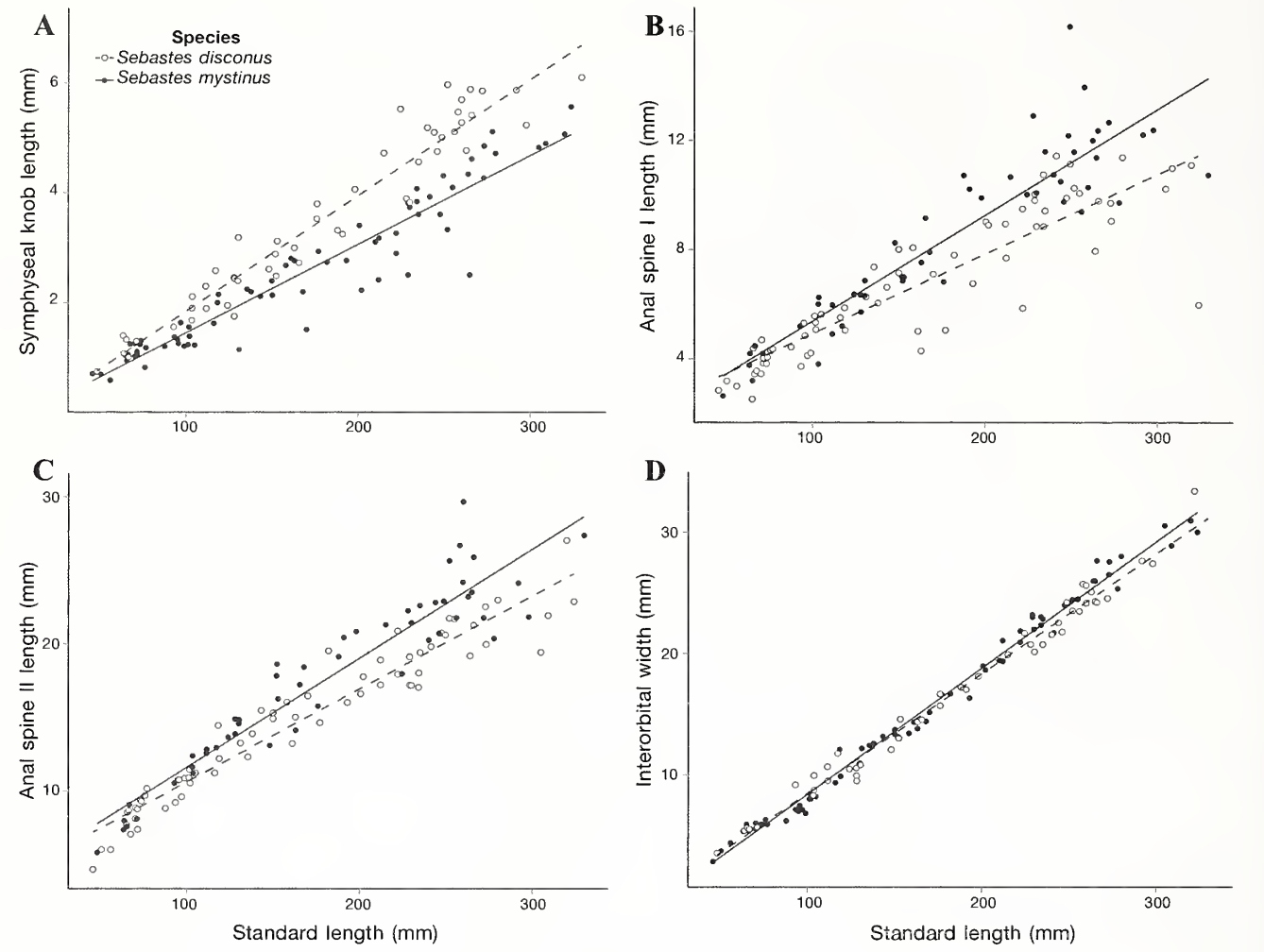

Figure 6

Linear regressions against standard length of the 4 morphometrics with significant allometric differences between *Sebastes mystinus* (blue rockfish; black dots, solid diagonal line) and *S. diaconus* (deacon rockfish; white dots, dashed diagonal line): (**A**) symphyseal knob length, (**B**) anal-fin spine I length, (**C**) anal-fin spine II length, and (**D**) ventral caudal peduncle length.

erages, and standard deviations for all specimens are provided in Table 3. Values in parentheses represent modes for meristic counts and means for morphometric ratios.

Dorsal-fin spines XXII or XXIII (XXIII), rays 14–17 (16); anal-fin spines III, rays 8 or 9 (9); pectoral-fin unbranched rays 9–10 (10), branched rays 6–8 (8), total pectoral rays 16–18 (18); pelvic-fin spines 1; pelvic-fin rays 5; total caudal-fin rays 38–41 (39); dorsal segmented caudal rays 8; ventral segmented caudal rays 8; dorsal procurrent caudal rays 11–13 (12); ventral procurrent caudal rays 11–12 (11); total vertebrae 26, rarely 27; anterior gill rakers 28–35 (33); posterior gill rakers 21–26 (22); scales ctenoid; lateral line complete and pronounced, lateral-line pores 41–51 (45); scales in lateral series on midline 56–68 (62).

Body deep and ellipsoid; depth at pelvic-fin origin 25.4–39.5% SL (34.4% SL); depth at anal-fin origin 22.0–34.8% SL (29.6% SL), lowest values in smallest specimens; depth at dorsal-fin origin 24.7–36.8% SL (33.5% SL). Dorsal margin of head sloping from supraoccipital crest to snout; HL 30.3–39.7% SL (34.6% SL); head depth 50.3–75.1% HL (59.4 HL); eye large, orbit diameter 20.9–33.0% HL (24.6% HL), orbit with bony ridge extending over anterodorsal margin; interorbital ridge moderately wide, interorbital area slightly convex, interorbital width 21.6–32.9% HL (25.9% HL); suborbital depth 2.5–8.5% HL (5.6% HL); snout length 17.2–27.4% HL (21.3% HL), nostrils anterior to central point of orbit, anterior nostril with spatulate flap extending posteriorly dorsal to posterior nostril and surpassing vertical bisecting posterior nostril when de-

Table 3

Mean, minimum, maximum, and standard deviation (SD) values of meristics and linear morphometrics for *Sebastes mystinus* (blue rockfish; n=68) and *S. diaconus* (deacon rockfish; n=58) examined for this study. Values for holotype of *S. diaconus*, new species, CAS 236653, and lectotype of *S. mystinus*, USNM 27085, are also provided. Standard length in millimeters. Linear morphometrics are given in proportions to standard length or head length for cephalic measurements (orbit length–symphyseal knob length).

	S. mystinus					*S. diaconus*				
	Lectotype	Mean	Min	Max	SD	Holotype	Mean	Min	Max	SD
Dorsal-fin spines	13	13	12	15	0.4	13	13	12	13	0.2
Dorsal-fin rays	15	15	13	17	0.7	16	16	14	17	0.8
Anal-fin spines	3	3	3	3	0.0	3	3	3	3	0.0
Anal-fin rays	9	9	8	10	0.5	9	9	8	9	0.4
Left total pectoral-fin rays	18	18	16	18	0.4	17	18	16	18	0.5
Right total pectoral-fin rays	17	18	17	19	0.6	18	18	17	18	0.5
Left unbranched pectoral-fin rays	10	10	9	12	0.4	10	10	9	10	0.3
Right unbranched pectoral-fin rays	10	10	9	11	0.4	10	10	10	10	0.3
Lateral-line pores	48	48	42	52	2.3	49	45	41	51	2.7
Scales in mid-lateral series	57	58	54	68	3.2	65	62	56	68	2.8
Anterior gill rakers	34	33	30	39	1.7	34	33	28	35	1.7
Posterior gill rakers	22	25	21	27	1.3	25	22	21	26	1.3
Dorsal procurrent caudal-fin rays	12	12	11	12	0.4	11	12	11	13	0.7
Ventral procurrent caudal-fin rays	12	11	11	12	0.5	12	11	11	12	0.5
Dorsal main caudal-fin rays	8	8	8	8	0.0	8	8	8	8	0.0
Ventral main dorsal-fin rays	8	8	8	8	0.0	8	8	8	8	0.0
Vertebrae	26	26	26	27	0.3	27	26	26	27	0.3
Standard length	249.6	164.2	45.7	324.0	80.6	260.0	181.3	48.2	330.0	73.8
Head length	34.7	33.7	29.9	36.4	1.5	35.3	34.5	30.3	39.7	1.9
Orbit length	7.3	24.6	17.3	30.4	2.7	7.5	24.6	20.9	33.0	2.7
Snout length	6.8	20.9	16.5	28.2	2.5	8.4	21.3	17.2	27.4	2.7
Interorbital width	9.7	26.2	18.1	32.0	3.3	9.9	26.0	21.6	32.9	2.0
Suborbital depth	2.4	6.0	4.0	8.9	0.9	2.6	5.6	2.5	8.5	1.2
Head depth	20.8	61.3	53.8	73.8	4.4	19.7	59.8	40.4	76.9	7.5
Upper jaw length	14.0	41.8	36.5	46.8	2.3	13.7	40.9	36.2	48.1	2.5
Lower jaw length	10.4	31.9	27.3	37.0	2.1	12.8	32.3	27.3	40.9	3.1
First gill arch length	14.7	43.3	30.6	53.5	4.0	14.0	42.3	32.3	49.0	3.5
Symphyseal knob length	1.7	4.5	2.6	5.7	0.7	2.0	5.5	4.0	7.0	0.7
Predorsal fin length	32.2	32.4	28.6	40.3	2.3	35.3	33.5	28.9	42.4	2.1
Prepelvic fin length	38.6	39.6	34.1	48.3	2.8	38.6	39.9	33.3	47.8	2.5
Preanal fin length	77.2	70.7	64.4	77.2	2.5	72.7	70.2	64.0	76.7	2.7
Depth at dorsal fin origin	36.2	34.4	28.4	39.8	2.0	34.2	33.5	24.7	36.8	2.0
Depth at pelvic fin origin	37.1	35.3	28.8	40.8	2.1	34.5	34.4	25.4	39.5	2.3
Depth at anal fin origin	31.7	29.8	23.0	34.1	2.2	32.5	29.7	22.0	34.8	2.3
Dorsal-fin spine I length	5.1	4.7	3.4	6.1	0.6	4.9	4.7	2.7	6.2	0.6
Dorsal-fin spine IV length	12.4	11.6	8.7	13.8	1.0	12.9	12.0	9.9	13.4	0.9
Spinous dorsal-fin base length	36.7	37.5	31.2	41.4	2.3	38.3	36.9	32.1	41.0	2.2
Soft rayed dorsal-fin base length	23.0	24.1	20.5	29.4	1.6	22.9	24.1	20.8	27.6	1.5
Pectoral-fin base depth	11.0	10.3	8.4	11.7	0.8	10.3	10.0	7.8	11.4	0.7
Pectoral fin length	30.5	29.3	25.6	32.7	1.8	29.2	28.8	23.7	32.0	1.7
Pelvic-fin ray length	20.6	20.2	16.3	23.4	1.7	22.1	19.8	16.8	22.4	1.3
Pelvic-fin spine length	13.8	12.7	8.9	15.6	1.3	12.9	12.4	9.3	14.7	1.2
Anal-fin base length	16.4	16.9	14.7	19.8	1.1	18.2	17.0	14.6	19.7	1.2
Anal-fin spine I length	4.5	4.5	1.8	6.7	1.0	6.2	4.8	3.3	6.7	0.8
Anal-fin spine II length	8.3	9.7	6.4	13.2	1.8	11.4	10.2	7.3	13.6	1.4
Anal-fin spine III length	11.8	10.7	7.5	13.8	1.4	10.9	11.0	6.7	14.2	1.4
Dorsal fin origin to anal fin origin	57.8	51.1	42.1	60.1	3.1	54.0	50.4	44.6	55.0	6.1
Caudal peduncle depth	11.1	10.6	8.6	12.5	0.9	11.0	10.5	8.9	12.7	0.7
Caudal peduncle dorsal length	10.8	11.8	8.6	15.3	1.6	8.2	12.3	8.2	16.3	1.7
Caudal peduncle ventral length	19.2	18.0	14.1	21.4	1.6	18.9	17.8	14.5	23.1	1.7

pressed, posterior nostril larger than anterior and without flap; cranial spines mostly absent with the exception of moderately weak nasal spines. Mouth terminal and moderately sized with posterior margin of maxilla extending to vertical through midpupil, posterior margin of maxilla slightly rounded, upper and lower jaw forming 30–35° angle to central axis of body when closed; upper jaw length 36.2–48.1% HL (40.9% HL), premaxilla with patches of minute conical teeth near symphysis transitioning into 2 then 3 rows of teeth along posterolateral portion, palatine and vomer covered in small conical teeth; lower jaw extending anteriorly slightly beyond upper jaw, protrusion becoming more distinct with growth, lower jaw length 27.4–40.9% HL (32.3% HL), mandibular pores minute or absent, mandible with 2–3 rows of minute conical teeth; tongue smooth; symphyseal knob pronounced and blunt (Fig. 7A), knob length 4.0–7.0% HL (5.5% HL); gill arch length 32.3–46.0% HL (42.3% HL); dorsal margin of opercular flap extending posteroventrally at a 25° angle to horizontal midline of the body, posterior margin of opercular flap straight, curving ventrally; opercular spines 2, dorsal spine stronger than ventral; preopercular spines 5, of which dorsal 3 are moderately developed, third largest, fourth weak and fifth very weak.

Figure 7

Comparison of the head of *Sebastes diaconus* (deacon rockfish; holotype; OS 18901), on the left side, with that of *S. mystinus* (blue rockfish; OS 18900), on the right side, to show differences in head shape and symphyseal protrusion.

Predorsal length 28.9–42.4% SL (33.5% SL); prepelvic length 33.3–47.8% SL (39.9% SL); preanal length 64.0–77.7% SL (70.3% SL). Dorsal-fin origin above posterior extent of opercular flap, dorsal-fin base length 55.0–68.2% SL (60.9% SL), spinous dorsal-fin base 32.1–41.0% SL (36.9% SL), first dorsal-fin spine 2.7–6.2% SL (4.7% SL), first spine shortest and subsequent spines rapidly increasing in height, longest dorsal-fin spine (IV) 9.9–13.4% SL (12.0% SL), spines IV–VII of approximately equal length with subsequent spines decreasing in size, 1 spine present at origin of rayed portion of dorsal fin, rayed dorsal-fin base 20.8–27.6% SL (24.0% SL), anterior rays longest and decreasing in size posteriorly, fin sloping posteroventrally and straight, not curved. Anal-fin margin perpendicular to body axis, posterior tips of rays forming nearly vertical line, anal-fin base 14.6–19.7% SL (17.0% SL), anterior anal-fin rays longest and decreasing in length posteriorly, anal-fin spine I length 3.3–6.7% SL (4.9% SL), anal-fin spine II length 7.3–13.6% SL (10.2% SL), thicker than others, anal-fin spine III length, usually longest, 6.7–14.2% SL (11.0% SL); pectoral-fin length 23.8–32.1% SL (28.8% SL), pectoral-fin base height 7.8–11.4% SL (10.0% SL), branched rays present on dorsal half of fin with transition to unbranched rays occurring 1 or 2 rays above the midline of the fin; pelvic-fin length 15.8–22.4% SL (19.7% SL), pelvic-fin rays decreasing in size from origin, posterior margin of pelvic fins slightly rounded; pelvic-fin spine length 9.3–14.7% SL (12.3% SL); caudal-peduncle depth 8.9–12.7% SL (10.5% SL), dorsal caudal-peduncle length 8.2–16.3% SL (12.3% SL); ventral caudal-peduncle length 14.5–23.1% SL (17.8% SL), caudal fin weakly emarginate, length not recorded because of extensive damage in many specimens.

Body covered in rough ctenoid scales; head entirely scaled, scales above dorsal opercular opening origin unorganized and very small, scales organized into loose rows on preopercle and opercle, scales on snout, premaxilla, maxilla and lower jaw minute and unorganized. Trunk scales moderately large, flanked by many small accessory scales, especially along posterior margins; lateral-line pores conspicuous and forming distinct line approximately one-quarter of body depth below dorsal margin of body, curving ventrally to reach midline of body axis at vertical through dorsal-fin insertion. Fins completely scaled, with exception of membranes between dorsal spines and posterior regions of unbranched pectoral-fin rays.

Coloration of live specimens (Figs. 1A and 8A) Body overall dark brown to blue-gray, becoming lighter posteriorly, ventrum white to light gray; small speckles covering sides of the body but not forming large blotches, pattern more evident in mature specimens. Juveniles (<100 mm SL) generally darker than adults, speckles indistinct or absent on trunk, and difficult to distinguish from other dark-bodied species. Head with 2 dark oblique bars extending posteriorly below orbit, 1 or 2 additional dark bars over cranium and opercular flap. Dorsal-fin membrane dark, lacking spots; caudal and anal fins uniformly blackish blue, thin light or unpigmented band on posterior margin of caudal fin; pelvic fins light with blue tips on rays, pelvic-fin spine white; pectoral fins dark blue dorsally, with light coloration on unbranched rays and ventral half of pectoral fins. Peritoneum dark, usually black to gray, typically

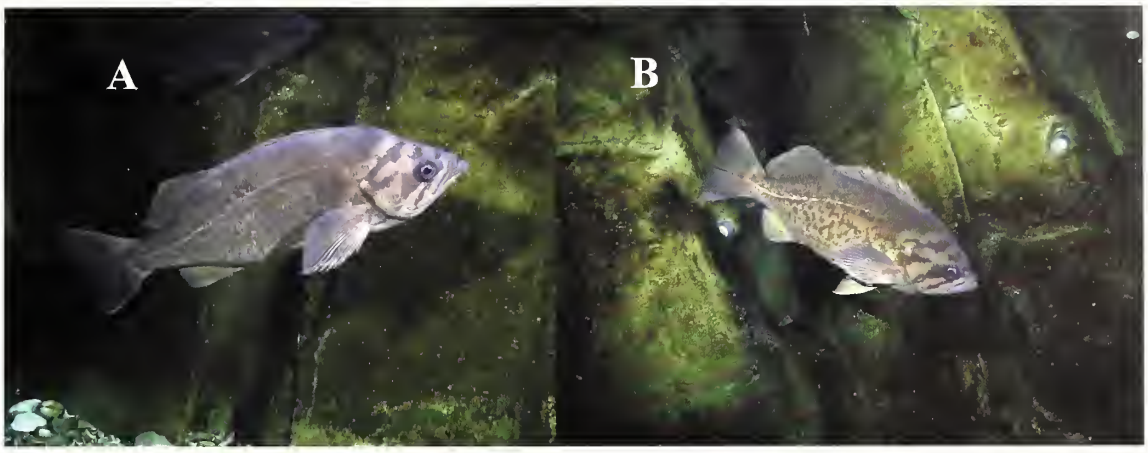

Figure 8

Photographs of live (**A**) *Sebastes diaconus* (deacon rockfish) and (**B**) *S. mystinus* (blue rockfish) in the Oregon Coast Aquarium, Newport, Oregon.

lighter in large specimens; stomach and other internal organs pale beige to grayish.

Coloration of preserved specimens (Fig. 1C) Shortly after death and during the process of preservation, trunk color becomes dull, dark gray to brown and the speckling pattern becomes less apparent; ventrum light brown to cream. Dorsal cranial bands fade and become indistinct, and 2 bands below orbit fade in color to match rest of body.

Etymology

Sebastes diaconus is derived from the Latinized ancient Greek διάκονος, the name for an acolyte or assistant to a priest. This name complements the species name of *S. mystinus*, which was intended to mean "priest" (Jordan and Evermann, 1898). This name highlights the similarity between the 2 species and the previous lack of differentiation.

Distribution

Sebastes diaconus is distributed from Vancouver Island in British Columbia to a southernmost record in Morro Bay, California (between 35°N and 48°N). All specimens with records of their collection depths were taken at depths of 8–50 m. The holotype and paratypes were collected from the Pacific Ocean off the coast of central Oregon (Fig. 9). Very little material was available from British Columbia and Alaska; therefore, the northern extent of the range remains unclear (Fig. 9). One poorly preserved specimen, USNM 54440, collected during an *Albatross* survey in 1897 off Killisnoo Island in southeastern Alaska may be a specimen of *S. diaconus*. However, it could also represent *S. ciliatus* and is excluded from the type and examined material. All other putative specimens of *S. mystinus* from Alaska that we examined had been misidentified and are mostly *S. ciliatus*. On the basis of this and previous work (Cope, 2004; Burford and Bernardi, 2008; Burford, 2009), *S. diaconus* appears to be much more abundant at latitudes higher than northern California.

Sebastes mystinus (Jordan and Gilbert, 1881)

English common name: blue rockfish

Figures 1, B and D, 2–6, 7B, 8B, 9, 10, and 11; Tables 1–3.

Sebastes variabilis (Pallas, 1814): Ayres, 1854:7 (specimens from California considered similar to but likely not that described in Pallas [1814]); Jordan and Gilbert, 1881:70.

Sebastichthys melanops (Girard, 1856): Jordan and Gilbert, 1880b:289.

Sebastodes melanops (Girard, 1856): Ayres, 1862:216 (in part, (not in fig. 66, but elsewhere in description); Jordan and Gilbert, 1881:70.

Sebastichthys mystinus Jordan and Gilbert, 1881 (for 1880b):455 (type localities: San Francisco and Monterey, California; described from 11 specimens).

Sebastodes mystinus (Jordan and Gilbert, 1881): Jordan and Gilbert (1882):659 (new combination).

Primospina mystinus (Jordan and Gilbert, 1881): Eigenmann and Beeson, 1893:669 (new combination).

Sebastosomus mystinus (Jordan and Gilbert, 1881): Jordan and J. Z. Gilbert, 1919:51 (new combination); Jordan and J. Z. Gilbert, 1920:32 (with mention that Jordan was inclined to elevate subgenus, but unclear if this decision was published); Jordan et al., 1930:365 (last reference to combination).

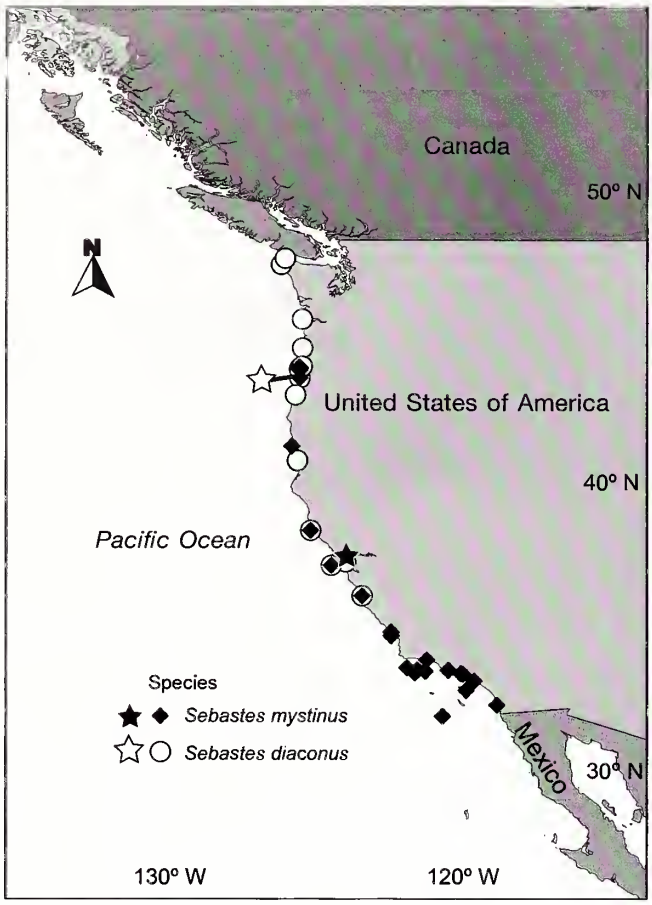

Figure 9

Distribution map of individuals of *Sebastes diaconus* (deacon rockfish; open circle; white star corresponding to holotype [OS 18901] locality) and *S. mystinus* (blue rockfish; black diamond; black star corresponding to lectotype [USNM 27085] locality) examined in this study.

Sebastes mystinus (Jordan and Gilbert, 1881): Hart, 1973:429; Eschmeyer and Herald, 1983:144; Orr et al., 2000:27; Love et al., 2002:215 (in part); Love, 2011:250–251 (in part).

Lectotype

USNM 27085, 1, 249 mm SL, off San Francisco, CA, 1880, D. S. Jordan.

Paralectotypes

MNHN A-3286 (ex-USNM 27085), 1, 185 mm SL, off San Francisco, CA, 1880, D. S. Jordan; MSNG 8327 (ex-USNM 26791), 1, 250 mm SL, off Monterey, CA, 1880, D. S. Jordan; MTD F 174 (ex-USNM 27085), 1, off San Francisco, CA, 1880, D. S. Jordan, desiccated specimen; RMNH-PISC 11530 (ex- USNM 26971), 1, 198 mm SL, off Monterey, CA, 1880, D. S. Jordan; USNM 26971, 212 mm SL, off Monterey, CA, 1880, D. S. Jordan; USNM 427237 (ex-USNM 27085), 1, 201 mm SL, off San Francisco, CA, 1880, D. S. Jordan; ZMUC P791064 (ex-USNM 27031), 1, 180 mm SL, off Monterey, CA, 1880, D. S. Jordan.

Additional material

CAS 13711, 1, 170 mm SL, off Southern California, east of Bishop Rock, 32°27′N, 119°7′59.10″W, 27.4 m depth, 28 July 1889, C. H. Eigenmann; CAS 14806, 4, 101–116 mm SL, Monterey Bay, Coast Guard Jetty, CA distance offshore 6.1–9.1 m, *Macrocystis* bed, 4.6–13.7 m depth, 14 August 1972, Behrens et al.; CAS 15439, 1, 193 mm SL, southern end of Santa Monica Bay, just north of Rocky Point, Palos Verdes Peninsula, CA, 24.4–27.4 m depth, 15 September 1972, E. W. Iverson; CAS 15440, 5, 150–182 mm SL, Santa Rosa Island, off Fraser Point, CA, 9.1–82.3 m, 21 September 1972, E. W. Iverson; CAS 234207, 1, 131 mm SL, off Santa Cruz Island, CA, 29 August 1954, E. Hunter; CAS 25884, 2, 64–70 mm SL, Pacific Grove, Monterey, CA, 6 October 1953, W. I. Follett; CAS 26469, 4 of 7, 130–176 mm SL, Souza Rock, Morro Bay, CA, 9 June 1953, G. D. Hanna; CAS 27719, 2, 50–101 mm SL, Point Arena, Arena Cove, CA, 38°54′56″N, 123°43′26″W, 9.1–12.2 m depth, 15 August 1972, R. Lea et al.; CAS 30262, 1, 265 mm SL, Santa Catalina Island, rocky bank off Avalon, CA, 6 June 1973, A. Loukashkin; SU 10149, 1, 273 mm SL, Cortez Bank, Baja California, Mexico, *Albatross* survey, U.S. Fish Commission; SU 15104, 1 of 10, 118 mm SL, Pacific Grove, pier at far end of city beach, California, 2 August 1948, E. Walker, C. Limbaugh, and A. Flechsig; SU 48885, 1, 76 mm SL, Morro Bay, beach just beyond PG&E intake on road to Morro Rock, San Luis Obispo, CA, 35°22′15″N, 120°55′20″W, 30 October 1995, B. W. Walker, UCLA party and San Simeon party; LACM 6607.001, 8, 65–77 mm SL, Leo Carillo State Park, Los Angeles, CA, 6 December 1964, E. S. Hobson and party. LACM 9482.002, 5 of 10, 136–234 mm SL, 8.0–9.7 km, north-northwest of San Miguel Island, CA, 6 December 1962, B. Wood; LACM 31864.024, 5, 88–100 mm SL, El Segundo, Los Angeles, CA, 25 March 1971, C. C. Swift and R. J. Lavenberg; LACM 35705.012, 1, 95 mm SL, off Huntington Beach power plant, CA, 11 June 1971, RV *Searcher*; LACM 47933.002, 241 mm SL, northeast end, 3.2 km offshore, Santa Rosa Island, CA, 5 June 1949, J. Fitch; LACM 47933.003, 46 mm SL, northeast end ~3.2 km offshore, Santa Rosa Island, CA, 5 June 1949, J. Fitch; LACM 48124.002, 2, 68–71 mm SL, point at Arguello Boat Station, Santa Barbara, CA, 22 October 1949, B. W. Walker and party; LACM 50157.002, 1, 56 mm SL, about 3.2 km north of San Simeon and 4.0 km south light at Coast Guard station, CA, 16 November 1999, B. W. Walker and class; OS 2618, 1, 222 mm SL, San Francisco Bay, CA, 15 May 1949, E. A. Brooks; OS 18881, 1, 257 mm SL, 1.4 km west of Tokatee Kloochman State Natural Site, OR, 44°12′26.28″N, 124°8′2.04″W,

19.2 m depth, 24 April 2012, D. W. Wagman and T. N. Frierson; OS 18886, 3, 223–300 mm SL, 1.3 km west of southern end of Lost Creek State Park, OR, 44°32′35.95″N, 124°5′33.61″W, 12.8 m depth, 24 April 2012, D. W. Wagman and T. N. Frierson; OS 18887, 3, 225–267 mm SL, 1.3 km west of south end of Lost Creek State Park, OR, 44°32′36.10″N, 124°5′33.40″W, 15.5 m depth, 20 April 2012, D. W. Wagman and T. N. Frierson; OS 18891, 3, 275–321 mm SL, 1.2 km west of north end of Lost Creek State Park, OR, 44°33′26.93″N, 124°5′18.17″W, 14.1 m depth, 20 April 2012, D. W. Wagman and T. N. Frierson; OS 18892, 1, 312 mm SL, 1.4 km west of north end of Lost Creek State Park, OR, 44°33′34.63″N, 124°5′45.02″W, 14.5 m depth, 8 May 2012, D. W. Wagman and T. N. Frierson; OS 18894, 2, 215–234 mm SL, 1.7 km northwest of Lost Creek State Park, OR, 44°33′51.12″N, 124°5′42.18″W, 14.3 m depth, 8 May 2012, D. W. Wagman and T. N. Frierson; OS 18896, 1, 295 mm SL, 1.5 km west of Lost Creek State Park, OR, 44°33′13.26″N, 124°5′38.54″W, 13.5 m depth, 8 May 2012, D. W. Wagman and T. N. Frierson; OS 18898, 1, 208 mm SL, 2.8 km west off south end of South Beach State Park, OR, 44°33′38.83″N, 124°6′36.47″W, 28.9 m depth, 15 May 2012, D. W. Wagman and T. N. Frierson; OS 18899, 1, 227 mm SL, 3.3 km west of south end of South Beach State Park, OR, 44°35′42.79″N, 124°6′35.82″W, 28.9 m depth, 15 May 2012, D. W. Wagman and T. N. Frierson OS 18900, 267 mm SL, 1.8 km west of Seal Rock, OR, 44°29′49.38″N, 124°6′30.48″W, 20.9 m depth, 20 April 2012, D. W. Wagman and T. N. Frierson; USNM 26947, 1, 163 mm SL, Santa Barbara, CA, 1880, D. S. Jordan; USNM 47154, 1, 270 mm SL, Cortez Banks, off Southern California, 37 m depth, 1889, *Albatross* expedition; USNM 63545, 1, 119 mm SL, Sausalito, CA, date unknown, *Albatross*; USNM 104771, 1, 161 mm SL, Point Pinos, Monterey, CA, 5 February 1923, C. L. Hubbs. UW 114028, 1, 210 mm SL, Scripps Canyon, La Jolla, CA, 32°49′59.88″N, 117°15′0″W, 14 November 2000, collector unknown.

Designation of lectotype

The original description by Jordan and Gilbert (1881) was published well before the establishment of the convention of holotype and paratypes designations. However, shortly after the original description, Jordan and Jouy (1881) published a listing of type material at the USNM for *Sebastichthys mystinus*. The type material listed includes USNM 26971 and 27031 from Monterey, California, and USNM 27085 from San Francisco, California, without any indication of the number of specimens in each lot. However, 10 syntypes are known to exist, including 5 in USNM: 26971 (1), 27031 (1), 27085 (3, of which 1 is an osteological preparation). In addition, there is 1 in each of 5 collections in Europe: MNHN A-3286 (ex-USNM 27085), MSNG 8327 (ex-USNM 26971), MTD F 174 (ex-USNM 27085, specimen desiccated), RMNH-PISC 11530 (ex-USNM 26971), and ZMUC P791064 (ex-USNM 27031). An eleventh syntype was sent to Philadelphia (ANSP 12119, ex-USNM 27085), but it is currently missing (Böhlke, 1984; Sabaj Peréz[3]). USNM 207085 was selected as the lectotype of *S. mystinus* because it is in the best condition of the original type material and has obvious blotched pigmentation (Fig. 11). One of the 10 extant syntypes of *S. mystinus*, USNM 27031, does not conform to the description of *S. mystinus*, clearly does not match the rest of the type series or the published illustration of this specimen (Jordan and Evermann, 1900: pl. 270, fig. 657; listed as fig. 656 in the index), and is a different species of *Sebastes* (see the *Remarks* section). We designate the remaining specimens in the syntype series, with the exceptions of the misidentified USNM 27031 and the missing ANSP 12119, as paralectotypes.

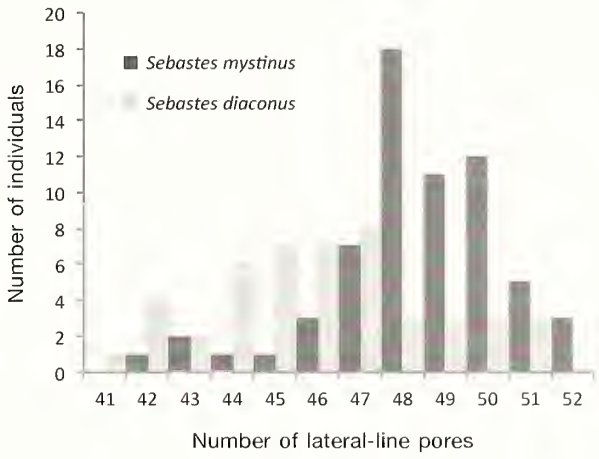

Figure 10

Histogram of lateral-line pore counts for specimens of *Sebastes diaconus* (deacon rockfish; n=47; gray bars) and *S. mystinus* (blue rockfish; n=68; black bars) examined in this study.

Diagnosis

A species of *Sebastes* differentiated from all congeners with the exceptions of *S. ciliatus*, *S. melanops*, and *S. diaconus* by possessing dark gray, blue, brown, or black body coloration, scales covering the mandible, and weak or absent head spination. *Sebastes mystinus* is distinguished from *S. ciliatus* and *S. melanops* by the maxilla not extending beyond the posterior margin of pupil when the mouth is closed. It is further distinguished from *S. ciliatus* by 4 bars of dark pigmentation extending across the head and nape versus an almost uniformly dark head coloration with 2 faint bars below orbit in *S. ciliatus*, 26–27 vertebrae versus

[3] Sabaj Peréz, M. 2013. Personal commun. Department of Ichthyology, The Academy of Natural Sciences, Philadelphia, PA 19103.

Figure 11

The lectotype of *Sebastes mystinus,* USNM 27085, 249 mm SL, collected by David Starr Jordan in 1880 off San Francisco Bay, California. Scale bar indicates 50 mm.

28–29 vertebrae in *S. ciliatus*, and a small or absent symphyseal knob versus a pronounced one. It is further distinguished from *S. melanops* by having a blue-gray trunk with large gray blotches, versus a darker black or gray trunk with irregular areas of dark pigmentation ranging from speckling to blotches in *S. melanops*, and by having dark dorsal-fin membranes without dark spots, versus the presence of such spots. *Sebastes mystinus* is distinguished from *S. diaconus* by a steel-blue to greenish-blue body coloration with large, distinct dark blotches versus a dark blue-brown to blue-gray body with a light, speckled pattern that characterizes *S. diaconus*. It is further distinguished from *S. diaconus* by the following set of character states in individuals over ~150 mm SL: ventral margin of head and ventrum generally rounded, giving the body a more ovoid appearance, versus the flat ventrum of *S. diaconus*; symphyseal knob short and not prominent (length of dentary symphysis 2.6–5.7% HL) versus well-developed (4.0–7.0% HL). Although these ranges overlap, symphyseal knob length differs diagnostically among specimens of equal size over 150 mm SL. This measurement can be diagnosed by reference to allometric plots (Fig. 6A).

Description

Description based on 68 specimens, 45.7–324.0 mm SL. Counts and measurements of lectotype and ranges, averages, and standard deviations for all specimens are provided in Table 3. Values in parentheses are modes for meristic counts and means of all specimens for morphometric ratios.

Dorsal-fin spines XXII to XXIV (XXIII) [1 with XXV], rays 13–17 (15); anal-fin spines III, rays 8–9, rarely 10 (9); pectoral-fin unbranched rays 9 or 10, rarely 11 (10), branched rays 7–9 (8), total pectoral rays 16–19 (18); pelvic-fin spines 1; pelvic-fin rays 5; total caudal-fin rays 38–40 (40); dorsal segmented caudal rays 8; ventral segmented caudal rays 8; dorsal procurrent caudal rays 11–12 (12); ventral procurrent caudal rays 11–12 (11); total vertebrae 26, rarely 27; anterior gill rakers 30–39 (33); posterior gill rakers 21–27 (25); scales ctenoid; lateral-line pores 42–52 (48); scales in lateral series on midline 54–68 (58).

Body deep and ovoid; depth at pelvic-fin origin 28.8–40.8% SL (35.3% SL); depth at anal-fin origin 23.0–34.1% SL (29.7% SL); depth at dorsal-fin origin 28.4–39.8% SL (34.3% SL). Dorsal margin of head slightly rounded (Fig. 6B); head length 29.9–36.4% SL (33.6% SL); head depth 53.8–73.8% HL (61.5 HL); eye moderately large, orbit diameter 17.3–30.4% HL (24.6% HL), bony ridge extending over anterodorsal margin of orbit; interorbital ridge wide and convex, interorbital width 18.1–32.0% HL (26.3% HL); suborbital depth 4.0–8.9% HL (6.0% HL); snout length 16.5–28.2% HL (20.9% HL). Nostrils anterior of mid-orbit, anterior nostril circular with wide spatulate nostril flap that extends to posterior side of posterior nostril when depressed, posterior nostril ovoid and larger than anterior nostril, posterior nostril without flap; cranial spines usually absent except for weak nasal spines, additional weak head spines have been rarely reported (Love et al., 2002). Terminal mouth with moderate gape, posterior tip of maxilla extending at least to vertical through center of orbit and at maximum to vertical through posterior margin of pupil, posterior margin of maxilla flat to minimally rounded. Jaws when closed forming dorsally slanted 30° angle to midline of body; upper jaw length 36.5–46.8% HL (41.8% HL), premaxilla with 2 broad patches of small unorganized conical teeth near symphysis, teeth forming 2–3 rows that terminate one-third premaxilla length before posterior tip of premaxilla, palatine and vomer with patches of minute conical teeth; anterior tip of lower jaw level with or slightly anterior to upper jaw when mouth closed, not exaggerated in larger

specimens, lower jaw length 27.3–37.0% HL (31.8% HL), mandible with patches of 5 or 6 rows of teeth near symphysis that become 3 rows of minute conical teeth away from symphysis, mandibular pores weak or absent, tongue smooth; symphyseal knob generally weak to absent, more pronounced in larger specimens, but not exaggerated, symphyseal knob length 2.6–5.9% HL (4.6% HL); gill arch length 30.6–53.5% HL (43.4% HL). Dorsal margin of opercular flap extends at posteroventral 18–20° angle with body midline, posterior margin of opercular flap straight, sloping at 65° anteroventral angle to body midline, curving anteriorly near ventral extreme; opercular spines 2, both weakly protruding from skin, dorsal spine slightly stronger than ventral spine; preopercular spines 5, dorsal 4 spines moderately developed, fifth spine small and weak.

Predorsal length 28.6–40.3% SL (32.4% SL); prepelvic length 34.1–48.3% SL (39.6% SL); preanal length 64.4–76.1% SL (70.6% SL). Origin of dorsal fin slightly anterior to posterior tip of opercular flap, dorsal-fin base length 55.3–67.4% SL (61.6% SL), spinous dorsal-fin base 31.2–41.2% SL (37.5% SL), spinous portion of dorsal fin slightly rounded, highest in middle, dorsal-fin spine I 3.4–6.1% SL (4.7% SL), first dorsal spine shortest, subsequent spines much longer, longest dorsal-fin spine (IV) 8.7–13.8% SL (11.6% SL), dorsal spines IV–VII roughly the same length, with posterior spines decreasing in length, 1 spine at origin of rayed section of dorsal fin, rayed dorsal-fin base 20.5–29.4% SL (24.1% SL), dorsal-fin rays decreasing in size posteriorly forming straight sloping edge with a slightly curved anterior portion; anal-fin base 14.7–19.8% SL (16.9% SL), anal-fin spine I length 2.6–6.7% SL (4.5% SL), anal-fin spine II length 6.4–13.2% SL (9.7% SL), anal-fin spine III length, usually the longest, 7.5–13.8% SL (10.7% SL), anal-fin rays decrease in size posteriorly, posterior tips of rays form line nearly perpendicular to body axis, not curved; pectoral-fin length 25.6–32.7% SL (29.2% SL), pectoral-fin base height 8.4–11.7% SL (10.3% SL), pectoral-fin rays on dorsal half of fin branched, ventral 9–10 rays unbranched, rays thick and cylindrical; pelvic-fin length 16.3–23.4% SL (20.1% SL), lateralmost pelvic-fin ray longest, rays decreasing in size medially, posterior margin of fin straight, pelvic-fin spine length 8.9–15.6% SL (12.6% SL); caudal-peduncle depth 8.6–12.5% SL (10.6% SL), dorsal caudal-peduncle length 8.6–15.3% SL (11.8% SL); ventral caudal-peduncle length 14.1–21.4% SL (17.9% SL), caudal fin broad, weakly emarginate.

Rough scales with many small ctenii covering most of body; head, including jaws, completely scaled, scales on cranium between supraoccipital crest and snout minute and unorganized, these scales also cover jaws, circumorbital area, and region ventral to orbit; preopercle and opercle covered in loosely organized rows of larger scales, posteriorly flanked by accessory scales. Scales on trunk moderate to large, largest scales near midline of body, most trunk scales also posteriorly flanked by unorganized accessory scales; lateral-line pores not associated one-to-one with scales, forming a slightly arched line along the dorsal third of the trunk originating at the dorsal insertion of opercular flap, curving to central midline of body at vertical through dorsal-fin insertion and terminating at caudal-fin base. Fins almost entirely scaled except for membranes of spinous dorsal and anal fins and posterior portions of the unbranched pectoral rays.

Coloration of live specimens (Figs. 1B and 8B) Overall body coloration somewhat variable, ranging from steel blue to greenish blue; ventrum white; sides of body with large, dark, angular blotches and no speckles; blotches easily discernible in larger juveniles (>100 mm SL) and mature adults; smaller juveniles generally solid brown-blue without distinct pattern of blotches. Head with 2 posteroventrally oriented dark bars, dorsal bar originating from orbit and extending to ventral margin of opercle, ventral bar running through orbit and over snout to terminate on ventral margin of opercular flap. One or 2 additional dark bars across dorsal surface of head behind orbit, terminating on opercular flap. Spinous dorsal-fin membrane completely dark and without spots, dorsal and caudal fin uniform dark blue to black, thin unpigmented strip on distal margin of caudal fin; anal fin slightly lighter, gray-blue to dark gray; pelvic fins light gray with blue tips, spine white to light gray; pectoral fins mostly dark blue-black, distal half of unbranched pectoral-fin rays light gray to white. Peritoneum usually black to dark gray, sometimes light in large specimens; stomach and other internal organs pale gray.

Coloration of preserved specimens (Figs. 1D and 11) After death and during process of preservation, body pattern becomes less distinct and overall color fades to dark blue-brown; blotched pattern still visible on specimens through at least first 30 years of preservation. Blotches absent in some long-preserved specimens; however, this absence may reflect variation in preservation technique or exposure to light. Ventrum cream to light brown, dorsal and caudal fin dark blue-black, anal fin dark gray to dark blue-black, pelvic fin light with black tips, pectoral fins mostly brown-black, but distal half of unbranched rays white. Bars on head fade slightly, but remain dark and distinct; orbit cloudy white-blue.

Etymology

The species name in *Sebastes mystinus* is an adjective derived from the Latinized form of the ancient Greek word μύστησ, which means initiated one or mystic (Hollmann[4]), although interpreted as "priest" (Jordan and Evermann, 1898). It was selected as the specific epithet because 19th century fishermen of Monterey, California,called the fish the "pêche prêtre" (translated as "priest-fish" by Goode, 1884) because of its overall

[4] Hollmann, A. 2015. Personal commun. Department of Classics, Univ. Wash., Seattle, WA 98195.

dark coloration and its light band between the head bars that resembles a clerical collar (Goode, 1884; Jordan and Evermann, 1898).

Distribution

The true range of *S. mystinus* extends from central Oregon to northern Baja California (specimens examined from 32.5°N to 44.5°N), with the highest concentration of the species occurring off the coast of central to southern California (Fig. 9). Specimens examined were collected at depths of 0.5–30.0 m. Jordan and Gilbert (1881) originally described *S. mystinus* from specimens collected "off" San Francisco and Monterey, California. Subsequent observations cited the species as occurring from Baja California, Mexico, northward into British Columbia, and even Alaska (Love et al., 2002). However, it is apparent that all specimens examined from central Oregon northward into British Columbia are the new species, *S. diaconus*, and not *S. mystinus*. All purported specimens of *S. mystinus* from Alaskan waters that we examined belong to other congeners, primarily *S. ciliatus*.

Remarks

Ten of the 11 surviving syntypes of *S. mystinus* are clearly conspecific and match the original description by Jordan and Gilbert (1881). However, USNM 27031 is clearly not *S. mystinus* or *S. diaconus*, on the basis of substantial morphological differences. This specimen possesses an exceptionally long symphyseal knob and a maxilla extending almost to the posterior margin of the eye. In addition, its opercular spines are very well developed and much longer than observed in any *S. mystinus* or *S. diaconus* specimens. This specimen lacks distinctive pigmentation, such as head bars or blotching on the trunk; in fact it is entirely devoid of dark pigment. The other specimen originally in the same lot, ZMUC P791064 (ex-USNM 27031), is clearly recognizable as *S. mystinus* in that it lacks a symphyseal knob and bears a maxilla that extends posteriorly only to the vertical through the pupil of the eye. Additionally, it possesses faint head bars and blotching on the trunk.

Given the major differences between USNM 27031 and the remainder of the syntype series, it seems strange that Jordan and Gilbert (1881) would have conflated them. An illustration of USNM 27031 published by Jordan and Evermann (1900: pl. 270, fig. 657; also see Mecklenburg et al., 2002:360) may help explain the apparent lapse. The specimen currently designated as USNM 27031 does not correspond with the body shape or lower jaw shape of the illustration, and length of the specimen (402 mm TL, with significant caudal fin damage) far exceeds the measurement of 300 mm TL cited in the 1900 work. On the basis of the length of the specimen and the obvious shape difference, it is clear the current USNM 27031 is not the specimen originally designated by Jordan and Gilbert (1881) and illustrated by Jordan and Evermann (1900).

It is unclear how the current specimen designated as USNM 27301 came to possess this number, but a note attached to USNM 27031 states "1 located Nov. 21, 1946; some sent UZM Copenhagen 1881-7." This note suggests that USNM 27031 was at one point lost and then relocated, presenting the possibility that the "relocated" specimen is not the original. The exact identification of USNM 27031 remains unclear. If it was originally dark-colored (now faded), it is most likely either an elongated specimen or a poorly preserved specimen of *S. melanops* or *S. ciliatus*. However, the lack of pigmentation could also indicate that this rockfish was originally light colored, a supposition supported by the fact that all other members of the syntype series retain some degree of dark coloration. If so, then the most likely species identification for this specimen is yellowtail rockfish *Sebastes flavidus* (Ayres, 1862). Either way, it undoubtedly does not represent *S. mystinus*, and we remove it from the paralectotype series.

Comparisons of *Sebastes mystinus, S. diaconus,* and similar congeners

Differentiation of the 2 species without the use of genetic techniques can be challenging, but the trunk coloration provides the most obvious difference between the 2 species. *Sebastes mystinus* is generally lighter colored, gray-blue to green-blue, and has a blotched pattern on the body, whereas *S. diaconus* is generally darker, blue to blue-brown, and has a distinct speckling pattern on the trunk (Fig. 1A). The difference in trunk pattern is apparent in juvenile specimens; however, smaller juveniles (<100 mm SL) of both species are almost entirely brown-gray with only subtle evidence of trunk markings. Coloration patterns are visible, but faint, in some preserved material making this diagnostic feature useful for historic specimens. *Sebastes diaconus* has a more pointed head and flat ventrum, as opposed to the generally rounded head and ventrum of *S. mystinus*. *Sebastes diaconus* specimens also have lower mean numbers of lateral-line pores (45 versus 48 in *S. mystinus*). Although the range of values overlaps almost completely (41–51 in *S. diaconus* versus 42–52, Fig. 10); only 16% of *S. diaconus* specimens possess more than 47 pored lateral-line scales versus 69% in *S. mystinus*, and the differences are statistically significant (Student's *t*-test: $P=8.87\times10^{-6}$).

Specimens over 150 mm SL differ between species in the prominence and average length of the symphyseal knob, which measures 2.6–5.9% HL (4.6% HL) in *S. mystinus* and 4.0–7.0% HL (5.9% HL) in *S. diaconus* (Fig. 6A). Many juvenile specimens of both species lack a distinctly developed symphyseal knob. Lower jaw length (9.1–12.3% SL [10.4% SL] versus 9.3–14.0% SL [11.1% SL] in *S. diaconus*) and overall HL (29.9–36.3% SL [33.2% SL] versus 30.3–39.7% SL [34.7% SL] in *S. diaconus*) are also higher in *S. diaconus*. The lower jaw of *S. diaconus* extends farther beyond the anterior margin of the upper jaw than it does in *S. mystinus*, and this length may increase allometrically in *S. diaco-*

nus. However, this measurement differed only slightly significantly in a pairwise comparison (Student's *t*-test: P=0.03). The posteriormost corner of the opercle appears to be pointed in *S. diaconus* rather than rounded in *S. mystinus*; however, this shape difference is not apparent in juvenile specimens and may best be used as a field character rather than as a diagnostic. *Sebastes diaconus* specimens also possess, on average, longer first and second anal-fin spines: anal-fin spine I: 2.6–5.3% (3.9%) SL in *S. mystinus* versus 3.3–6.2% SL (4.6% SL) in *S. diaconus*, anal-fin spine II: 6.4–9.9% SL (8.3% SL) versus 7.3–12.2% SL (9.5% SL) in *S. diaconus*. The slopes of regressions for these spine lengths versus SL differ significantly (Figure 6, B and C).

Collection and dissection of specimens from off the Oregon coast between 2009 and 2014 indicate that ovary color of breeding females may also differ diagnostically (Hannah et al.[5]). Ovaries of breeding female *S. diaconus* examined immediately after capture were always pink-cream, whereas the ovaries of *S. mystinus* were always bright yellow. We did not observe this difference in the specimens used for genetic analysis; however, those specimens were not freshly deceased at the time of dissection.

Both *S. mystinus* and *S. diaconus* can be distinguished from the other potentially co-occurring dark-colored *Sebastes* species, such as *S. melanops* and *S. ciliatus*, on the basis of morphology and pigmentation. The color pattern of *S. diaconus* is very similar to that of some *S. melanops*; however, *S. melanops* tends to be darker black to brown with irregular gray blotches, mottling or speckling. The trunk coloration of *S. mystinus*, with large gray blotches, is generally lighter than that of *S. melanops*, and *S. melanops* is generally darker and more irregular in coloration. Additionally, both *S. diaconus* and *S. mystinus* have a smaller gape than that of *S. melanops*, with maxilla extending only to or just beyond the posterior margin of the pupil rather than beyond the posterior margin of the orbit. Some sources cite anal-fin shape to differentiate *S. mystinus* (and likely *S. diaconus*): a rounded anal fin versus a straight anal fin in *S. melanops* (Kramer and O'Connell, 1995). However, this character does not seem to be discrete because variation in fin shape between rounded and straight occurs in all 3 species.

Sebastes diaconus and *S. mystinus* are distinguished from *S. ciliatus* by having 4 bars of dark pigmentation across the head and nape, whereas *S. ciliatus* usually has uniform cephalic coloration (2 faint bars appear below the orbit occasionally) (Orr and Blackburn, 2004). As in *S. melanops*, the gape of *S. ciliatus* is larger than that of the other 2 species, with the maxilla extending to the posterior margin of the orbit. *Sebastes ciliatus* is further distinguished from *S. mystinus* by having a more pronounced symphyseal knob, similar to that of *S. diaconus*. *Sebastes ciliatus* is known to occur mainly in Alaska and may range into northern British Columbia (Orr and Blackburn, 2004), whereas *S. mystinus* and *S. diaconus* occur farther south (all specimens of "*S. mystinus*" from Alaska examined were *S. ciliatus* or *S. variabilis*). Finally, *S. mystinus* and *S. diaconus* possess 26–27 vertebrae, and *S. ciliatus* has 28–29 vertebrae (Orr and Blackburn, 2004).

Discussion

Potential mechanisms for segregation

Although both pre- and postzygotic barriers may separate the 2 species, Burford et al. (2011a) suggested that a prezygotic explanation is more likely owing to the lack of hybrid individuals and strong Wahlund effect in areas of sympatry. Sympatric species of *Hexagrammos* in the northeastern Pacific show similar patterns of segregation (Crow et al., 2010). Prezygotic barriers may result generally from variable courtship behavior, incompatible reproductive morphological features, different reproductive timing, segregation of habitat type, or a combination of these factors. A least 3 of these factors are plausible in the specific case of *S. mystinus* and *S. diaconus*.

If differential courtship helps isolate these species, the development of species-specific characteristics at a size near, or preceding, early estimates of the length of first maturity (~150 mm SL in California populations of *S. mystinus*, Wyllie Echeverria, 1987; Love et al., 2002; Key et al.[6]; however, see Hannah et al.[5]) may facilitate prezygotic isolation by allowing breeding pairs to cue visually and tactilely on differences in body color (Fig. 1), in the size of the symphyseal knob (Fig. 6), or in the length of the lower jaw. In the only study to describe courtship behavior in *S. mystinus,* individuals were observed in Southern California (and, therefore, were clearly not *S. diaconus*) and during courtship the male was found to graze the snout of the female with its body (Helvey, 1982:fig. 3). The presence or absence of a moderately large symphyseal knob and longer lower jaw may act as an indication of species identity at this point. Comparison of the mating behavior of both species would be an important first step in exploring this hypothesis. Additionally, more recent work on both species in Oregon waters indicates larger lengths at first maturity for both species: around 260 mm fork length (FL) for *S. mystinus* and 270 mm FL for the other species (Hannah et al.[5]). The inclusion of more morphometric data from large individuals could elucidate further species-specific sexual characteristics.

[5] Hannah, R. W., D. W. Wagman, and L. A. Kautzi. 2015. Cryptic speciation in the blue rockfish (*Sebastes mystinus*): age, growth and female maturity of the blue-sided rockfish, a newly identified species, from Oregon waters. Fish Div., Oregon Dep. Fish Wildl. Inf. Rep. 2015-01, 24 p. [Available at website.].

[6] Key, M., A. D. MacCall, J. Field, D. Aseltine-Neilson, and K. Lynn. 2007. The 2007 assessment of blue rockfish (*Sebastes mystinus*) in California, 112 p. Pacific Fishery Management Council, Portland, OR. [Available at website.]

The differences between *S. mystinus* and *S. diaconus* in length of the anal-fin spines may imply additional mechanistic differences in internal fertilization. Helvey (1982) noted that at the probable point of insemination, male and female *S. mystinus* embrace with bodies in a C-shape position with their anal pores and anal fins tightly joined, indicating the use of anal-fin elements in copulation. The sexual dimorphism in anal-fin spine length in *S. melanops* (Wyllie Echeverria, 1986) and *S. mystinus* (Wyllie Echeverria, 1986; Lenarz and Wyllie Echeverria, 1991) further suggests a role for anal fin elements in internal fertilization among *Sebastes*. We did not observe sexual dimorphism in anal-fin spine lengths in this study, although sex was only verified on a subsample of specimens, and the use of anal-fin elements in sperm transfer has not been proven for these species. Therefore, the conjecture of differential reproductive morphological features remains speculative.

Differential reproductive timing may also play a role in prezygotic isolation of these 2 species. Hannah et al.[5] observed ovary development for both species off central Oregon and identified a potential difference of a month in the timing of parturition with *S. diaconus* beginning in January and *S. mystinus* in February. However, sampling per month was uneven, and larger samples sizes may be necessary to confirm this difference.

Prezygotic isolation can also stem from habitat differences and particularly from differences among spawning sites. Although previous studies (Burford, 2009; Burford et al., 2011a, 2011b) found no clear evidence of differential habitat or depth preference between the 2 species, anecdotal evidence from fishermen and port samplers in central Oregon (Phillips[7]) indicates that adult *S. diaconus* are collected more frequently in deeper waters farther offshore than are adult *S. mystinus*, which are caught closer to shore in shallower waters. This variation in depth preference could explain the lack of type-1 (*S. diaconus*) adults found by Burford et al. (2011b) in nearshore surveys. Only new data on fisheries catches and intensive field observation will discern whether these species inhabit different physical environments.

Although previous research (Burford, 2011a) and evidence from this study support the possibility of segregation by means of prezygotic barriers, the possibility of segregation by postzygotic barriers, such as hybrid sterility or zygotic inviability, cannot be ruled out completely. Postzygotic barriers could be explored with controlled laboratory hybridization studies; however, breeding in captivity may not be realistic as rockfish mature slowly.

Implications for fisheries

The molecular analyses of Cope (2004) and of Burford and colleagues (Burford and Larson, 2007; Burford and Bernardi, 2008; Burford, 2009; Burford et al., 2011a, 2011b), combined with our morphological results, indicate definitively that 2 types of blue rockfish differ sufficiently to merit recognition as distinct species. We concur with Burford et al.'s (2011a, 2011b) argument that fisheries management must recognize that distinction, because the 2 species may react differently to varying ocean conditions and may experience drastically different levels of fishing pressure. In the known area of sympatry (from Newport, Oregon, south through northern California), these 2 species hold substantial recreational importance and, to a lesser degree, commercial value. In northern California, blue rockfish (likely both species) are the most commonly caught species of rockfish by recreational fishermen and are the second largest recreational rockfish fishery after *S. melanops* in Oregon (Love et al., 2002). Central and southern California populations of blue rockfish (either *S. mystinus* or both species) have declined drastically and many of the fish currently being caught are juvenile, indicating stock depletion in these areas (Love et al., 2002). In response to the known decline, most of the fishery and life history research on blue rockfish has focused on southern California populations, likely *S. mystinus* (VenTresca et al., 1995; Laidig et al., 2003; Key et al.[6]), and very little appears to be known about *S. diaconus* from Oregon and Washington. Moreover, it is unknown whether fishing pressure in the zone of overlap affects 1 of the 2 species more than the other.

Our study provides fisheries managers the crucial diagnostic tool needed to answer these questions: namely, the characters that readily distinguish the adults of the 2 species, *S. mystinus* and *S. diaconus*, in the form of color pattern, size of the symphyseal knob and lower jaw, ventrum shape (rounded versus flat), and potentially ovary color. Although pelagic, young-of-year and early settled juveniles are more difficult to distinguish, as is the case with many young *Sebastes* (Love et al., 2002), genetic analysis or collection locality can help assign those individuals to these 2 species. Additional sampling and observational studies may also be able to elucidate ecological and habitat differences. Even with some gaps in our knowledge, formal recognition of these lineages as distinct species permits the development of proper management regimes for these important groundfishes along the Pacific coast of the United States.

Acknowledgments

We would like to thank D. Catania (CAS), M. Crag (ZMUC), G. Doria (MSNG), R. Fenney (LACM), K. Pearson Maslenikov (UW), T. Pietsch (UW), S. Raredon (USNM), P. Rask Møller (ZMUC), L. Rocha (CAS), R. de Ruiter (RMNH), M. Sabaj Peréz (ANSP), E. Taylor (UBC), and N. Vasset (MNHN) for providing access specimens or images, M. Burford for providing genetic samples, S. S. Heppell, K. Hoekzema, T. Laidig, M. Love, D. Markle, J. Orr, and K. Schmidt for providing

[7] Phillips, J. 2013. Personal commun. Hatfield Marine Science Center, Oregon State Univ., Newport, OR 97365.

feedback and support, our undergraduate helpers, A. Martin and E. Peterson, A. Hollmann (UW) for elucidating Ancient Greek etymology and for assisting with naming the new species, and the Oregon Coast Aquarium for access to exhibits. Support was provided by National Science Foundation Division of Biological Infrastructure NSF DBI 1057452 and U.S. Fish and Wildlife Service Federal Assistance Award OR F-186-R-9.

Literature cited

An, H. S., J. Y. Park, M.-J. Kim, E. Y. Lee, and K. K. Kim.
2009. Isolation and characterization of microsatellite markers for the heavily exploited rockfish *Sebastes schlegeli*, and cross-species amplification in four related *Sebastes* spp. Conserv. Genet. 10:1969–1972.

Ayres, W. O.
1854. Description of new fishes from California. Proc. Calif. Acad. Nat. Sci. 1:3–22.
1862. Descriptions of fishes believed to be new. Proc. Calif. Acad. Nat. Sci. 2:206–218.

Bean, T. H.
1882. Notes on a collection of fishes made by Captain Henry E. Nichols, U.S.N., in British Columbia and southern Alaska, with descriptions of new species and a new genus (*Delolepis*). Proc. U.S. Natl. Mus. 4:463–474.

Böhlke, E. B.
1984. Catalog of type specimens in the ichthyological collection of the Academy of Natural Sciences of Philadelphia. Special Publication 14, 216 p. Acad. Nat. Sci. Phil., PA.

Burford, M. O.
2009. Demographic history, geographical distribution and reproductive isolation of distinct lineages of blue rockfish (*Sebastes mystinus*), a marine fish with a high dispersal potential. J. Evol. Biol. 22:1471–1486.

Burford, M. O., and G. Bernardi.
2008. Incipient speciation within a subgenus of rockfish (*Sebastosomus*) provides evidence of recent radiations within an ancient species flock. Mar. Biol. 154:701–717.

Burford, M. O., G. Bernardi, and M. H. Carr.
2011a. Analysis of individual year-classes of a marine fish reveals little evidence of first generation hybrids between cryptic species in sympatric regions. Mar. Biol. 158:1815–1827.

Burford, M. O., M. H. Carr, and G. Bernardi.
2011b. Age-structured genetic analysis reveals temporal and geographic variation within and between two cryptic rockfish species. Mar. Ecol. Prog. Ser. 442:201–215.

Burford, M. O., and R. J. Larson.
2007. Genetic heterogeneity in a single year-class from a panmictic population of adult blue rockfish (*Sebastes mystinus*). Mar. Biol. 151:451–465.

Burnaby, T. P.
1966. Growth-invariant discriminant functions and generalized distances. Biometrics 22:96–110.

Clemens, W. A., and G. V. Wilby.
1961. Fishes of the Pacific coast of Canada, 2nd ed. Fish. Res. Board Can. Bull. 68, 443 p.

Cope, J. M.
2004. Population genetics and phylogeography of the blue rockfish (*Sebastes mystinus*) from Washington to California. Can. J. Fish. Aquat. Sci. 61:332–342.

Crow, K. D., H. Munehara, and G. Bernardi
2010. Sympatric speciation in a genus of marine fishes. Mol. Ecol. 19:2089–2105.

Earl, D. A., and B. M. vonHoldt.
2012. STRUCTURE HARVESTER: a website and program for visualizing STRUCTURE output and implementing the Evanno method. Conserv. Genet. Res. 4:359–361.

Eigenmann, C. H., and C. H. Beeson.
1893. Preliminary note on the relationship of the species usually united under the generic name *Sebastodes*. Am. Nat. 27:668–671. [Available at website.]

Eschmeyer, W. N., E. S. Herald, and H. Hammann.
1983. A field guide to Pacific Coast fishes of North America, 336 p. Houghton Mifflin Co., Boston, MA.

Falush, D., M. Stephens, and J. K. Pritchard.
2003. Inference of population structure using multilocus genotype data: linked loci and correlated allele frequencies. Genetics 164:1567–1587.

Gharrett, A. J., A. P. Matala, E. L. Peterson, A. K. Gray, Z. Li, and J. Heifetz.
2005. Two genetically distinct forms of Rougheye rockfish (*Sebastes aleutianus*) are different species. Trans. Am. Fish. Soc. 134:242–260.

Girard, C. F.
1856. Contributions to the ichthyology of the western coast of the United States, from specimens in the museum of the Smithsonian Institution. Proc. Acad. Nat. Sci. Phila. 8:131–137.

Gomez-Uchida, D., E. A. Hoffman, W. R. Ardren, and M. A. Banks.
2003. Microsatellite markers for the heavily exploited canary (*Sebastes pinniger*) and other rockfish species. Mol. Ecol. Notes 3:387–389.

Goode, G. B.
1884. The fisheries and fishery industries of the United States. Section I: natural history of useful aquatic animals, 895 p. Government Printing Office, Washington, D.C.

Hammer, Ø., D. A. T. Harper, and P. D. Ryan.
2001. PAST: paleontological statistics software package for education and data analysis. Palaeontologia Electronica 4(1):1–9. [Available at website.]

Hart, J. L.
1973. Pacific fishes of Canada. Fish. Res. Board Can. Bull. 180, 740 p.

Helvey, M.
1982. First observations of courtship behavior in rockfish, genus *Sebastes*. Copeia 1982:763–770.

Hyde, J. R., and R. D. Vetter.
2007. The origin, evolution, and diversification of rockfishes of the genus *Sebastes* (Cuvier). Mol. Phylogen. Evol. 44:790–811.

Hyde, J. R., C. A. Kimbrell, J. E. Budrick, E. A. Lynn, and R. D. Vetter.
2008. Cryptic speciation in the vermilion rockfish (*Sebastes miniatus*) and the role of bathymetry in the speciation process. Mol. Ecol. 17:1122–1136.

Jordan, D. S., and B. W. Evermann.
1898. The fishes of North and Middle America: a descriptive catalogue of the species of fish-like vertebrates found in the waters of North America, north of the Isthmus of Panama, part II. Bull. U.S. Natl. Mus. 47:1241–2183.
1900. The fishes of North and Middle America: a descriptive catalogue of the species of fish-like verte-

brates found in the waters of North America, north of the Isthmus of Panama, part IV. Bull. U.S. Natl. Mus. 47:3137–3313 +pls.1–392.

Jordan, D. S., B. W. Evermann, and H. W. Clark.
1930. Check list of the fishes and fishlike vertebrates of North and Middle America north of the northern boundary of Venezuela and Colombia. Rep. U.S. Comm. Fish. 1928, part II, 670 p.

Jordan, D. S., and C. H. Gilbert.
1880a. Description of a new species of *Sebastichthys* (*Sebastichthys miniatus*) from Monterey Bay, California. Proc. U.S. Natl. Mus. 3:70–73.
1880b. Description of seven new species of sebastoid fishes, from the coast of California. Proc. U.S. Natl. Mus. 3:287–298.
1881. Description of *Sebastichthys mystinus*. Proc. U.S. Natl. Mus. 4:70–72.
1882. Synopsis of the fishes of North America. Bull. U.S. Natl. Mus. 16:1–1018.

Jordan, D. S. and J. Z. Gilbert.
1919. Fossil fishes of the Miocene (Monterey) formations of Southern California. *In* Fossil fishes of Southern California, p. 13–60. Stanford Univ. Press, Stanford, CA.
1920. Fossil fishes of diatom beds of Lompoc, California, 45 p. + 39 pls. Stanford Univ. Press, Stanford, CA.

Jordan, D. S. and P. L. Jouy.
1881. Check-list of duplicates of fishes from the Pacific coast of North America, distributed by the Smithsonian Institution in behalf of the United States National Museum, 1881. Proc. U.S. Natl. Mus. 4:1–18.

Kramer, D. E., and V. O'Connell.
1995. Guide to northeast Pacific rockfishes genera *Sebastes* and *Sebastolobus*, 2nd rev. Alaska Sea Grant, Mar. Adv. Bull. 25, 78 p.

Laidig, T. E., D. E. Pearson, and L. L. Sinclair.
2003. Age and growth of blue rockfish (*Sebastes mystinus*) from central and northern California. Fish. Bull. 101:800–808.

Lenarz, W. H., and T. Wyllie Echeverria.
1991. Sexual dimorphism in *Sebastes*. *In* Rockfishes of the genus *Sebastes*: their reproduction and early life history (G. W. Boehlert and J. Yamada), p. 71–80. Springer Science+Business Media, Dordrecht, Netherlands.

Love, M. S.
2011. Certainly more than you wanted to know about the fishes of the Pacific coast, a postmodern experience, 650 p. Really Big Press, Santa Barbara, CA.

Love, M. S., M. Yoklavich, and L. Thorsteinson.
2002. The rockfishes of the northeast Pacific, 405 p. Univ. Calif. Press, Los Angeles, CA.

Matsubara, K.
1934. Studies on the scorpaenoid fishes of Japan. I. Descriptions of one new genus and five new species. J. Imp. Fish Inst. Tokyo 30:199–210.

Mecklenburg, C. W., T. A. Mecklenburg, and L. K. Thornsteinson.
2002. Fishes of Alaska, 1116 p. Am. Fish. Soc., Bethesda, MD.

Miller, J. A., M. A. Banks, D. Gomez-Uchida, and A. L. Shanks.
2005. A comparison of population structure in black rockfish (*Sebastes melanops*) as determined with otolith microchemistry and microsatellite DNA. Can. J. Fish. Aquat. Sci. 62:2189–2198.

Narum, S. R., V. P. Buonaccorsi, C. A. Kimbrell, and R. D. Vetter.
2004. Genetic divergence between gopher rockfish (*Sebastes carnatus*) and black and yellow rockfish (*Sebastes chrysomelas*). Copeia 2004:926–931. [Available at website.]

Orr, J. W., and J. E. Blackburn.
2004. The dusky rockfishes (Teleostei: Scorpaeniformes) of the North Pacific Ocean: resurrection of *Sebastes variabilis* (Pallas, 1814) and a redescription of *Sebastes ciliatus* (Tilesius, 1813). Fish. Bull. 102:328–348.

Orr, J. W., M. A. Brown, and D. C. Baker.
2000. Guide to rockfishes (Scorpaenidae) of the genera *Sebastes, Sebastolobus*, and *Adelosebastes* of the Northeast Pacific Ocean, 2nd ed. NOAA Tech. Memo. NMFS-SWFC-117, 47 p. [Available at website.]

Orr, J. W., and S. Hawkins.
2008. Species of the rougheye rockfish complex: Resurrection of *Sebastes melanostictus* (Matsubara, 1934) and a redescription of *Sebastes aleutianus* (Jordan and Evermann, 1898) (Teleostei: Scorpaeniformes). Fish. Bull. 106:111–134.

Pallas, P. S.
1814. Zoographia Rosso-Asiatica, sistens omnium animalium in extenso Imperio Rossico et adjacentibus maribus observatorum recensionem, domicilia, mores et descriptiones anatomen atque icones plurimorum, vol. 3, 428 p. Acad. Sci. Imp., St. Petersburg, Russia.

Phillips, J. B.
1957. A review of the rockfishes of California (Family Scorpaenidae). Calif. Dep. Fish Game, Fish. Bull. 104, 158 p.

Pritchard, J. K., M. Stephens, and P. Donnelly.
2000. Inference of population structure using multilocus genotype data. Genetics 155:945–959.

R Core Team.
2013. R: a language and environment for statistical computing. R Foundation for Statistical Computing, Vienna, Austria. [Available at website, accessed May 2013.]

Roques, S., D. Pallotta, J.-M. Sévigny, and L. Bernatchez.
1999. Isolation and characterization of polymorphic microsatellite markers in the North Atlantic redfish (Teleostei: Scorpaenidae, genus *Sebastes*). Mol. Ecol. 8:685–687.

Sabaj Pérez, M. H (ed.).
2013. Standard symbolic codes for institutional resource collections in herpetology and ichthyology: an online reference, version 4.0. [Available at website, accessed June 2013].

Schuelke, M.
2000. An economic method for the use of fluorescent labeling of PCR fragments. Nat. Biotechnol. 18: 233–234.

Tilesius, W. G. von.
1813. Iconum et descriptionum piscium Camtschaticorum continuatio tertia tentamen monographiae generis Agoni blochiani sistens. Mem. Acad. Imp. Sci. St. Petersbg. 4:406–478.

VenTresca, D. A., R. H. Parrish, J. L. Houk, M. L. Gingras, S. D. Short, and N. L. Crane.
1995. El Niño effects on the somatic and reproductive condition of blue rockfish, *Sebastes mystinus*. CalCOFI Rep. 36: p. 167–174.

Warton, D. I., R. A. Duursma, D. S. Falster, and S. Taskinen.
2012. smatr 3—an R package for estimation and inference about allometric lines. Methods Ecol. Evol. 3:257–259.

Westerman, M. E., V. P. Buonaccorsi, J. A. Stannard, L. Galver, C. Taylor, E. A. Lynn, C. A. Kimbrell, and R. D. Vetter.
2005. Cloning and characterization of novel microsatellite DNA markers for the grass rockfish, *Sebastes rastrelliger*, and cross-species amplification in 10 related *Sebastes* spp. Mol. Ecol. Notes 5:74–76.

Whiteaves, J. F.
1887. On some marine Invertebrata dredged or otherwise collected by Dr. G.M. Dawson, in 1885, on the coast of British Columbia; with a supplementary list of a few land and fresh water shells, fishes, birds, etc., from the same region, 137 p. Dawson Brothers Publishers, Montreal, Canada.

Wickham, H.
2009. ggplot2: elegant graphics for data analysis, 213 p. Springer, New York.

Wyllie Echeverria, T.
1986. Sexual dimorphism in four species of the rockfish genus *Sebastes* (Scorpaenidae). Environ. Biol. Fish. 15:181–190.
1987. Thirty-four species of California rockfishes: maturity and seasonality of reproduction. Fish. Bull. 85:229–250.

Yoshida, K., M. Nakagawa, and S. Wada.
2005. Multiplex PCR system applied for analysing microsatellite loci of Schlegel's black rockfish, *Sebastes schlegeli*. Mol. Ecol. Notes 5:416–418.

NOAA
National Marine
Fisheries Service

Fishery Bulletin
established 1881

Spencer F. Baird
First U.S. Commissioner
of Fisheries and founder
of *Fishery Bulletin*

Factors driving the density of derelict crab pots and their associated bycatch in North Carolina waters

Christine M. Voss[1]
Joan A. Browder[2]
Andrew Wood[3]
Adriane Michaelis[3]

Email address for contact author: c.m.voss.unc@gmail.com

[1] Institute of Marine Sciences
University of North Carolina
3431 Arendell Street
Morehead City, North Carolina 28557

[2] Southeast Fisheries Science Center
National Marine Fisheries Service, NOAA
75 Virginia Beach Drive
Miami, Florida 33149

[3] Audubon North Carolina
7741 Market Street
Unit D
Wilmington, North Carolina 28411

Abstract—Lost or derelict fishing gear can impair fisheries by contributing to the depletion of target species populations and can reduce nontarget fish and wildlife populations. We measured the density of derelict crab pot (DCPs) using side-scan sonar and examined bycatch associated with DCPs in nearshore waters (depths ≤4 m) of 6 waterbodies important to the North Carolina blue crab fishery, the state's most valued commercial fishery. Extrapolated mean DCP density was 105 DCP/km^2 of open water (range: 6–301). Densities of DCPs differed significantly among waterbodies but not among habitats (marsh creeks, estuarine edge ≤50 m from shore, and Atlantic Intracoastal Waterway margin). Extrapolated DCP densities were generally greater than those concurrently observed for actively fished crab pots within the 201 1-km^2 cells sampled during 23 survey days between April and November 2010. Of the DCPs examined, 41% contained bycatch (unintentional catch) and 37% remained capable of trapping organisms. Bycatch was dominated by blue crab (*Callinectes sapidus*) and Florida stone crab (*Menippe mercenaria*) and included 5 diamondback terrapin (*Malaclemys terrapin*) and 1 clapper rail (*Rallus crepitans*). Based on monitoring of four 1-km^2 cells, annual DCP "recruitment" was 1.5 DCP/km^2 (1 SD). Reducing recruitment, persistence, and entrapment capability of DCPs would benefit the blue crab and Florida stone crab fisheries, as well as help conserve at-risk wildlife populations.

Manuscript submitted 21 January 2014.
Manuscript accepted 2 July 2015.
Fish. Bull.: 113:378–390 (2015).
Online publication date: 21 July 2015.
doi: 10.7755/FB.113.4.2

More than 1 million commercial crab pots are used annually in North Carolina, and an annual loss rate of 17% has been estimated by the North Carolina Division of Marine Fisheries (NCDMF[1]). Estimated annual rates of crab pot losses were 30% in the lower York River, Virginia, for commercial and recreational pots combined (Havens et al., 2008) and 25% in the Gulf of Mexico for commercial pots only (Guillory et al.[2]). Because pots that are lost or abandoned can continue to capture crabs, terrapins, fishes, and other wildlife for years, derelict crab pots (DCPs) pose a serious conservation problem in the coastal wetlands and shallow estuarine waters of North Carolina and elsewhere along the coasts of the U.S. Atlantic and Gulf of Mexico. North Carolina in recent years has ranked third or fourth among all states in annual commercial landings of hard-shell blue crab (NMFS, 2007–2014). The industry for hard-shelled blue crab (*Callinectes sapidus*) alone is the most highly valued commercial fishery in North Carolina (Burgess and Bianchi[3]). Landings and value of

[1] NCDMF (North Carolina Division of Marine Fisheries). 2008. Assess the effects of hurricanes on North Carolina's blue crab resource, 178 p. [Available from NCDMF, North Carolina Dep. Environ. Nat. Resour., 3441 Arendell St., Morehead City, NC 28557.]

[2] Guillory, V., A. McMillen-Jackson, L. Hartman, H. Perry, T. Floyd, T. Wagner, and G. Graham. 2001. Blue crab derelict traps and trap removal programs. Gulf States Mar. Fish. Comm. Publ. 88, 13 p. [Available at website.]

[3] Burgess, C. C., and A. J. Bianchi. 2004. An economic profile analysis of the commercial fishing industry of North Carolina including profiles for state-managed species, 123 p. Div. Mar. Fish., North Carolina Dep. Environ. Nat. Resour., Morehead City, NC. [Available at website.]

peeler crab and soft-shell crab add to the value and are reported separately. In addition, a substantial recreational blue crab fishery exists in North Carolina. Crab pots are the principal fishing gear for all the hard-shell crab fisheries in North Carolina.

The unharvested "take" of blue crab and other fishery species in DCPs represents substantial mortality (Guillory, 1993; Guillory[4]) and is a drain on fishery catches and incomes. Substantial unintended incidental take, or bycatch, of wildlife also occurs in pots meant to capture blue crab (Havens et al., 2008; Morris et al., 2011). We extend the definition of *bycatch* to include blue crab and Florida stone crab (*Menippe mercenaria*), both live and dead, found in DCPs because the DCP catch is rendered unavailable to the fishery.

In a NCDMF[1] study during 2002–2005, the capture, mortality, and escapement rates of blue crab in DCPs in 4 regions (Alligator River, Pamlico River, Bogue Sound, and Middle Sound) of coastal North Carolina were estimated at an average yearly catch of 40.4 individuals/DCP for legally marketable blue crab. In that study, the overall mortality for blue crab in DCPs was 45%, and the estimated annual escapement of blue crab from DCPs was 55%; estimated annual finfish mortality was 2.5 individuals/DCP. In Virginia, Havens et al. (2008) estimated that about 50 marketable blue crab are killed per DCP each year. Other fishery and non-fishery species have been found either in or entangled by DCPs (Havens et al., 2011; NCDMF[1]; Guillory et al.[2]). Both actively fished crab pots (AFCPs) and DCPs pose a significant threat of drowning to diamondback terrapin (*Malaclemys terrapin*), a coastal species of concern in the states of Connecticut, Delaware, Maryland, Massachusetts, New Jersey, New York, North Carolina, Rhode Island, and Virginia (Roosenburg et al., 1997; Grosse et al., 2009). Organisms that die in a DCP can attract additional organisms that can become bycatch until that DCP is no longer capable of retaining organisms (degrades) or is removed.

The demographics of DCPs are not yet known for North Carolina. One might assume that DCP abundance is related to the number of AFCPs used in each waterbody. Likewise, the number of years that DCPs continue to trap animals is unknown. Shively[5] found that, depending upon salinity, the functional life expectancy of vinyl-coated pots was 2 years or more in Texas. The research of Havens et al. (2008) in Virginia indicates that lost crab pots trapped animals for more than 1 year in higher-salinity areas (annual mean salinity=20) and probably longer in lower-salinity areas (annual mean salinity=6), where pots were slower to degrade. The rate at which pots become incapacitated can be affected by their rate of decomposition, bioerosion, and engulfment through encrustation by sessile organisms. These processes are likely to differ with habitat because of variation in salinity, dissolved oxygen, temperature, and other factors.

The type of habitat where DCPs are most likely to occur is poorly understood. Storms and currents often redistribute DCPs (Bishop, 1983), not necessarily to places where crabbing has taken place. In North Carolina, Avissar (2006) found that crabbers relocated their crab pots shoreward into shallow-water areas and tidal marsh creeks to avoid damage to the pots from sea turtles attempting to remove the bait, and Grant[6] noted that capture rates of diamondback terrapin decreased with distance from shore. In Maryland, Roosenburg et al. (1999) noted that juvenile and male diamondback terrapin were more frequently observed in nearshore shallow areas, where they are more likely to interact with DCPs. Information about DCP density, transport, deposition, and longevity is needed if the limited resources available for DCP removal efforts are to be used more effectively.

The objectives of this study were to quantify the density, distribution, and bycatch of DCPs in 6 selected waterbodies on the central and southern coast of North Carolina, from Core Sound south to Cape Fear River, within 3 habitat types typically fished by crabbers that use hard-shell crab pots, marsh creek, margin of the Atlantic Intracoastal Waterway (ICW), and estuarine edge (within 50 m of shoreline). We test whether the density of DCPs differs among these waterbodies and the habitats.

Materials and methods

Study area and mapping procedure for stratified random sampling

The geographical range of this study spanned from Core Sound south to Cape Fear River, an area that includes 14 of 29 North Carolina inshore waterbodies. The 6 waterbodies that we sampled accounted for, on average, 74% of fishery landings of hard-shell crab in crab pots and 61% of fishing trips for hard-shell crab during which crab pots were used in the area from Core Sound south to the South Carolina border (NCDMF[7]) from 2006 to 2008. The sampled waterbodies, listed from north to south, were Core Sound, Newport River, Bogue Sound, Topsail Sound, Masonboro Sound, and the lower 16 km of the Cape Fear River (Fig. 1).

[4] Guillory, V. 2001. A review of incidental fishing mortalities of blue crabs. *In* Proceedings: blue crab mortality symposium. Gulf States Mar. Fish. Comm. Publ. 90; Lafayette, LA, 28–29 May 1999 (V. Guillory, H. Perry, and S. Vanderkooy (eds.), p. 28–41. [Available at website.]

[5] Shively, J. D. 1997. Degradability of natural materials used to attach escapement panels to blue crab traps in Texas, 18 p. [Available from Natl. Mar. Fish. Serv., Southeast Reg., 9721 Executive Center Dr., North, St. Petersburg, FL 22702.]

[6] Grant, G. S. 1997. Impact of crab pot excluder devices on diamondback terrapin mortality in commercial crab catch, 9 p. Unpubl. report. Univ. North Carolina at Wilmington, Wilmington, NC.

[7] NCDMF (North Carolina Division of Marine Fisheries). 2009. Unpubl. data. [Hard crabs and other species reported in crab pot landings in 2006–2009.] NCDMF, Morehead City, NC 28557.

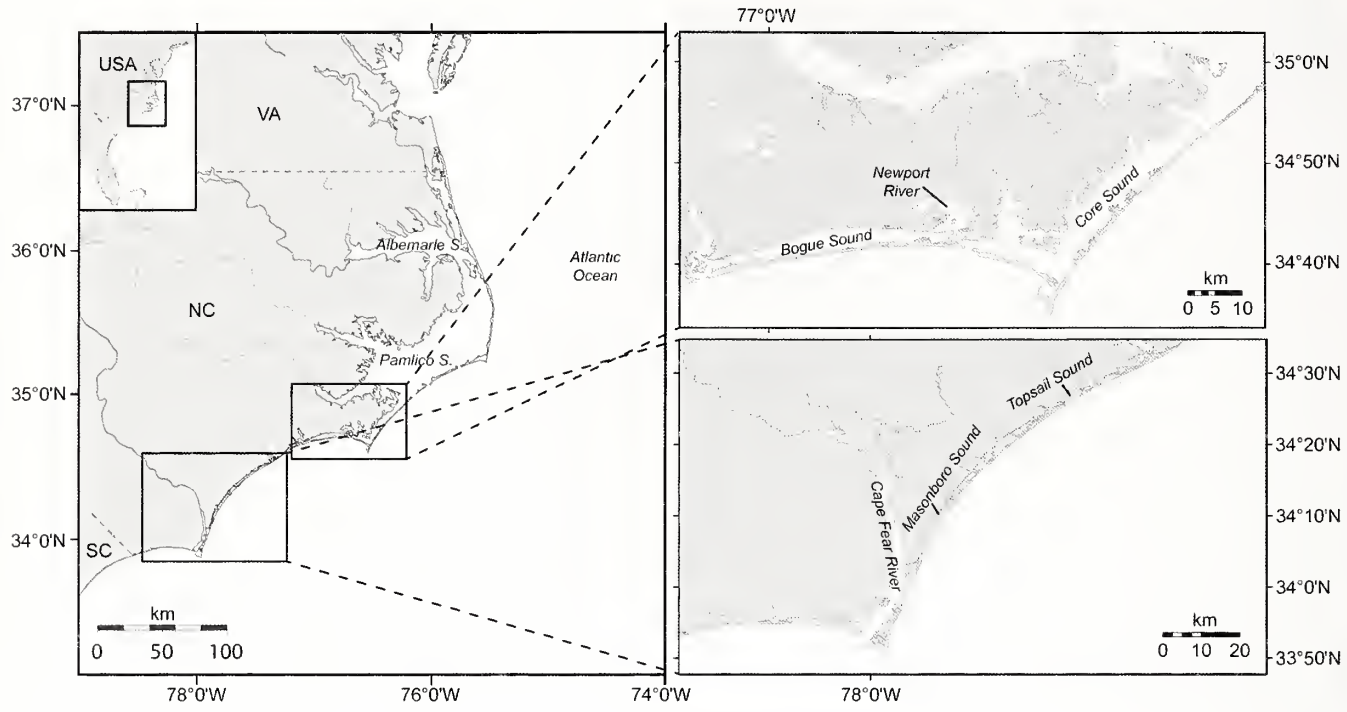

Figure 1

The locations of waterbodies sampled for assessing density of bycatch in derelict crab pots in North Carolina from April to November 2010: Bogue and Core sounds and Newport River (within the Central District of the North Carolina Division of Marine Fisheries) and Masonboro and Topsail sounds and Cape Fear River (within the Southern District).

We distinguished and sampled 3 habitat types in each waterbody: 1) marsh creeks; 2) estuarine edges (areas of open water within 50 m of the shoreline); and 3) areas adjacent to the ICW. Because one goal was to examine the interactions of diamondback terrapin with DCPs, we limited our surveys to nearshore waters with depths ≤4 m, where diamondback terrapins and DCPs were most likely to co-occur. Given Avissar's (2006) observation that most blue crab fishermen now locate their pots near to shore to avoid sea turtle interference, our focus on the nearshore habitat probably provides good coverage of the area of activity for crab pot fishing.

With ArcMap,[8] vers. 9.3.1 (Esri, Redlands, CA), we used readily available maps and shapefiles to classify areas as adjacent to the ICW or as estuarine edge; however, we had to create by hand a unique shapefile for marsh creek areas in each waterbody, digitizing these creeks with Google Earth software. A grid of 1-km^2 cells was placed over the habitat-classified map, and then each cell in our entire study area was assigned to one or more habitat types. The 1-km^2 grid was placed over our study area in the habitat-classified map with Google Earth software, which allowed us to eliminate inappropriate cells (i.e., estuarine edge cells with insufficient water surface area, and marsh creek cells where the entire natural shoreline was hardened) from the pool of possible cells. Approximately 20% open water was considered sufficient water surface area in most cases; very few marsh creek cells were as low as 10% open water. All sufficient cells had much more than the 24,000-m^2 area of water that we sampled within each cell. In addition, we eliminated cells known to be in an area included in the NCDMF program for removing and disposing of lost and abandoned crab pots.

A stratified random sampling design was used to select the cells to be sampled. A total of 1088 cells formed our sampling pool. Each cell was designated by habitat type within each waterbody, with the possibility that a given cell could represent more than one habitat type. Using ArcMap, we delineated the 1-km^2 cells, determined the latitude and longitude of cell centroids, and calculated the area of open water for each cell. We determined that our resources allowed us to survey approximately 200 cells overall, a count that could include some of the same cells twice (as separate samples because they represented 2 different habitat types). The number of cells to be sampled in each waterbody was determined by a weighting method for both the relative numbers of fishing trips with hard-shell crab pots (averaging NCDMF[7] data for 2006–2008) and the

[8] Mention of trade names or commercial companies is for identification purposes only and does not imply endorsement by the National Marine Fisheries Service, NOAA.

Table 1

Distribution of sampling effort and raw abundance of derelict crab pots (DCPs) and actively fished crab pots (AFCPs) found within cells (each 1 km^2) sampled in 2010 during a survey of marsh creek, estuarine edge, and adjacent Atlantic Intracoastal Waterway (ICW) habitats in Bogue, Core, Masonboro, and Topsail sounds and Cape Fear and Newport rivers in North Carolina. Abundance of DCPs is the number observed in the 24,000-m^2 areas surveyed in sampled cells, and abundance of AFCPs is the number observed in the entirety of the 1-km^2 cells. Note that the ICW does not traverse Core Sound and was not sampled in Cape Fear River because depths were >4 m.

	Number of cells sampled			Total	DCP abundance				AFCP abundance			
Waterbody	Marsh creek	Estuarine edge	Adjacent ICW	cells sampled	Marsh creek	Estuarine edge	Adjacent ICW	Total DCPs	Marsh creek	Estuarine edge	Adjacent ICW	Total AFCPs
Bogue Sound	8	8	8	24	8	1	1	10	58	106	94	258
Cape Fear River	30	30	–	60	14	13	–	27	48	51	–	99
Core Sound	30	30	–	60	9	8	–	17	369	219	–	588
Masonboro Sound	9	9	9	27	20	19	4	43	20	53	55	128
Newport River	5	5	5	15	0	1	0	1	43	24	20	87
Topsail Sound	5	5	5	15	1	3	4	8	19	14	18	51
Totals	87	87	27	201	52	45	9	106	557	467	187	1211

relative combined area of marsh creek, estuarine edge, and ICW-margin habitats within each waterbody.

For each waterbody, we multiplied the proportion of total trips by the proportion of total area of the 3 habitat types combined. Sampling effort, or the number of cells to be sampled, was then allocated to waterbodies in proportion to the product of the 2 proportions. Each of 1088 cells was categorized by waterbody and habitat type and a random number generator was used to rank the priority of the cells for sampling. We determined that a 201-cell sampling design allowed us to balance effort among habitat types within waterbodies. To distribute the 201 1-km^2 cells to be sampled across the 6 waterbodies, the number of cells assigned to each waterbody were divided equally among the 3 habitat types (Table 1), with the exceptions of the 2 waterbodies that lacked appropriate ICW habitat: Core Sound, which the ICW does not traverse, and the lower Cape Fear River, where the ICW is a major shipping channel with all depths >4 m. In those 2 waterbodies, the number of cells to be sampled was divided evenly between the habitat types of marsh creek and estuarine edge (Table 1).

Field sampling

Sampling was conducted within 99 cells over 11 field days, between 28 April and 3 June 2010 in the Core Sound, Newport River, and Bogue Sound (within the Central District of the NCDMF) and within 102 cells over 12 field days, between 10 May and 10 August and on 11 November 2010 in Topsail Sound, Masonboro Sound, and Cape Fear River (within the Southern District of the NCDMF) (Fig. 1). Of the 201 cells sampled, 23 cells that were randomly selected to represent 2 different habitat types were sampled twice, accounting for 46 of the 201 samples. A team from the University of North Carolina at Chapel Hill Institute of Marine Sciences conducted surveys in the Central District, and a team from Audubon North Carolina conducted surveys in the Southern District. Two scientists, one from each sampling team, met to discuss details of sampling protocols, and subsequently practiced and standardized techniques during a day on the water dedicated to standardize methods before sampling was conducted.

The latitude and longitude of each target cell's centroid were used to locate cells in the field with a handheld GPS (GPSMAP 76Cx or 60CSx, Garmin International, Inc., Olathe, KS). GPS also was used to determine the cell boundaries in relation to each centroid. This method of field demarcation enabled the definition of each 1-km^2 cell, within which both DCPs and AFCPs were counted. DCPs, which lacked surface buoys, were detected with the use of side-scan sonar, and AFCPs, which had one floating buoy per pot, were detected visually.

Within each sampled 1-km^2 cell, 4 separate transects (30 m wide by 200 m long) were haphazardly chosen and surveyed by boat with no overlap of sampling area (for a total sampled area of 24,000 m^2) to detect DCPs with Humminbird 1197c high definition side imaging sonar (Johnson Outdoors Marine Electronics, Inc., Racine, WI), combined with a GPS. Transect distances were verified by both one of the handheld GPSMAPs and the Humminbird sonar. Each team surveyed transects in either a linear or a curved pattern that was tailored to the shape of estuarine contours within a given cell. In some cases, shallow water allowed DCPs to be located visually. During the same survey, all AFCPs, with their required float visible on the water's surface, were counted visually, within each 1-km^2 cell that was demarcated by using both the handheld and Humminbird GPSs.

Figure 2

Photograph of derelict crab pots retrieved from Bogue Sound and the Newport River, North Carolina, in May 2010: (left) a pot in poor condition (rank of 9), with a partial wall collapse that allowed unrestricted movement of organisms, and (right) a pot in fair condition (rank of 5), well fouled yet structurally intact and capable of trapping organisms.

Crab pots were distinguished from other benthic objects and debris in images from the side-scan sonar on the basis of their square shape, dimensions, and acoustic shadow distal to the nadir (Havens et al., 2008; Morison and Murphy, 2009). The crab pots typically used in both the commercial and recreational hard-shell blue crab fishery are 60 cm in length, 60 cm in width, and 50 cm in height, and they are constructed of vinyl-coated wire, with a center chamber in which bait is secured (Fig. 2). Metal rebar is often wired to a pot's bottom surface to ensure that it is properly oriented as it settles upon the estuarine floor after deployment. When a DCP was discovered, the time and GPS coordinates were recorded. A 30-m waterman's rope (a rope to which bent nails are attached in increments of 30 cm) or a grapple was used to retrieve DCPs and haul them aboard the boat for inspection and to record bycatch metrics; in some cases, pots were in such poor condition that they were ripped apart upon haul-out and only pot parts were recovered.

Data on DCP construction (wire type and pot design) and condition (functionality ranking, from 1 to 10, with 1 for structurally sound and 10 for totally dilapidated; Table 2), an estimate of each DCP's time in water (soak time), and the identification and percent cover of fouling organisms on each DCP were recorded. Estimates of DCP soak times were determined by the same researcher in each region who had participated in the technique-standardization trip, on the basis of the degree of fouling and bivalve recruitment that had accumulated on pots. Although soak time was a subjective measure, each of the researchers who estimated soak times had >40 years of experience working in estuaries to guide their estimates. These estimates were consistent with the descriptions and images of crab pots after known soak times in North Carolina high-salinity (annual mean salinity=30) estuaries that were provided in the NCDMF[1] report. In general, DCPs that received a condition score of ≤4 had estimated soak times of ≤1 year, and pots that had a condition rank ≥9 had estimated soak times of ≥2 years.

Environmental data (temperature, salinity, and dissolved oxygen) for each cell were recorded with a YSI ProPlus water quality meter (YSI, Inc., Yellow Springs, OH), and, for each DCP found in a cell, its distance from shore was recorded. Aquatic organisms found in bycatch or living on recovered DCPs were identified (according to Gosner, 1971, Robins et al., 1986; Ruppert and Fox, 1988; FishBase, vers. 2/2010, available at website) to the lowest possible taxonomic level, classified as living or dead, counted, measured, and released. The total length of fishes and the carapace width (CW), point to point (distance between posterior lateral spines of the carapace) of crabs were used as standard measures of organism size. For blue crab, adults were distinguished from juveniles by having a CW ≥5.6 cm CW, the smallest size considered mature for a female crab with a full apron (NCDMF[9]); legal market size for this species in North Carolina is ≥12.5 cm CW for males and ≥17 cm CW for females (NCDMF[9]). For Florida stone crab, adults were distinguished from juveniles by having a CW ≥3.0 cm; coloration patterns did not differ with age (Lindberg and Marshall[10]).

[9] NCDMF (North Carolina Division of Marine Fisheries). 2004. North Carolina Fishery Management Plan: Blue Crab, 133 p. +app. Div. Mar. Fish., North Carolina Dep. Environ. Nat. Resour., Morehead City, NC. [Available at website.]

[10] Lindberg, W. J., and M. J. Marshall. 1984. Species profiles: life histories and environmental requirements of coastal fishes and invertebrates (south Florida) stone crab. U.S. Fish Wildl. Serv. FWS/OBS-82/11.21 and U.S. Army Corps Eng. TR EL-82-4, 17 p. [Available at website.]

Table 2

Condition of derelict crab pots was ranked on a scale of 1–10. This table provides the descriptors used to rank the condition of pots.

Condition rank	Descriptors
1	Structural integrity of pot sound; some rust or discoloration may be seen
2	Pot retains original shape but shows wear and abrasion
3	Pot structure intact, with obvious flaws in wall or floor
4	Pot likely misshapen; walls or floor beginning to degrade
5	Observable decay of structure, with pits in walls or floor
6	Small voids in walls or floor
7	Walls or floor are clearly deteriorated; partial collapse likely
8	Holes ≥10 cm in walls or floor
9	Structural integrity of pot has failed; walls or floor well decayed
10	Total dilapidation; parts of walls or floor well disintegrated

Bivalve size was measured by the perpendicular axes of height, from umbo to distal tip, and length, the longest axis from anterior to posterior ends. All size measurements were recorded to the closest 1 mm. After all data were collected and all animals were released from a pot, it was flattened and taken for proper disposal.

To estimate the recruitment rate of DCPs in areas where crabbing commonly occurs in North Carolina, we carefully removed all DCPs from four 1-km^2 cells, one cell each in Bogue Sound (near Archer's Creek) and in the eastern area of Newport River in the Central District and in Topsail Sound (behind Figure Eight Island), and Masonboro Sound (behind Masonboro Island) in the Southern District in spring 2010. These 4 cells were intensively resurveyed for newly recruited DCPs after 1 year (52 and 51 weeks later in the Central and Southern Districts, respectively). We worked with the North Carolina Marine Patrol of the NCDMF to ensure that the 4 areas used for this study component were >5 km from state waters included in the NCDMF program for removing and disposing of lost and abandoned crab pots (Anthony and Knudsen[11]).

Data analyses

Data on DCPs, AFCPs, coordinates for surveyed transect area, and DCP bycatch and attached organisms for all 6 waterbodies were combined. SYSTAT, vers. 13.00.05 (Systat Software, Inc., San Jose, CA) and JMP, vers. 8.0 (SAS Institute, Inc., Cary, NC) software packages were used for statistical analyses. Because the area of some sampled 1-km^2 cells included land, we used a conversion factor to standardize the data to the proportion of open water in each cell as computed by ArcMap. Here, the number of DCPs found in each 24,000-m^2 area or ACFPs in a 1-km^2 cell was multiplied by the proportion-open-water conversion factor, with DCPs also multiplied by 41.667, to calculate the density of DCPs and AFCPs as the number of pots per square kilometer of open water. Density values for both DCPs (λ: −0.6) and AFCPs (λ: −0.2) were Box-Cox transformed to preclude significant departure from homogeneity of variance as confirmed afterward by either O'Brien's or Bartlett's tests (α=0.05).

Two-way analyses of variance (ANOVAs) were conducted on data to test whether waterbody or habitat type were significant factors explaining differences in DCP and AFCP density and to test whether interactions between habitat type and waterbody existed. Tukey's honestly significant difference tests were conducted post hoc to examine differences in DCP and AFCP densities among the waterbodies and habitats we sampled. Because of the lack of a linear relationship between DCPs and AFCPs, analysis of covariance was unwarranted. Two-way ANOVAs were used to compare bycatch abundance of blue and Florida stone crabs by waterbody and habitat type, as well as to determine whether an interaction between factors existed. The bycatch abundance data for both blue and Florida stone crabs were Box-Cox transformed to meet normality criteria before ANOVAs. To investigate the effects of including cells that represented more than one habitat type, results from 2-way ANOVAs that included all (n=201) cells were compared with 2-way ANOVAs that excluded the cells that served for 2 habitat types (n=155). In cases where the arithmetic mean is given, the standard deviation (SD) is also presented in parentheses.

Results

Density of crab pots

The 201 cells within the selected 6 waterbodies in North Carolina were scanned with a side-scan sonar and 106 DCPs were detected (Table 1). By extrapolat-

[11]Anthony, S., and H. Knudsen. 2010. Personal commun. Marine Patrol, Div. Mar. Fish., North Carolina Dep. Environ. Nat. Resour., Morehead City, NC 28557.

ing the values of DCP abundance found in the 24,000-m^2 areas surveyed within cells to estimate the number of DCPs in each square kilometer of open water, we computed a mean of 105 DCP/km^2 in open water in the 6 waterbodies that produced 61–74% of the commercial hard-shell crab catch in 2006–2008 in North Carolina from Core Sound south to the South Carolina border. Extrapolated DCP densities in open water for each waterbody ranged from 6 DCP/km^2 in the Newport River to 301 DCP/km^2 in Topsail Sound (Fig. 3). Two-way ANOVA revealed that estimates of DCP densities differed significantly by waterbody ($F_{(3)}$=4.18, P=0.007) but not by habitat type ($F_{(1)}$=0.043, P=0.84), and revealed no interaction between these factors ($F_{(8)}$=0.448, P=0.89) (Fig. 3). Likewise, we did not detect differences in DCP density ($P \geq 0.37$) by habitat type when analyzed within each waterbody.

During our sampling of the 201 1-km^2 cells over 23 survey days from April to November 2010, 1211 AFCPs were observed concurrently with DCPs (Table 1), yielding a mean AFCP density of 19 AFCP/km^2 in open water. The densities of AFCPs in open water ranged from 8 AFCP/km^2 in Cape Fear River to 32 AFCP/km^2 in Bogue Sound (Fig. 3). Using 2-way ANOVA, we did not detect differences in the densities of AFCPs by waterbody ($F_{(3)}$=0.232, P=0.87) or by habitat type ($F_{(1)}$=0.627, P=0.26), and any interaction between these factors ($F_{(8)}$=0.66, P=0.73) (Fig. 3). As with the DCPs, the density of AFCPs did not differ significantly ($P \geq 0.29$) by habitat type when analyzed within each waterbody.

Of the 201 cells sampled, 23 cells represented 2 different habitat types (accounting for 46 of 201 samples because they were sampled twice) and 155 cells represented only 1 habitat type. A 2-way ANOVA of the 155 cells that represented only 1 habitat type yielded results similar to those of the analyses that included all 201 cells. For the subset of 155 cells, DCP densities differed significantly by waterbody ($F_{(3)}$=3.56, P=0.012) but not by habitat type ($F_{(1)}$=0.18, P=0.89), and there was no interaction between these factors ($F_{(8)}$=1.06, P=0.39). In contrast, for this subset of cells, we detected no differences in ACFP densities by waterbody ($F_{(3)}$=0.50, P=0.66) or by habitat type, ($F_{(1)}$=0.77, P=0.38) and no interaction ($F_{(8)}$=0.72, P=0.67) between these factors. Additionally, we detected no differences in DCP density or AFCP density among habitat types within waterbodies.

Characterization of derelict crab pots

Of the 106 DCPs found during field surveys, 92 (86.8%) were retrieved. These 92 DCPs were in the water for an estimated mean of 2.09 years (SD 1.30). For retrieved DCPs, condition was ranked on a scale ranging from 1 to 10 with a mean value of 6.8 (SD 2.74) (see ranking system in Table 2; see Fig. 2 for examples of DCPs in poor [rank value of 9] and fair [5] condition). Of these pots, 34 DCPs (37%) were functional and capable of trapping organisms (Fig. 2), and these DCPs had no markings or floats that would make visual detection possible from the surface. About 51% or 47 of the 92 DCPs were buried in estuarine sediments and had a mean burial depth of 7.87 cm (SD 10.57) measured from pot bottom. With organisms, such as macroalgae, soft corals, sponges, tunicates, bivalves, and bryozoans growing on their walls, 27 DCPs supported fouling communities.

Bycatch of derelict crab pots

Of the 92 DCPs retrieved for analysis of bycatch (Table 3), 38 DCPs (41.3%) contained bycatch organisms. A total of 45 taxa were identified in or on these pots. Of these 45 identified taxa, 18 species (Table 4), represented by 531 individuals, were bycatch, inhibited from leaving the DCP. The most abundant bycatch species of fisheries interest were blue crab and Florida stone crab; sheepshead (*Archosargus probatocephalus*) and black sea bass (*Centropristis striata*) were also among DCP bycatch (Fig. 4).

Of the 25 blue crab found as bycatch, all were considered adults (CW ≥5.6 cm [point to point], the minimum size of mature females as defined in NCDMF[9]; females also had to exhibit a rounded abdominal apron), 10 were dead, and 11 were of legal market size (males ≥12.7 cm CW and females ≥17 cm CW [NCDMF[9]]); for 3 of these 25 crab, size was estimated allometrically from claw size. Of the 69 Florida stone crab found as bycatch, only 1 was dead and 23 (33%) were juveniles (CW: 1.25–3.00 cm; Lindberg and Marshall[10]).

Blue crab bycatch abundance did not differ significantly among waterbodies ($F_{(2)}$=1.50, P=0.23) or among habitat types ($F_{(1)}$=0.06, P=0.80) (Fig. 4). The interaction between these factors was significant ($F_{(6)}$=2.66, P=0.02) as a consequence of relatively high numbers of blue crab found in estuarine edge habitat in Core Sound and in marsh creek habitat in the Cape Fear River. The relative proportions of available estuarine edge and marsh creek habitats in these respective waterbodies did not explain patterns in abundances of blue crab in DCPs. Bycatch abundance of Florida stone crab did not differ significantly among waterbodies ($F_{(2)}$=0.37, P=0.70) or among habitat types ($F_{(1)}$=2.74, P=0.10) (Fig. 4). The interaction between these factors was not significant ($F_{(6)}$=2.16, P=0.056), yet it was influenced by the relatively high abundance of Florida stone crab found in estuarine edge habitat in Core Sound, which was dominated by juveniles, and in marsh creek habitat in Bogue Sound.

The most important bycatch species of conservation interest were 5 diamondback terrapin and 1 clapper rail (*Rallus crepitans*). Other abundant nonfishery species were mud crabs (family Xanthidae), portly spider crab (*Libinia emarginata*), blennies (suborder Blennioidei), pinfish (*Lagodon rhomboides*), and oyster toadfish (*Opsanus tau*). Eastern oyster (*Crassostrea virginica*) had recruited to 16 of the 92 pots retrieved, and recruitment of northern quahog (*Mercenaria mercenaria*) was also substantial. Several species of bryozoans (phy-

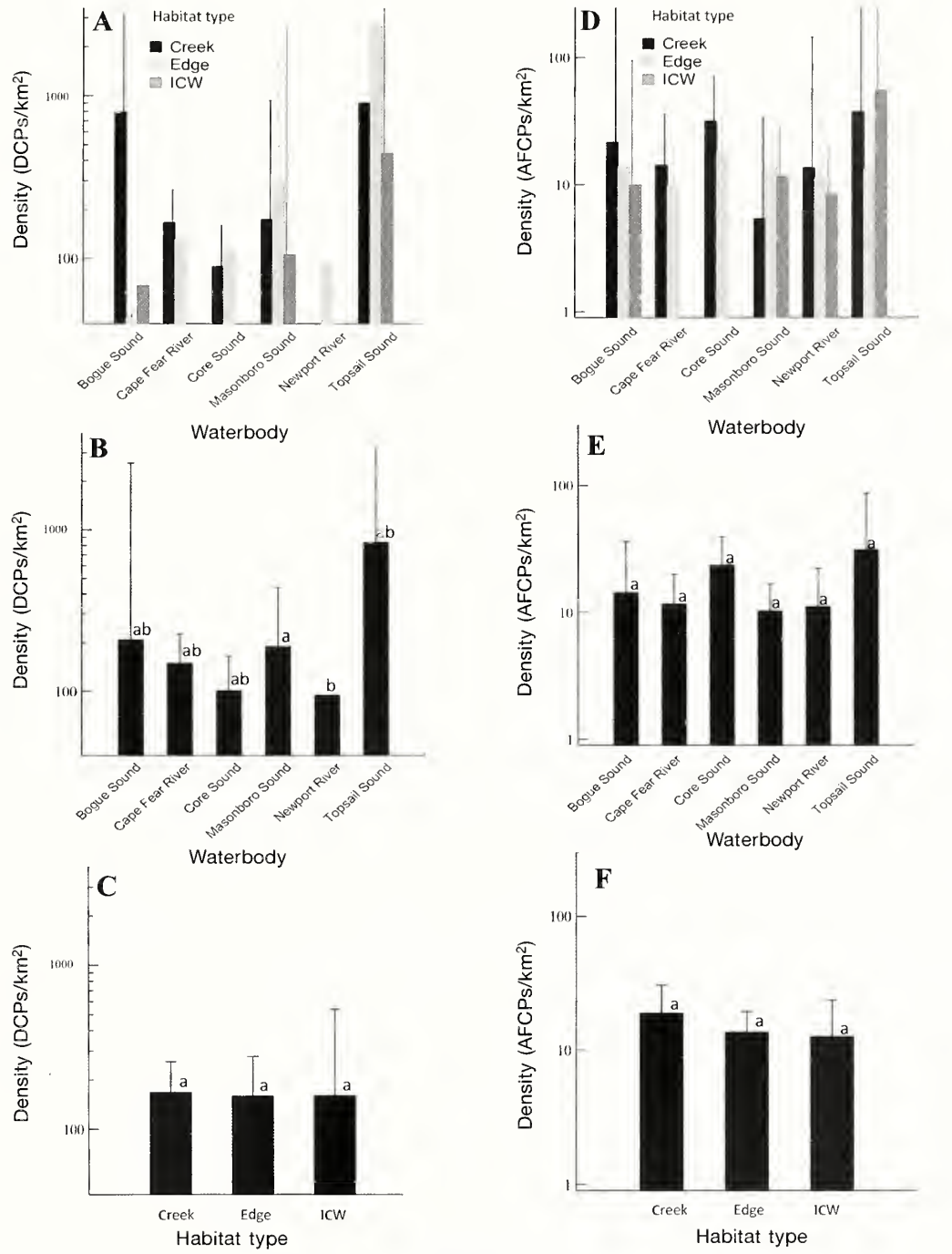

Figure 3

Mean densities of derelict crab pots (DCPs), extrapolated to the number of DCPs per square kilometer of open water (**A**) by habitat type (marsh creek, estuarine edge, and areas adjacent to the Atlantic Intracoastal Waterway [ICW]) and by each of 6 waterbodies in North Carolina (Bogue, Core, Masonboro, and Topsail sounds and Cape Fear and Newport rivers), (**B**) by waterbody, and (**C**) by habitat type, and mean densities of actively fished crab pots (AFCPs) extrapolated to number of AFCPs per square kilometer of open water of open water (**E**) by habitat type and by each of the 6 waterbodies, (**F**) by waterbody, and (**F**) by habitat type, as observed by side-scan sonar or visually, from April to November 2010. Note that the logarithmic scales used on the *y*-axes differ between graphs for DCP densities and graphs for AFCP densities. Levels not sharing the same letter differ significantly ($P \leq 0.05$) in Tukey's honestly significant difference post-hoc comparison of least square means of Box-Cox transformed data (panels B, C, E, and F). Error bars indicate standard errors.

Table 3

Abundance of derelict crab pots (DCPs) retrieved for collection of bycatch data during surveys of marsh creek, estuarine edge, and adjacent Atlantic Intracoastal Waterway (ICW) habitats in Bogue, Core, Masonboro, and Topsail Sounds and the Cape Fear and Newport rivers in North Carolina from April to November 2010. Note that the ICW does not traverse Core Sound and was not sampled in Cape Fear River because depths were >4 m.

Waterbody	Habitat type			Total number of DCPs retrieved
	Marsh creek	Estuarine edge	Adjacent ICW	
Bogue Sound	4	1	1	6
Cape Fear River	13	9	–	22
Core Sound	5	6	–	11
Masonboro Sound	20	19	4	43
Newport River	0	1	0	1
Topsail Sound	1	4	4	9
Total DCPs retrieved	43	40	9	92

lum Bryozoa), tunicates (subphylum Urochordata), and estuarine algae also were growing on retrieved DCPs.

Recruitment of derelict crab pots

Surveys of DCPs 1 year after meticulous removal of DCPs present in 4 cells (each 1 km^2, all 100% open water) resulted in the finding of 6 new pots: 1 in each of 3 cleared cells (Bogue and Masonboro sounds and Newport River) and 3 in the cleared cell near Figure Eight Island in Topsail Sound. On the basis of these recoveries, we estimated an annual DCP recruitment rate of 1.0 DCP/km^2 in Bogue and Masonboro sounds and Newport River and of 3 DCP/km^2 in Topsail Sound. From this survey of only four 1-km^2 cells, we found an overall annual mean DCP recruitment rate of 1.5 DCPs/km^2 (SD 1.0), yielding lower and upper 95% confidence levels of −0.09 and 3.09 DCPs/km^2, respectively. Of the

Table 4

Faunal bycatch (trapped and unrestricted) species and number caught in 92 derelict crab pots retrieved between April and November 2010 from Bogue, Core, Masonboro, and Topsail Sounds and the Cape Fear and Newport rivers in North Carolina. Trapped organisms were those that were confined, and escape was unlikely, once they entered pots. Unrestricted organisms were those that were free to pass through pot walls yet were captured when the pots were retrieved.

Common name	Taxonomic name	Number of organisms trapped	Number of unrestricted organisms
Blue crab	*Callinectes sapidus*	25	0
Florida stone crab	*Menippe mercenaria*	46	23
Mud crabs	Xanthidae.	0	267
Spider crabs	Majidae.	15	0
Oyster toadfish	*Opsanus tau*	40	0
Sheepshead	*Archosargus probatocephalus*	4	0
Blennies.	Suborder Blennioidei	0	47
Black sea bass	*Centropristis striata*	1	0
Pinfish	*Lagodon rhomboides*	1	0
Snapping shrimps	Alpheoidea	0	27
Banded tulip	*Fasciolaria lilium*	0	1
Polychaetes	Polychaeta	0	4
Brittle star	Ophiuroidea	0	20
Anemone	Anemone	0	1
Clapper rail	*Rallus crepitans*	1	0
Diamondback terrapin	*Malaclemys terrapin*	5	0
Hermit crabs	Paguroidea	0	2
Purple sea urchin	*Strongylocentrotus purpuratus*	0	1

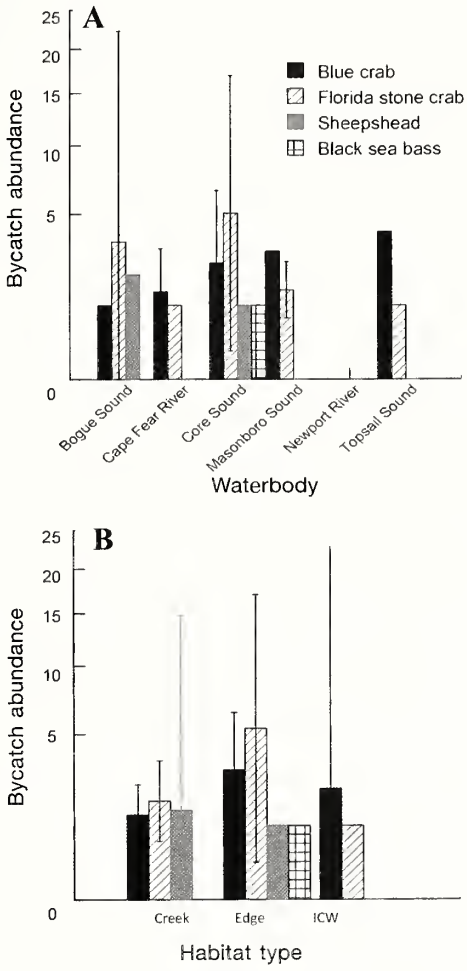

Figure 4

Abundance of 4 fishery species per km^2—the blue crab (*Callinectes sapidus*), Florida stone crab (*Menippe mercenaria*), sheepshead (*Archosargus probatocephalus*), and black sea bass (*Centropristis striata*)—found among the bycatch of derelict crab pots (**A**) by waterbody and (**B**) by habitat type from April to November 2010 in 6 waterbodies (Bogue, Core, Masonboro, and Topsail sounds and Cape Fear and Newport rivers) of North Carolina.

6 retrieved DCPs, 2 were estimated to have been in the water for at least 2 years, on the basis of degree of fouling and size of attached eastern oysters. Three other introduced DCPs, each estimated to have been in the water for 1–1.5 years, were heavily fouled with algae and tunicates and were still capable of capturing bycatch. Live adult blue crab (5), Florida stone crab (8), and an oyster toadfish (1) were found in the 6 recovered DCPs, but they were not included in our bycatch database. One DCP was thought to have become derelict within a few months of retrieval because its rebar was still intact.

Discussion

The occurrence of DCPs is a serious problem throughout North Carolina and in other states where the blue crab fishery that uses hard-shell crab pots contributes to the local heritage and economy. We were able to produce quantitative estimates of DCP density and abundance and of bycatch by waterbody and habitat in North Carolina. Our results document the magnitude of the problem and may help focus future cleanout efforts. This study shows that DCPs are introduced into areas not necessarily associated with crabbing activity because pots were probably transported by tides and storm currents. Further, a previously unrecognized source of mortality for fishery species and other wildlife—stacked pots stored on the marsh—was observed.

Derelict crab pots were abundant in 5 of the 6 waterbodies (Table 1) and were present in each of the 3 types of habitat surveyed (Table 1; Fig. 3), despite current crab pot regulations, management efforts to limit pot loss or abandonment, and programs to remove derelict gear. Lack of a significant difference in DCP density among habitat types may have been a result of the ecological similarity of the 3 habitats examined. All were situated in shallow water, they were adjacent to one another, and each was a likely focus of crabbing effort. Crabbers traditionally set lines of pots along the shallow edge of deeper water areas (such as channels) or in areas adjacent to salt marshes. Avissar (2006) found that crabbers moved their pots into shallower waters at the estuarine edge or toward the heads of marsh creeks to avoid pot damage caused by sea turtles seeking the enclosed bait. Hence, we expected to find higher DCP densities in marsh creek or estuarine edge habitats. Of all observed DCPs, 50% were discovered in marsh creek habitat; however, this finding could result from lower sampling effort overall in ICW habitat or from the lack of appropriate ICW habitat in 2 of the studied waterbodies (Table 1).

We sampled with replacement for a selection of cells to represent each habitat type within each waterbody. This procedure resulted in 23 randomly selected cells being surveyed as 2 different habitat types, effectively duplicating results in 46 of the 201 sampled cells and possibly hindering our ability to detect differences in DCP density among habitat types. However, analysis of the subset of 155 single-habitat cells yielded the same patterns found in the analysis of the complete 201-cell data set, with significant differences in DCP densities found among the 6 waterbodies but not among the 3 habitat types and with no differences in AFCP densities detected among these factors.

Found in 46% of the 201 sampled cells, AFCPs were much more widely distributed than DCPs, which were found in only 9% of the sampled cells. This difference may have resulted from the 11-fold higher number of

observed AFCPs than of observed DCPs, 1211 versus 106 (Table 1) and from the 41 times greater survey area over which AFCPs were counted, 1 km^2 versus 24,000 m^2 (or 0.024 km^2).

The results of our limited study of the re-introduction of DCPs into specific areas from which all had been removed indicate that pots were relocated from the areas of their original deployment and loss. In all 4 of the cells where annual recruitment was assessed, DCPs were found with a degree of fouling or with sizes of encrusting eastern oysters that implied submergence ≥1 year (5 out of 6 DCPs), although all crab pots were removed from these areas 1 year before, indicating that relocation rather than deployment within the last year was responsible for their presence in the cleared plots. We cannot conclude that natural physical processes necessarily caused these relocations of DCPs because human intervention, such as transport and discard by trawlers, could also explain the movement of these DCPs. In contrast to this evidence of DCP mobility, 51% of the 6 DCPs retrieved showed evidence of at least partial burial by estuarine sediments, a situation that would limit their subsequent movement.

Regulations of a NCDMF crab pot clean-out program that began in 2003 require commercial crabbers to remove all pots from the water for a period of 2–3 weeks, and a crab potting moratorium occurs typically from late January to early February. During this time, NCDMF crews remove DCPs that they find in North Carolina waters. This program is quite limited in scope and targets popular crabbing areas. Derelict crab pots retrieved by NCDMF are either disposed of, if no identification is present, or returned to the owner with a fine, if the mandated identification tag remained attached to the pot. From 2003 through 2011, NCDMF removed 21,338 DCPs from coastal waters in North Carolina (NCDMF[12]).

In one heavily fished waterbody, few DCPs were found, possibly because fishermen were regularly removing derelict gear. Only 4 DCPs were found in the 9 cells surveyed in Jarrett Bay, within Core Sound, which has historically experienced substantial fishing and crabbing effort (Avissar, 2006; Cahoon and Hart[13]; Hooper[14]; and Purifoy[15]). Part of this bay was open to a trawl fishery in 2010, and traditional crab potting areas bordered the trawl areas. Perhaps peer pressure from other fishermen or inadvertent collection and removal by trawlers was responsible for the unexpected low number of DCPs in Jarrett Bay.

Bycatch or residents?

What motivates organisms to occupy DCPs? Of the retrieved DCPs, 41% contained bycatch, most of which was alive. A separate but relevant study (senior author, unpubl. data) in Bogue Sound, North Carolina, found that scavengers quickly take remains of organisms that die in crab pots. Dead bycatch is either consumed or becomes so fragmented that it is washed out of the pot through the mesh. Only chitinous components and large bones remain for ≥4 days; therefore, deaths attributable to DCPs are generally underestimated when using only the counts of bycatch found in recovered pots.

Living blue crab and Florida stone crab were found as DCP bycatch in every waterbody and every habitat type (Florida stone crab found in the cell in Newport River that was sampled for our DCP recruitment study were not part of the quantitative survey and therefore not included in the bycatch data set). Of the crabs found in DCPs, 44% of blue crab and 67% of Florida stone crab were of marketable size.

The range of the Florida stone crab has expanded northward into the region of our study. Warming surface water temperatures in North Carolina estuaries, such as the 1.4°C increase in the daily mean surface temperatures in Bogue Sound from 1985 to 2005 (Micheli et al., 2008), have probably facilitated the poleward expansion of populations of Florida stone crab. Populations of Florida stone crab have become well established as far north as Pamlico Sound (just north of our study area), where salinities are higher than 15, at population densities similar to densities observed for the Florida Panhandle (Rindone and Eggleston, 2011). Habitat changes may have also contributed to the increase in Florida stone crab abundance in our study area. We found more Florida stone crab in estuarine edge habitats compared with the abundance observed in marsh creek or adjacent ICW habitats (Fig. 4), a pattern that may be related to the presence of abundant rock revetments along shorelines that abut estuarine edges. Hard rock and crevice substrate is a favorable habitat for Florida stone crab and growing use of rocks to stabilize estuarine shorelines may have increased abundance of Florida stone crab in such areas (Wong et al., 2010). The degree to which Florida stone crab use DCPs and, perhaps, other structural marine debris as refuge habitat is unclear.

Some blue crab and Florida stone crab may escape from DCPs; however, as long as they are trapped they are not available to the fishery. Nonetheless, increases in abundance of Florida stone crab indicate a potential for commercial and recreational fisheries of Florida stone crab in North Carolina. Although not historically developed as a commercial fishery in North Carolina,

[12]NCDMF. 2011. Unpub. data. Marine Patrol, Div. Mar. Fish., North Carolina Dep. Environ. Nat. Resour., Morehead City, NC 28557 [Records obtained 27 Jan 2011.]

[13]Cahoon, R., and K. Hart. 2004. Evaluating the efficiency and necessity of requiring bycatch reduction devices on pots in the peeler crab fishery: qualifying and characterizing spatial and temporal overlap of activities between diamondback terrapins (*Malaclemys terrapin*) and the commercial fishery for peeler blue crabs (*Callinectes sapidus*), 13 p. North Carolina Sea Grant Project no. 03-FEG-18. [Available from North Carolina Sea Grant, 303 College Circle, Morehead City, NC 28557.]

[14]Hooper, M. 2010. Personal commun. Hooper Family Seafood, Smyrna, NC 28579.

[15]Purifoy, J. 2010. Personal commun. Inst. Mar. Sci., Univ. North Carolina Chapel Hill, Morehead City, NC 28557.

landings of Florida stone crab are highly valued in Florida and prized along the U.S. Gulf Coast (NCDMF[9]).

Species of concern, such as the diamondback terrapin and several coastal birds and mammals, are perhaps the most serious captures among DCP bycatch (Bishop, 1983). The results of this study and others (Bishop, 1983; Havens et al., 2011) indicate that crab pots that become derelict near marshes, essential terrapin habitat, are likely to attract terrapins and often result in their drowning. All 5 diamondback terrapins found in this study were associated with marsh habitat: 1 terrapin in a DCP in a marsh creek of the Cape Fear River and 4 juvenile terrapins in a DCP in Topsail Sound, where the ICW traverses marsh habitat. All 5 diamondback terrapin were dead yet sufficiently intact for clear identification. Hart and Crowder (2011) found that all terrapin captures in Jarrett Bay occurred between April and mid-May in baited hard-shell and peeler crab pots located <321 m from the estuarine shore.

If they are improperly stored when not in use, crab pots can become a threat to wildlife. In Core Sound, 115 crab pots were tagged and properly outfitted for crabbing, stacked, and stored neatly on the marsh adjacent to the area where they were likely to be deployed. We found the remnants of bycatch organisms that included blue crab, portly spider crab, whelks or hermit crabs, and juvenile birds (skulls) in the area of dead marsh vegetation adjacent to the stacked pots and presumably where pots had been stacked previously. Large numbers of crab pots were also stacked along marsh edges at locations within Topsail Sound. Neither the stacked crab pots found on marshes nor their contents were included in the results of this study.

Derelict crab pots can provide structural habitat for organisms, initially supporting a fouling community, which subsequently provides forage and refuge habitat for other organisms. Organisms, such as Florida stone crab and mud crabs, may have chosen to reside in the DCPs that were recovered, and others, such as bivalves, algae, and tunicates, may have dispersed as propagules and then have settled on the pot surfaces. Many of the organisms that could freely pass through the pot mesh obviously elected to be part of the DCP living community and were probably subsidized energetically by organisms that became entrapped and died in pots. Eastern oysters had recruited to 17% of the retrieved DCPs and therefore specific environmental conditions and pot features may have facilitated bivalve recruitment. Perhaps DCPs made incapable of retaining bycatch could be left in the estuary to support structural habitats such as oyster reefs (Fodrie[16]).

Future management considerations

Various management actions have been used to reduce the bycatch in DCPs: 1) reduction of the numbers of DCPs (e.g., as per NCDMF[9]); 2) promotion of the use of pots with panels that allow bycatch species and legally undersize blue crab to escape; and 3) promotion of the use of pots with replaceable biodegradable materials that will not remain intact for long after a pot becomes derelict. The results of our study may help to evaluate the potential effectiveness of these actions and guide strategic planning to improve fishery yields and reduce wildlife mortality attributable to DCPs. For example, our project showed that substantial numbers of DCPs were in the water despite the seasonal crab pot clean-out program of the NCDMF. That program is limited in its effectiveness by the low numbers of marine patrol staff available to participate. The clean-out program could yield a greater positive effect if other groups or individuals were allowed to remove crab pots during the crabbing moratorium period, with a requirement that they report their findings to NCDMF.

Commercial and recreational crab pots in North Carolina are distinguishable only by the color of their float; therefore, when the float is no longer attached, it is almost impossible to determine whether a DCP came from the recreational or commercial fishery. Through establishing separate recruitment study sites in areas known to be used exclusively by each fishery, the rate at which pots become derelict could be determined from the activities of each fishery. This information could help fishery managers better allocate between the fisheries incentives used for reducing crab pot loss or abandonment and resources used for DCP retrieval.

Our observations of bycatch associated with stacked crab pots on the marsh revealed that terrestrial species may also be killed as bycatch associated with the blue crab fishery. In addition, strong storms may transport these stored pots into the estuary and turn a crabber's lost investment into DCPs that ghost fish and kill fishes, crabs, terrapin, and other wildlife. Mandatory rules for permit holders that specify proper storage of crab pots might reduce the effect of stored crab pots on fishery species and other wildlife.

The geographic area of this study was limited by logistic and budgetary constraints to selected waterbodies in North Carolina, within the Central and Southern Districts of the NCDMF. Because Albemarle Sound, which is within the Northern District, produced an average of 52% of the blue crab landings in North Carolina from 2006 to 2008 (NCDMF[7]) and was not included in our study, a similarly designed study conducted in the Northern District, especially in Albemarle Sound, would likely expand the knowledge of DCP density in the waters of North Carolina.

Acknowledgments

This study was funded in part by the NOAA Marine Debris Program, with thanks to H. Bamford, S. Morison, and C. Arthur. Specific thanks to D. Lee of The Tortoise Reserve for input on study protocols. We thank C. Rivero for providing essential GIS support for our sampling plan. We thank J. Purifoy for sharing his

[16]Fodrie, J. F. 2010. Personal commun. Inst. Mar. Sci., Univ. North Carolina Chapel Hill, Morehead City, NC 28557.

invaluable skills and expertise on the water. We also thank W. Golder, N. Loft, A. Mangiameli, R. Nelson, C. H. Peterson, R. Sicheneder, M.-K. Spillane, P. Shrestha, J. Vicente, C. Wood, R. Wood, and A. Zasadny for their contributions.

Literature cited

Avissar, N.
2006. Sea turtle damage and bycatch in North Carolina's blue crab fishery. M.S. thesis, 65 p. Nicholas School of the Environment and Earth Sciences, Duke Univ., Durham, NC. [Available at website.]

Bishop, J. M.
1983. Incidental capture of Diamondback Terrapin by crab pots. Estuaries 6:426–430.

Gosner, K. L.
1971. Guide to identification of marine and estuarine invertebrates, 693 p. Wiley-Interscience, John Wiley and Sons, New York.

Grosse, A. M., D. J. Van Dijk, K. L. Holcomb, and J. C. Maerz.
2009. Diamondback terrapin mortality in crab pots in a Georgia tidal marsh. Chelonian Conserv. Biol. 80:98–100.

Guillory, V.
1993. Ghost fishing in blue crab traps. N. Am. J. Fish. Manage. 13:459–466.

Hart, K. M., and L. B. Crowder.
2011. Mitigating by-catch of diamondback terrapins in crab pots. . Wildl. Manage. 75:264–272.

Havens, K. J., D. M. Bilkovic, D. Stanhope, K. Angstadt, and C. Hershner.
2008. The effects of derelict blue crab traps on marine organisms in the Lower York River, Virginia. N. Am. J. Fish. Manage. 28:1194–1200.

Havens, K., D. M. Bilkovic, D. Stanhope, and K. Angstadt.
2011. Fishery failure, unemployed commercial fishers, and lost blue crab pots: an unexpected success story. Environ. Sci. Policy. 14:445–450.

Micheli, F., M. J. Bishop, C. H. Peterson, and J. Rivera.
2008. Alteration of seagrass species composition and function over two decades. Ecol. Monogr. 78:225–244.

Morison. S. E., and P. M. Murphy (eds.).
2009. Proceedings of the NOAA Submerged Derelict Trap Detection Methods Workshop; Silver Spring, MD, 2–4 June. NOAA Tech. Memo. NOS-OR&R-32, 36 p. [Available at website.]

Morris, A. S., S. M. Wilson, E. F. Dever, and R. M. Chambers.
2011. A test of bycatch reduction devices on commercial crab pots in a tidal marsh creek in Virginia. Estuar. and Coasts 34:386–390.

NMFS (National Marine Fisheries Service).
2007. Fisheries of the United States 2006. Current Fishery Statistics No. 2006, 104 p. Natl. Mar. Fish. Serv., NOAA, Silver Spring, MD. [Available at website.]
2008. Fisheries of the United States 2007. Current Fishery Statistics No. 2007, 103 p. Natl. Mar. Fish. Serv., NOAA, Silver Spring, MD. [Available at website.]
2009. Fisheries of the United States 2008. Current Fishery Statistics No. 2008, 103 p. Natl. Mar. Fish. Serv., NOAA, Silver Spring, MD. [Available at website.]
2010. Fisheries of the United States 2009. Current Fishery Statistics No. 2009, 103 p. Natl. Mar. Fish. Serv., NOAA, Silver Spring, MD. [Available at website.]
2011. Fisheries of the United States 2010. Current Fishery Statistics No. 2010, 103 p. Natl. Mar. Fish. Serv., NOAA, Silver Spring, MD. [Available at website.]
2012. Fisheries of the United States 2011. Current Fishery Statistics No. 2011, 124 p. Natl. Mar. Fish. Serv., NOAA, Silver Spring, MD. [Available at website.]
2013. Fisheries of the United States 2012. Current Fishery Statistics No. 2012, 124 p. Natl. Mar. Fish. Serv., NOAA, Silver Spring, MD. [Available at website.]
2014. Fisheries of the United States 2013. Current Fishery Statistics No. 2013, 129 p. Natl. Mar. Fish. Serv., NOAA, Silver Spring, MD. [Available at website.]

Rindone, R. R., and D. B. Eggleston.
2011. Predator–prey dynamics between recently established stone crabs (*Menippe* spp.) and oyster prey (*Crassostrea virginica*). J. Exp. Mar. Biol. Ecol. 407:216–225.

Robins, C. R., G. C. Ray, and J. Douglass.
1986. A field guide to Atlantic Coast fishes of North America, 354 p. Houghton Mifflin, Boston, MA.

Roosenburg, W. M., W. Cresko, M. Modesitte, and M. B. Robbins.
1997. Diamondback terrapin (*Malaclemys terrapin*) mortality in crab pots. Conserv. Biol. 11:1166–1172.

Roosenburg, W. M., K. L. Haley, and S. McGuire.
1999. Habitat selection and movements of diamondback terrapins, *Malaclemys terrapin*, in a Maryland estuary. Chelonian Conserv. Biol. 3:425–429.

Ruppert, E., and R. Fox.
1988. Seashore animals of the Southeast: a guide to common shallow-water invertebrates of the southeastern Atlantic coast, 429 p. Univ. South Carolina Press, Columbia, SC.

Wong, M. C., C. H. Peterson, and J. Kay.
2010. Prey size selection and bottom type influence multiple predator effects in a crab–bivalve system. Mar. Ecol. Prog. Ser. 409:143–156.

NOAA
National Marine
Fisheries Service

Fishery Bulletin
established 1881

Spencer F. Baird
First U.S. Commissioner
of Fisheries and founder
of Fishery Bulletin

Climate-related meteorological and hydrological regimes and their influence on recruitment of Gulf menhaden (*Brevoortia patronus*) in the northern Gulf of Mexico

Guillermo Sanchez-Rubio (contact author)
Harriet Perry

Email address for contact author: guillermo.sanchez@usm.edu

Gulf Coast Research Laboratory
Center for Fisheries Research and Development
University of Southern Mississippi
703 East Beach Drive
Ocean Springs, Mississippi 39564

Abstract—Abundances of Gulf menhaden (*Brevoortia patronus*) in the northern Gulf of Mexico (GOM) are heavily influenced by physical and biological processes that affect refuge and food availability. This study identified specific decadal and interannual responses in the recruitment of Gulf menhaden to local meteorological and hydrological regimes imposed by the coupling of Atlantic Multidecadal Oscillation (AMO) and North Atlantic Oscillation (NAO) phases and by El Niño Southern Oscillation (ENSO) events. Numbers of age-0 menhaden in fishery-independent surveys and numbers and proportions of Gulf menhaden ages 1–6 in commercial purse-seine landings in the northern GOM were used to investigate those responses. High postlarval abundance of Gulf menhaden (3.6/beam plankton haul) in the central region was related to the decadal wet regime associated with AMO cold and NAO positive phases. Elevated numbers of menhaden species (38.3/seine haul) in the western region were related to interannual wet regimes associated with ENSO warm and neutral events. High commercial landings of Gulf menhaden (10 million fish/vessel ton week) were related to the decadal average hydrological regime associated with AMO cold and NAO negative phases. Climate regimes may favor growth and survival by structuring offshore and inshore nursery habitats or by synchronizing release of larvae when offshore and inshore nursery conditions are favorable.

Manuscript submitted: 13 September 2013.
Manuscript accepted: 16 July 2015.
Fish. Bull. 113:391–406 (2015).
Online publication date: 14 August 2015.
doi: 10.7755/FB.113.4.3

Gulf menhaden (*Brevoortia patronus*) spawn in offshore marine waters and juvenile development occurs in nearshore nursery areas. Spawning occurs in the late fall and winter, peaking between December and February (Gunter, 1945; Guillory and Roussel, 1981; Shaw et al., 1985; Christmas et al.[1]). On the basis of the distribution of eggs, Fore (1970) noted that spawning occurred mainly over the continental shelf in the northcentral Gulf of Mexico (GOM) and that the greatest concentrations were found in waters between 8 and 70 m off Texas and Louisiana and near the Mississippi River Delta. Christmas and Waller (1973) and Sogard et al. (1987) also found high densities of larvae near the Mississippi River. Late-stage larvae recruit to estuaries during the winter and spring, and there they transform into juveniles and remain for several months before moving back to open Gulf waters (Suttkus, 1956; Christmas and Waller, 1973) in the summer and fall (Suttkus, 1956). After metamorphosis of larvae into juveniles, Gulf menhaden change their feeding habits from a carnivorous diet to an omnivorous filter-feeding diet.

The capacity of estuaries to support growth and development was considered by Reintjes (1970) to be critical to survival of young Gulf menhaden. A host of studies have examined the effects of meteorological and hydrological variables on recruitment success (numbers of juvenile fish moving into the estuary) and most have focused on annual fluctuations. More recent data indicate that global climate factors associated with decadal and multidecadal oscillations in the Pacific and Atlantic influence population abundances of estuarine species in addition to the annual and interannual factors noted in earlier studies.

The Pacific Decadal Oscillation (PDO), Atlantic Multidecadal Oscillation (AMO), North Atlantic Oscillation (NAO), and El Niño Southern Oscillation (ENSO) are associated with river flows across the continental United States (Tootle et al., 2005; Tootle and Piechota, 2006). The combination of PDO, AMO, and NAO and

[1] Christmas, J. Y., D. J. Etzold, L. B. Simpson, and S. Meyers (eds.). 1988. The menhaden fishery of the Gulf of Mexico United States: a regional management plan. Gulf States Mar. Fish. Comm. 18, 134 p. [Available at website.]

the coupling of AMO and NAO phases were found to be important drivers of long-term flows in the Mississippi River and Atchafalaya River and in the Pearl River and Pascagoula River, respectively (Sanchez-Rubio et al., 2011a). The effect of ENSO on river flow is more evident in smaller river basins closely associated with the Gulf Coast environment (Sanchez-Rubio et al., 2011a).

Mississippi River flow is tightly linked to physical and biological processes associated with the development and survival of early stages of Gulf menhaden on the continental shelf and in estuaries of the north-central GOM (Grimes and Finucane, 1991; Govoni and Grimes, 1992). From fall through early spring, biological productivity is enhanced by offshore transport and upwelling induced by northerly (north–south wind direction) and easterly (east–west wind direction) winds. Vector winds (Hitchcock et al., 1997) spread and project the Mississippi–Atchafalaya River plume over shelf waters as far as 100 km (Riley, 1937), resulting in a buoyant, nutrient-rich, freshwater mass with a well-defined frontal zone that veers westward in spring (Govoni et al., 1989; Govoni and Grimes, 1992; Hitchcock et al., 1997). Gulf menhaden larvae aggregate in the river plume front on the continental shelf where the Coriolis force, wind speed, and wind direction shape the trajectory and properties of the plume that transports larvae (Govoni et al., 1989; Govoni and Grimes, 1992; Hitchcock et al., 1997) as far west as Texas (Dinnel and Wiseman, 1986).

Mississippi–Atchafalaya river flow is positively related to the seaward projection and areal coverage of the plume (Wright and Coleman, 1971; Walker and Rouse[2]) and to the influx of nutrient-rich river water (Bratkovich et al., 1994). Seaward projection and areal expansion through high river discharge may prolong shoreward transport of larvae and increase vulnerability to predation (Govoni, 1997). Nutrient enhancement (Riley, 1937; Lohrenz et al., 1990; Dagg and Whitledge, 1991) during high river discharge increases food availability and growth, thereby decreasing predation and increasing survival of Gulf menhaden larvae (Govoni, 1997). The river plume eventually enters the coastal current (Cochrane and Kelly, 1986; Wiseman and Kelly, 1994), exchanging water (Dinnel and Wiseman, 1986; Wiseman and Garvine, 1995) and transporting Gulf menhaden larvae (Govoni, 1993) between the current and the coastal boundary zone. Larvae, once they are within the coastal boundary zone, enter estuaries with the vernal rise in sea level (Shaw et al., 1985).

Juvenile development takes place in the estuary. During this period, interannual, strong northerly winds (coming from the north) promote coastal upwelling, increase nearshore productivity, and produce extremely low tide levels along the Gulf Coast with a resultant die off of marsh vegetation (Kirby, 1972; Day et al., 1973). This vegetation, accumulated during the winter, is later washed out by spring flood tides, stimulating spring plankton production (Guillory et al., 1983). The availability of food is further increased by high river flow that introduces new organic material to inshore waters and re-suspends existing detritus (Deegan and Thompson, 1985; Madden et al., 1988), fostering faster growth and increased survival of young Gulf menhaden (Deegan, 1990).

For early life history stages, food availability is a critical aspect of habitat suitability (Christmas et al., 1982; Deegan, 1986), and climate plays a crucial role in the structuring of habitats. Despite the economic and ecological importance of Gulf menhaden, studies of climate-related hydrological regimes on population abundances have been limited primarily to the study of annual and interannual factors thought to influence survival of larvae and juveniles. In this study, the effects of decadal AMO and NAO phases as well as interannual ENSO events on northern GOM hydrological conditions were examined and related to abundances of menhaden documented in fishery-independent and fishery-dependent data.

Two other species of menhaden have overlapping distribution ranges with the Gulf menhaden (Tolan and Newstead, 2004). In the western GOM, juveniles of the finescale menhaden (*Brevoortia gunteri*) may co-occur with Gulf menhaden, and juvenile populations in that area are therefore referred to in this manuscript as *menhaden species* (Tolan and Newstead, 2004; Anderson and Karel, 2014). The range of yellowfin menhaden (*B. smithi*) overlaps that of Gulf menhaden in the eastern portion of the northern GOM; however, estuarine collections of *Brevoortia* in Alabama bays have yielded only Gulf menhaden (Boschung et al., 2004). Menhaden in fishery-independent studies in the central GOM (Louisiana, Mississippi, and Alabama) are almost exclusively Gulf menhaden (SEDAR[3]). A host of studies have examined stock structure in the northern GOM, and all reveal that the fishery is composed of Gulf menhaden and other menhaden species, the latter of which represent less than 1% of the harvest (VanderKooy and Smith[4]).

We examined fishery-independent data and fishery-dependent data to identify the responses of menhaden populations to local meteorological and hydrological conditions imposed by the coupling of AMO and NAO phases and by ENSO events. Fishery-independent data included data 1) on Gulf menhaden from surveys conducted with beam plankton trawls [BPLs] in the central region, 2) on Gulf menhaden from

[2] Walker, N. D., and L. J. Rouse Jr. 1993. Satellite assessment of Mississippi River discharge plume variability. OCS Study MMS 93-0044. U.S. Dep. Interior, Minerals Manage. Serv., Gulf of Mexico OCS Region, New Orleans, 50 p. [Available at website.]

[3] SEDAR (Southeast Data, Assessment, and Review). 2013. SEDAR 32A—Gulf of Mexico menhaden assessment report, 422 p. SEDAR, North Charleston, NC. [Available at website.]

[4] VanderKooy, S. J, and J. W. Smith (eds.). 2015. The menhaden fishery of the Gulf of Mexico, United States: a regional management plan, 181 p. Gulf States Mar. Fish. Comm. 240 [Available at website.]

Table 1

Periods and sources of climatological, meteorological, hydrological, and biological data used in analysis of the effect of climate-related factors on the recruitment of menhaden in the northern Gulf of Mexico. N:P ratio=nitrogen to phosphorus ratio; BPL= beam plankton trawl; hPa=hectopascal; h=hour.

Variables	Units	Years	Months	Sources
Atlantic Multidecadal Oscillation	°C	1962–2010	Jul–Jun	ESRL[1]
North Atlantic Oscillation	hPa	1962–2010	Apr–Mar	NCAR[2]
El Niño Southern Oscillation	°C	1962–2010	May–Feb	ESRL[3]
Coastal air temperature	°C	1962–2010	Nov–Mar	NCDC[4]
Precipitation	Mm	1962–2010	Sep–Aug	NCDC[4]
River flows	m^3/s	1962–2010	Sep–Aug	USGS[5]
Palmer Drought Severity Index		1962–2010	Sep–Aug	NCDC[4]
Sea level	Mm	1962–2010	Nov–May	GLOSS[6]
Offshore wind momentum	$[N/m^2]h$	1973–2010	Oct–Mar	NDBC[7]
Sea-surface temperature	°C	1973–2010	Oct–Mar	NDBC[7]
N:P ratio of Mississippi River influx		1974–2010	Sep–Aug	USGS[8]
Postlarval abundance index from BPL surveys		1981–2008	Nov–May	ADCNR[9]; MSDMR[10]
Early juvenile abundance index from seine surveys		1985–2008	Jan–Aug	ADCNR[9]; LDWF[11] MSDMR[10]; TPWC[12]
Numbers and proportions per vessel ton week by age in the purse-seine fishery		1964–2010	Mid-Apr–Oct	Smith and Vaughan[13]

[1] ESRL (Earth Systems Research Laboratory). AMO unsmoothed from the Kaplan SST V2. [Available at website, accessed May 2012.]

[2] NCAR (National Center for Atmospheric Research). Hurrell NAO Index (PC-based). [Available at website, accessed May 2012.]

[3] ESRL (Earth Systems Research Laboratory). ENSO: 3.4 SST Region. [Available at website, accessed May 2012.]

[4] NCDC (National Climatic Data Center). Air temperature, precipitation, and Palmer Drought Severity Index. [Available at website, accessed May 2012.]

[5] USGS (U.S. Geological Survey). River flows along the Gulf Coast. [Available at website, accessed May 2012.]

[6] GLOSS (Global Sea Level Observing System). Sea level for Pensacola and Galveston. [Available at website, accessed May 2012.]

[7] NDBC (National Data Buoy Center). Wind direction, wind speed, and sea-surface temperature from 42001 and 42002 buoy stations. [Available at website, accessed May 2012.]

[8] USGS (U.S. Geological Survey). Mississippi River predicted loads of monthly nutrients. [Available at website, accessed May 2012.]

[9] ADCNR (Alabama Department of Conservation and Natural Resources). 2011. Unpubl. data. [Beam plankton net and bag seine data from fishery monitoring program.] ADCNR, Montgomery, AL 36130.

[10] MSDMR (Mississippi Department of Marine Resources). 2011. Unpubl. data. [Beam plankton net and bag seine data from fishery monitoring program.] MSDMR, Biloxi, MS 39530.

[11] LDWF (Louisiana Department of Wildlife and Fisheries). 2011. Unpubl. data. [Bag seine data from fishery monitoring program.] LDWF, Baton Rouge, LA 70898.

[12] TPWC (Texas Parks and Wildlife Commission). 2011. Unpubl. data. [Bag seine data from fishery monitoring program.] TPWC, Austin, TX 78744.

[13] Smith, J. W., and D. S. Vaughan. 2011. Harvest, effort, and catch-at-age for Gulf menhaden. Southeast Data, Assessment, and Review SEDAR 27-DW05, 28 p. [Available at website.]

seine hauls in the central region, and 3) menhaden species from seine hauls in the western region. Fishery-dependent data included numbers and proportions of Gulf menhaden by age captured in the reduction purse-seine fishery. Meteorological conditions used in analyses were north–south and east–west wind momentum, precipitation, and air temperature, and hydrological conditions comprised sea-surface temperature (SST), Palmer Drought Severity Index (PDSI), river flow, and Mississippi River nitrogen to phosphorus (N:P) ratio.

Materials and methods

Data sets and sampling locations used to identify responses of juvenile (age 0) and adult (ages 1–6) populations of Gulf menhaden to local meteorological and hydrological conditions imposed by the coupling of AMO and NAO phases and by ENSO events are presented in Table 1 and Figure 1, respectively. Table 1 provides details on periods and sources of climatological, meteorological, hydrological, and biological data used in our analysis of the effect of climate-related factors on the

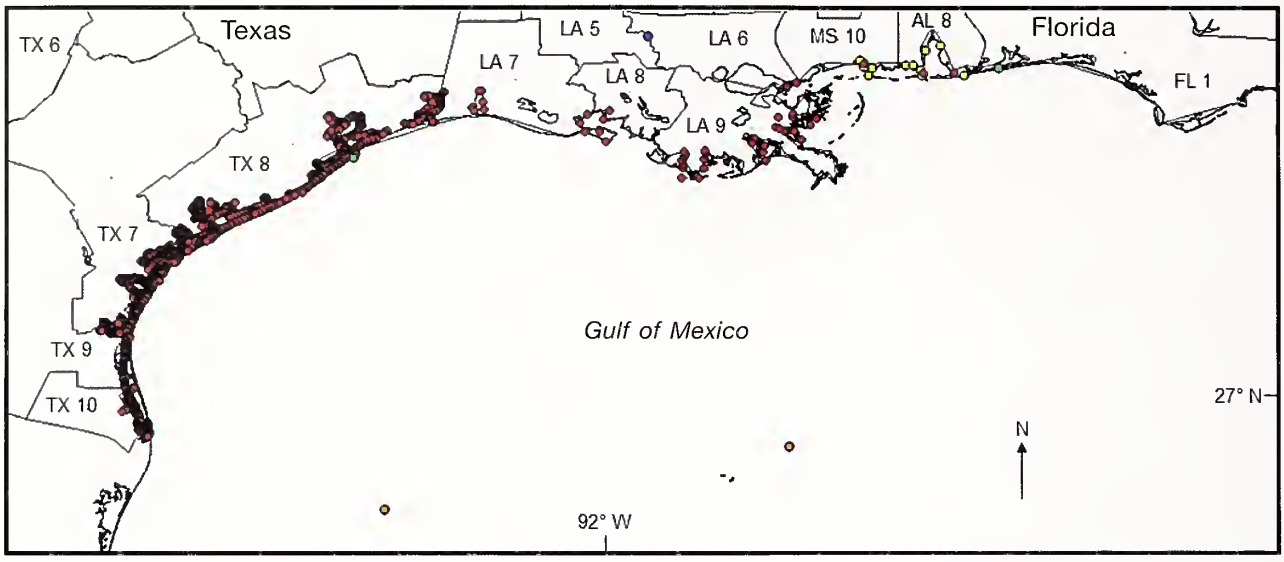

Figure 1

Map of the northern Gulf of Mexico showing the NOAA climate divisions from the western (Texas: TX6–10) and central (Louisiana, LA5–9; Mississippi, MS10; Alabama, AL8; and Florida, FL1) regions, the locations of stations from the U.S. Geological Survey near St. Francisville, Louisiana (1 blue dot seen at boundary between LA5 and LA6), the NOAA National Data Buoy Center (2 orange dots offshore), and the Global Sea Level Observing System (2 green dots), and the sites where biological data were collected with seines (red dots) and beam plankton trawls (yellow dots).

recruitment of menhaden species in the northern Gulf of Mexico. Meteorological and hydrological data were divided into 2 climate areas: central (Louisiana, Mississippi, Alabama, and Florida panhandle) and western (Texas). Annual values of wind momentum (north–south and east–west directions), SST, and Mississippi River nutrient influx (N:P ratio) were calculated for the months in which larvae of Gulf menhaden inhabit offshore waters. Annual values of air temperature, precipitation, PDSI, and sea level were calculated for the months critical to the inshore growth and development of early life history stages of Gulf menhaden. Annual catch values were calculated by using catch data collected for the months in which juveniles and adults were sampled by fishery-independent and fishery-dependent methods.

The lag in months among AMO, NAO, and ENSO indices and meteorological and hydrological response parameters in offshore waters of the northern GOM (wind momentum and SST), in central and western Gulf Coast regions (air temperature, precipitation, PDSI, and river flow), and in the Mississippi River nutrient influx (N:P ratio) was in agreement with the lag reported by Sanchez-Rubio et al. (2011a). Those authors reported a monthly lag in hydrological responses (e.g., river flow input) in the northcentral GOM to changes in AMO, NAO, and ENSO phases.

Decadal AMO and NAO phases and interannual ENSO events

For this study, the phases of AMO during the period 1948–2004 and phases of NAO and ENSO during 1950–2004 that were described in Sanchez-Rubio et al. (2011a) were revised, refined, and extended through the use of new AMO (1899–1947), NAO (1899–1949), and ENSO (1895–1949) values from paleontological reconstruction data and new values for all indices (2005–2011) from observational monitoring (see Table 1 for sources of AMO, NAO, and ENSO data). Use of new historical and observational data increased the time period of survey coverage and allowed for more accurate interpretation of climate descriptors. For this study, years classified within phases of AMO, NAO, and ENSO from 1962 to 2010 were considered.

The AMO cold and warm years were defined as years with below-average and above-average SST across the North Atlantic from 0° to 70°N (Enfield et al., 2001). The NAO negative and positive years were defined as years with below-average and above-average meridional oscillation in sea-level pressure between Iceland and the Azores (Hurrell and Van Loon, 1997). The ENSO warm and cold years were defined as years with above-average (>0.75°C) and below-average (< −0.75°C) SST in the Niño 3.4 region of the equatorial Pacific, the area defined by 120–170°W and from 5° S to 5°N (Rogers and Coleman, 2003). Years were considered ENSO neutral years when SST deviated between −0.75°C and 0.75°C from the average conditions.

The characterization of years within AMO phases described by Sanchez-Rubio et al. (2011a) were modified in this study; years with more than 9 consecutive months of above-average or below-average conditions were characterized as AMO warm or cold years. As a result, the AMO warm year in 1965 (Sanchez-

Rubio et al., 2011a) was reclassified as an AMO cold year.

The long-term phases of NAO were identified according to the proportion of total number of seasonal values (winter: January–March; spring: April–June; summer: July–September; and fall: October–December) that were negative and positive within a long-term NAO phase. A long-term period with a higher proportion of negative seasonal values was classified as a NAO negative phase, and a long-term period with a higher proportion of positive values was identified as a NAO positive phase. If the NAO negative and positive phases also had negative and positive averaged values, the above classification of phases of NAO was confirmed. The NAO positive (1959, 1995, 1996) and NAO negative (1971, 1972) years classified by Sanchez-Rubio et al. (2011a) were reclassified as NAO negative and NAO positive years, respectively.

The prior classification of ENSO years by Sanchez-Rubio et al. (2011a) was also revised with the new available monthly values of ENSO. To classify a year's event, 3 or more monthly values from May through February were averaged. As a result, the previously classified ENSO cold years in 1971 and 1995 were reclassified as ENSO neutral years.

Meteorological and hydrological data for coastal divisions

Data sets of monthly precipitation, PDSI, and air temperature were obtained by climate division, the spatial scale by which the NOAA National Climate Data Center divides data from stations within a state. Data sets were acquired for 17 climate divisions along coastal areas from Texas to Florida: Texas (divisions TX6–10), Louisiana (divisions LA5–9), Mississippi (division MS10), Alabama (division AL8), and Florida (divisions FL1–5). Monthly precipitation (in inches to the hundredths place) and PDSI values were averaged for the water year (defined as September of the current year to August of the subsequent year) from 1899 through 2011. Annual precipitation values were converted into millimeters. Monthly (November-March) air temperature values were averaged across the period 1899–2011.

To compare hydrological conditions (precipitation and PDSI) among climate divisions, single linkage (nearest neighbor) agglomerative clustering based on Pearson correlation coefficients was carried out with SPSS Statistics[5] software, vers. 20.0 (IBM Corp., Armonk, NY). Three clusters of precipitation and PDSI climate divisions from the eastern (FL2–5), central (LA5–9, MS10, AL8, FL1), and western (TX6–10) regions were found along the Gulf Coast. A Mann-Whitney test was used to test differences among correlation coefficients in groups derived from the cluster analysis. When the null hypothesis of no difference was rejected, annual values of precipitation, PDSI, and air temperature from grouped climate divisions were averaged to obtain data sets for each variable by region.

For this study, annual environmental data sets were restricted to the western and central regions (from Texas to Alabama) where data were collected for menhaden. Annual regional anomalies were calculated by subtracting the average value by year from the annual value of wind momentum (north–south and east–west directions) and air temperature. Annual values of air temperature (November–March) and sea level (November–May) were taken for the months that corresponded to the recruitment of Gulf menhaden to inshore nursery habitats and to their early juvenile development. Annual values of precipitation, PDSI, and river flow were calculated for the period September–August, the months of early inshore development. Annual regional anomalies were calculated by subtracting the average value by year from the annual value of river flows.

Meteorological and hydrological data: offshore waters

Hourly SST, wind speed, and wind direction were obtained from offshore monitoring stations (platform 42001, monitored since 1975, and platform 42002, monitored since 1973) maintained by the NOAA National Data Buoy Center (available at website). Hourly values of SST were transformed to daily and monthly values by using averaged values for each of the buoys. To increase the number of available years, we averaged highly correlated (coefficient of correlation $[r]=0.946$, $P<0.001$) monthly values of SST from buoys at both stations. Because of the potential influence of SST on the development of Gulf menhaden larvae, annual average values of SST were calculated for the spawning season of Gulf menhaden (October of the previous year to March of the following year).

For each of the stations, hourly values of wind direction were used to categorize winds as easterlies, westerlies, northerlies, or southerlies. Wind data from each direction were treated separately. Hourly wind speed data were averaged and transformed to daily and monthly values. Hours of recorded winds from each direction were added to obtain monthly values. Because the sampling hours were different among months, the monthly hours for each direction of the wind were divided by the total monthly hours when wind direction was sampled. Monthly values of wind speed and direction were correlated ($r>0.726$, $P<0.001$), and data from both stations were averaged. These data were used to calculate wind stress (T), measured as newtons per square meter:

$$T = \rho \times CD \times U_{10}^2, \quad (1)$$

where ρ (the density of air) = 1.225 kg/m^3;
U_{10} (wind speed in m/sec) = wind speed at 10 m above the water surface; and
CD = the drag coefficient for which Smith (1980) proposed a formula to calculate CD:

$$1000\ CD = 0.44 + (0.063 \times U_{10}). \quad (2)$$

[5] Mention of trade names or commercial companies is for identification purposes only and does not imply endorsement by the National Marine Fisheries Service, NOAA.

The monthly values of T were multiplied by the proportion of monthly hours to obtain wind momentum. To encompass transport-recruitment processes, annual average values of wind momentum (north–south and east–west wind directions) were calculated from October of the previous year to March of the following year, the months when larvae inhabit offshore nursery habitats and early juveniles recruit to estuaries.

Riverine influx of nutrients

The predicted monthly loads of nutrients for the Mississippi River from October 1974 through September 2011 were obtained from the U.S. Geological Survey (USGS, data available from website). Monthly influx of nutrients (in metric tons) for the mainstem Mississippi River Basin was based on approved water quality data near St. Francisville, Louisiana, and represented stream flows from the Mississippi River at Tarbert Landing, Mississippi, and near Knox Landing, Louisiana, and Thebes, Illinois, and from the Ohio River at Metropolis, Illinois. Monthly concentrations of nutrients were averaged for the water year (September of the previous year to August of the following year). Those months covered the period of early offshore and inshore development of Gulf menhaden. The potential conditions limiting the availability of nutrients were evaluated by calculating the annual average ambient N:P ratio in water (Smith, 1984) and by comparing that value with the average value of ambient N:P ratio in phytoplankton (Redfield, 1958).

Biological data

Fishery-independent data on abundances of menhaden postlarvae and juveniles were acquired from BPL samples in Mississippi and Alabama and from seine surveys conducted by state agencies in all the major coastal bay systems of Texas (Texas Parks and Wildlife Commission), Louisiana (Louisiana Department of Wildlife and Fisheries), Mississippi (Mississippi Department of Marine Resources), and Alabama (Alabama Marine Resources monitoring programs) (Table 1). Biological data were analyzed by region (central and western). Within these 2 regions, 19 coastal study areas or bay systems were identified: Lake Borgne–Chandeleur Sound; Breton Sound; Barataria Bay; Terrebonne-Timbalier Bay; Lake Mechant–Caillou Lake; Vermilion Bay; Calcasieu Lake; Biloxi; Mobile Bay; Sabine Lake; Galveston Bay; Cedar Lakes; East Matagorda Bay; West Matagorda Bay; San Antonio Bay; Aransas Bay; Corpus Christi Bay; Upper Laguna Madre; and Lower Laguna Madre.

Data from seine surveys in Alabama, Mississippi, and Louisiana were grouped into a single data set for the central region (sampling gear and protocols used for surveys in these states are similar and follow those of Christmas [1973]), and data from seine surveys in Texas were placed in the western region. Detailed specifications for seine collections are found in SEDAR.[6][7][8][9][10][11] In Alabama and Mississippi, small-mesh BPLs with 1.6-mm-mesh wings and a 750-μ codend were used, and data from sampling with these BPLs were grouped to form a single data set. The BPL is described in Renfro (1963). Catches in BPL hauls comprised late-stage larvae and postlarvae (11–20 mm standard length [SL]); catches in seine hauls were primarily postlarvae and early juveniles (17–49 mm SL). According to Shaw et al. (1988), lengths for postlarval Gulf menhaden range between 15 and 25 mm SL. Transformation to the juvenile stage begins at ~20 mm SL and ends at ~30 mm SL (Suttkus, 1956; Hettler, 1984).

Fishery-independent surveys have been conducted in Texas estuaries from 1977 to the present, in Louisiana since 1986, in Alabama since 1981, and in Mississippi from 1973 to the present. Disparity in survey periods, sampling effort, and areal coverage between years and among and within bay systems complicated comparisons of abundance among and within areas in early years with the result that periods of abundance were restricted to those years with adequate sampling coverage and effort. The following years and months were analyzed for this study: seine data, all states, 1985–2008 (January–August); BPL data, Mississippi and Alabama, 1981–2008 (November–May). Yearly catch was calculated by month and gear mentioned above. Annual catch by station within each bay system was calculated by dividing the total catch by the total number of hauls. To obtain yearly catch for each of the 19 bay systems, the annual catches from the stations within a bay system were added and then divided by the number of stations in that system. The catches from bay systems within a region were added and then divided by the number of bay systems within that region to produce a regional annual catch for relevant gear types. Data were analyzed regionally in a manner that ensured equality across each study area (the same weight was given to each station and each bay system).

The purse-seine fishery for menhaden has been in operation since the late 1940s. Gulf menhaden dominate this fishery, and finescale and yellowfin menhaden compose less than 1% of the annual landing (Ahrenholz, 1981). The fishery is prosecuted from the state

[6] SEDAR (Southeast Data, Assessment, and Review). 2011. Fishery-independent sampling: Alabama. SEDAR27-RD-01, 2 p. [Available at website.]

[7] SEDAR (Southeast Data, Assessment, and Review). 2011. Fishery-independent sampling: Mississippi. SEDAR27-RD-02, 5 p. [Available at website.]

[8] SEDAR (Southeast Data, Assessment, and Review). 2011. Fishery-independent sampling: Florida SEDAR27-RD-03, 57 p. [Available at website.]

[9] SEDAR (Southeast Data, Assessment, and Review). 2011. Fishery-independent sampling: Texas. SEDAR27-RD-04, 11 p. [Available at website.]

[10] SEDAR (Southeast Data, Assessment, and Review). 2011. Fishery-independent sampling: SEAMAP trawl. SEDAR27-RD-05, 6 p. [Available at website.]

[11] SEDAR (Southeast Data, Assessment, and Review). 2011. Fishery-independent sampling: Louisiana. SEDAR27-RD-06, 9 p. [Available at website.]

line between Mississippi and Alabama to as far west as northcentral Texas. Anderson (2007) used mitochondrial DNA to denote a single population in the western GOM and more recent data indicate a single unit stock throughout the northern GOM (Vanderkooy and Smith[4]).

Fishery-dependent data from landings of the reduction purse-seine fishery for Gulf menhaden by age during the period 1964–2010 were obtained from Smith and Vaughan.[12] Descriptions of the fishery-dependent data and the method used to generate that time series are provided in Vaughan et al. (2007). Total landings of Gulf menhaden, numbers and proportions of fish by age per vessel-ton-week (vtw, defined as the net tonnage of a vessel multiplied by the number of weeks that vessel unloaded fish at least one day (Smith, 1991), were used in this study.

Analyses

Annual meteorological data (air temperature and north–south and east–west wind stress), hydrological data (precipitation, PDSI, river flow, sea level, SST, and Mississippi River N:P ratio) and biological data (fishery-independent age-0 abundance of Gulf menhaden in the central region and of menhaden species in western region; fishery-dependent numbers and proportions of Gulf menhaden in commercial landings) were compared among decadal regimes associated with the couplings of AMO cold and NAO negative (average regime: 1964–1970), AMO cold and NAO positive (wet regime: 1971–1994), and AMO warm and NAO negative (dry regime: 1995–2010) phases and among interannual regimes associated with ENSO warm events (wet years: 1963, 1965, 1968–1969, 1972, 1976–1977, 1982, 1986–1987, 1991–1994, 1997, 2002, 2004, 2006, 2009), neutral events (average years: 1962, 1966–1967, 1971, 1978–1981, 1985, 1989–1990, 1995-1996, 2001, 2003), and cold events (dry years: 1964, 1970, 1973–1975, 1983–1984, 1988, 1998–2000, 2005, 2007–2008, 2010). Nonparametric rank-sum tests (Kruskal-Wallis H-test, χ^2 statistic; Mann–Whitney U-test, Z statistic) were performed with SPSS Statistics, vers. 20.0, on the meteorological, hydrological, and biological responses imposed by the coupling of AMO and NAO phases and by ENSO events. To adjust the P-values for multiple comparisons, the alpha level of each individual test was adjusted downward by using the Bonferroni correction method. Linear associations among abiotic variables were checked with the variance inflation factor to quantify the severity of collinearity. This test was performed with linear regression analysis in SPSS, vers. 20.0. To linearize relationships and approximate normality, annual river flows from the western region were logarithmically transformed and annual north–south wind values were cube-root–transformed. All abiotic variables were standardized to a mean of 0 and variance of 1 by subtracting the mean and dividing by the standard deviation.

Two multivariate techniques were used to determine the relationships between abundance of menhaden and climate-related meteorological and hydrological variables. Principal component analysis (PCA) was used on the correlation matrix of abiotic variables to reduce data. The PCA transformed the original set of variables into a smaller set of orthogonal linear combinations of abiotic variables that account for a major portion of the variance in the original set (Chatfield and Collins, 1980; Dillon and Goldstein, 1984). A high number of abiotic variables were reduced to few principal components by using the factor procedure in SPSS Statistics, vers. 20.0. The scree plot was examined to determine where the curve started to flatten between principal components, and only the components with eigenvalues higher than 1 were retained for interpretation. The component scores that were retained were correlated against annual abundances of age-0 Gulf menhaden in BPL and seine hauls in the central region, annual abundances of age-0 menhaden species in seine hauls in the western region, and annual landings (numbers and proportions) of Gulf menhaden by age from offshore waters of the area studied in the northern GOM.

Because abundance determined with BPL surveys in the central region was not linear, those annual values were cube-root–transformed. Covariability between principal components and biotic variables was examined by performing a Pearson correlation analysis in SPSS Statistics, vers. 20.0. To adjust the P-values for multiple correlation analyses, the alpha level of each individual test was adjusted downward with the Bonferroni correction method. In the case of significant correlations, it was assumed that the variables with larger eigenvectors (coefficients of structure or correlations) for the axis were the ones that most influenced the abundance of Gulf menhaden. Further covariability analysis was performed between the actual climate-related meteorological and hydrological variables and data on fishery-independent catches and fishery-dependent landings of menhaden species. The alpha level of each individual test was also adjusted downward with the Bonferroni correction method.

To identify models of climate-related meteorological and hydrological parameters that contributed to the variability in recruitment of menhaden from Alabama through Texas, the retained component scores were used as predictors of fishery-independent catches (abundances of age-0 Gulf menhaden per BPL or seine haul in the central region and abundances of age-0 menhaden species per seine haul in the western region) and fishery-dependent landings (numbers and proportions of age-1 Gulf menhaden per vtw) in an automatic linear modeling procedure in SPSS Statistics, vers. 20.0. A predictive model was developed by regressing fishery-independent recruits to age 0 ($R_{0,t}$) and fishery-dependent recruits to age 1 ($R_{1,t+1}$) on

[12]Smith, J. W., and D. S. Vaughan. 2011. Harvest, effort, and catch-at-age for Gulf menhaden. Southeast Data, Assessment, and Review SEDAR 27-DW05, 28 p. [Available at website.]

principal components (PC) of climate-related meteorological and hydrological parameters in years t with t equal to 1981–2008 for recruits to age 0 and 1964–2010 for recruits to age 1,

$$R_{0,t} = b_0 + b_1 PC_{1,t} + b_2 PC_{2,t} + \varepsilon \text{ and} \quad (3)$$

$$R_{1,t+1} = b_0 + b_1 PC_{t-1} + b_2 PC_{2,t-1} + \varepsilon, \quad (4)$$

where b_0, b_1, and b_2 are estimated parameters; and
error ε is normally distributed $\varepsilon \sim N(0,\sigma^2)$.

To find the best-fitting model, the model selection method of best subsets was used with Akaike's information criterion (AIC; Akaike, 1981). The models with the lowest AIC values were considered most reliable and their coefficients of determination (r^2) were recorded.

Results

Climate-related meteorological and hydrological regimes and population levels of menhaden

Analyses of fishery-independent data Influence of decadal and interannual climate-related meteorological and hydrological regimes on early juveniles of Gulf menhaden was evident. Early juvenile abundances from the BPL surveys in the central region ($Z=-2.212$, $P=0.027$; Fig. 2A) and the N:P ratio of the Mississippi River influx ($Z=-2.520$, $P=0.012$; Fig. 2B) were higher during the decadal wet regime than during the decadal dry regime. During the wet regime, Mississippi River waters had an average N:P ratio closer to the Redfield (1958) ratio of 16:1, a ratio that indicates no limitation in N. During the dry regime, Mississippi River waters had an average N:P ratio of less than 10, a value that usually indicates conditions under which phytoplankton production is nitrogen limited (Ram and Plotkin, 1983; Sakshaug and Olsen, 1986).

Abundance of early juveniles from seine surveys was higher in the central region than in the western region (Texas, $Z=-5.938$, $P<0.001$), supporting the need for a regional analysis of data. Mean ranks of seine catches ($\chi^2=8.814$, $P=0.012$) and air temperature ($\chi^2=7.066$, $P=0.029$) in the western region and of PDSI in the central and western regions ($\chi^2>9.858$, $P<0.007$) were different among ENSO events. Seine catches of early juveniles in the western region ($Z<-2.441$, $P<0.016$; Fig. 3A) and of PDSI in the central region ($Z<-2.620$, $P<0.010$; Fig. 3B) were higher during wet and average ENSO years than during dry ENSO years. In addition, PDSI in the western region was higher during wet ENSO years than during dry ENSO years ($Z=-2.928$, $P=0.003$; Fig. 3C).

With principal component analysis we extracted 5 components of climate-related meteorological and hydrological parameters associated with BPL catches of Gulf menhaden (Table 2). Correlation analysis of BPL catches with the 5 extracted principal components showed that catches of early juvenile Gulf menhaden in BPL hauls in the central region were correlated with the third ($r=-0.494$, $P=0.010$) and fifth ($r=0.624$, $P=0.001$) extracted components. In order of importance, the variables loaded on the third extracted component were air temperature from the central region, north–south and east–west wind directions from offshore waters, NAO from the North Atlantic Ocean, air temperature from the western region, river flow from the central region, and PDSI and precipitation from the western region. In order of importance, the variables loaded on the fifth component extracted were cube-

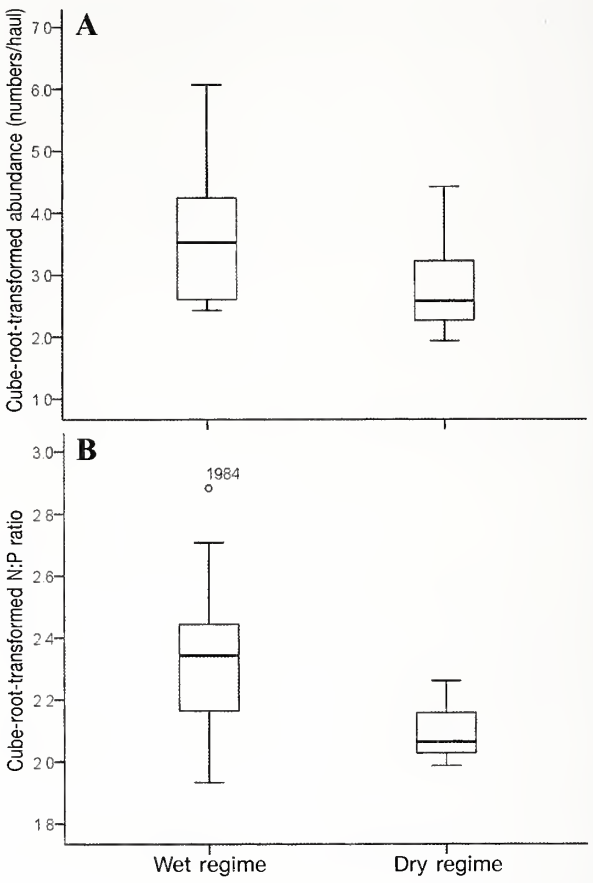

Figure 2

Box plots of (**A**) cube-root–transformed abundance of postlarval Gulf menhaden (*Brevoortia patronus*) in beam plankton trawl (BPL) surveys, measured as numbers per BPL haul (1981–2008), and (**B**) cube-root–transformed N:P ratio of the Mississippi River influx in the central region of the Gulf Coast (1981–2008) under 2 contrasting climate-related hydrological regimes: the wet regime, or the cold phase of the Atlantic Multidecadal Oscillation (AMO) and the positive phase of the North Atlantic Oscillation (NAO) in 1981–1994, and the dry regime, or the AMO warm–NAO negative phase in 1995–2008. Horizontal lines for each box plot indicate the 5th, 25th, 50th (median), 75th, and 95th percentiles. Outliers are shown as dots, and they are labeled by year.

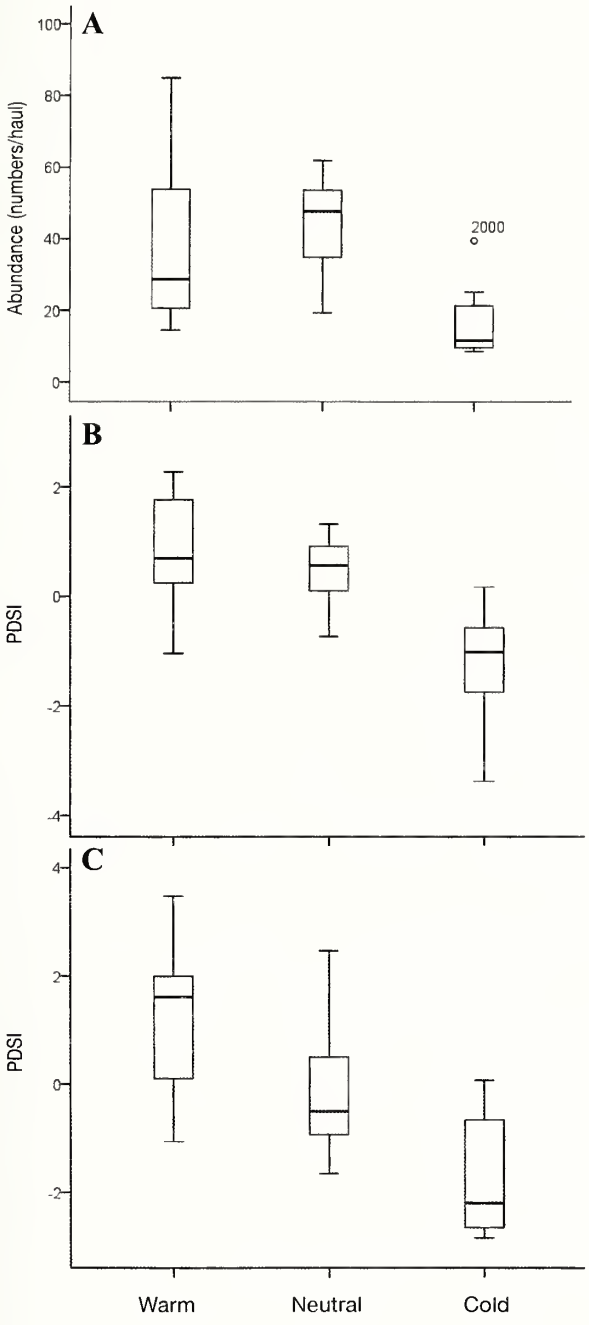

Figure 3

Box plots of (**A**) abundance of early juveniles of menhaden species in seine surveys, measured as numbers per haul, in the western region of the Gulf Coast and Palmer Drought Severity Index (PSDI) in the (**B**) central and (**C**) western regions during the period 1985–2008 under interannual hydrological events associated with the El Niño Southern Oscillation (ENSO). Horizontal lines for each box plot indicate the 5th, 25th, 50th (median), 75th, and 95th percentiles. Outliers are shown as dots, and they are labeled by year.

root–transformed N:P ratio of Mississippi River influx and north–south wind direction. Correlation analysis of BPL catches with the actual environmental variables showed that catches in the BPL hauls were correlated with the cube-root–transformed Mississippi River N:P ratio (r=0.670, P<0.001). Although numbers of early juveniles in seine hauls were not related to any of the extracted components, abundances of early juveniles in seine hauls in the western region were correlated with cube-root–transformed Mississippi River N:P ratio (r=0.591, P=0.002). These results indicate that high (3.6/BPL haul) abundances of age-0 Gulf menhaden from BPL hauls in the central region and high (38.3/seine haul) abundances of age-0 menhaden species from seine hauls in the western region were found during periods of a high (2.3) N:P ratio of Mississippi River influx.

Multiple regression analyses were performed between abundance of Gulf menhaden from fishery-independent BPL surveys and the 5 extracted components. According to the regression models developed from AIC, 2 significant predictors (third and fifth components) with negative and positive regression coefficients, respectively, explained 60% of the variance contained in cube-root–transformed BPL catches of early juvenile Gulf menhaden (Table 3, Fig. 4A). These results indicate that the variability in abundance of age-0 Gulf menhaden was partially explained by climate-related meteorological and hydrological conditions in the northern GOM.

Analyses of fishery-dependent data Mean ranks of commercial harvest (numbers and proportions of age-1 Gulf menhaden; χ^2>7.340, P<0.026) and climate-related hydrological parameters (precipitation, PDSI, river flow, and sea level in the central region and sea level in the western region; χ^2>6.041, P<0.05) were different among the coupling of AMO and NAO phases. Proportions of age-1 Gulf menhaden in landings (Z= −2.982, P=0.003; Fig. 5A), PDSI (Z= −2.429, P=0.015; Fig. 5B), and river flow (Z= −2.595, P=0.009; Fig. 5C) in the central region were higher during the decadal wet regime than during the decadal dry regime. Numbers (Z= −2.673, P=0.008; Fig. 6A) and proportions (Z= −3.274, P=0.001; Fig. 5A) of age-1 fish in landings were higher during the decadal average regime than during the dry regime, but sea level (Z< −2.672, P<0.009) in the western (Fig. 6B) and central (Fig. 6C) regions was lower during the decadal average regime than during the dry regime.

Principal component analysis revealed 3 components of climate-related meteorological and hydrological parameters associated with Gulf menhaden commercial landings (Table 4). Correlation analysis of commercial landings with the 3 extracted principal components showed that landings of age-1 Gulf menhaden were correlated with 1 of the 3 extracted components. Numbers (r= −0.689, P=0.000) and proportions (r= −0.571, P=0.000) of age-1 Gulf menhaden were correlated with the second component. In order of importance, the variables loaded on the second extracted component were

Table 2

The 5 extracted principal components of climate-related meteorological and hydrological variables that are considered to have influenced the variability of catches of Gulf menhaden (*Brevoortia patronus*) in beam plankton trawl (BPL) surveys from 1981 through 2008 in the northern Gulf of Mexico. E–W=east–west; N–S=north–south; N:P=nitrogen to phosphorus ratio. Data were divided into 2 climate regions: central (Louisiana, Mississippi, Alabama, and Florida panhandle) and western (Texas).

		Extracted principal components				
Regions	Variables	1st	2nd	3rd	4th	5th
North Atlantic	North Atlantic Oscillation	0.467		0.549		
Offshore waters	E–W wind direction		0.408	−0.592	0.308	
	N–S wind direction			−0.635	0.474	−0.356
Central region	Cube-root–transformed N:P ratio		−0.375		0.479	0.761
	Sea level	0.535			0.585	
	River flow	0.583	−0.494	0.469		
	Precipitation	0.795	−0.372			
	Palmer Drought Severity Index	0.771	−0.419			
	Air temperature		0.666	0.684		
Western region	Precipitation	0.788		−0.314		
	Palmer Drought Severity Index	0.822		−0.378		
	Cube-root–transformed river flow	0.663	0.398		−0.439	
	Air temperature		0.760	0.482		
	Sea level	0.611	0.638		0.327	
	Eigenvalue	4.269	2.605	2.433	1.368	1.008
	Variance explained (%)	30.489	18.604	17.377	9.774	7.203
	Cumulative variance explained (%)	30.489	49.093	66.470	76.244	83.447

air temperature from the western and central regions, sea level from the western and central regions, and PDSI from the western region.

Correlation analysis of commercial landings with environmental variables showed that numbers and proportions of age-1 Gulf menhaden were correlated with air temperature and sea level in the western region (r< −0.485, P<0.002): high numbers (10 million fish/vtw) and proportions (74%/vtw) were found during periods of low (0.87°C below average) air temperature and (6954 mm) sea level. Low (6.2 million fish/vtw) numbers of age-1 Gulf menhaden were correlated with high (0.47°C above average) air temperature and (7258 mm) sea level (r< −0.446, P<0.003) in the central region. High (74%/vtw) proportions of age-1 Gulf menhaden in fishery landings were correlated with AMO cold years (r= −0.497, P=0.000).

Multiple regression analyses were performed to determine which of the 3 extracted components individually or combined best resembled the variability of fishery-dependent landings of Gulf menhaden. According to the regression models developed from AIC, a significant predictor (second component) with a negative regression coefficient explained 46% of the variance contained in the numbers of age-1 Gulf menhaden (Table 3, Fig. 4B). In addition, 2 significant predictors (first and second components) with positive and negative regression coefficients, respectively, explained 34% of the variance contained in the proportion of age-1 Gulf menhaden in landings (Table 3, Fig. 4C).

Discussion

Differences in responses of menhaden to decadal and annual meteorological and hydrological regimes were evident in this study, providing additional support for the notion that climate plays a role in structuring suitable habitat and, therefore, in survival of larvae and juveniles of menhaden. The specific meteorological and hydrological conditions identified as determinates of abundance estimates, however, differed from those identified in past studies. We found that a high recruitment of menhaden postlarvae (3.6/BPL haul), juveniles (38.3/seine haul), and age-1 fish in landings (10 million/vtw) was associated with cold, wet spawning and recruitment seasons characterized by high PDSI (0.45) and coastal river flow (401.6 m^3/s above average), by a Mississippi River N:P ratio of 2.3, and by low sea level (7065 mm); low recruitment occurred in warm, dry seasons. In contrast, Guillory et al. (1983) found that elevated juvenile recruitment was associated with cold, dry winters and poor recruitment with warm, wet winters. Contradictory results between studies may be related to 1) differences in data selected for analysis, 2) gear types and associated differences in life history stages and habitats, and 3) spatial and temporal differences in the characterization of meteorological and hydrological conditions that drive recruitment of menhaden species.

Data reviewed in the Guillory et al. (1983) and Govoni (1997) studies span what the authors described as

Table 3

Linear models fitted to fishery-independent and fishery-dependent data on Gulf menhaden (*Brevoortia patronus*) in the northern Gulf of Mexico during the periods from 1981 through 2008 and from 1964 through 2010, respectively. BPL=beam plankton trawl; vtw=vessel ton week in the purse-seine fishery; F=F-test; r^2=coefficient of determination; AIC=Akaike's information criterion. Adjusted r^2 would be sufficient.

Model	Response variables	Explanatory variables	df	Sum of squares	F	$P(>F)$	r^2	AIC	Adjusted r^2
1	cube-root–transformed abundance per BPL haul	5th component	1	15.568	19.841	0.000	0.679	–21.5	0.62
		3rd component	1				–0.493		0.21
		Intercept					3.219		
2	Age-1 landing per vtw	2nd component	1	230.728	40.740	0.000	–2.240	83.7	0.46
		Intercept					7.657		
3	Age-1 proportion of total landings per vtw	2nd component	1	0.501	12.344	0.000	–0.100	–179.7	0.33
		1st component					0.032		0.01
		Intercept					0.572		

2 climate periods, a series of years of low river flows followed by years of high river flows. Sanchez-Rubio et al. (2011a) and Sanchez-Rubio and Perry,[13] using climatic indices that spanned the time period preceding and during the low river flow conditions of Guillory et al. (1983) and high river flow period of Govoni (1997), characterized the years during their studies as average (1964–1970) and high (1971–1994) river flow periods. The high river flow regime ended in 1994 and was followed by low river flow conditions brought on by a change in the phases of AMO and NAO in 1995 (Sanchez-Rubio and Perry[13]).

At the decadal scale, Govoni (1997) found increased numbers of Gulf menhaden under conditions of high river flow in the years following 1975. He attributed this increase to enhanced nutrient availability and suggested "discharge of the Mississippi River was positively associated with recruitment over decadal scales." A relationship between decadal oscillations of Mississippi River flow and abundance of another estuarine organism, the blue crab (*Callinectes sapidus*), was reported by Sanchez-Rubio et al. (2011b). Both blue crab and Gulf menhaden in northern GOM estuaries appear to respond positively to wet regimes, although the factors responsible for driving abundances differ between the 2 species. Decreased predation, associated with a reduced predator guild in waters with lowered salinities, was found to be responsible for increased numbers of juvenile blue crab during wet regimes. In this study, decadal abundance of early juvenile Gulf menhaden in the BPL surveys was higher during the decadal cold, wet regime (throughout the coupling of AMO cold and NAO positive phases) characterized by high (2.3) cube-root–transformed N:P ratio of Mississippi River influx than during other considered regimes.

The importance of nutrients to recruitment was evident in this study. The Mississippi River N:P ratio and north–south wind direction explained 41% of variability in abundance of early juvenile Gulf menhaden. In Louisiana, northerly winds produce extremely low tides, high transport of organic material into open waters, and strong upwelling events (Moeller et al., 1993). The contribution of other environmental factors, such as NAO, east–west wind direction in offshore waters, air temperature and river flow in the central region, and PDSI, precipitation, and air temperature in the western region, accounted for 21% of the variability.

Commercial landings also showed decadal fluctuations in the proportion of age-1 Gulf menhaden in relation to the total landings, measured as numbers of fish per vtw. The proportion of age-1 Gulf menhaden in the catch (Alabama–Texas) was significantly higher during the decadal cold, wet regime characterized by high (0.56) values of PDSI and high (401.6 m^3/s above average) river flows in the central region than during the decadal warm, dry regime. A decrease in both early juvenile abundance (fishery-independent surveys) and the proportion of age-1 fish in the commercial landings occurred with the 1995 shift in climate regimes from cold and wet to warm and dry, indicating diminished recruitment over the warm, dry period. Although the abundance of age-1 fish in commercial landings decreased, the numbers of Gulf menhaden of ages 2–6 remained stable with a slight increase observed for age-2 fish (Vanderkooy and Smith[4]). The increase in numbers and relative stability of age-2 fish in commercial landings indicated continued recruitment to the fishery.

[13]Sanchez-Rubio, G., and H. Perry. 2013. Climate-related meteorological and hydrological regimes and their influence on Gulf menhaden (*Brevoortia patronus*) recruitment in the northern Gulf of Mexico: final administrative report, 30 p. Saltonstall-Kennedy project no. NA10NMF4270195. [Available from Office of Management and Budget, Natl. Mar. Fish. Serv., NOAA, 1315 East-West Hwy., Silver Spring, MD.]

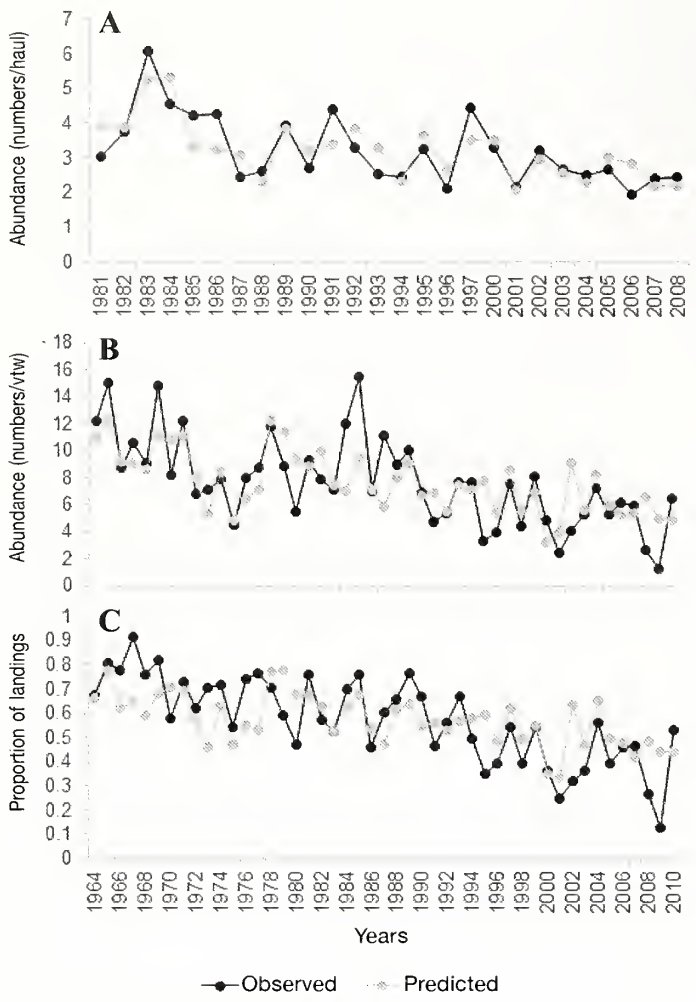

Figure 4

Observed (black line) and predicted (gray line) yearly values for (**A**) numbers of postlarval Gulf menhaden (*Brevoortia patronus*) in surveys conducted with beam plankton trawls (BPLs) during 1981–2008 in Mississippi and Alabama, (**B**) numbers of age-1 Gulf menhaden in commercial landings (millions of fish per vessel-ton/week [vtw]), and (**C**) proportion of age-1 Gulf menhaden in landings per vtw taken in the purse-seine fishery in the northern Gulf of Mexico in 1964–2010.

The steady decreases in age-0 and -1 Gulf menhaden that have been observed since 1964 may have been a function of the fishery-dependent and fishery-independent sampling strategies and changes in the physiography of nearshore environments in the northern GOM. Fixed fishery-independent sampling stations may account for some portion of the perceived decline in abundance of early juvenile Gulf menhaden as fish moved farther up into estuaries in response to elevated salinities (Vanderkooy and Smith[4]). The downward trend of age-1 Gulf menhaden in commercial landings (numbers and proportions) from 1964 to 2010 was accompanied by a steady rise of sea level in the study area. Numbers and proportions of age-1 Gulf menhaden in commercial landings were high (10 million fish/vtw; 74%/vtw) during the decadal average hydrological regime characterized by low (6954 mm) sea level. Proportion of age-1 Gulf menhaden in commercial landings was average (61%/vtw) during the decadal cold, wet regime characterized by high (0.56) PDSI and high (401.6 above average) river flows. Numbers and proportions of age-1 Gulf menhaden in commercial landings were low (6.2 million fish/vtw; 44%/vtw) during the decadal warm, dry regime with high (7016 mm) sea level, low (–0.57) PDSI, and low (247.6 below-average) river flows.

Changes in the physiography of estuaries due to sea level rise and conversion of wetlands to open water may play a major role in structuring inshore nursery habitats for Gulf menhaden, and declining numbers of age-1 fish in the commercial harvest may reflect a response to those changes. The stable numbers of age-2 fish in the commercial harvest indicate that age-1 Gulf menhaden were remaining in nearshore waters and entering the fishery at a later age (SEDAR[3]). Air temperature and sea level in the western and central regions and PDSI in the western region explained 46% and 32% of the variability in numbers and proportions of age-1 Gulf menhaden. Only an additional 1% of the variability in proportion of age-1 Gulf menhaden was explained by adding meteorological and hydrological factors, such as PDSI from the central region and precipitation and river flows from the central and western regions.

The influence of Mississippi River discharge on annual recruitment of Gulf menhaden has been analyzed over the last 30 years. Previous studies found an inverse annual association between Mississippi River discharge (November–March) and estimates of juvenile recruits (Guillory et al., 1983; Govoni, 1997; Vaughan et al., 2000, 2007). Govoni (1997) explained this relationship by suggesting that high flow of the Mississippi River and the resultant plume pushed larvae farther offshore, prolonging shoreward transport of larvae and increasing larval vulnerability to predation. Results of this study indicate a positive association between ENSO-related meteorological (e.g., northerly cold winds) and hydrological (e.g., river discharge and flooding events) conditions and the recruitment of Gulf menhaden—a finding that is contradictory to the results of these previous studies.

The influence of ENSO on recruitment of Gulf menhaden can be explained by its effect in structuring suitable offshore and inshore nursery habitats. In offshore waters, high seaward projection and areal coverage of the nutrient-rich plume of the Mississippi River are

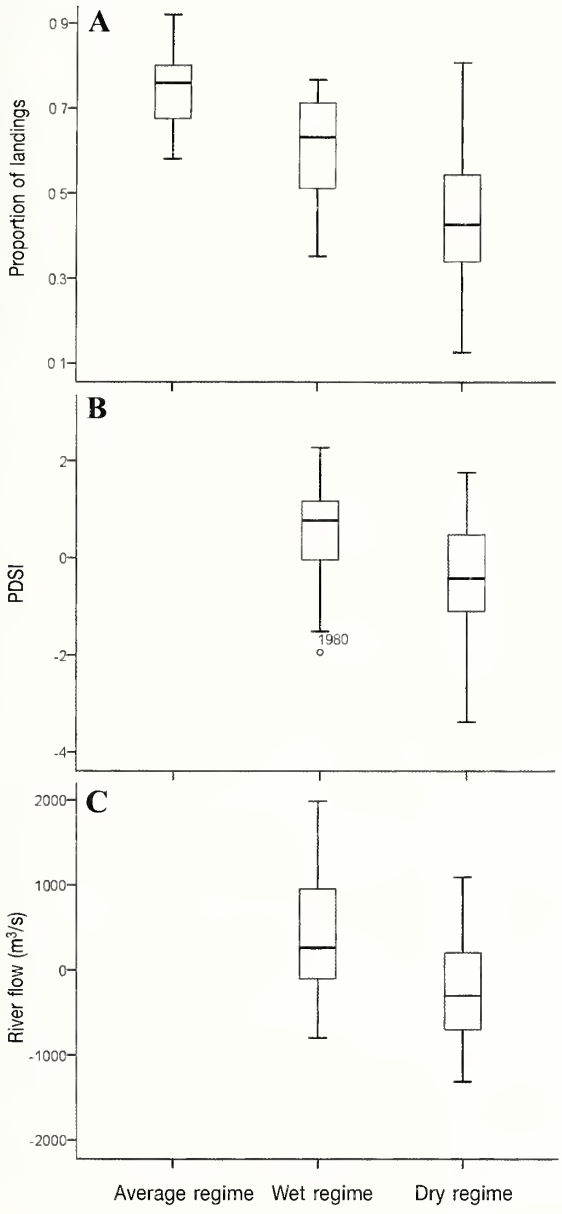

Figure 5

Box plots of (**A**) proportion of age-1 Gulf menhaden (*Brevoortia patronus*) in total landings per vessel-ton-week (vtw) in the purse-seine fishery, (**B**) Palmer Drought Severity Index (PSDI), and (**C**) river flow in the central region during the 3 dominant climate-related hydrological regimes in the Gulf of Mexico: average regime, or the AMO cold–NAO negative phase in 1964–1970; wet regime, or the cold phase of the Atlantic Multidecadal Oscillation (AMO) and the positive phase of the North Atlantic Oscillation (NAO) in 1971–1994; and dry regime, or the AMO warm–NAO negative phase in 1995–2010. Horizontal lines for each box plot indicate the 5th, 25th, 50th (median), 75th, and 95th percentiles. Outliners are shown as dots and they are labeled by year.

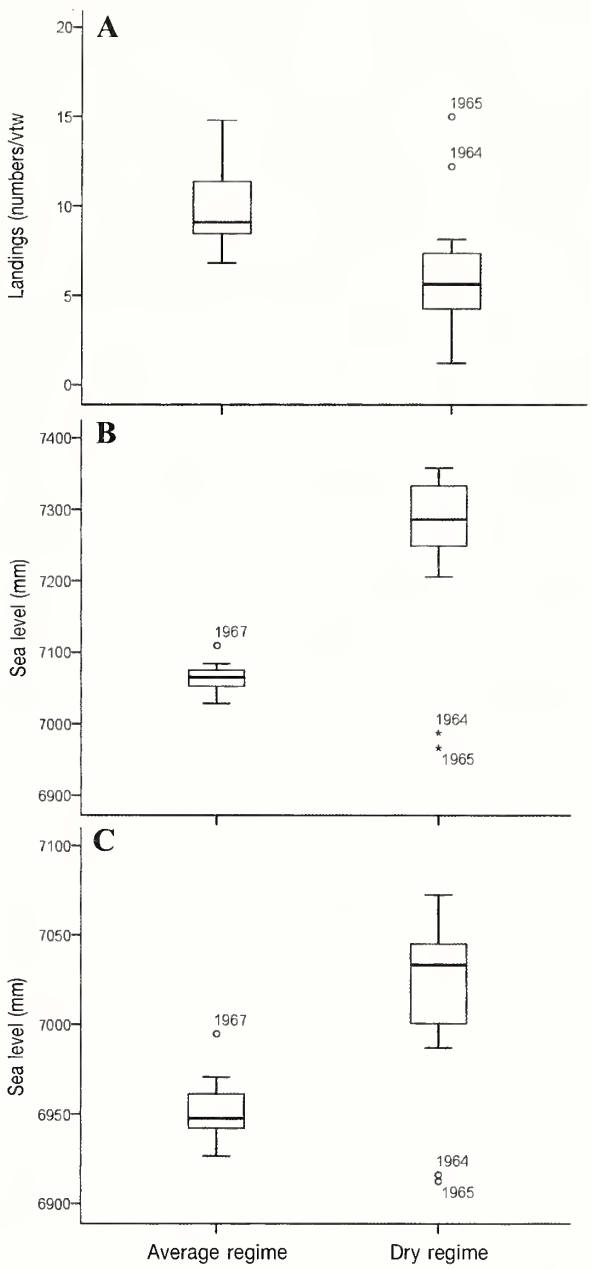

Figure 6

Box plots of (**A**) numbers (millions of fish) of age-1 Gulf menhaden (*Brevoortia patronus*) per vessel-ton-week (vtw) in total landings of the purse-seine fishery in the northern Gulf of Mexico and sea levels in the (**B**) western and (**C**) central regions under decadal climate-related hydrological regimes: average regime, or the cold phase of the Atlantic Multidecadal Oscillation (AMO) and the negative phase of the North Atlantic Oscillation (NAO) in 1964–1970, and dry regime, or the AMO warm–NAO negative phase in 1995–2010. Horizontal lines for each box plot indicate the 5th, 25th, 50th (median), 75th, and 95th percentiles. Outliers are shown as dots, and they are labeled by year.

Table 4

The 3 extracted principal components of climate-related meteorological and hydrological variables that are considered to have influenced the variability of commercial landings (numbers and proportions per vessel ton week) of Gulf menhaden (*Brevoortia patronus*) from 1964 through 2010 in the northern Gulf of Mexico. Data were divided into 2 climate regions: central (Louisiana, Mississippi, Alabama, and Florida panhandle) and western (Texas).

		Extracted principal components		
Regions	Variables	1st	2nd	3rd
Central region	Precipitation	0.776		−0.459
	Palmer Drought Severity Index	0.740		−0.463
	River flow	0.719		−0.563
	Air temperature	0.342	0.855	
	Sea level	0.727	0.533	
Western region	Palmer Drought Severity Index	0.714	−0.381	0.500
	Air temperature		0.940	
	Sea level	0.651	0.578	
	Precipitation	0.689		0.575
	Cube-root–transformed river flow	0.673		0.559
	Eigenvalue	4.173	2.648	1.660
	Variance explained (%)	41.734	26.482	16.596
	Cumulative variance explained (%)	41.734	68.216	84.812

driven by the strong, coastal upwelling and high river flow associated with meteorological (e.g., frequency of cold fronts and, therefore, low air temperatures associated with northerly winds; Henderson and Vega, 1996) and hydrological (e.g., precipitation; Douglas and Englehart, 1981) conditions related to the warm phase of ENSO. These conditions have the potential to enhance larval development and survival of Gulf menhaden (Riley, 1937; Dagg and Whitledge, 1991; Grimes and Finucane, 1991; Hitchcock et al., 1997). In the intertidal zone, extreme winter low tides and cold temperatures associated with meteorological (e.g., northerly cold winds and cold fronts; Henderson and Vega, 1996) conditions related to the ENSO warm phase produce an accumulation of detritus through the die off of marsh grasses (Kirby, 1972; Day et al., 1973). In spring, plant detritus collected during the winter is washed to open waters by flooding events produced by the prevailing southeasterly winds. During this season, juveniles move from the intertidal zone to open waters, where the availability of detritus as a food source becomes crucial for their development and survival (Darnell, 1958).

Acknowledgments

The authors thank V. Guillory, K. Ibos, J. Adriance, P. Cook, and M. Harbison from the Louisiana Department of Wildlife and Fisheries, F. Martinez-Andrade from the Texas Parks and Wildlife Department, L. Hartman from the Marine Resources Division of the Alabama Department of Conservation and Natural Resources, and J. Anderson from the Center for Fisheries Research and Development at the Gulf Coast Research Laboratory, University of Southern Mississippi for providing us with the fishery-independent data used in this study. Commercial landings data were furnished by D. Vaughan and J. Smith of the National Marine Fisheries Service, NOAA. Data used in this publication was assimilated under NOAA 2010 Saltonstall-Kennedy Grant NA10NMF4270195: climate-related hydrological regimes and their influence in Gulf menhaden recruitment in the northcentral GOM.

Literature cited

Ahrenholz, D. W.
1981. Recruitment and exploitation of Gulf menhaden, *Brevoortia patronus*. Fish. Bull. 79:325–335.

Akaike, H.
1981. Likelihood of a model and information criteria. J. Econometrics 16:3–14.

Anderson, J. D.
2007. Systematics of the North American menhadens: molecular evolutionary reconstructions in the genus *Brevoortia* (Clupeiformes: Clupeidae). Fish. Bull. 105:368–378.

Anderson, J. D., and W. J. Karel.
2014. Limited genetic structure of Gulf Menhaden (*Brevoortia patronus*), as revealed by microsatellite markers developed for the genus *Brevoortia* (Clupeidae). Fish. Bull. 112:71–81.

Boschung, H. T. Jr., R. L. Mayden, and J. R. Tomelleri.
2004. Fishes of Alabama, 960 p. Smithsonian Books, Washington, D.C.

Bratkovich, A., S. P. Dinnel, and D. A. Goolsby.
1994. Variability and prediction of freshwater and nitrate fluxes for the Louisiana–Texas shelf: Mississippi and Atchafalaya River source functions. Estuaries 17:766–778.

Chatfield, C., and A. J. Collins.
1980. Introduction to multivariate analysis, 246 p. Chapman and Hall, London.

Christmas, J. Y.
1973. Area description: phase I. *In* Cooperative Gulf of Mexico estuarine inventory and study, Mississippi (J. Y. Christmas, ed.), p. 1–71. Gulf Coast Research Laboratory. Ocean Springs, MS.

Christmas, J. Y., J. T. McBee, R. S. Waller, and F. C. Sutter III.
1982. Habitat suitability models: Gulf menhaden. U.S. Dep. Int. Fish Wildl. Serv. FWS/OBS 82/10.23, 23 p. [Available at website.]

Christmas, J. Y., and R. S. Waller.
1973. Mississippi: estuarine vertebrates. *In* Cooperative Gulf of Mexico estuarine inventory and study, Mississippi (J. Y. Christmas, ed.), p. 320–434. Gulf Coast Research Laboratory, Ocean Springs, MS.

Cochrane, J. D., and F. J. Kelly.
1986. Low-frequency circulation on the Texas-Louisiana shelf. J. Geophys. Res., C 91:10645–10659.

Dagg, M. J., and T. E. Whitledge.
1991. Concentrations of copepod nauplii in the nutrient-rich plume of the Mississippi River. Cont. Shelf Res. 11:1409–1423.Darnell, R. M.
1958. Food habits of fishes and larger invertebrates of Lake Pontchartrain, Louisiana, an estuarine community. Publ. Inst. Mar. Sci., Univ. Texas 5:353–416.

Day, J. W. Jr., W. G. Smith, P. Wagner, and W. Stowe.
1973. Community structure and carbon budget in a salt marsh and shallow bay estuarine system in Louisiana. Sea Grant Publ. LSU-SG-72–04, 80 p. Cent. Wetland Resour., Louisiana State Univ., Baton Rouge, LA.

Deegan, L. A.
1986. Changes in body composition and morphology of young-of-the-year gulf menhaden, *Brevoortia patronus* Goode, in Fourleague Bay, Louisiana. J. Fish Biol. 29:403–415.1990. Effects of estuarine environmental conditions on population dynamics of young-of-the-year gulf menhaden. Mar. Ecol. Prog. Ser. 68:195–205.

Deegan, L. A., and B. A. Thompson.
1985. The ecology of fish communities in the Mississippi River deltaic plain. *In* Fish community ecology in estuaries and coastal lagoons: towards an ecosystems integration (A. Yanez-Arancibia, ed.), p. 35–56. UNAM-ICML Publishers, Mexico City.

Dillon, W. R., and M. Goldstein.
1984. Multivariate analysis: methods and applications, 608 p. John Wiley & Sons, New York.

Dinnel, S. P., and W. J. Wiseman.
1986. Fresh water on the Louisiana and Texas shelf. Cont. Shelf Res. 6:765–784.

Douglas, A. V., and P. J. Englehart.
1981. On a statistical relationship between autumn rainfall in the central equatorial Pacific and subsequent winter precipitation in Florida. Mon. Weather Rev. 109: 2377–2382.

Enfield, D. B., A. M. Mestas-Nuñez, and P. J. Trimble.
2001. The Atlantic Multidecadal Oscillation and its relation to rainfall and river flows in the continental U.S. Geophys. Res. Lett. 28:2077–2080.

Fore, P. L.
1970. Oceanic distribution of eggs and larvae of the Gulf menhaden. *In* Report of the Bureau of Commercial Fisheries Biology Laboratory, Beaufort, N. C., for the fiscal year ending June 30, 1968. U.S. Fish Wildl. Serv. Circ. 341:11–13.

Govoni, J. J.
1993. Flux of larval fishes across frontal boundaries: examples from the Mississippi River plume front and the western Gulf Stream front in winter. Bull. Mar. Sci. 53:538–566.
1997. The association of the population recruitment of gulf menhaden, *Brevoortia patronus*, with Mississippi River discharge. J. Mar. Syst. 12:101–108.

Govoni J. J., D. E. Hoss, and D. R. Colby.
1989. The spatial distribution of larval fishes about the Mississippi River plume. Limnol. Oceanogr. 34:178–187.

Govoni, J. J., and C. B. Grimes.
1992. The surface accumulation of larval fishes by hydrodynamic convergence within the Mississippi River plume front. Cont. Shelf Res. 12:1265–1276.

Grimes, C. B., and J. H. Finucane.
1991. Spatial distribution and abundance of larval and juvenile fish, chlorophyll and macrozooplankton around the Mississippi River discharge plume, and the role of the plume in fish recruitment. Mar. Ecol. Prog. Ser. 75:109–119.

Guillory, V., J. Geaghan, and J. Russel.
1983. Influence of environmental factors of Gulf menhaden recruitment: an update. La. Dep. Wildl. Fish. Tech. Bull. 37, 32 p.

Guillory, V., and J. Roussel.
1981. Seasonal and areal abundance of Gulf menhaden in Louisiana estuaries. Proc. Annu. Conf. Southeast. Assoc. Fish Wildl. Agencies 35:365–371.

Gunter, G.
1945. Studies on marine fishes of Texas. Publ. Inst. Mar. Sci., Univ. Tex. 1:1–190.

Henderson K. G., and A. J. Vega.
1996. Regional precipitation variability in the southern United States. Phys. Geogr. 17:93–112.

Hettler, W. F., Jr.
1984. Description of eggs, larvae, and early juveniles of gulf menhaden, *Brevoortia patronus*, and comparisons with Atlantic menhaden, *B. tyrannus*, and yellowfin menhaden, *B. smithi*. Fish. Bull. 82:85–95.

Hitchcock, G. L., W. J. Wiseman Jr., W. C. Boicourt, A. J. Mariano, N. Walker, T. A. Nelsen, and E. Ryan.
1997. Property fields in an effluent plume of the Mississippi River. J. Mar. Syst. 12:109–126.

Hurrell, J. W., and H. Van Loon.
1997. Decadal variations in climate associated with the North Atlantic Oscillation. Clim. Change 36:301–326.

Kirby, C. J.
1972. The annual net primary production and decomposition of the salt marsh grass *Spartina alterniflora* Loisel in the Barataria Bay estuary of Louisiana. Ph. D. diss., 81 p. Louisiana State Univ., Baton Rouge, LA.

Lohrenz, S. E., M. J. Dagg, and T. E. Whitledge.
1990. Enhanced primary production at the plume/oceanic interface of the Mississippi River. Cont. Shelf Res. 10:639–664.

Madden, C. J., J. W. Day Jr., and J. M. Randall.
1988. Freshwater and marine coupling in estuaries of the Mississippi River deltaic plain. Limnol. Oceanogr. 33:982–1004.

Moeller, C. C., O. K. Huh, H. H. Roberts, L. E. Gumley, and W. P. Menzel.
1993. Response of Louisiana coastal environments to a cold front passage. J. Coast. Res. 9:434–447.

Ram, N. M., and S. Plotkin.
1983. Assessing aquatic productivity in the Housatonic River using the algal assay bottle test. Water Res. 17:1095–1106.

Redfield, A. C.
1958. The biological control of chemical factors in the environment. Am. Sci. 46:205–222. [Available at website.]

Reintjes, J. W.
1970. The Gulf menhaden and our changing estuaries. Proc. Gulf Caribb. Fish. Inst. 22:87–90.

Renfro, W. C.
1963. Small beam net for sampling postlarval shrimp. *In* Biological Laboratory, Galveston, Tex., fishery research for the year ending June 30, 1962, p. 86–87. U.S. Fish Wildl. Serv. Circ. 161. [Available at website.]

Riley, G. A.
1937. The significance of the Mississippi River drainage for biological conditions in the northern Gulf of Mexico. J. Mar. Res. 1:60–74.

Rogers, J. C., and J. S. M. Coleman.
2003. Interactions between the Atlantic Multidecadal Oscillation, El Niño/La Niña, and the PNA in winter Mississippi Valley stream flow. Geophys. Res. Lett. 30:1518.

Sakshaug, E., and Y. Olsen.
1986. Nutrient status of phytoplankton blooms in Norwegian waters and algal strategies for nutrient competition. Can. J. Fish. Aquat. Sci. 43:389–396.

Sanchez-Rubio, G., H. M. Perry, P. M. Biesiot, D. R. Johnson, and R. N. Lipcius.
2011a. Oceanic–atmospheric modes of variability and their influence on riverine input to coastal Louisiana and Mississippi. J. Hydrol. 396:72–81.
2011b. Climate-related hydrological regimes and their effects on abundance of blue crabs (*Callinectes sapidus*) in the northcentral Gulf of Mexico. Fish. Bull. 109:139–146.

Shaw, R. F., B. D. Rogers, J. H. Cowan Jr., and W. H. Herke.
1988. Ocean-estuary coupling of ichthyoplankton and nekton in the northern Gulf of Mexico. Am. Fish. Soc. Symp. 3:77–89.

Shaw, R. F., W. J. Wiseman Jr., R. E. Turner, L. J. Rouse Jr., R. E. Condrey, and F. J. Kelley.
1985. Transport of larval gulf menhaden *Brevoortia patronus* in continental shelf waters of western Louisiana: a hypothesis. Trans. Am. Fish. Soc. 114:452–460. Article

Smith, J. W.
1991. The Atlantic and gulf menhaden purse fisheries: origins, harvesting technologies, biostatistical monitoring, recent trends in fisheries statistics, and forecasting. Mar. Fish. Rev. 53:28–39.

Smith, S. D.
1980. Wind stress and heat flux over the ocean in gale force winds. J. Phys. Oceanogr. 10:709–726.

Smith, S. V.
1984. Phosphorus versus nitrogen limitation in the marine environment. Limnol. Oceanogr. 29:1149–1160.

Sogard, S. M., D. E. Hoss, and J. J. Govoni.
1987. Density and depth distribution of larval gulf menhaden, *Brevoortia patronus*, Atlantic croaker, *Micropogonias undulatus*, and spot, *Leiostomus xanthurus*, in the northern Gulf of Mexico. Fish. Bull. 85:601–609.

Suttkus, R. D.
1956. Early life history of the Gulf menhaden, *Brevoortia patronus*, in Louisiana. Trans. N. Am. Wildl. Conf. 21:390–407.

Tootle, G. A., and T. C. Piechota.
2006. Relationships between Pacific and Atlantic ocean sea surface temperatures and U.S. streamflow variability. Water Resour. Res. 42, W07411.

Tolan, J. M., and D. A. Newstead.
2004. Descriptions of larval, prejuvenile, and juvenile finescale menhaden (*Brevoortia gunteri*) (family Clupeidae) and comparisons to gulf menhaden (*B. patronus*). Fish. Bull. 102:723–732.

Tootle, G. A., T. C. Piechota, and A. Singh.
2005. Coupled oceanic-atmospheric variability and U.S. streamflow. Water Resour. Res. 41, W12408.

Vaughan, D. S., J. J. Govoni, and K. W. Shertzer.
2011. Relationship between Gulf menhaden recruitment and Mississippi River flow: model development and potential application for management. Mar. Coast. Fish. 3:344–352.

Vaughan, D. S., K. W. Shertzer, and J. W. Smith.
2007. Gulf menhaden (*Brevoortia patronus*) in the U.S. Gulf of Mexico: fishery characteristics and biological reference points for management. Fish. Res. 83:263–275.

Vaughan, D. S., J. W. Smith, and M. H. Prager.
2000. Population characteristics of Gulf menhaden, *Brevoortia patronus*. NOAA Tech. Rep. NMFS 149. 19 p.

Wiseman, W. J. Jr., and R. W. Garvine.
1995. Plumes and coastal currents near large river mouths. Estuaries 18:509–517.

Wiseman, W. J. Jr., and F. J. Kelly.
1994. Salinity variability within the Louisiana coastal current during the 1982 flood season. Estuaries 17: 732–739.

Wright L. D., and J. M. Coleman.
1971. Effluent expansion and interfacial mixing in the presence of a salt wedge, Mississippi River delta. J. Geophys. Res. 76:8649–8661.

NOAA
National Marine
Fisheries Service

Fishery Bulletin
established 1881

Spencer F. Baird
First U.S. Commissioner
of Fisheries and founder
of Fishery Bulletin

Per-recruit stock assessment of wahoo (*Acanthocybium solandri*) in the southwest Pacific Ocean

Mitchell T. Zischke (contact author)[1,2]
Shane P. Griffiths[2]

Email address for contact author: mitchell.zischke@gmail.com

[1] School of Biological Sciences
The University of Queensland
Brisbane, Queensland 4072, Australia
Present address: Purdue University
Department of Forestry and Natural Resources
195 Marsteller St
West Lafayette, Indiana 47907, United States

[2] Oceans and Atmosphere Flagship
Commonwealth Scientific and Industrial Research Organisation
GPO Box 2583
Dutton Park, Queensland 4102, Australia

Abstract—A stock assessment incorporating sensitivity in biological parameters and potential fishery management strategies for wahoo (*Acanthocybium solandri*) in the southwest Pacific Ocean was undertaken to assess the stock status of this species for 2008–2010. Selectivity probabilities at age were similar for 2 commercial longline fisheries and a recreational sport fishery. However, the median exploited length and age were slightly higher in the commercial fisheries than in the recreational fishery. Current fishing mortality ($F_{current}$) was predicted to be lower than limit and target reference points, with the exception that $F_{current}$ exceeded the target reference point F_{SSB40} (fishing mortality at which the spawning stock biomass per recruit [SSB/R] is 40% of the SSB/R at F=0). This result indicates that wahoo may be at a greater risk of recruitment overfishing than of growth overfishing. Of the fishery management scenarios tested, introduction of a slot limit in the recreational fishery had the greatest effect on assessment results; however, this effect was relatively minor and may not be practical to implement. Given the relatively short life span of wahoo, ongoing biological monitoring and rigorous collection of catch and effort data may facilitate continued assessment of this species in the southwest Pacific Ocean.

Manuscript submitted 20 March 2014.
Manuscript accepted 21 July 2015.
Fish. Bull. 113:407–418 (2015)
Online publication date: 10 August 2015.
doi: 10.7755/FB.113.4.4

Wahoo (*Acanthocybium solandri*) is a pelagic scombrid with a tropical and subtropical distribution in oceanic waters worldwide (Collette and Nauen, 1983). This species is caught incidentally and retained as a byproduct in commercial pelagic longline, purse-seine, and trolling fisheries that target tunas and mackerels (Scombridae), broadbill swordfish (*Xiphias gladius*), and dolphinfishes (*Coryphaena* spp.) (Zischke, 2012). The average annual global catch of wahoo in these fisheries has remained around 3000 metric tons (t) since 1996 (Global Production Statistics 1950–2012, FAO, available at website, accessed October 2012). Commercial catches in the Pacific Ocean have increased 10-fold over the past 15 years (Global Production Statistics 1950–2012, FAO) because of increases in effort in tuna fisheries in this region. Wahoo is also an important target and nontarget species in subsistence and artisanal fisheries, as well as a prized catch in recreational fisheries throughout the western Pacific Ocean (Zischke, 2012). Although catch and effort data from subsistence, artisanal, and recreational fisheries are scarce, evidence indicates that the recreational catch of wahoo may exceed the commercial catch off eastern Australia (Zischke et al., 2012), as has been reported for the Atlantic Ocean (SAFMC[1]).

Off eastern Australia, wahoo are retained as byproduct in the Commonwealth-managed Eastern Tuna and Billfish Fishery (ETBF). The ETBF is a pelagic longline fishery with a quota on species that include albacore (*Thunnus alalunga*), yellowfin tuna (*T. albacares*) and bigeye tuna (*T. obesus*), as well as broadbill

[1] SAFMC (South Atlantic Fishery Management Council). 2003. Fishery management plan for the dolphin and wahoo fishery of the Atlantic including a final environmental impact statement, regulatory impact review, initial regulatory flexibility analysis, and social impact assessment/fishery impact statement, 308 p. SAFMC, Charleston, SC. [Available at website].

swordfish and striped marlin (*Kajikia audax*) (AFMA[2]). The mean annual catch of wahoo in the ETBF has been 20.1 t (standard error [SE] 2.7) over the last 15 years, and the majority of catch has been derived from the northeastern area of Australia's Exclusive Economic Zone (EEZ) (AFMA[3]). Apart from an arbitrary combined possession limit for wahoo, butterfly mackerel (*Gasterochisma melampus*) and slender tuna (*Allothunnus fallai*) of 20 fish per trip (AFMA[2]), no species-specific assessment or management framework exists for wahoo in this fishery. Wahoo also are caught in low quantities (<5 t annually) in state-managed trolling fisheries that target narrow-barred Spanish mackerel (*Scomberomorus commerson*) in Queensland and New South Wales (DAF[4]; DPI[5]).

Elsewhere in the southwest Pacific Ocean, wahoo are retained as byproduct in the commercial pelagic longline fishery of New Caledonia, which targets species similar to those targeted by the ETBF. Catch of wahoo in this fishery is similar to the ETBF, with a mean annual catch of 25.1 t (SE 3.5) since 1997. No management measures exist for wahoo in this fishery.

Specialized recreational fisheries exist for wahoo off eastern Australia, and, although total catch is poorly understood, recent evidence indicates that it may be equal to or exceed the total commercial catch in some regions (Zischke et al., 2012). Management measures for recreational fisheries differ by state: a minimum legal length of 75 cm in total length (TL) and a possession limit of 2 fish per person has been mandated in Queensland (according to the Queensland Fisheries Regulation 2008) but there is no minimum legal length and a possession limit of 5 fish per person in New South Wales (according to the New South Wales Fisheries Management [General] Regulation 2010).

Wahoo are low priority as a commercial species, a status that is likely to be responsible for the lack of biological research on the species that has hindered the undertaking of rigorous stock assessments (Zischke, 2012). However, preliminary stock assessments have been completed for wahoo in the Atlantic Ocean and the waters off Taiwan. The Atlantic assessment in 2000 considered wahoo in the subtropical western North Atlantic, Caribbean, and Gulf of Mexico to be a single stock and used median annual catch as a proxy for fishing mortality (F) to indicate a maximum sustainable yield (MSY) of 640–740 t, but an assessment of the current status of the stock was not undertaken (SAFMC[1]). In the waters off Taiwan, an age-structured model was used in 2007 to assess the current fishing mortality ($F_{current}$) against the reference points of 1) fishing mortality at which the slope of the yield-per-recruit (Y/R) curve is 10% of the slope at the origin ($F_{0.1}$) and 2) the fishing mortality at which the spawning stock biomass per recruit (SSB/R) is 40% of the SSB/R at F=0 (F_{SSB40}) obtained from a Y/R model, and results from that model indicated that wahoo were being fished at sustainable levels (Lee, 2008).

Despite exploitation by multiple fishing sectors and an increasing commercial catch in the southwest Pacific Ocean, no stock assessment has been completed for wahoo in this region. Recent research has provided comprehensive information on the stock structure, age, growth, and reproductive biology of this species in this region (Zischke et al., 2013a; 2013b; 2013c). Wahoo grow quickly and reach sexual maturity at less than 1 year old (Zischke et al., 2013a; 2013b). Most wahoo in fisheries catches, and their populations in general, are 1–2 years old. Biological data, in conjunction with fishery data from Australia and New Caledonia, were used to conduct the first stock assessment for wahoo in the southwest Pacific Ocean, and we present the results here. The objectives of the present study were 1) to apply an age-structured per-recruit model to the wahoo stock, 2) to examine the sensitivity of the population status derived by a per-recruit model after incorporating variability in biological parameters, and 3) to investigate potential management strategies for ensuring the long-term sustainability of wahoo in this region.

Materials and methods

Study area

The global stock structure of wahoo is uncertain. Although the species is reputed to exist as a single panmictic population worldwide (Theisen et al., 2008), recent evidence suggests that wahoo may exist as multiple phenotypic populations throughout the Pacific Ocean (Zischke et al., 2013c). A fine-scale, spatially explicit analysis of morphometrics and parasites has indicated that wahoo off eastern Australia form part of a single stock in the southwest Pacific Ocean (Zischke et al., 2013c). Because the geographic extent of this stock has not been resolved, we have adopted a precautionary approach, defining the stock for assessment as consisting of wahoo from the EEZ off eastern Australia and the EEZ of New Caledonia (Fig. 1).

Fishery data used for stock assessment

Limited catch and effort data are available for wahoo in the southwest Pacific Ocean because wahoo are not targeted in any commercial fisheries and are taken as part of the specialized recreational sport fishery in this region (Zischke, 2012; Zischke et al., 2012). In the

[2] AFMA (Australian Fisheries Management Authority). 2011. Eastern Tuna and Billfish Fishery (ETBF) management arrangements booklet: 2011 fishing season, 31 p. AFMA, Canberra, Australia. [Available at website].

[3] AFMA (Australian Fisheries Management Authority). 2011. Unpubl. data. [Eastern Tuna and Billfish Fishery commercial logbook data.] AFMA, Canberra, 2610, Australia.

[4] DAF (Department of Agriculture and Fisheries). 2011. Unpubl. data. [Queensland commercial and charter fisheries logbook data.] Queensland DAF, Brisbane, 4001, Australia.

[5] DPI (Department of Primary Industries). 2011. Unpubl. data. [New South Wales commercial fisheries logbook data.] New South Wales DPI, Port Stephens, 2316, Australia.

ETBF, catch, effort, and CPUE (catch per unit of effort) data for wahoo has been recorded in commercial logbooks since 1996 (AFMA[3]). Similarly, in the commercial pelagic longline fishery in New Caledonia, logbook data have been recorded since 1997 (SPC[6]).

In addition to catch and effort data in commercial longline fisheries, size composition data are available for most fisheries. For Australian fisheries, onboard scientific observers from the Australian Fisheries Management Authority have recorded size composition data for wahoo in the ETBF since 2002. No catch and effort data are available from recreational fisheries. However, limited size composition data from the recreational fishery off eastern Australia (EC Rec) are available from an on-site survey of this fishery in 2010 (Zischke et al., 2012), as well as from a volunteer tagging program since 1973 (DPI[7]). Limited size composition data from commercial and recreational fisheries off eastern Australia also are available from biological research conducted between 2008 and 2011 (Zischke et al., 2013a; 2013b). To supplement data from Australian fisheries, size composition data were obtained from observers and port samplers in the fishery in New Caledonia (SPC[6]).

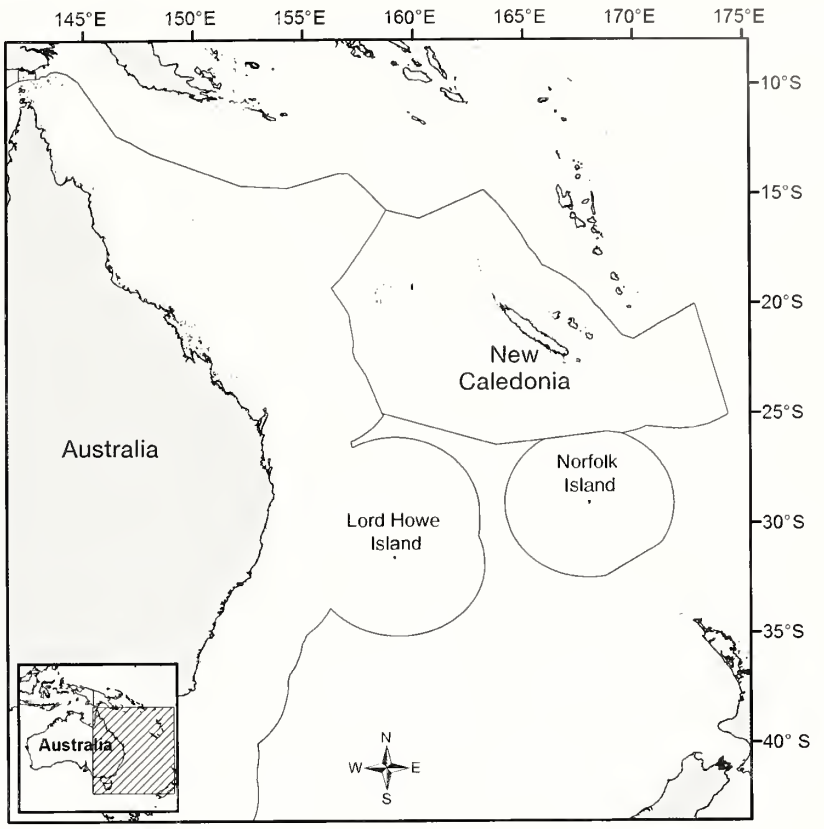

Figure 1

Map of the southwest Pacific Ocean with the exclusive economic zones of Australia (including Lord Howe and Norfolk islands) and New Caledonia indicated by the solid lines. Data for the per-recruit assessment were collected throughout these zones.

Size composition data from all fisheries were restricted to the period 2008–2010 for all analyses because biological data were collected during this period. Age distributions were calculated by converting fork length (FL) to age with a von Bertalanffy growth function reported by Zischke et al., 2013b (Table 1), who noted that age could not be calculated for any fish with an FL greater than the maximum theoretical fork length (L_∞) because such a fish would be assigned an infinite age.

Estimation of mortality

Natural mortality is a key component of fish stock dynamics because it directly influences the productivity of a stock and the optimum fishery yield that can be obtained. One of the most reliable methods for estimating the natural mortality of a stock is through mark-recapture experiments (Vetter, 1988). However, such experiments are expensive to implement and require extensive fishing effort to ensure high numbers of initial marking and adequate recaptures for analysis. Mark-recapture work was outside the scope of this study; therefore, 2 empirical equations were used to provide estimates of natural mortality (M) of wahoo in the southwest Pacific Ocean.

The first model was that of Pauly (1980):

$$\mathrm{Log}M = -0.0066 - 0.279\log L_\infty + 0.6543\log K + 0.4634\log T, \quad (1)$$

where L_∞ and K = von Bertalanffy growth parameters (Table 1), respectively (Zischke et al., 2013b); and

T = the mean sea-surface temperature off eastern Australia at 22.9°C (CSIRO[8]).

The second model used to estimate M was that of Hoenig (1983):

$$M = \frac{-\ln(0.01)}{t_m}, \quad (2)$$

[6] SPC (Secretariat of the Pacific Community). 2011. Unpubl. data [Commercial fisheries logbook data.] SPC, 98848 Noumea, New Caledonia.

[7] DPI (Department of Primary Industries). 2011. Unpubl. data [Gamefish Tagging Program tagging data.] New South Wales DPI, Port Stephens, 2316, Australia.

[8] CSIRO (Commonwealth Scientific and Industrial Research Organisation). 2012. Unpubl. data. [Sea-surface temperature data.] CSIRO, Dickson ACT 2602, Australia.

Table 1

Means and 95% confidence intervals (CI) for biological parameters used in the stock assessment of wahoo (*Acanthocybium solandri*) in the southwest Pacific Ocean during 2008–2010. TL=total length, FL=fork length, W_B=body weight, VBGF=von Bertalanffy growth function, L_t=length at time t, and m_L=maturity at length. Length, weight, and VBGF parameters (L_∞, K, and t_0) were obtained from Zischke et al. (2013b), and maturity parameters were obtained from Zischke et al. (2013a).

Model	Equation	Parameter	Mean	95% CI
TL (mm) and FL (mm)	$TL = aFL + b$	a	1.01	1.00–1.02
		b	34.97	26.23–43.71
W_B (g) and FL(mm)	$\mathrm{Log}W_B = a\mathrm{Log}FL + b$	a	3.28	3.20–3.36
		b	−13.95	−14.01–13.89
VBGF 1465.80–1531.50	$L_t = L_\infty[1 - e^{-K(t - t_0)}]$	L_∞	1498.65	
		K	1.58	1.23–1.93
		t_0	−0.17	−0.35–0.01
Maturity	$m_L = \frac{e^{-a+bL_F}}{1+e^{-a+bL_F}}$	a	−16.98	−22.25–−11.71
		b	0.02	0.01–0.02

where t_m = a maximum age of 7 years (Zischke et al., 2013b). In the absence of exploitation, it was assumed that 1% of fish in the population would reach t_m (Quinn and Deriso, 1999). An estimate of 7 years for t_m was based on the maximum observed age in a biological study in the southwest Pacific Ocean (Zischke et al., 2013b). However, because wahoo may reach an age greater than that observed in the study by Zischke et al. (2013b), and have undergone exploitation by commercial and recreational fisheries for at least 15 years, this estimate should be viewed with caution.

Age-based catch curves are often used to estimate the annual instantaneous mortality rate (Z) according to the description of Beverton and Holt (1957). However, for tropical species that have fast growth and a short lifespan, length-converted catch curves may be more useful (Sparre et al., 1989). Therefore, length-frequency data from the 3 fisheries (i.e., the 2 commercial fisheries, ETBF and New Caledonia, and the EC Rec) were used to construct length-converted catch curves according to the methods of Pauly (1983, 1984a, 1984b). Size-frequency data were converted to age-frequency data with the von Bertalanffy growth parameters (Table 1; Zischke et al., 2013b).

Selectivity may differ with fish size or age, as well as with different fisheries, especially for those fisheries that use different gear types. Total mortality at age (Z_t) can be expressed in an equilibrium state in this way:

$$Z_t = M_t + S_t^{\mathrm{ETBF}} F_t^{\mathrm{ETBF}} + S_t^{\mathrm{EC\ Rec}} F_t^{\mathrm{EC\ Rec}} + S_t^{\mathrm{New\ Cal}} F_t^{\mathrm{New\ Cal}}, \quad (3)$$

where M_t = the natural mortality at age t; and
S_t and F_t = the selectivity and fishing mortality at age for the ETBF, EC Rec, and New Caledonia (New Cal) fisheries, respectively.

Selectivity at age in each fishery was estimated with standard linear length-converted catch curves by using backward extrapolation of the descending regression line to include younger fish that were likely to be under-represented in catches (Sparre et al., 1989). All fisheries in this study were hook-and-line fisheries, which tend to have selectivity probabilities that follow a logistic function because the fishing gear is capable of catching any fish larger than the size at which all fish are recruited to the fishery (Hovgard and Lassen, 2000). Therefore, the selectivity (S_t) at age (t) in each fishery was determined with the following equation:

$$S_t = \frac{1}{1+e^{a+bt}}, \quad (4)$$

where a = the intercept; and
b = the slope of a linear regression line fitted to the observed selection at age (Sparre et al., 1989).

Numbers of fish in each age class for each fishery were adjusted according to their respective selectivity probability before the catch-curve analysis. Given the similar selectivity of the 3 fisheries (see *Results* section), an estimate of Z was obtained from the slope of a linear regression line fitted to a length-converted catch curve for all fisheries combined, and instantaneous F was calculated as $F=Z-M$.

Per-recruit analysis

The Y/R and SSB/R of wahoo in the southwest Pacific Ocean were assessed by using the model of Quinn and Deriso (1999). This model defines the age-specific exploitation fraction (μ_t) in this manner:

$$\mu_t = \frac{F_t}{F_t + M}(1 - e^{-\Delta t(F_t + M)}), \quad (5)$$

where Δt = the change in age; and
F_t = the fishing mortality at age, which is a product of fishing mortality and selectivity at age for each fishery:

$$F_t = \sum_j S_{t,j} F_j = \sum_j F_{t,j}, \quad (6)$$

where $S_{t,j}$ = the selectivity at age; and
F_j = the fishing mortality of the jth fishery (Quinn and Deriso, 1999).

A recent reproductive study for wahoo off eastern Australia reported the FL at which 50% of females are mature (L_{50}) as 1046 mm, which corresponds to an age at 50% maturity (A_{50}) of approximately 7 months (Zischke et al., 2013a). No estimate of L_{50} was reported for male wahoo; however, as growth parameters do not differ significantly between sexes (Zischke et al., 2013a), it is assumed to be similar to that of females. The maturity-at-length (m_L) logistic function reported in this study was used to calculate SSB/R (Table 1).

Wahoo are exploited by multiple fisheries, including recreational sport fisheries that often practice catch and release; therefore, it is important to account for the effect of discard mortality on stock biomass. Discard mortality is the product of the probability that a fish is discarded and the probability that, if released, the fish still dies because of the physiological stress of capture. Discard mortality at age (H_t) is likely to be fishery specific, where the fishing mortality for the jth fishery (F'_j) can be expressed with the following equation:

$$F'_j = -\ln(1 - H_{t,j}(1 - e^{-F_{t,j}})), \quad (7)$$

where $F_{t,j}$ = a product of the fishing mortality at age and the selectivity at age (Quinn and Deriso, 1999; see Eq. 6).

Postrelease mortality is expensive to evaluate, particularly for large oceanic fishes, and there is currently no species-specific estimate for wahoo. Two electronic tagging studies of wahoo have reported relatively low levels of postrelease mortality. Theisen (2007) deployed pop-up satellite archival tags on 3 wahoo in the Atlantic Ocean, and all fish survived more than 5 days after release, a time period that is often used to assess postrelease mortality (Domeier et al., 2003; Kerstetter and Graves, 2006). In the eastern Pacific Ocean, Sepulveda et al. (2011) deployed 108 archival tags on wahoo caught by using recreational fishing techniques and had up to 62% tag recovery in areas with high fishing effort. These results indicate that postrelease mortality may be relatively low. Similarly, for juvenile bluefin tuna (*T. thynnus*), another scombrid, in the Atlantic Ocean, Skomal et al. (2002) reported postrelease mortality of 28% when recreational fishing techniques were used. As such, we assumed the postrelease mortality of wahoo from the EC Rec was also 28%. Approximately 6–38% of wahoo were reported as released by the EC Rec (Zischke et al., 2012). Assuming a mean release percentage of 20%, combined with a postrelease mortality of 28%, the percentage of fish at age t incurring mortality in the EC Rec fishery is 86%, or H_t=0.86.

Discard mortality may be higher for pelagic longline fisheries because a large proportion of fish are already dead once they are hauled onto a vessel (Kerstetter and Graves, 2008). Observer data from the ETBF were investigated to identify the life status of wahoo upon hauling—ranging from dead and in rigor mortis to alive and vigorous. Less than 10% of wahoo were alive (sluggish or vigorous) upon hauling, and only 3% of all wahoo were released. As such, it was assumed that 100% of longline-caught fish died (H_t=1.0).

Per-recruit analysis was undertaken by using an age-structured virtual population model with 1-month time intervals to capture the variability in the biological dynamics of wahoo (e.g., growth and maturity) that occurs primarily within the first year of life (Zischke et al., 2013a; Zischke et al., 2013b). To assess the status of the wahoo stock in the study area, $F_{current}$ was compared with 2 limit and 2 target reference points. From the Y/R analysis, the limit reference point was the fishing mortality at which maximum Y/R is produced (F_{max}), and the target reference point was $F_{0.1}$. For the SBB/R analysis, the limit and target reference points were defined as the fishing mortality at which the SSB/R is 25% of the SSB/R at F=0 (F_{SSB25}) and as F_{SSB40}, respectively.

Sensitivity and management simulations

A sensitivity analysis was conducted to examine the effect of variability in growth and maturity estimates on Y/R and SSB/R. Rather than use mean biological parameters, new parameters were randomly selected from a normal distribution defined by the mean and standard error for each parameter (Table 1). Randomly selected parameters were used in all subsequent calculations, including M (Eq.1 only), catch-curve analysis, selectivity, and the per-recruit analysis. To investigate uncertainty in stock assessment outputs under this scenario (S1), 100 model iterations were conducted. With this scenario, M is assumed to be constant throughout the life of a fish; however, M has been shown to vary ontogenetically in pelagic tunas and may be an order of magnitude higher for small fishes (Hampton, 2000). To examine variable mortality for wahoo, we also ran a scenario (S2) in which natural mortality at age was set at an order of magnitude higher for fish 0–2 months old and mortality for all other age classes (i.e., >2 months old) remained unchanged.

To assess the efficacy of potential fishery management measures, a number of model scenarios were explored with the same iterative approach outlined previously. Currently, the only size restriction for wahoo in any Australian recreational fishery is a minimum legal length of 75 cm TL in Queensland. Because L_{50} is considered to be 104.6 cm TL (Zischke et al., 2013a), for the first fishery management scenario

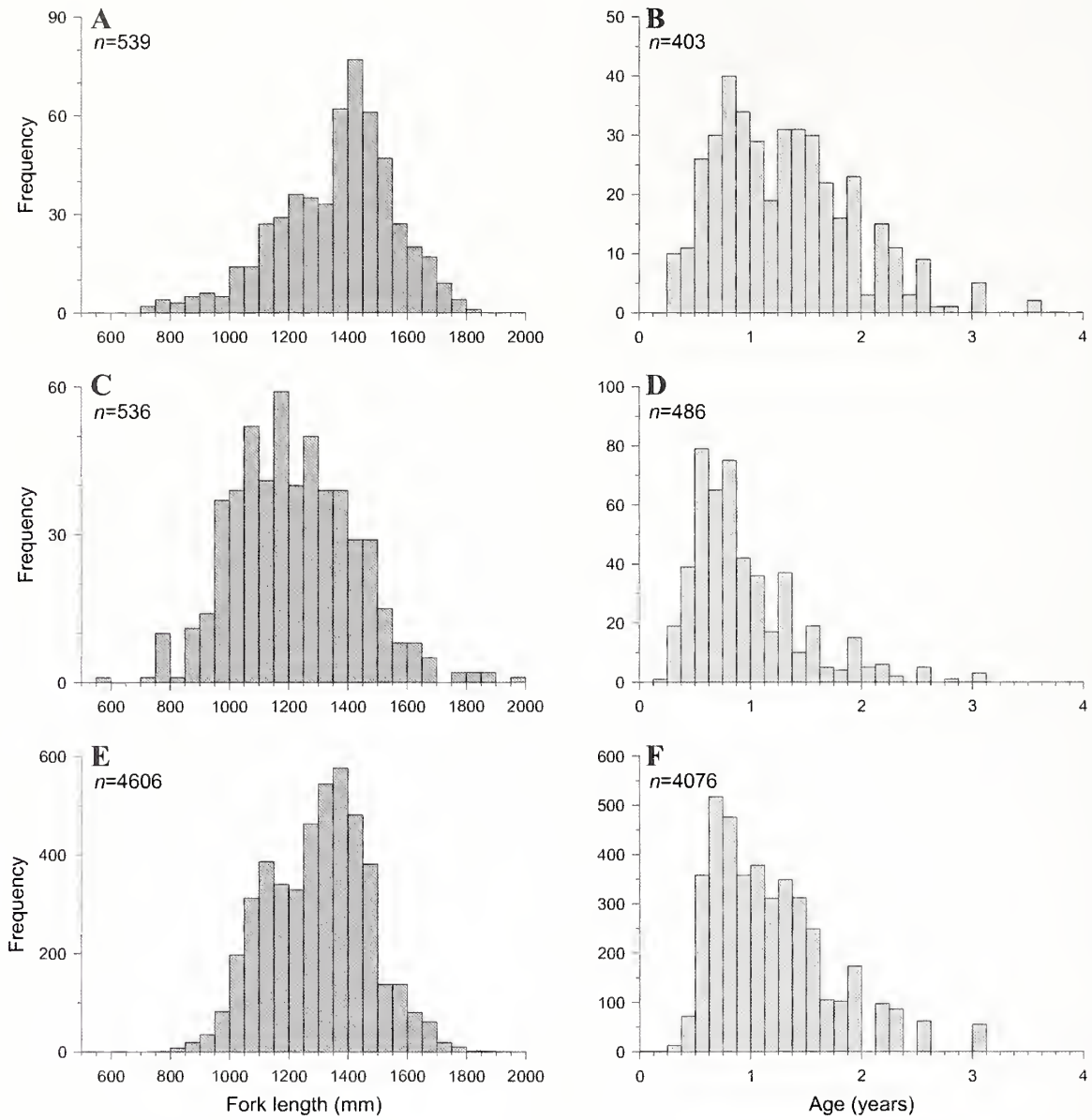

Figure 2

Length- and age-frequency distributions of wahoo (*Acanthocybium solandri*) caught in the (**A** and **B**) Eastern Tuna and Billfish Fishery (**C** and **D**) recreational fishery off eastern Australia and (**E** and **F**) the commercial longline fishery in New Caledonia between 2008 and 2010. Note that the sample sizes were lower for age-frequency distributions because age could not be calculated for all fish with a fork length greater than the theoretical length of infinite age (i.e., FL>1499 mm).

(F1), the effect of imposing a minimum legal length of 100 cm TL for the entire recreational fishery was explored. Although this length is slightly smaller than L_{50}, its simplicity may be easier for recreational fishermen to remember and management agencies to enforce. For scenarios F2 and F3, variations of these size limits were examined, including a maximum legal length of 150 cm TL (based on size distributions for the recreational fishery; see Fig. 2), and a slot limit where only fish 100–150 cm TL may be retained, respectively. As the F from the recreational sector represents only about one-third of the total F in the southwest Pacific Ocean, we used an additional scenario (F4) to explore changes to commercial longline fisheries. This scenario reduced the postrelease mortality of wahoo from 90% to 50%, following the hypo-

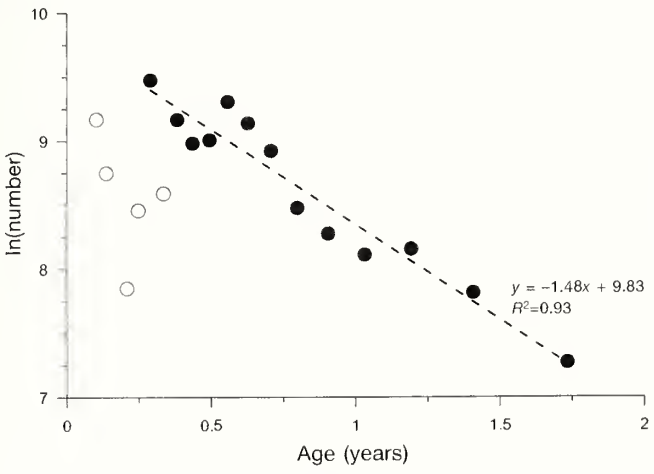

Figure 3

A length-converted catch curve for wahoo (*Acanthocybium solandri*) in the southwest Pacific Ocean (all fisheries combined) between 2008 and 2010. Numbers of fish in each age class were corrected with selectivity probability at age for all fisheries combined. Only values indicated by the solid black symbols were used in the regression analysis to estimate total mortality. R^2=coefficient of multiple determination.

thetical implementation of shorter soak times in the pelagic longline fishery, thereby allowing more fish to remain alive at haul back, and introduced a 20% discard rate similar to that observed for the recreational fishery. All analyses were undertaken with R software, vers. 3.0.2 (R Core Team, 2013).

Results

Size and age structure of exploited wahoo

Length- and age-frequency distributions of wahoo were similar for the 3 fisheries examined in the southwest Pacific Ocean, but the recreational fishery tended to catch slightly smaller and younger fish (Fig. 2). The median FLs for the ETBF, New Caledonia, EC Rec were 1400 mm (mean: 1366), 1320 (1304) mm, and 1209 (1222) mm. Corresponding median ages for the ETBF, New Caledonia, and EC Rec were 1.25 (mean: 1.31) years, 1.08 (1.18) years, and 0.82 (0.95) years. These median and mean ages are underestimates, however, because age could not be calculated for fish with an FL greater than 1499 mm (i.e., L_∞).

Age and size selectivity of fisheries

The selectivity probability at age for wahoo was similar for the 3 fisheries. The age (and FL) at which 50% of wahoo were selected in the ETBF, EC Rec, and New Caledonia was 0.58 years (mean: 1041 mm), 0.60 years (1055 mm), and 0.63 years (1076 mm), respectively.

Mortality estimates

Estimates of M obtained from the use of mean biological parameters (Table 1) in the 2 empirical equations were 0.66–0.74/year. Catch-curve analysis where the mean biological parameters for all fisheries were combined between 2008 and 2010 produced an estimate of Z of 1.48/year (Fig. 3). Subtracting M from Z, the annual $F_{current}$ for wahoo in the southwest Pacific Ocean was estimated as 0.74–0.82/year.

Sensitivity and management simulations

In the base scenario (S1), $F_{current}$ was lower than both limit reference points (i.e., F_{max} and F_{SSB25}) and the target reference point $F_{0.1}$, but it was higher than F_{SSB40} (Table 2). Introduction of a 10-fold increase in M for young fish (S2) caused a decrease in overall Y/R and SSB/R (Fig. 4) but resulted in $F_{current}$ exceeding the reference points in a lower percentage of iterations than the percentage seen in S1 (Table 2). In all of the fishery management scenarios (F1–F4) examined, $F_{current}$ was lower than all reference points (Table 2). Scenario F2 produced the most favorable results with respect to Y/R as $F_{current}$ exceeded the target and limit reference points in 2% and 0% of iterations (Table 2). With respect to SSB/R, scenario F3 produced the most favourable results, as $F_{current}$ exceeded the target and limit reference points in 27% and 2% of iterations (Table 2).

Discussion

Size selectivity of fisheries

The 3 fisheries examined in this study had similar selectivity probabilities at age; however, there were differences in the size distribution of wahoo caught in these fisheries, particularly between the commercial and recreational fisheries off eastern Australia. Numerous characteristics of pelagic longline gear may influence the probability of capture. These characteristics include the time of day (i.e., night or day) when the gear is soaking in relation to the peak feeding times of wahoo, the depth of hooks in relation to the depth distribution of the fish, and the size of the hook (and bait) relation to the maximum gape of the mouth. For example, in a trial where circle hooks were 57% wider than the traditional Japanese tuna hooks resulted in lower catch rates of smaller nontarget species, including wahoo (Curran and Bigelow, 2011). Circle hooks are widely used in the ETBF; and, therefore, these larger hooks may select for larger fish.

Recreational fishing gear used to catch wahoo (either intentionally or incidentally) off eastern Australia varies considerably among individual fishermen and includes heavy tackle, large hooks, baits, and lures used

Table 2

Results of the per-recruit analysis for wahoo (*Acanthocybium solandri*) in the southwest Pacific Ocean during 2008–2010 under sensitivity (S1–S2) and fishery management scenarios (F1–F4). For each scenario, means and 95% confidence intervals (CI) are given for current fishing mortality ($F_{current}$) and 4 biological reference points: fishing mortality at which maximum yield per recruit is produced (F_{max}), fishing mortality at which the slope of the yield-per-recruit curve is 10% of the slope at the origin ($F_{0.1}$), and fishing mortalities at which the spawning stock biomass per recruit (SSB/R) is 25% (F_{SSB25}) and 40% (F_{SSB40}) of the SSB/R at F=0. For each scenario, 100 iterations were conducted, and the percentage of iterations in which $F_{current}$ exceeded the reference point are given here for each scenario.

Model scenario	Mean (95% CI) $F_{current}$	Mean (95% CI) target reference points		Mean (95% CI) limit reference points		Iterations in which $F_{current}$ exceeds target reference points (%)		Iterations in which $F_{current}$ exceeds limit reference points (%)	
		$F_{0.1}$	F_{SSB40}	F_{max}	F_{SSB25}	$F_{current}$ >$F_{0.1}$	$F_{current}$ >F_{SSB40}	$F_{current}$ >F_{max}	$F_{current}$ >F_{SSB25}
S1	0.85 (0.82–0.89)	0.96 (0.95–0.98)	0.82 (0.78–0.85)	2.22 (2.18–2.26)	1.57 (1.48–1.65)	18%	53%	0%	4%
S2	0.80 (0.77–0.83)	0.95 (0.94–0.96)	0.81 (0.77–0.85)	2.22 (2.18–2.26)	1.55 (1.46–1.65)	11%	43%	0%	2%
F1	0.80 (0.77–0.83	0.96 (0.95–0.98)	0.87 (0.84–0.91)	2.32 (2.27–2.37)	1.72 (1.63–1.81)	8%	29%	0%	2%
F2	0.81 (0.78–0.84)	1.03 (1.02–1.05)	0.86 (0.82–0.90)	2.28 (2.24–2.32)	1.65 (1.55–1.74)	2%	36%	0%	3%
F3	0.87 (0.83–0.90)	1.07 (1.05–1.08)	0.96 (0.92–0.99)	2.46 (2.41–2.50)	1.89 (1.80–1.99)	7%	27%	0%	2%
F4	0.82 (0.80–0.85)	1.00 (0.99–1.02)	0.93 (0.89–0.97)	2.40 (2.36–2.44)	1.94 (1.82–2.05)	9%	32%	0%	0%

for targeting large marlins (Istiophoridae) and light tackle and smaller terminal equipment used to specifically target wahoo and similar-size mackerels and tunas. In addition to fishing gear, there are spatiotemporal differences in fishing effort between fishing sectors because the majority of fishing effort in the recreational fishery is expended during the day in more southern areas of the EEZ that are relatively close to the coast (Zischke et al., 2012). Therefore, differences in the size (and age) distributions of wahoo caught by commercial and recreational fisheries off eastern Australia may be due to the spatiotemporal differences in fishing areas between sectors (cf., Griffiths, 2010), rather than due to the selectivity of fishing gears, particularly if wahoo of different sizes or ages display different spatial distributions. It is important to quantify fishery-specific selectivity probabilities for stock assessment and to understand how potential management changes might influence selectivity.

Per-recruit analysis

Dynamic pool models and virtual population analysis can be useful in situations (e.g., in developing fisheries) in which there are little historical catch and effort data (Gabriel and Mace, 1999). We provided an assessment of $F_{current}$ against a traditional limit reference point F_{max}. However, because per-recruit models assume constant recruitment regardless of spawning stock size, estimates of F_{max} may not be sufficient to ensure sustainability (Gabriel and Mace, 1999). We also estimated $F_{0.1}$, a precautionary target reference point that may reduce the chance of overfishing and stock collapse, particularly in data-poor fisheries (Gulland and Boerema, 1973). Constant recruitment is assumed in a yield-per-recruit model and therefore is independent of variations in stock size, and recruitment overfishing is not able to be detected (Quinn and Deriso, 1999). We investigated recruitment overfishing by conducting an SBB/R analysis to assess $F_{current}$ against a limit reference point of F_{SSB25} and a target reference point of F_{SSB40} (Goodyear, 1993).

Current levels of F of wahoo in the southwest Pacific Ocean are below both limit (F_{max}) and target ($F_{0.1}$) reference points for Y/R and the limit reference point (F_{SSB25}) for SSB/R, but they are similar to the target reference point (F_{SSB40}) for SSB/R (Table 2; Fig. 4). This finding indicates that, under current fishing practices in commercial and recreational fisheries, wahoo may be at higher risk of recruitment overfishing than of growth overfishing—an observation that may be attributed to their fast growth and the low selectivity of juvenile fish by fisheries. Chale-Matsau et al. (1999) obtained similar results from a per-recruit analysis of the closely related Kanadi kingfish (*Scomberomorus plurilineatus*) in South Africa; in that study, $F_{0.1}$ greatly exceeded F_{SSB50}, and the authors suggested that F_{SSB50} be used as a biological reference point for that species as a safeguard to minimize the risk of recruitment overfishing.

Sensitivity and management simulations

The iterative approach to the per-recruit model allowed us to explore the likelihood that $F_{current}$ exceeded reference points because of uncertainty in biological param-

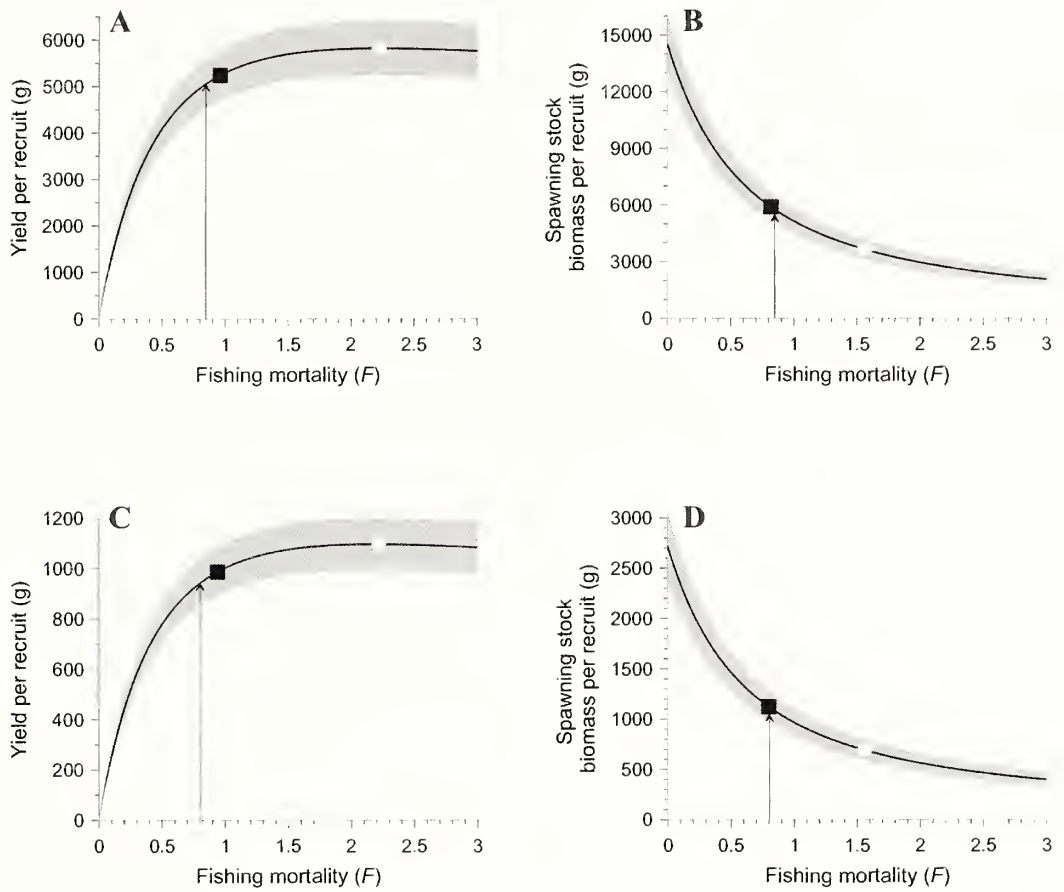

Figure 4

Mean estimates (solid line) and 95% confidence intervals (gray shaded area) of yield per recruit (Y/R) and spawning stock biomass per recruit (SSB/R) for wahoo (*Acanthocybium solandri*) in the southwest Pacific Ocean during 2008–2010: (**A**) Y/R and (**B**) SSB/R for a model scenario with constant natural mortality for all ages (scenario 1 [S1]; see *Materials and methods* section) and (**C**) Y/R and (**D**) SSB/R for a model scenario where natural mortality is 10-fold higher for juvenile fish than for adults (S2; see *Materials and methods* section). Arrows indicate current fishing mortality. Black squares represent target reference points of fishing mortality at which the slope of the Y/R curve is 10% of the slope at the origin in panels A and C and target reference points of fishing mortality at which the SSB/R is 40% of the SSB/R at F=0 in panels B and D. Open circles represent limit reference points of fishing mortality at which maximum Y/R is produced in panels A and C and reference points of fishing mortality at which the SSB/R is 25% of the SSB/R at F=0 in panels in B and D.

eters. The base scenario (S1), including variability in growth and maturity parameters, resulted in 95% confidence intervals of approximately 10% for both Y/R and SSB/R. Although recent research has provided the most reliable account of wahoo growth dynamics (Zischke et al., 2013b), further biological research is needed to validate the periodicity of growth increment formation to ensure that length-at-age relationships used in future assessments are reliable. Future assessment of wahoo stocks should prioritize research that provides regional estimates of growth parameters. Similar effects of variability in age and growth have been shown for walleye pollock (*Gadus chalcogrammus*) in the eastern Bering Sea, where aging error has had little effect on estimates of growth and mortality but has produced sufficiently different results in a Y/R analysis conducted to infer overfishing (Lai and Gunderson, 1987).

The iterative approach also allowed us to assess the impact of potential management changes on Y/R and SSB/R. For example, F_{current} exceeded F_{SSB40} in 53% of iterations under the standard scenario (S1), but this percentage decreased to 27% when a slot limit in the recreational fishery was introduced (F3; Table 2). Overall, fishery management scenarios (F1–F4) had little effect on the results of the per-recruit model because F_{current} was already lower than 3 (and similar to 1) of

the reference points in the base scenario (S1). A similar outcome was seen in a per-recruit analysis of longtail tuna (*T. tonggol*) in Australian waters, whereby increases in recreational size limits and post-release survival did not change the relationship between $F_{current}$ and biological reference points (Griffiths, 2010). It is likely that this finding results from low selectivity of immature fish of both species in recreational fisheries. In contrast, the recreational fishery for largemouth queenfish (*Scomberoides commersonnianus*) in Australian waters had a relatively high selectivity for immature fish; therefore, increasing minimum size limits to reflect L_{50} had a drastic improvement on the status of that stock (Griffiths et al., 2006).

Future directions

We compared $F_{current}$ for wahoo against traditionally used reference points for target species in commercial fisheries. Alternative reference points, such as catch rate, mortality rate, and potential biological removal, have been suggested for data-poor bycatch species (Moore et al., 2013). However, because wahoo represent an important byproduct in the 2 commercial fisheries assessed in this article, reference points based on yield may still be appropriate. Management objectives for recreational fisheries, which generally value high catch rates and large average size of fish, differ from those for commercial fisheries, which value total yield and high profit. In regions where recreational fisheries represent a significant proportion of total F for wahoo, alternative reference points that reflect the preferences of these fisheries (e.g. more large fish) may be appropriate.

Per-recruit analysis cannot directly explore the effect of reducing catch and effort on the status of a stock. However, input (effort-based) and output (catch-based) management measures are commonly used in both commercial and recreational fisheries. For example, the efficacy of current commercial trip limits or recreational possession limits for wahoo could not be examined with per-recruit analysis. A population model should be adopted in future assessments of this species in the southwest Pacific Ocean, such as MULTIFAN-CL (Fournier et al., 1998; Kleiber et al., 2003), that is structured by size, age, and spatial distribution. This model can integrate fishery-specific catch, effort, and length-frequency data, as well as tag and release data, to provide time-series estimates of recruitment, biomass, and F, as well as to summarize the stock status against various reference points.

This approach has been used extensively for pelagic target species in commercial fisheries throughout the western and central Pacific Ocean (Davies et al.[9]; Hoyle et al.[10]; Langley et al.[11]). Although such assessments are data intensive and, therefore, costly to implement, they allow management strategy evaluations to explore outcomes for fishery and population sustainability objectives. Alternatively, cost-effective methods for assessing all species that a fishery interacts with, such as the quantitative ecological sustainability assessment for fishing effects developed by Zhou and Griffiths (2008), may be more appropriate for wahoo and other byproduct and bycatch species.

Although wahoo may still be considered a low-priority species for most commercial fisheries, their steadily increasing catches worldwide may require species-specific management in the future. We collated biological and fishery information for wahoo in the southwest Pacific Ocean and present the first quantitative assessment of their status in this region. The results of this assessment indicate that $F_{current}$ for wahoo is lower than limit reference points and the target reference point for Y/R and that it is slightly higher than the target reference point for SBB/R. It is important that these fisheries be re-assessed periodically because their dynamics (e.g., effort, catch, or management arrangements) may change through time. In addition to providing a baseline assessment for wahoo, this study provides an approach that may be useful for data-poor, nontarget species in other fisheries worldwide.

Acknowledgments

We thank the Australian Fisheries Management Authority and Secretariat of the Pacific Community for providing catch, effort and, size-frequency data from commercial fisheries. We would like to thank 3 anonymous reviewers for constructive feedback that improved the quality of the final manuscript. We also thank I. Tibbetts (UQ) for comments on an earlier draft of the manuscript. M.T.Z was funded by a University of Queensland Research Scholarship, with support provided by the Division of Marine and Atmospheric Research of the Commonwealth Scientific and Industrial Research Organisation.

Literature cited

Beverton, R. J. H., and S. J. Holt.
1957. On the dynamics of exploited fish populations, 533 p. Chapman & Hall, London.

Chale-Matsau, J. R., A. Govender, and L. E. Beckley.
1999. Age and growth of the queen mackerel *Scomb-*

[9] Davies, N., S. Hoyle, S. Harley, A. Langley, P. Kleiber, and J. Hampton. 2011. Stock assessment of bigeye tuna in the western and central Pacific Ocean. Western and Central Pacific Fisheries Commission WCPFC-SC7-2011/SA- WP-02, 119 p. [Available at website.]

[10] Hoyle, S., J. Hampton, and N. Davies. 2012. Stock assessment of albacore tuna in the South Pacific Ocean. Western and Central Pacific Fisheries Commission WCPFC-SC8-2012/SA-WP-04-REV1, 123 p. [Available at website.]

[11] Langley, A., S. Hoyle, and J. Hampton. 2011. Stock assessment of yellowfin tuna in the western and central Pacific Ocean. Western and Central Pacific Fisheries Commission WCPFC-SC7-2011/SA- WP-03, 124 p. [Available at website.]

eromorus plurilineatus from KwaZulu-Natal, South Africa. Fish. Res. 44:121–127.

Collette, B. B., and C. E. Nauen.
1983. FAO species catalogue, vol. 2. Scombrids of the world. FAO Fish. Synop. 125, 137 p. FAO, Rome.

Curran, D., and K. Bigelow.
2011. Effects of circle hooks on pelagic catches in the Hawaii-based tuna longline fishery. Fish. Res. 109:265–275.

Domeier, M. L., H. Dewar, and N. Nasby-Lucas.
2003. Mortality rate of striped marlin (*Tetrapturus audax*) caught with recreational tackle. Mar. Freshw. Res. 54:435–445.

Fournier, D. A., J. Hampton, and J. R. Sibert.
1998. MULTIFAN-CL: a length-based, age-structured model for fisheries stock assessment, with application to South Pacific albacore, *Thunnus alalunga*. Can. J. Fish. Aquat. Sci. 55:2105–2116.

Gabriel, W. L., and P. M. Mace.
1999. A review of biological reference points in the context of the precautionary approach. *In* Proceedings of the fifth national NMFS stock assessment workshop: providing scientific advice to implement the precautionary approach under the Magnuson-Stevens Fishery Conservation and Management Act; Key Largo, FL, 24–26 February 1998 (V. R. Restrepo, ed.), p. 34–45. NOAA Tech Memo NMFS-F/SPO-40.

Goodyear, C. P.
1993. Spawning stock biomass per recruit in fisheries management: foundation and current use. *In* Risk evaluation and biological reference points for fisheries management (S. J. Smith, J. J. Hunt, and D. Rivard, eds.), p. 67–81. Can. Spec. Publ. Fish. Aquat. Sci. 120.

Griffiths, S. P.
2010. Stock assessment and efficacy of size limits on longtail tuna (*Thunnus tonggol*) caught in Australian waters. Fish. Res.102:248–257.

Griffiths, S. P., G. C. Fry, and T. D. van der Velde.
2006. Population dynamics and fishery benefits of a large legal size of a pelagic sportfish, the Talang queenfish, *Scomberoides commersonnianus*, in northern Australia. Fish. Res. 83:74–86.

Gulland, J. A., and L. K. Boerema.
1973. Scientific advice on catch levels. Fish. Bull. 71:325–335.

Hampton, J.
2000. Natural mortality rates in tropical tunas: size really does matter. Can. J. Fish. Aquat. Sci. 57:1002–1010.

Hoenig, J. M.
1983. Empirical use of longevity data to estimate mortality rates. Fish. Bull. 82:898–903.

Hovgard, H., and H. Lassen.
2000. Manual on estimation of selectivity for gillnet and longline gears in abundance surveys. FAO Fish. Tech. Paper 397, 84 p.

Kerstetter, D. W., and J. E. Graves.
2006. Survival of white marlin (*Tetrapturus albidus*) released from commercial pelagic longline gear in the western North Atlantic. Fish. Bull. 104:434–444.
2008. Postrelease survival of sailfish caught by commercial pelagic longline gear in the southern Gulf of Mexico. N. Am. J. Fish. Manage. 28:1578–1586.

Kleiber, P., J. Hampton, and D. A. Fournier.
2003. MULTIFAN-CL User's Guide, 152 p. [Available at website.]

Lai, H. L., and D. R. Gunderson.
1987. Effects of ageing errors on estimates of growth, mortality and yield per recruit for walleye pollock (*Theragra chalcogramma*). Fish. Res. 5:287–302.

Lee, T. M.
2008. Estimation of life history parameters, biological reference points, and associated uncertainties for wahoo (*Acanthocybium solandri*) in the waters off eastern Taiwan. M.S. thesis, 75 p. National Taiwan Univ., Taipei, Taiwan.

Moore, J. E., K. A. Curtis, R. L. Lewison, P. W. Dillingham, J. M. Cope, S. V. Fordham, S. S. Heppell, S. A. Pardo, C. A. Simpfendorfer, G. N. Tuck, and S. Zhou.
2013. Evaluating sustainability of fisheries bycatch mortality for marine megafauna: a review of conservation reference points for data-limited populations. Environ. Conserv. 40:329–344.

Pauly, D.
1980. On the interrelationships between natural mortality, growth parameters, and mean environmental temperature in 175 fish stocks. J. Cons. 39:175–192.
1983. Length-converted catch curves: a powerful tool for fisheries research in the tropics (Part I). Fishbyte 1:9–13.
1984a. Length-converted catch curves: a powerful tool for fisheries research in the tropics (III: Conclusion). Fishbyte 2:9–10.
1984b. Length-converted catch curves: a powerful tool for fisheries research in the tropics (Part II). Fishbyte 2:17–19.

Quinn, T. J., and R. B. Deriso.
1999. Quantitative fish dynamics, 560 p. Oxford Univ. Press, New York.

R Core Team.
2013. R: a language and environment for statistical computing. R Foundation for Statistical Computing, Vienna, Austria. [Available at website, accessed October 2013]

Sepulveda, C. A., S. A. Aalbers, S. Ortega-Garcia, N. C. Wegner, and D. Bernal.
2011. Depth distribution and temperature preferences of wahoo (*Acanthocybium solandri*) off Baja California Sur, Mexico. Mar. Biol. 158:917–926.

Skomal, G. B., B. C. Chase, and E. D. Prince.
2002. A comparison of circle hook and straight hook performance in recreational fisheries for juvenile Atlantic bluefin tuna. Am. Fish. Soc., Symp. 30:57–65.

Sparre, P., E. Ursin, and S. C. Venema.
1989. Introduction to tropical fish stock assessment. Part 1. Manual. FAO Fish. Tech. Pap. 306.1, 337 p. FAO, Rome.

Theisen, T. C.
2007. Population genetic structure, movement patterns, and environmental preferences of the pelagic wahoo, *Acanthocybium solandri*. Ph.D. thesis, 98 p. Florida Atlantic Univ., Boca Raton, FL.

Theisen, T. C., B. W. Bowen, W. Lanier, and J. D. Baldwin.
2008. High connectivity on a global scale in the pelagic wahoo, *Acanthocybium solandri* (tuna family Scombridae). Mol. Ecol. 17:4233–4247.

Vetter, E. F.
1988. Estimation of natural mortality in fish stocks: a review. Fish. Bull. 86:25–43.

Zhou, S. and S. P. Griffiths.
2008. Sustainability Assessment for Fishing Effects (SAFE): a new quantitative ecological risk assessment method and its application to elasmobranch bycatch in an Australian trawl fishery. Fish. Res. 91:56–68.

Zischke, M. T.
2012. A review of the biology, stock structure, fisheries and status of wahoo (*Acanthocybium solandri*), with reference to the Pacific Ocean. Fish. Res. 119–120:13–22.

Zischke, M. T., J. H. Farley, S. P. Griffiths, and I. R. Tibbetts.
2013a. Reproductive biology of wahoo, *Acanthocybium solandri*, off eastern Australia. Rev. Fish Biol. Fish. 23:491–506.

Zischke, M. T., S. P. Griffiths, and I. R. Tibbetts.
2012. Catch and effort from a specialised recreational pelagic sport fishery off eastern Australia. Fish. Res. 127–128:61–72.
2013b. Rapid growth of wahoo (*Acanthcybium solandri*) in the Coral Sea, based on length-at-age estimates using annual and daily increments on sagittal otoliths. ICES J. Mar. Sci. 70:1128–1139.

Zischke, M. T., S. P. Griffiths, I. R. Tibbetts, and R. J. G. Lester.
2013c. Stock identification of wahoo (*Acanthocybium solandri*) in the Pacific and Indian Oceans using morphometrics and parasites. ICES J. Mar. Sci. 70:164–172.

NOAA
National Marine
Fisheries Service

Fishery Bulletin
established 1881

Spencer F. Baird
First U.S. Commissioner
of Fisheries and founder
of *Fishery Bulletin*

Genetic structure and dispersal capabilities of dolphinfish (*Coryphaena hippurus*) in the western central Atlantic

Wessley B. Merten (contact author)[1,3]
Nikolaos V. Schizas[1]
Matthew T. Craig[2]
Richard S. Appeldoorn[1]
Donald L. Hammond[3]

Email address for contact author: wessleymerten@gmail.com

[1] Department of Marine Sciences
University of Puerto Rico, Mayagüez
P.O. Box 9000
Mayagüez, Puerto Rico 00681

[2] Department of Marine Science and Environmental Studies
University of San Diego
5998 Alcalá Park
San Diego, California 92110

[3] Cooperative Science Services LLC
Dolphinfish Research Program
961 Anchor Road
Charleston, South Carolina 29412

Abstract—The dolphinfish (*Coryphaena hippurus*) is of major recreational and commercial importance, and landings have increased in recent years around Puerto Rico, throughout the Caribbean Sea, and along the U.S. East Coast, yet its genetic structure among these localities is uncertain. A portion of the mitochondrial nicotinamide adenine dinucleotide (NADH) dehydrogenase subunit 1 (ND1; 1288 base pairs) gene was used at 2 spatial scales to investigate the population structure of dolphinfish. In a comparison of 183 specimens of dolphinfish between the northern and southern coasts of Puerto Rico over 4 consecutive years (2010–2013), no genetic differentiation was detected (Φ_{ST}= −0.002, P=0.640). On a broader scale, patterns of genetic variation of ND1 were compared for samples collected throughout the western central Atlantic from Florida, South Carolina, North Carolina (southeastern United States; N=90); Puerto Rico (northeastern Caribbean Sea; N=183); Barbados, Dominica, and Trinidad and Tobago (eastern Caribbean Sea; N=43); and the central North Atlantic in the Azores Islands (N=8), and 199 haplotypes were identified from all of the regions combined. Analysis of all samples (N=324) revealed shallow genetic structure (Φ_{ST}=0.009, P=0.023), but pairwise regional comparisons did not, indicating low population differentiation of dolphinfish throughout the western central Atlantic.

Manuscript submitted 26 May 2014.
Manuscript accepted 28 July 2015.
Fish. Bull. 113:419–429 (2015).
Online publication date: 14 August 2015.
doi: 10.7755/FB.113.4.5

The combination of tagging and genetic approaches (e.g., DNA sequencing and microsatellite analyses) has led to significant improvements in characterizing the stock and population structure of marine pelagic fishes, in interpreting biomass dynamic models, in generating stock-recruitment curves, and in conducting cohort analyses (Graves, 1998; Reiss et al., 2009). Specifically, tag and genetic data can be used to estimate regional biomass exchange and define stocks demographically; this information is useful in the stock assessment process (Waples et al., 2008). Alternatively, tag or genetic data have allowed scientists to refine assessment models and facilitate a more precise allocation of management effort. Therefore, this combination of approaches provides more realistic estimates of immigration, emigration, mortality (natural and anthropogenic), and the extent of population mixing, all of which are informative in assessment models (Hilborn and Walters, 1992).

The results of these models provide fishery managers with information necessary to adjust fishing effort, set size limits and quotas, identify seasonal hot spots and essential fish habitat (e.g., *Sargassum*), and protect spawning stocks to safeguard recruitment and future landings (Allendorf et al., 1987), although the applicability of management measures can vary depending on effective population size (i.e., small versus large). Nevertheless, tag and genetic data are increasingly used to manage highly migratory fish stocks because they provide better estimates of spatiotemporal population differentiation and effective population sizes (Hauser and Carvalho, 2008)

The large population sizes and high dispersal capabilities of marine pelagic fishes (e.g., tunas, swordfishes, and jacks) are thought to contribute to low genetic differentiation among their populations (Graves and Dizon, 1989; Graves and McDowell, 2003; Theisen et al., 2008). The lack of genetic heterogeneity among regional samples in these pelagic species is believed to be an outcome of reduced genetic drift due to high gene flow among the locations sampled (Hauser and Ward, 1998). Studies with the use of various nuclear and mitochondrial DNA (mtDNA) markers of yellowfin (*Thunnus albacares*) and bigeye (*T. obesus*) tuna (Graves and Dizon, 1989), striped (*Kajikia audax*) and white (*K. albida*) marlin (Graves and McDowell, 1994, 2001), swordfish (*Xiphias gladius*) (Alvarado Bremer et al., 1996, 2005), and wahoo (*Acanthocybium solandri*) (Theisen et al., 2008) have revealed limited intra- and interocean divergence. Yet, some pelagic fishes (e.g., bluefin tuna [*T. thynnus*]) are now recognized as distinct species in the Pacific and Atlantic (Collette et al., 2001), and others show considerable genetic divergence among ocean basins (e.g., Indo-Pacific versus eastern Pacific, or Gulf of Mexico versus Mediterranean Sea) owing to physical isolation or the existence of separate spawning areas (Graves and McDowell, 2003).

In the Atlantic, no genetic heterogeneity has been detected over widespread areas for blue marlin (*Makaira nigricans*) (McDowell et al., 2007), sailfish (*Istiophorus platypterus*) (Graves and McDowell, 2003), and wahoo (Garber et al., 2005). High rates of large-scale migration and subsequent mixing may reduce the probability of small-population structure. For example, movement data for blue marlin show transatlantic, interocean (Atlantic to Indian Ocean), and Atlantic transequatorial crossings over large spatial and temporal scales, and no subpopulations have been evident (Witzell and Scott, 1990; McDowell et al., 2007). However, population subdivision has been shown between bluefin tuna populations in the Atlantic despite observed transatlantic movements between the Gulf of Mexico and Mediterranean Sea from satellite and conventional tagging data (Boustany et al., 2008). Using microsatellite and mtDNA markers, Boustany et al. (2008) detected genetic heterogeneity between those populations that was likely the result of strong natal homing to either the Gulf of Mexico or the Mediterranean Sea to reproduce.

The dolphinfish (*Coryphaena hippurus*) is similar to many large circumtropically distributed pelagic fish species (many thunnins, istiophorids) in that the species is abundant and has a high dispersal potential in all life stages. However, although istiophorid species have varied fecundity (Eldridge and Wares, 1974; Salcedo-Bojorquez and Arreguin-Sanchez, 2011) and spawning grounds (Richardson, 2008), the dolphinfish is highly fecund, spawns throughout a wide geographical range, has an early age at first maturity, and a short generation time (Palko et al., 1982; Ditty et al., 1994; Benetti et al., 1995; Oxenford, 1999). Together, these features indicate that genetic differentiation would be limited in this species, yet such differentiation has been detected at several spatial scales.

At the largest spatial scale, genetic differentiation was reported between eastern Atlantic and western Pacific dolphinfish populations, presumably because of dispersal limitations and vicariance between basins (Díaz-Jaimes et al., 2010). At the basin-wide scale, Díaz-Jaimes et al. (2010), using mtDNA nicotinamide adenine dinucleotide (NADH) dehydrogenase subunit 1 (ND1) sequences, observed genetic divergence between the western (Caribbean Sea) and eastern Atlantic (Senegal). In the Pacific, analyses of mtDNA (Díaz-Jaimes et al., 2006) and microsatellite loci (Tripp-Valdez et al., 2010) showed no population separation in the Gulf of California or eastern central Pacific. However, Rocha-Olivares et al. (2006) did show population separation using analyses of restriction fragment length polymorphism (RFLP) when comparing dolphinfish sampled in the eastern Pacific (Los Cabos, Mexico) and central Pacific (Hawaii).

In the past, Oxenford and Hunte (1986) inferred population subdivision in the western central Atlantic from regional differences in peak landings, growth rates, size of oocytes, maturity stage of gonads, and a limited survey of allozyme variation. Their analyses led to the hypothesis that dolphinfish exist as northern (U.S. East Coast to northern Caribbean Sea) and southern (southern Caribbean Sea to Brazil) stocks.

Around Puerto Rico, anecdotal reports from fishermen and recorded observations support the differential timing of the annual arrival of adult dolphinfish along the north (fall; October–January) and south coast (spring; January–April) (Rivera and Appeldoorn, 2000). As a result, it has long been thought that these seasonal "runs" represent different dolphinfish stocks. To examine dolphinfish stock structure around Puerto Rico, Rivera and Appeldoorn (2000) examined growth rates of dolphinfish sampled around the island to detect any significant growth differences between the northern and southern runs of dolphinfish. Within the 2 stock hypothesis advanced by Oxenford and Hunte (1986), fish around Puerto Rico are thought to belong to a northern stock and would, therefore, exhibit much slower growth rates than fish in the southern stock in Barbados. However, no growth differences were detected in fish sampled around Puerto Rico or between Puerto Rico and Barbados; Rivera and Appeldoorn (2000) suggested that stock structure and migration patterns were likely to be more complicated than postulated by Oxenford and Hunte (1986).

In this study, we investigated the genetic population structure of dolphinfish around Puerto Rico and in the western central Atlantic at 2 spatial scales, using the mtDNA ND1 gene. At the larger scale, comparisons were made from distinct regions within the western central Atlantic: 1) Puerto Rico (northeastern Caribbean Sea); 2) Florida, South Carolina, and North Carolina (southeastern United States); 3) Dominica, Barbados, and Trinidad and Tobago (eastern Caribbe-

Table 1

Genetic diversity and summary statistics of dolphinfish (*Coryphaena hippurus*) based on mitochondrial nicotinamide adenine dinucleotide (NADH) dehydrogenase subunit 1 (ND1) sequences by region in the western central Atlantic. N=number of samples; *Nh*=number of haplotypes per location; *h*=haplotype diversity; π=nucleotide diversity; θ_s=Watterson's theta; F_s=Fu's F_s; H_{ri}=Harpending's raggedness index; SSD=sum of squared differences from mismatch analysis. Bold values indicate significance at $P<0.05$. In this study, the region of the southeastern United States included North Carolina, South Carolina, and Florida; the northeastern Caribbean Sea consisted of the northern and southern shores of Puerto Rico; the eastern Caribbean Sea comprised Dominica, Barbados, and Trinidad and Tobago; and the central North Atlantic consists of the Azores Islands.

Regions	N	*Nh*	*h*	π	θ_s	F_s	H_{ri}	SSD
Southeastern United States	90	59	0.9763	0.0040	17.75	**−25.46**	0.010	0.001
Northeastern Caribbean Sea	183	100	0.9768	0.0035	19.02	**−25.42**	0.017	0.050
Eastern Caribbean Sea	43	33	0.9623	0.0046	16.41	**−24.59**	0.009	0.002
Central North Atlantic	8	7	0.9643	0.0026	4.24	**−2.87**	0.065	0.017
Mean	Σ=324	Σ=199	0.9699	0.0038	14.35	**−19.58**	0.025	0.175

an Sea); and 4) the Azores Islands (central North Atlantic). At the smaller scale, comparisons were made within regions (e.g., within the northeastern Caribbean Sea between the northern and southern coasts of Puerto Rico). The results from these investigations were used to examine how stock structure and stock connectivity of this species in relation to Puerto Rico are reflected in the variation of the ND1 gene around the western central Atlantic and the central North Atlantic.

Materials and methods

Field sampling

Dolphinfish were primarily sampled at various locations in the western central Atlantic (Table 1, Fig. 1). Tissue samples (~1 g; fin clip) were collected from landing sites, when fish at recreational fishing tournaments were weighed, or in situ with hook-and-line techniques along the northern and southern coasts of Puerto Rico from 2010 through 2013, along the southeastern United States in 2012, and from Barbados in 2014. Tissue samples were taken individually, immediately preserved in individual vials containing >95% ethanol solution, and stored at −20°C once in the laboratory. Additional samples from the Azores Islands (N=8) and Barbados (N=5) collected in 1998 were obtained from the South Carolina Department of Natural Resources; these samples included fin clips or heart tissue stored in a Sarkosyl-urea solution (1% Sarkosyl, 6 M urea, 100 mM Tris at pH 6.8–7.0). The samples in Sarkosyl-urea solution were stored at room temperature. Additional sequence data from the southeastern United States (N=1) and eastern Caribbean Sea (N=12) were acquired from public databases (GenBank accession numbers: AF272054–AF272061, AF290386–AF290390, AF256056).

DNA extraction, PCR amplification, and sequencing

Total genomic DNA was extracted through the use of a DNeasy[1] kit (Qiagen Inc., Valencia, CA) according to the manufacturer's instructions. Polymerase chain reaction (PCR) was used to amplify a fragment, with 1437 base pairs (bp) of the mitochondrial genome consisting of the ND1 gene and portions of the flanking transfer RNAs (tRNAs) by using the L3324 (5′-GTCCTACGTGATCTGAGTTCAG-3″) and H4716 (5-TACATGTTTGGGGTATGGGC-3′) primers (Chapman[2]). After quality assessment and trimming to a common length, a 1288-bp fragment was used for all analyses containing 126 bp of the 16S RNA upstream, the entire tRNA Leu (72 bp) and tRNA Ile (69 bp) genes, a portion of the tRNA Gln (49 bp) gene downstream, and the entire ND1 gene (972 bp). PCR amplifications in 25-µL volumes were prepared with BioMix Red solution (Bioline USA Inc., Taunton, MA) according to the manufacturer's instructions with the addition of 10 ng of DNA and 5 µM of each primer. Thermal cycling consisted of an initial denaturation step for 2 min at 94°C, followed by 35 cycles of 94°C for 30 s, 53°C for 25 s, and 72°C for 45 s, with a final 10 min extension at 72°C. Sanger sequencing in both forward and reverse directions was performed by the High Throughput Genomics Center in Seattle, Washington. All sequences and final alignment have been submitted to GenBank (accession numbers: KP057921–KP058244).

Data analysis

For visualization, quality assessment, contig (contiguous) assembly, and editing, DNA trace files were im-

[1] Mention of trade names or commercial companies is for identification purposes only and does not imply endorsement by the National Marine Fisheries Service, NOAA

[2] Chapman, R. 2012. Personal commun. Hollings Marine Lab, Charleston, SC 29412.

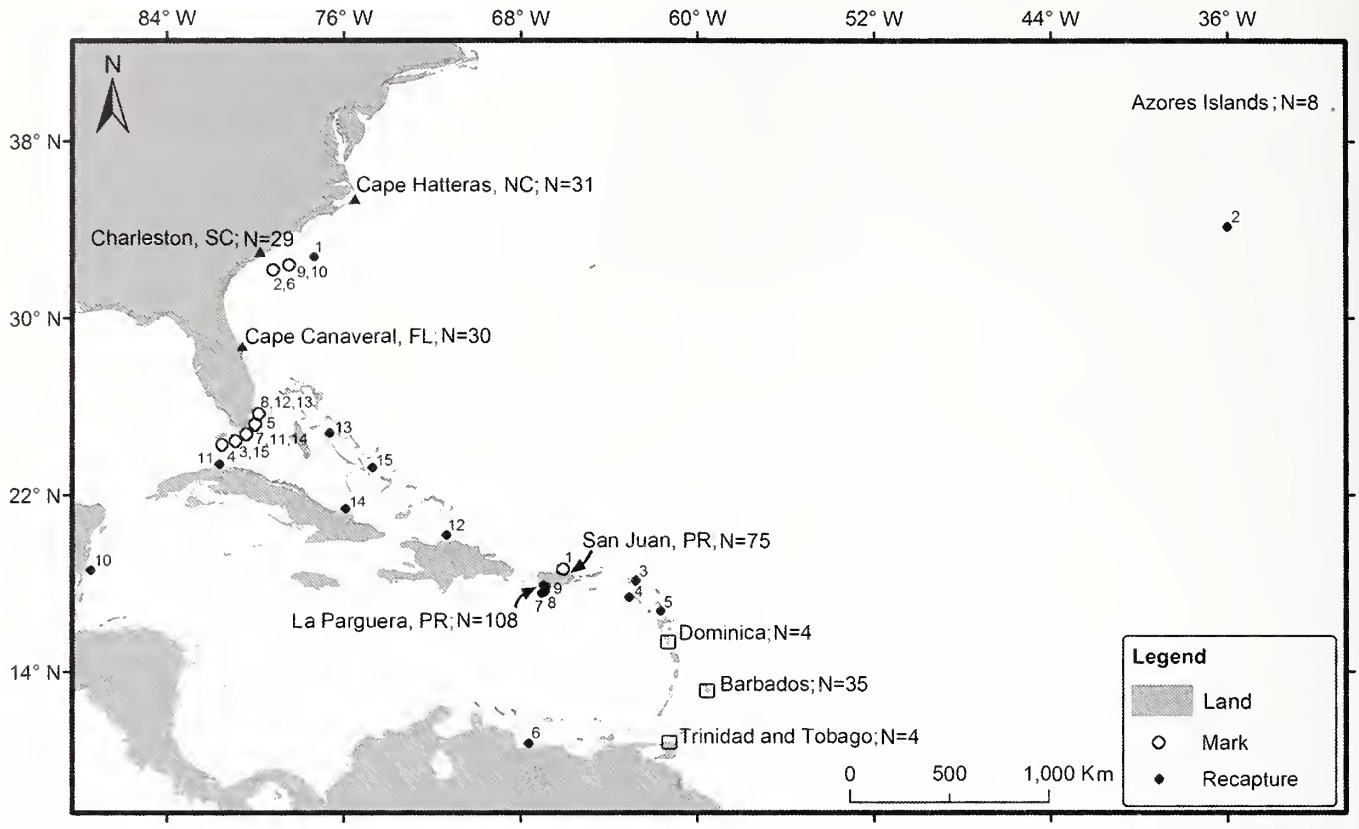

Figure 1

Tissue sample distribution and conventional tagging movements of dolphinfish (*Coryphaena hippurus*) in the western central and central North Atlantic. Tissue samples were taken from fish collected at different landing sites in each of the 3 regions in the western central Atlantic, including the southeastern United States in 2012 (triangles), northeastern Caribbean Sea during 2010–2013 (arrows), and eastern Caribbean Sea (open squares) during 1998 and 2014; samples from fish collected in the central North Atlantic (Azores Islands) were taken in 1998. The numbers adjacent to open circles (fish release locations) and closed circles (fish recapture locations) correspond to the tagging information in Table 4.

ported to CodonCode Aligner, vers.4.2.5 (CodonCode Corp., Centerville, MA). Sequences were aligned and trimmed to a common length with Mesquite, vers. 2.75 (Maddison and Maddison, 2011). Haplotype (h) and nucleotide diversity (π) were calculated with Arlequin, (vers. 3.5; Excoffier and Lischer, 2010). Population differentiation and the geographical pattern of variation were examined with hierarchical analyses of molecular variance (AMOVA) (Excoffier and Lischer, 2010) and pairwise comparisons of Φ_{ST} through the use of the Tamura-Nei model (Tamura and Nei, 1993). Significance of Φ-statistics was assessed by 10,000 permutations of groups and haplotypes. A gamma distribution parameter of α=0.881 was used to run AMOVA. This parameter was selected by prior sequence comparisons in jModelTest, vers. 2.1.3, after the GTR+I+G DNA substitution model was selected as the best-fit model on the basis of the Akaike information criterion (Posada, 2008; Darriba et al., 2012).

Fu's F_S (Fu, 1997) was used to test for deviation from the neutral model of molecular evolution (Kimura, 1968). The demographic parameters τ, θ_0, and θ_1 were estimated from pairwise sequence distribution of mismatches according to the demographic and spatial expansion models. The translation of demographic parameters to estimates of effective population size were obtained by following Bowen et al. (2006). To evaluate a null hypothesis of a population expansion, Harpending's raggedness index was calculated; failure to reject the null hypothesis (i.e., nonsignificant raggedness values) indicates that there is no support for a stable (nonexpanding) population (Rogers and Harpending, 1992). Additional demographic and spatial expansion parameters, including time since expansion in years (T), effective female population size (Ne), and immigration rate from neighboring demes (m), were generated according to the method of Díaz-Jaimes et al. (2006, 2010), using a maximum generation time of 3 years for dolphinfish (Mahon and Oxenford, 1999) and a mutation rate of 1.2% per million years for marine teleosts (Bermingham et al., 1997).

To test for differences in genetic structure between seasonal runs thought to occur around Puerto Rico, pairwise Φ_{ST} comparisons of samples taken from the

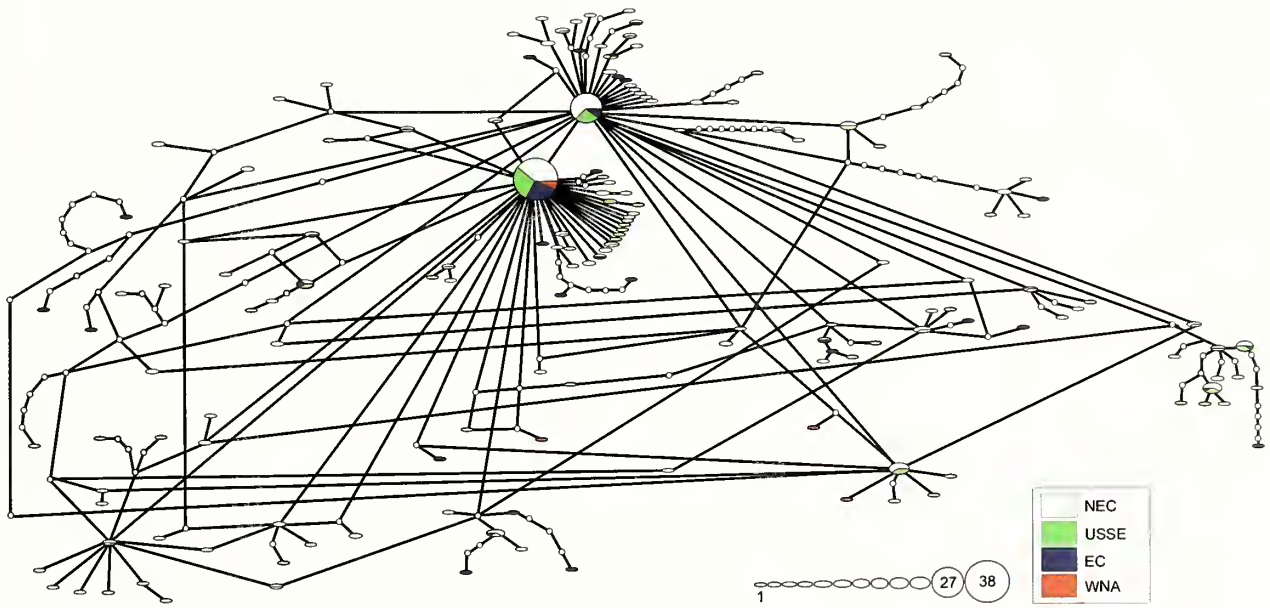

Figure 2

Statistical parsimony network for dolphinfish (*Coryphaena hippurus*) based on mitochondrial nicotinamide adenine dinucleotide (NADH) dehydrogenase subunit 1 (ND1) sequences. The size of circles is proportional to the number of shared haplotypes represented as pie charts. The small white circles on the connecting lines indicate the number of mutations among haplotypes and internal nodes. The color of a section in pie charts indicates a region: northeastern Caribbean Sea (NEC); southeastern United States (USSE); eastern Caribbean Sea (EC); central North Atlantic (CNA). The circles next to the legend indicate the proportionality of the number of haplotypes to the size of the circles (1–10, 27, and 38).

northern and southern coasts were compared over 4 consecutive years (2010–2013). All samples were then compared with samples collected from the southeastern United States during 2012, from the eastern Caribbean Sea during 1998 and 2014, and from the central North Atlantic during 1998. Lastly, a statistical parsimony network was generated for all haplotypes with TCS, vers. 1.2.1 (Clement et al., 2000) and redrawn in Adobe Photoshop CS5.

Results

From 324 specimens of dolphinfish collected primarily around the western central Atlantic, 199 haplotypes of a 1288-bp fragment containing ND1 and its adjacent tRNAs were resolved (Fig. 1). The haplotype network was characterized by a high number of singletons (Fig. 2). The most numerically dominant haplotype (N=38) was found in all sampling locations and mean h was high (0.9699), ranging from 0.9623 in the eastern Caribbean Sea to 0.9768 in the northeastern Caribbean Sea (Table 1).

Population structure

Significant overall population differentiation (Φ_{ST}=0.009, P=0.023) was revealed through AMOVA of all samples, but AMOVA did not reveal differentiation among areas within regions (i.e., between northern and southern Puerto Rico within the northeastern Caribbean Sea, among North Carolina, South Carolina, and Florida within the southeastern United States, or among Barbados, Dominica, and Trinidad and Tobago within the eastern Caribbean Sea) (Φ_{SC}=0.014, P=0.059) and among regions (i.e., northeastern Caribbean Sea versus southeastern United States versus eastern Caribbean Sea) (Φ_{CT}= −0.005, P=0.301) (Table 2). Pairwise comparisons among regions failed to reveal significant differences. In addition, pairwise comparisons between the northern and southern coasts of Puerto Rico did not reveal significant differences (Φ_{ST}= −0.002, P=0.640).

Population expansion

For all regions, Fu's F_S showed significant (P<0.05) negative departures from neutrality and supported the spatial-population-expansion model (Table 1, Fig. 3). In addition, nonsignificant raggedness values supported the spatial-population-expansion model (Table 1). Estimates of τ (time in generations) were similar among all regions and compatible with the timing of recent population expansion beginning around 80,500 years ago (Table 3). For the southeastern United States, northeastern Caribbean Sea, and the Azores Islands, there

Table 2

Analysis of molecular variance (AMOVA) of dolphinfish (*Coryphaena hippurus*) based on mitochondrial nicotinamide adenine dinucleotide (NADH) dehydrogenase subunit 1 (ND1) sequences by region in the western central Atlantic. Total population differentiation was estimated by using maximum likelihood DNA sequence pairwise distances (Tamura-Nei correction). The fixation indices for differentiation within a population among samples (Φ_{ST}=0.009, P=0.023), among regions (Φ_{CT}), and among areas within regions (Φ_{SC}) are presented. The areas and regions in this study were the northern and southern coasts of Puerto Rico in the northeastern Caribbean Sea; Florida, South Carolina, and North Carolina within the southeastern United States; Dominica, Barbados, and Trinidad and Tobago in the eastern Caribbean Sea; and the Azores Islands in the central North Atlantic.

Source of variation	Sum of squares	Variance	Variation (%)	Fixation indices
Among regions	8.179	−0.1354	−0.55	Φ_{CT}= −0.005 (P=0.301)
Among areas within regions	17.997	0.3509	1.41	Φ_{SC}=0.014 (P=0.059)
Within areas	775.105	2.4607	99.13	
Total	801.281	2.4822		

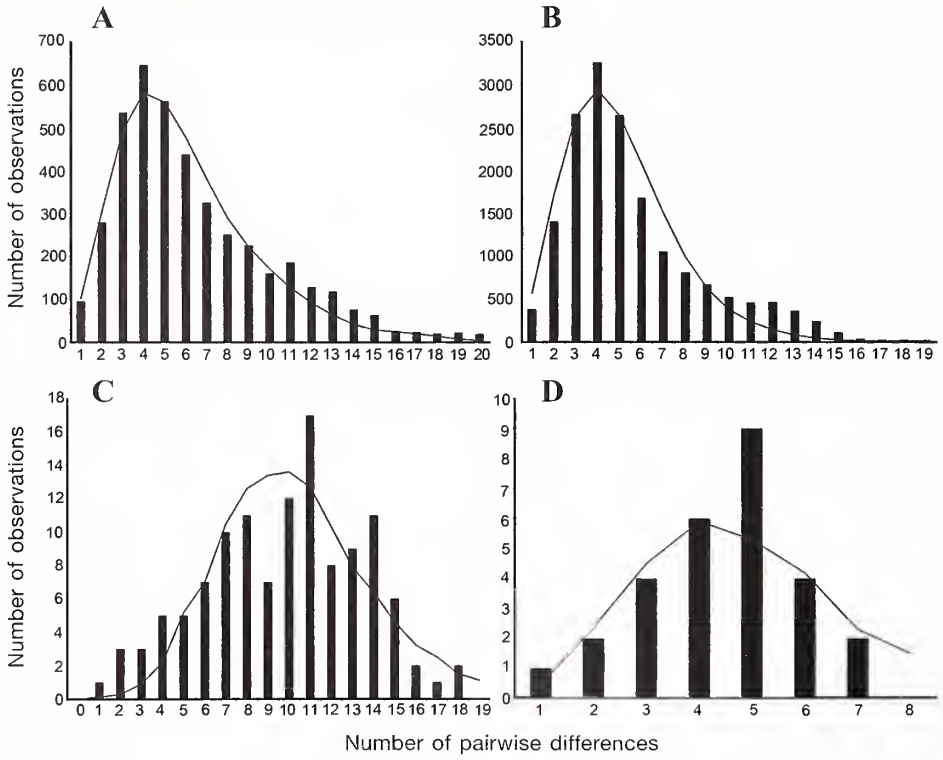

Figure 3

Number of pairwise differences from mismatch distributions of dolphinfish (*Coryphaena hippurus*) based on analyses of mitochondrial nicotinamide adenine dinucleotide (NADH) dehydrogenase subunit 1 (ND1) sequence data from fish sampled in the (**A**) southeastern United States in 2012, (**B**) northeastern Caribbean Sea in 2010–2013, (**C**) eastern Caribbean Sea in 1998 and 2014, and (**D**) central North Atlantic in 1998. Bars indicate the observed distributions under the spatial expansion model. The curve indicates the simulated distribution.

Table 3

Mismatch parameters used in the estimation of population expansion of dolphinfish (*Coryphaena hippurus*) based on mitochondrial nicotinamide adenine dinucleotide (NADH) dehydrogenase subunit 1 (ND1) sequence data analyzed in this study. τ=coalescence time in generations (τ=2μT); μ=mutation rate 1.2% per million years; T=years since expansion; θ=value used to estimate initial effective population size (N_0) before and after (θ_1) expansion; N_1=population size after expansion; M=scaled migration rate; m=immigration rate from adjacent population; P_{SSD}=probability of the expected mismatch distribution to fit the expansion model. The bold value is significant at P<0.001. Modified following Díaz-Jaimes et al. (2010). USSE=southeastern United States; NEC=northeastern Caribbean Sea; EC=eastern Caribbean Sea; CNA=central North Atlantic.

Region	Demographic expansion parameters							Spatial expansion parameters						
	τ	T	θ	N_0	θ_1	N_1	P_{SSD}	τ	T	θ	N	M	m	P_{SSD}
USSE	2.21	71,400	0.00	0.00	99,999	2.1×10^9	**>0.001**	2.21	71,400	2.97	64,000	99,999	0.78	0.760
NEC	2.31	74,700	1.89	40,700	99,999	2.1×10^9	0.370	2.31	74,700	1.89	40,900	99,999	1.22	0.280
EC	1.59	51,400	5.25	113,200	1205	2.5×10^7	0.800	1.61	52,000	5.23	112,700	298.00	0.0013	0.810
CNA	3.85	124,500	0.00	0.00	99,999	2.1×10^9	0.590	3.85	124,500	0.007	15.1	99,999	3311	0.530
Mean	2.49	80,500	1.78	38,475	75,300	1.6×10^9	0.440	2.50	80,650	2.52	54,353	75,073	828.25	0.595

were large differences in θ_0 (twice the product of the effective population size [N_0] and mutation rate [μ]) and in θ_1 (2 (N_1*μ)), indicating rapid demographic expansions. The average value of θ_0 among regions (1.78) indicated a small initial size for the female breeding population (N_0 ~38,475) followed by very rapid population expansion (N_1=~1.6×10^9).

Discussion

Analyses of the ND1 gene in dolphinfish revealed genetic homogeneity around Puerto Rico and shallow genetic heterogeneity across the western central Atlantic but failed to identify regional genetic differences among the southeastern United States, northeastern Caribbean Sea, eastern Caribbean Sea, and central North Atlantic. These results, when examined with tag data (Fig. 1), indicate that substantial mixing is occurring throughout the western central Atlantic and that the entire region could be identified as a single stock. It is clear that migration across the region is high and the degree of reproductive isolation is low. However, although migration and reproductive isolation are critical attributes considered for stock identification, biological data sources (e.g., catch data, growth rates, fecundity at age) should be considered in future studies to strengthen the support for or against the identification of individual dolphinfish stocks in the Atlantic (Begg and Waldman, 1999).

Haplotypes were randomly distributed (Fig. 2)—a finding that indicates the presence of a single panmictic population. A possible explanation for this panmixis is Gulf Stream intensification (Coëtlogon et al., 2006) and the recirculation tendency of surface waters around the North Atlantic subtropical gyre (Richardson, 1993). This current pattern may facilitate significant migration of dolphinfish among locations in the North Atlantic by larval dispersal and as a result of the propensity of juvenile and subadult fish to exhibit strong fidelity with floating objects (e.g., *Sargassum* and flotsum) (Farrell et al., 2014; Merten et al., 2014a)

The dispersal capability of large pelagic species like dolphinfish is high in the absence of obvious barriers (e.g., temperature and land). Presumably, the highly migratory nature of dolphinfish, coupled with widespread spawning activity, resulted in the moderate levels of gene flow and low genetic differentiation found in this study. This pattern is characteristic of intrabasin distributions of other pelagic fishes, including blue marlin (McDowell et al., 2007), sailfish (Graves and McDowell, 2003), and wahoo (Theisen et al., 2008). However, oceanographic features, such as gyres, or population isolation due to coastal geomorphology, could limit population mixing and lead to genetic heterogeneity. In the case of bluefin tuna, Carlsson et al. (2006) observed a slight genetic separation of stocks in the Atlantic Ocean, likely a result of geographically separated spawning areas due to coastal geomorphology, and suggested the population consists of a mixed-stock fishery.

The potential for year-round spawning behavior and the lack of reproductive isolation in dolphinfish are important life-history characteristics that contribute to the observed genetic homogeneity. Dolphinfish have been characterized as batch spawners because of the presence of several size classes of eggs in the ovaries occurring simultaneously at geographically separate regions (Palko et al., 1982; Ditty et al., 1994; Oxenford, 1999), a reproductive characteristic that indicates that females spawn over broad times and locations as they migrate throughout the region. Female dolphinfish often are active reproductively from November through July in the Straits of Florida and from May through July off Cape Hatteras, North Carolina (Palko et al.,

Table 4

Conventional mark and recapture movements of dolphinfish (*Coryphaena hippurus*) reported from recreational and commercial fishermen participating in the Dolphinfish Research Program in the western and central North Atlantic and Caribbean Sea from 2004-2012. DAL=days at liberty.

Tag (no.)	Date tagged	Date recaptured	DAL	Distance (km)[a]	Speed (km/d)	Nearest locality to tagging location	Nearest locality to recapture location
1	8-Nov-2011	30-May-2012	203	1916.22	9.43	San Juan, PR	Charleston, SC
2	15-May-2004	11-Feb-2005	240	4002.77	17.94	Charleston, SC	Azores Islands
3	20-Jun-2011	2-Mar-2012	256	2049.59	8.00	Marathon, FL	St. Barthélemy
4	10-Jun-2008	17-May-2009	341	2058.68	6.03	Big Pine Key, FL	St. Kitts
5	19-Jun-2004	4-Feb-2005	230	2109.22	9.17	Biscayne, FL	Antigua
6	8-Jun-2007	26-Feb-2008	263	2651.57	10.08	Charleston, SC	Puerto Columbia, Venezuela
7	23-Jul-2004	26-Mar-2005	246	1610.13	6.54	Islamorada, FL	Guanica, Puerto Rico
8	1-Jun-2011	9-Dec-2012	557	1613.39	2.89	Miami, FL	Guanica, Puerto Rico
9	7-Aug-2009	26-Mar-2010	231	1975.73	8.55	Charleston, SC	Guanica, Puerto Rico
10	15-May-2004	11-Feb-2005	330	1711.23	5.18	Charleston, SC	Costa Maya, Mexico
11	1-Aug-2007	18-Mar-2008	230	198.47	0.86	Islamorada, FL	Playa Escondido, Cuba
12[b]	2-Jun-2010	12-Dec-2010	192	1140.57	5.94	Miami, FL	Puerto Plata, DR
13[b]	14-Jul-2011	22-Feb-2012	223	342.56	1.53	Miami, FL	Exuma Sound, Bahamas
14[b]	24-Jul-2004	2-Apr-2005	252	598.91	2.37	Islamorada, FL	Playa Blanca, Cuba
15[b]	10-Jun-2009	24-Apr-2010	318	657.21	2.06	Big Pine Key, FL	Long Island, Bahamas

[a]Minimum straight-line distance.
[b]Previously published data taken with permission from Merten et al. (2014b).

1982). However, larvae and early juveniles have been collected year-round off the southeastern United States and in the Caribbean Sea (Rose and Hassler, 1968; Ditty et al., 1994).

Length-frequency distributions based on data collected around the region indicate the seasonal arrival and departure of different cohorts (Rivera and Appeldoorn, 2000), again indicating multiple spawning events. However, the seasonal arrival of different cohorts may also result from schooling behavior and swimming speeds of similar-size fish or from the seasonal dynamics of the "delivery system" (e.g., cycling of *Sargassum* mats, which serve as a mobile habitat that constantly supports recruitment); the cycling of *Sargassum* may be more of an influence than reproductive timing on dolphinfish population dynamics, especially off Puerto Rico (Rivera and Appeldoorn, 2000).

Movements of dolphinfish found by conventional mark and recapture methods linked most sampled regions and provide a basis for regional connectivity and population mixing (Table 4; Fig. 1). Along the U.S. East Coast, dolphinfish move north (Merten et al., 2014a) and appear to make circuits around the Sargasso Sea and multiple movements from Florida to the Bahamas, Dominican Republic, and Cuba (Merten et al., 2014b). Movements to the Caribbean Sea are likely extensions of these shorter circuits, determined by how far north dolphinfish exit from waters of the U.S. East Coast. Exiting north of Little Bahama Bank will result in shorter migratory routes around the western central Atlantic than staying with the Gulf Stream and exiting off the Mid-Atlantic Bight. The former would result in a more direct route to the Bahamas, but the latter would likely result in eventual movement toward the northeastern Caribbean Sea. Together, the low genetic structure and the evidence of high dispersal capabilities of this species support recognition of a single stock (both fishery and genetic) throughout the western central Atlantic, with exchange between the central North Atlantic on the basis of sequence data and observed movement to the Azores Islands (Table 4, Fig. 1).

A population is composed of individuals that co-occur in space and time and interbreed, and a stock is a subgroup of the main population, capable of interbreeding, but differs in some way from the main population (i.e., timing of migration, percent occurrence by location, or growth rates) (Waples et al., 2008). Here, the high potential for long-distance migration indicated by the tagging data and the low reproductive isolation indicated by the genetic analyses of dolphinfish sampled in the western central Atlantic do not support the identification of 2 stocks as proposed by Oxenford and Hunte (1986). However, the number of samples was low from the eastern Caribbean Sea (N=43) and the central North Atlantic (N=8), and those low numbers of samples represent a major constraint in this study. With only 8 samples from the central North Atlantic, it is unlikely that genetic structure would be detected with any type of genetic marker. Additionally, the number of tagged fish showing movement between the eastern

Caribbean Sea and other areas was small, and their movements were largely unidirectional.

In this study, genes adjacent to the coding region were incorporated into genetic analyses to add sensitivity to DNA sequence comparisons. The use of the entire ND1 gene was considered appropriate to preliminarily describe the genetic structure of dolphinfish in the western central Atlantic at different spatial scales. It is important to note that, from the onset of this study, the choice to use the ND1 marker may have influenced the outcome of results. Therefore, faster-evolving nuclear markers (e.g., microsatellites or single-nucleotide polymorphisms) may have been more suitable to detect genetic differences of dolphinfish at the scale of this study.

More samples (N>50) should be compared in future studies, the sampling area should be expanded to Brazil and west Africa, and more sensitive markers should be used to address the multistock question for dolphinfish across the broader Atlantic. More extensive tagging studies need to be conducted in poorly sampled areas, such as the eastern Caribbean Sea and the Azores Islands. Using more sensitive techniques, Díaz-Jaimes et al. (2010) detected low genetic structure between the Caribbean Sea and Senegal, west Africa, and suggested that isolation of dolphinfish in the Mediterranean Sea caused genetic differentiation between populations in the Mediterranean and western North Atlantic. They concluded that alternative markers should be used to define stock structure at the within-ocean level. In the eastern Pacific, Rocha-Olivares et al. (2006) observed significant genetic heterogeneity, using RFLP analyses of dolphinfish between Hawaii and Baja California (straight-line distance= ~4660 km); this observation was likely the result of lower gene flow among these locations but merits future investigation with more powerful molecular markers (e.g., microsatellites or single-nucleotide polymorphisms). In the Caribbean Sea and Atlantic, the spatial scale of our study (Miami, Florida, to the Azores Islands= ~4796 km) was not sufficient to resolve stock-related differences.

Fu's F_S departed significantly from expectations in all sampled regions. The driving force of significant departures from neutrality in our samples was the excess of singletons, an outcome that is indicative of past population expansions (Aris-Brosou and Excoffier, 1996). Pairwise mismatch distributions were unimodal for all regions, indicating relatively recent range expansions with continued gene flow between populations through time (Fig. 3) (Rogers and Harpending, 1992; Díaz-Jaimes et al., 2006). In the central North Atlantic, the low number of samples could have heavily influenced the extremely low F estimation observed in the mismatch analyses (P=0.013). Owing to the low numbers of samples from both the eastern Caribbean Sea and central North Atlantic, mismatch distributions should not be considered conclusive of population expansions until more samples are included into future model analyses.

Because of extensive mixing on a fishery stock level and support for a single regionally linked population across the sampled region, we suggest that a multijurisdictional and international approach to management is necessary. The most accurate landings information should be shared among all jurisdicitions where dolphinfihs are caught. However, we leave open the question of whether the eastern Caribbean Sea can be managed separately (though still internationally), and it is not clear how the central North Atlantic (i.e., Azores Islands) should be grouped as a result of a low number of samples; in future studies, more samples from this region should be collected and compared.

Our results are similar to those of Díaz-Jaimes et al. (2006), who found a single panmictic eastern Pacific population of dolphinfish that occurs within the northern portion of the Gulf of California and off Chiapas in southern mainland Mexico. The major difference between the 2 regions is the number of jurisdictions where dolphinfish are harvested. In the eastern Pacific, the geographic extent of the Díaz-Jaimes et al. (2006) study spanned only one exclusive economic zone (EEZ); in contrast, as many as 30 EEZs (Mahon, 1996) exist in the area examined in our study. Therefore, in the western central Atlantic, stock assessments will become inherently more complex because of the shared nature of the resource among many resource users. Subsequently, to effectively manage dolphinfish in the western central Atlantic, stock assessments need to incorporate the movement of dolphinfish through distant and adjacent EEZs, the timing of arrival to different EEZs, the amount landed in each location, and the demographics of this species at different scales.

Acknowledgments

This research was supported by funding through the U.S. Fish and Wildlife and Puerto Rico Department of Natural and Environmental Resources F-66.1 project to the Department of Marine Sciences, University of Puerto Rico at Mayagüez. We thank R. Chapman and the Marine Resources Division of the South Carolina Department of Natural Resources and H. Oxenford and N. Simpson of the Centre for Resource Management and Environmental Studies at the University of the West Indies for providing additional samples for use in this study. We also thank J. Hyde for providing a preliminary review on an earlier version of this manuscript. Lastly, we thank M. Botello, I. Báez, A. Alfalla, C. Whitley, M. Lugo, E. Martínez, M. Carlo, A. Santiago, and O. Espinosa for help in the field collecting samples.

Literature cited

Allendorf, F. W., N. Ryman, and F. M. Utter.
1987. Genetics and fishery-management: past, present, and future. *In* Population genetics and fishery management (N. Ryman and F. Utter, eds.), p. 1–20. Univ. Washington Press, Seattle, WA.

Alvarado Bremer, J. R., J. Mejuto, J. Gómez-Márquez, F. Boán, P. Carpintero, J. M. Rodríguez, J. Viñas, T. W. Greig, and B. Ely.
2005. Hierarchical analyses of genetic variation of samples from breeding and feeding grounds confirm the genetic partitioning of northwest Atlantic and South Atlantic populations of swordfish (*Xiphias gladius* L.). J. Exp. Mar. Biol. Ecol. 327:167–182.

Alvarado Bremer, J. R., J. Mejuto, T. W. Greig, and B. Ely.
1996. Global population structure of the swordfish (*Xiphias gladius* L.) as revealed by analysis of the mitochondrial DNA control region. J. Exp. Mar. Biol. Ecol. 197:295–310.

Aris-Brosou, S., and L. Excoffier.
1996. The impact of population expansion and mutation rate heterogeneity on DNA sequence polymorphism. Mol. Biol. Evol. 13:494–504.

Begg, G. A., and J. R. Waldman.
1999. An holistic approach to fish stock identification. Fish. Res. 43:35–44.

Benetti, D. D., R. W. Brill, and S. A. Kraul Jr.
1995. The standard metabolic rate of dolphinfish. J. Fish. Biol. 46:987–996.

Bermingham, E., S. S. McCafferty, and A. P. Martin.
1997. Fish biogeography and molecular clocks: perspectives from the Panamanian isthmus. *In* Molecular Systematics of Fishes (T. D. Kocher and C. A. Stepien, eds.), p. 113–128. Academic Press, San Diego, CA.

Boustany, A. M., C. A. Reeb, and B. A. Block.
2008. Mitochondrial DNA and electronic tracking reveal population structure of Atlantic bluefin tuna (*Thunnus thynnus*). Mar. Biol. 156:13–24.

Bowen, B. W., A. Muss, L. A. Rocha, and W. S. Grant.
2006. Shallow mtDNA coalescence in Atlantic pygmy angelfishes (genus *Centropyge*) indicates a recent invasion from the Indian Ocean. J. Hered. 97:1–12.

Carlsson, J., J. R. McDowell, J. E. L. Carlsson, D. Ólafsdóttir, and J. E. Graves.
2006. Genetic heterogeneity of Atlantic bluefin tuna caught in the eastern North Atlantic Ocean south of Iceland. ICES J. Mar. Sci. 63:1111–1117.

Collette, B. B., C. Reeb, and B. A. Block.
2001. Systematics of the tunas and mackerels (Scombridae). Fish Physiol. 19:1–33.

Clement, M., D. Posada, and K. A. Crandall.
2000. TCS: a computer program to estimate gene genealogies. Mol. Ecol. 9:1657–1659.

Coëtlogon, G. de, C. Frankignoul, M. Bentsen, C. Delon, H. Haak, S. Masina, and A. Paradaens.
2006. Gulf Stream variability in five oceanic general circulation models. J. Phy. Oceanog. 36:2119–1235.

Darriba, D., G. L. Taboada, R. Doallo, and D. Posada.
2012. jModelTest 2: more models, new heuristics and parallel computing. Nat. Methods 9:772.

Díaz-Jaimes, P., M. Uribe-Alcocer, S. Ortega-García, and J.-D. Durand.
2006. Spatial and temporal mitochondrial DNA genetic homogeneity of dolphinfish populations (*Coryphaena hippurus*) in the eastern central Pacific. Fish. Res. 80:333–338.

Díaz-Jaimes, P., M. Uribe-Alcocer, A. Rocha-Olivares, F. J. García-de-León, P. Nortmoon, and J. D. Durand.
2010. Global phylogeography of the dolphinfish (*Coryphaena hippurus*): the influence of large effective population size and recent dispersal on the divergence of a marine pelagic cosmopolitan species. Mol. Phylogenet. Evol. 57:1209–1218.

Ditty, J. G., R. F. Shaw, C. B. Grimes, and J. S. Cope.
1994. Larval development, distribution, and abundance of common dolphin, *Coryphaena hippurus*, and pompano dolphin, *C. equiselis* (family: Coryphaenidae), in the northern Gulf of Mexico. Fish. Bull. 92:275–291.

Eldridge, M. B., and P. G. Wares.
1974. Some biological observations of billfishes taken in the eastern Pacific Ocean, 1967–1970. *In* Proceedings of the international billfish symposium, Pt. 2. Review and contributed papers; Kailua-Kona, HI, 9–12 August 1972 (R. S. Shomura and F. Williams, eds.), p. 89–101. NOAA Tech. Rep. NMFS SSRF-675.

Excoffier, L., and H. E. L. Lischer.
2010. Arlequin suite ver 3.5: a new series of programs to perform population genetics analyses under Linux and Windows. Mol. Ecol. Resour. 10:564–567.

Farrell, E. R., A. M. Boustany, P. N. Halpin, and D. L. Hammond.
2014. Dolphinfish (*Coryphaena hippurus*) distribution in relation to biophysical ocean conditions in the northwest Atlantic. Fish. Res. 151:177–190.

Fu, Y. X.
1997. Statistical tests of neutrality against population growth, hitchhiking and background selection. Genetics 147:915–925.

Garber, A. F., M. D. Tringali, and J. S. Franks.
2005. Population genetic and phylogeographic structure of wahoo, *Acanthocybium solandri*, from the western central Atlantic and central Pacific Oceans. Mar. Biol. 147:205–214.

Graves, J. E.
1998. Molecular insights into the population structures of cosmopolitan marine fishes. J. Hered. 89:427–437.

Graves, J. E., and A. E. Dizon.
1989. Mitochondrial DNA sequence similarity of Atlantic and Pacific albacore tuna. Can. J. Fish. Aquat. Sci. 46:870–873.

Graves, J. E., and J. R. McDowell.
1994. Genetic analysis of striped marlin (*Tetrapturus audax*) population structure in the Pacific Ocean. Can. J. Fish. Aquat. Sci. 51:1762–1768.
2001. A genetic perspective on the stock structures of blue marlin and white marlin in the Atlantic Ocean. Collect. Vol. Sci. Pap. ICCAT 53:180–187. [Available at website.]
2003. Stock structure of the world's istiophorid billfishes: a genetic perspective. Mar. Freshw. Res. 54:287–298.

Hauser, L., and G. R. Carvalho.
2008. Paradigm shifts in marine fisheries genetics: ugly hypotheses slain by beautiful facts. Fish Fish. 9:333–362.

Hauser, L., and R. D. Ward.
1998. Population identification in pelagic fish: the limits of molecular markers. *In* Advances in molecular ecology (G. R. Carvalho, ed.), p. 191–224. IOS Press, Amsterdam.

Hilborn, R., and C. J. Walters.
1992. Quantitative fisheries stock assessment: choice, dynamics, and uncertainty, 570 p. Routledge, Chapman, & Hall, New York.

Kimura, M.
1968. Evolutionary rate at the molecular level. Nature 217:624–626.

Maddison, W. P., and D. R. Maddison.
2011. Mesquite: a modular system for evolutionary analysis, version 2.75. [Available at website.]
Mahon, R.
1996. Fisheries and research for tunas and tuna-like species in the western central Atlantic: implications of the agreement for the implementation of the provisions of the United Nations convention on the law of the sea 10 December 1982 relating to the conservation and management of straddling fish stocks and highly migratory fish stocks. FAO Fish Tech. Pap. 357, 62. [Available at website.]
Mahon, R., and H. A. Oxenford.
1999. Precautionary assessment and management of dolphinfish in the Caribbean. Sci. Mar. 63:429–438.
McDowell, J. R., J. E. L. Carlsson, and J. E. Graves.
2007. Genetic analysis of blue marlin (*Makaira nigricans*) stock structure in the Atlantic Ocean. Gulf Caribb. Res. 19:75–82.
Merten, W., R. Appeldoorn, and D. Hammond.
2014a. Movements of dolphinfish (*Coryphaena hippurus*) along the U.S. east coast as determined through mark and recapture data. Fish. Res. 151:114–121.
2014b. Spatial differentiation of dolphinfish (*Coryphaena hippurus*) movements relative to the Bahamian archipelago. Bull. Mar. Sci. 90:849–864.
Oxenford, H. A.
1999. Biology of the dolphinfish (*Coryphaena hippurus*) in the western central Atlantic: a review. Sci. Mar. 63:277–301.
Oxenford, H. A., and W. Hunte.
1986. A preliminary investigation of the stock structure of the dolphin, *Coryphaena hippurus*, in the western central Atlantic. Fish. Bull. 84:451–460.
Palko, B. J., G. L. Beardsley, and W. J. Richards.
1982. Synopsis of the biological data on *Coryphaena hippurus* Linnaeus and *Coryphaena equiselis* Linnaeus. NOAA Tech. Rep. NMFS Circ. 443, 35 p.
Posada, D.
2008. jModelTest: phylogenetic model averaging. Mol. Biol. Evol. 25:1253–1256.
Reiss, H., G. Hoarau, M. Dickey-Collas, and W. J. Wolff.
2009. Genetic population structure of marine fish: mismatch between biological and fisheries management units. Fish Fish. 10:361–395.
Richardson, D. E.
2008. Physical and biological characteristics of billfish spawning habitat in the Straits of Florida. Ph.D. diss., 194 p. Univ. Miami, Coral Gables, FL.
Richardson, P. L.
1993. A census of eddies observed in North Atlantic SOFAR float data. Prog. Oceanog. 31:1–50.
Rivera, G. A., and R. S. Appeldoorn.
2000. Age and growth of dolphinfish, *Coryphaena hippurus*, off Puerto Rico. Fish. Bull. 98:345–352.
Rocha-Olivares, A., M. Bobadilla-Jiménez, S. Ortega-García, N. Saavedra-Sotelo, and J. R. Sandoval-Castillo.
2006. Mitochondrial variability of dolphinfish (*Coryphaena hippurus*) populations in the Pacific Ocean. Cienc. Mar. 32:569–578. [Available at website.]
Rogers, A. R., and H. Harpending.
1992. Population growth makes waves in the distribution of pairwise genetic differences. Mol. Biol. Evol. 9:552–569.
Rose, C. D., and W. W. Hassler.
1968. Age and growth of the dolphin, *Coryphaena hippurus* (Linnaeus), in North Carolina waters. Trans. Am. Fish. Soc. 97:271–276.
Salcedo-Bojorquez, S., and F. Arreguin-Sanchez.
2011. An exploratory analysis to identify reproductive strategies of billfishes. J. Fish. Aquat. Sci. 6:578–591.
Tamura, K., and M. Nei.
1993. Estimation of the number of nucleotide substitutions in the control region of mitochondrial DNA in humans and chimpanzees. Mol. Biol. Evol. 10:512–526.
Theisen, T. C., B. W. Bowen, W. Lanier, and J. D. Baldwin.
2008. High connectivity on a global scale in the pelagic wahoo, *Acanthocybium solandri* (tuna family Scombridae). Mol. Ecol. 17:4233–4247.
Tripp-Valdez, M. A., F. J. García de León, S. Ortega-García, D. Lluch-Cota, J. López-Martínez, and P. Cruz.
2010. Population genetic structure of dolphinfish (*Coryphaena hippurus*) in the Gulf of California, using microsatellite loci. Fish. Res. 105:172–177.
Waples, R. S., A. E. Punt, and J. M. Cope.
2008. Integrating genetic data into management of marine resources: how can we do it better? Fish Fish. 9:423–449.
Witzell, W. N., and E. L Scott.
1990. Blue marlin, *Makaira nigricans*, movements in the western north Atlantic Ocean: results of a cooperative game fish tagging program, 1954–88. Mar. Fish. Rev. 52(2):12–17.

NOAA
National Marine
Fisheries Service

Fishery Bulletin
established 1881

Spencer F. Baird
First U.S. Commissioner
of Fisheries and founder
of *Fishery Bulletin*

Behavior-dependent selectivity of yellowtail flounder (*Limanda ferruginea*) in the mouth of a commercial bottom trawl

Melanie J. Underwood (contact author)[1,2,3]
Paul D. Winger[3]
Anders Fernö[2]
Arill Engås[1,2]

Email address of contact author: melanie.underwood@imr.no

[1] Institute of Marine Research
P.O. Box 1870
Nordnes, 5817 Bergen, Norway

[2] Department of Biology
University of Bergen,
P.O. Box 7800
NO-5020 Bergen, Norway

[3] Fisheries and Marine Institute
Memorial University of Newfoundland
P.O. Box 4920
St. John's, Newfoundland, Canada A1C 5R3

Abstract—To improve the efficiency of a commercial bottom trawl for catching yellowtail flounder (*Limanda ferruginea*), we studied the behavior of individuals in the middle of the trawl mouth. Observations were conducted with a high-definition camera attached at the center of the headline of a trawl, during the brightest time of day in June 2010 off eastern Newfoundland. Behavioral responses were quantified and analyzed to evaluate predictions related to fish behavior, orientation, and capture. Individuals showed 3 different initial responses independent of fish size, gait, and fish density: they swam close to (75%), were herded away from (19%), or moved vertically away from (6%) the seabed. Individuals primarily swam in the direction of initial orientation. No fish were oriented against the trawling direction. Fish in the center of the trawl mouth tended to swim along the bottom in the trawling direction. Only individuals that were stimulated to leave the bottom were caught. Individuals in peripheral locations within the trawl mouth more often swam inward and upward. Fish that swam inward were twice as likely to be caught. Fish size, gait, and fish density did not influence the probability of capture. A trawl that stimulates yellowtail flounder to orient inward and leave the bottom would increase the efficiency of a trawl.

Manuscript submitted 9 September 2014.
Manuscript accepted 5 August 2015.
Fish. Bull. 113:430–441 (2015).
Online publication date: 2 September 2015.
doi: 10.7755/FB.113.6.

The bottom trawl fishery in Newfoundland for yellowtail flounder (*Limanda ferruginea*), hereafter called "yellowtail," re-opened in 1998 after a moratorium from 1994 to 1997. As a result of efforts to maintain a sustainable fishery after the re-opening, the industry faced restrictions that included yearly quotas, minimum legal sizes, discard bans, and short-term area closures due to summer spawning, as well as closures resulting from bycatches of American plaice (*Hippoglossoides platessoides*) and Atlantic cod (*Gadus morhua*). In addition, declines in the quality of fish that occur before the spawning season create an incentive to harvest the entire quota while the market value for yellowtail is highest. Therefore, ensuring that the harvesting of this species is not only sustainable but also efficient is a key concern for the fishing industry for yellowtail in Newfoundland.

Understanding fish behavior can help to improve the harvesting process (Winger, 2008). How fishes respond to demersal trawls is indicative of their catchability and has been studied for the different catch zones of a trawl where individuals may occur either 1) in the path of a trawl (i.e., the area between the wings of a trawl net), which results in a high probability of capture; 2) in the path of the sweeps (i.e., the area swept by the doors and ground wires), where they have a lower but still significant probability of capture; or 3) outside the paths of the trawl and sweeps, where there is a minimal probability of capture. Only fishes that stay in or are herded into the path of the trawl mouth (i.e., the area where the footgear connects to the net) are ultimately caught in the net (see Winger et al. [2010] for review).

Flatfishes, because of their generally poor swimming ability that can be attributed to their unique body

Table 1

Date, location, start depth, vessel's course over ground, percentage of yellowtail flounder (*Limanda ferruginea*), American plaice (*Hippoglossoides platessoides*), and witch flounder (*Glyptocephalus cynoglossus*), and the number of observations of yellowtail flounder made in analyses of video footage from 5 tows of a bottom trawl in June 2010 on the southern Grand Bank off eastern Newfoundland.

Tow	Date (m/d)	Start latitude (°)	Start longitude (°)	Start depth (m)	Course over ground (°)	Catch size (kg)	Percentage of flatfishes in catch			Observations
							Yellowtail flounder	American plaice	Witch flounder	Number of yellowtail
1	6/17	45.463	-51.871	82.3	162	2875	86	14		44
2	6/20	45.438	-52.219	73.2	20	1725	92	8		38
3	6/22	45.430	-51.871	80.5	270	2944	84	15	1	27
4	6/23	45.393	-51.175	69.5	344	2530	92	8		46
5	6/24	45.454	-51.283	69.5	142	2392	90	10		35

shape, exhibit a close association with the seabed. Their strategy to avoid natural predators is a combination of burying themselves in sediment, cryptic coloration, and low activity, all of which minimize their detection (Gibson, 2005). As a predator advances, a flatfish will either remain immobile or flee to a short distance to maintain distance from the predator, settling only when the encounter ceases. Similar behavior in relation to trawls has been observed in other flatfishes (Main and Sangster, 1981; Bublitz, 1996; Ryer and Barnett, 2006; Ryer et al., 2010), which react to a gear at short distances and commonly move at a 90° angle to the trawl. This response occurs multiple times along the sweeps until flatfishes congregate in the mouth of a trawl. Once they are in the trawl mouth, escapement under the footgear is a particular problem (Albert et al., 2003; Ryer and Barnett, 2006). Consequently, the mouth of the trawl is a critically important area when considering how to improve gear efficiency (Engås and Godø, 1989; Walsh, 1992).

As a first step to improve the efficiency of the yellowtail fishery, we developed a high-definition camera system (Underwood et al., 2012) because flatfish species were not able to be easily distinguished in most previous studies (e.g., Beamish, 1966; 1969; Walsh and Hickey, 1993; Bublitz, 1996; Kim and Wardle, 2003; Chosid et al., 2012; Bryan et al., 2014). Then we examined the behavior of yellowtail in the central part of the trawl mouth during commercial bottom trawling operations. The influence of fish size (Walsh, 1992; Peake and Farrell, 2004), swimming endurance and gait (Winger et al., 1999, 2004), orientation (Beamish, 1966), and density (Godø et al., 1999) on general flatfish behavior have been examined in these studies; however, each factor was examined separately. In contrast, we conducted an in-depth, quantitative study and applied statistical models to simultaneously assess all of the above factors and explain what drives the behavior of individual fish and overall outcome for yellowtail in the mouth of the trawl.

We anticipated that the orientation of a fish in or on the substrate and that previous herding by sweeps (previous experience of fish with gear) would affect the probability of capture of individual yellowtail. A flatfish observed in a trawl mouth would be either a fish that had been lying in the path of the trawl and is encountering the gear for the first time or a fish that had been herded previously by the sweeps. In contrast, fish observed along the periphery of the footgear of a trawl would be expected to have been herded previously by the sweeps and, therefore, more likely to orient toward the opposite side of the trawl. Because the morphological features of flatfishes make it difficult for them to turn left or right (Stickney et al., 1973), most yellowtail would be expected to swim in the direction they are facing; therefore, fish oriented inward, if they swam on their current trajectory, would observe the trawl gear earlier in their field of view and hit the footgear, increasing their probability of being captured. Previously herded fish are also likely to be more fatigued than first-time herded fish (Winger et al., 1999)—a state that could affect their response to a trawl and determine whether an individual fish is caught or not.

Materials and methods

Experiments were conducted during the first tow of a bottom trawl each afternoon in June 2010 onboard the FV *Aqviq*, a 49-m groundfish trawler (2450 bhp) of Ocean Choice International,[1] on the southern Grand Bank off eastern Newfoundland (Table 1). The gear used in these experiments was a 2-bridle, 2-seam bottom trawl (Fig. 1) that had a 4-m extended upper panel (square) and that was equipped with rockhopper footgear (52.5-cm-diameter rubber discs with 20-cm spacers). Towing speeds varied from 1.5 to 1.7 m/s,

[1] Mention of trade names or commercial companies is for identification purposes only and does not imply endorsement.

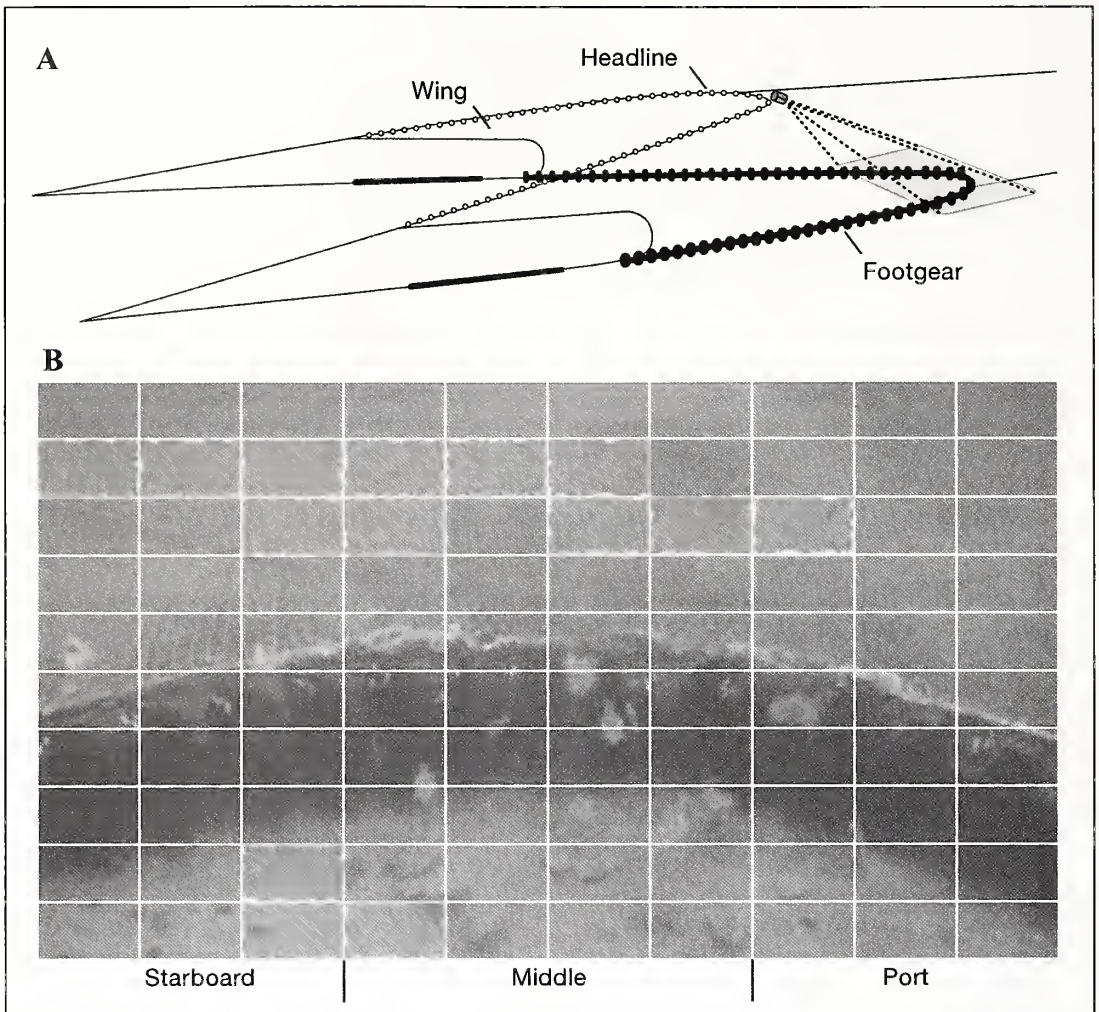

Figure 1

(**A**) Schematic illustration of the bottom trawl used to collect video images of yellowtail flounder (*Limanda ferruginea*) in June 2010 on the southern Grand Bank off eastern Newfoundland and (**B**) an example of the grid used for the analysis of video footage. The gray square in panel A indicates the area observed by the camera (3 m high×4 m wide field of view), which was ~5 m from the center of the footgear (and 3 m from seabed; the headline was 4 m in front of the footgear). Video frames, as shown in panel B, were divided into 100 squares, with the middle 4 columns representing the center of the footgear and the 3 columns on either side representing port and starboard of the footgear.

and durations of tows were in a range of 2–3 h. Tow direction was decided by commercial operations and was different for each tow. The height of the headline was approximately 3 m and was recorded with a sensor (Marport Stout Inc., Snohomish, WA) attached to the headline on all tows without the use of camera documentation during the cruise. The door spread ranged from 113 to 123 m and was measured with spread sensors (Marport Stout Inc.) placed on the trawl doors.

During 5 tows, more than 12 h of video footage of flatfishes were collected at depths of 70–82 m, at bottom temperatures ranging from 0.6°C to 1.2°C. A new high-definition, self-contained underwater camera system without artificial lights (72% accuracy for identification of yellowtail; for details, see Underwood et al. [2012]) was used to observe approximately a quarter of the footgear (i.e., the central region, excluding the wings; Fig 1). Observational techniques, such as the use of artificial lights, may influence the behavior for some species (Walsh and Hickey, 1993; Weinberg and Munro, 1999). Therefore, time of year and day was chosen to optimize natural underwater light for the camera and so that artificial lights were not needed. The camera system was attached to the inside of the center of the headline (Fig. 1A). The straight-line distance from the camera to the center of the footgear was ~5 m, providing a field a view 3 m high by 4 m wide of the lower first belly and the central part of the footgear.

Video analysis

Analysis of the video footage was conducted in the laboratory by using Observer XT software, vers. 10.1 (Noldus Information Technology, Wageningen, Netherlands). A grid of 100 squares was placed over a 1080p high-definition monitor, and the use of that grid made it possible to provide information on where a fish was in relation to the gear (Fig. 1B). Our approach was similar to that of Albert et al. (2003), but we increased the number of squares in the grid from 49 to 100 to more accurately record the location of individual fish in relation to the footgear.

A square within the grid was selected from a list of randomly generated numbers and, while the video footage was playing, the behavior sequence of the first individual fish seen in that square was recorded. If the selected square included the trawl gear, then the next grid square on the list was selected. Only behaviors for individuals seen resting on the substrate were recorded because it was unclear whether a fish seen swimming into a frame had interacted with the sweeps or footgear. To reduce autocorrelation, observations were restricted to following a single fish in the video footage at any given time. After a sequence was analyzed, playing of the video footage was stopped, and the next grid square was selected from the list of randomly generated numbers. The process was repeated until the footage ended or until it was impossible to identify individuals on or in the substrate because of reduced natural light or the presence of sand clouds. The video footage was reviewed a second time to identify segments greater than 30 s in duration that had not been evaluated previously. The additional observations collected from this second round of analysis were added to the data set.

Individual flatfishes were categorized as either yellowtail (identified by their pointed snout and small mouth; Collette and Klein-MacPhee, 2002) or as unidentified. The analysis of video footage was limited to yellowtail because of the dominance of this species in the footage, but the numbers of unidentified flatfishes were included in values for the "start density" category, which is described later.

Categorical variables used for analysis (Table 2) were derived from similar behavioral studies (e.g., Walsh and Hickey, 1993; Albert et al., 2003; Piasente et al., 2004; Ryer and Barnett, 2006). *Location* of an individual in relation to the footgear was recorded at the start of the observation and categorized into the following 3 groups. Individuals within 2 squares of and on either side of the center of the footgear were categorized as in the "middle" of the footgear. Individuals observed greater than 2 squares to the port side or starboard side of the center of the footgear were classified as "port" and "starboard", respectively (Fig. 1B). The *orientation* of an individual fish on or in the substrate was recorded at the start of each observation (i.e., before the individual rose from the seabed), and *swimming direction* was recorded when a fish left the seabed (i.e., displayed initial behavior; Table 2). *Previous gear experience* was assumed to influence the orientation of an individual fish, and peripherally located individuals (i.e., those not in the 4 middle squares, Fig. 1B) that were facing inward (i.e., individuals on the port side facing starboard and vice versa) were recorded as "previously herded."

Fish *length* was estimated on the basis of the known dimensions of footgear components (one rockhopper disc and spacer together measured 30 cm in width) within the field of view that corresponded with the minimum legal size of yellowtail (30 cm). Measurements were taken when a single fish was close to the footgear, and each fish was then classified as being either larger or smaller than 30 cm. Individuals that were close to the reference length (~28–32 cm) or that were not visible or close to the footgear were grouped as "unmeasured." Given that fish of different sizes swim at different levels within their swimming performance range, the choice of *gait* used by each fish was also recorded (Table 2; Webb, 1994; see review by Winger et al. [2010]).

Responses of flatfishes to the footgear and sweeps had been classified into the 4 categories "pass under," "hop," "rise," and "run" in previous studies (Ryer and Barnett, 2006; Ryer, 2008; Ryer et al., 2010; Table 2). We adopted this classification and added a fifth category, "slope." After leaving the seabed, the swimming behavior of individual fish was classified into these 5 categories of "initial behavioral response" (Table 2). Run and slope led to the initiation of herding by the footgear, and the behavioral responses of the other 3 categories were seen as nonherding responses (Ryer et al., 2010). If a subsequent change in the initial response of an individual was observed, then it was noted in "change in response" (Table 2) and the second behavioral response was recorded. The response of individuals that maintained their initial behavioral response was recorded as "continued." The capture outcome of each individual was recorded as "escaped" or "captured" and the method of escapement or capture was noted (i.e., "actively entered or sought escapement," "overtaken," or "collided with the footgear").

The time, in seconds, from the point when an individual left the seabed until it passed over or under the footgear was recorded as the *residence* time. Total flatfish densities, estimated as the number of stationary and moving flatfishes in each video frame, were recorded at the start of each observation (*start density*). After all video footage was analyzed, the behaviors of 190 yellowtail were available for statistical analysis, representing approximately 1% of the total yellowtail catch from the 5 tows.

Statistical analysis

We concentrated on 4 main areas of analysis, looking at the influence of multiple variables on orientation (model 1: orientation=location), initial response (model 2: initial response=location+swimming direction+length+gait+start density+tow [random factor]), change in response (model 3: change in re

Table 2

Detailed description of each categorical variable used in the analysis of video footage from 5 tows with a bottom trawl in June 2010 on the southern Grand Bank off eastern Newfoundland.

	Location	Orientation and swimming direction (coded separately)	Previous gear experience	Length	Gait [a]	Initial and second behavioral response [b] (coded separately)	Change in response	Capture outcome	Interaction with trawl
1	Port: greater than 2 squares to the port side of the center of the footgear	Facing the vessel: between 315° and 45°	Herded: located on the port, facing starboard or located on the starboard, facing port	Small: <30 cm	Kick-swim: caudal fin moves steadily between high tailbeat amplitudes (≥1 tailbeat/s)	Pass under: no reaction to gear before passing under the footgear	Changed: changed initial response and displayed a second response	Caught: entered the trawl	Actively escaped: Sought gear and escaped
2	Middle: within 2 squares either side of the center of the footgear	Facing starboard: between 45° and 135°	Not herded: all other locations and orientations	Large: >30 cm	Cruising: caudal fin moves steadily without high tailbeat amplitudes (<1 tailbeat/sec)	Hop: 1 or 2 body movements without swimming before passing over the footgear	Continued: continued initial response with no second response	Escaped: did not enter the trawl	Overtaken and escaped: overtaken by gear
3	Starboard: greater than 2 squares to the starboard side of the center of the footgear	Facing the trawl: between 135° and 225°		Unmeasured	Burst and coast: caudal fin moves steadily between periods of no movement	Rise: swimming vertically, leaving the seabed			Overtaken and caught: overtaken by trawl while facing the vessel
4		Facing port: between 225° and 315°				Run: swimming close to the seabed (< 1 body length), in front of the footgear			Actively entered: swam into trawl
5						Slope: swimming upward while maintaining distance to the footgear			Collided and caught: collided with the gear and entered the trawl
6									Collided and escaped: collided with the gear and escaped

[a] Gait employed by fishes (Webb, 1994; Winger et al., 2004).

[b] Behavioral responses based on the descriptions in Ryer and Barnett (2006), Ryer (2008), and Ryer et al. (2010); pass under and hop were considered only for initial herding.

Table 3

Summary of the 3 statistical models used for analyses of behavioral responses of yellowtail flounder (*Limanda ferruginea*) observed in video footage from 5 tows of a bottom trawl in June 2010 on the southern Grand Bank off eastern Newfoundland. Initial herding response: initial response=location+swimming direction+length+gait+start density+tow (random factor). Change in herding response: change in response=location+swimming direction+length+gait+initial response+residence+start density+tow (random factor). Capture outcome: capture outcome=previous gear experience+length+gait+initial response+residence+start density+tow (random factor). Variables indicated in bold are significant in the reduced models ($P<0.05$). Z value is the Wald-Z test. Location 1: port vs. starboard; location 2: port vs. middle; swimming direction 1: port vs. starboard; swimming direction 2: port vs. vessel; initial response 1: slope vs. run; initial response 2: slope vs. rise.

	Initial herding response		Change in herding response		Capture outcome	
Variable	Z-value	P (>Z)	Z-value	P (>Z)	Z-value	P (>Z)
Intercept	0.416	0.68	−2.384	0.02	−2.240	0.03
Location 1	0.939	0.35	−0.057	0.95		
Location 2	0.570	0.57	−0.159	0.87		
Swimming direction 1	1.415	0.16	0.275	0.78		
Swimming direction 2	**2.404**	**0.02**	−0.607	0.54		
Previous gear experience					**-2.031**	**0.04**
Length	0.213	0.83	0.390	0.70	0.278	0.78
Gait	0.616	0.54	−1.573	0.12	−1.590	0.11
Initial response 1			**3.465**	**<0.001**	**3.366**	**<0.001**
Initial response 2					0.000	0.99
Residence			1.037	0.30	−1.117	0.26
Start density	−0.494	0.62	0.237	0.81	−0.029	0.98

sponse=location+swimming direction+length+gait+initial response+residence+startdensity+tow [random factor]), and capture outcome (model 4: capture outcome=previous gear experience+length+gait+initial response+residence +start density+tow [random factor]).

The influence of fish location in relation to the footgear on the orientation of 190 individual yellowtail on the substrate (previous gear experience, specifically for previously herded fish) was tested for uniformity (nonrandomness) with the Rayleigh test by using Oriana software, vers. 3 (Kovach Computing Services, Anglesey, Wales).

Because we were interested in the effect of fish length, along with other covariates, in shaping behavioral responses, 40 individual yellowtail that had no length data (i.e., fish that were unmeasured) were dropped from the analysis for models 2–4 (initial response, change in response, and capture outcome). For the initial response model, we initially attempted a multinominal analysis. However, we had zero observations for hop and pass under responses and only 9 observations for the rise response, thereby invalidating any further multicategorical analysis. The statistical analysis for the initial response model was then focused on the herded individuals, and binomial analysis was used with the initial response variable categories of run and slope for 141 observations. The model, therefore, was altered and named "initial herding response." The statistical analysis for the change-in-response model was also focused on only the herded individuals (i.e., initial response variable categories of run and slope), and binomial analysis was used with the change-in-response variable categories of changed and continued for 141 observations. The model, therefore, was altered and named "change in herding response." However, with the capture outcome model, we examined all initial responses (i.e., initial response variable categories of run, slope, and rise), using binomial analysis with capture outcome variable categories of caught and escaped for 150 observations.

To account for the variance between tows and pseudo replication (Millar and Anderson, 2004) in analysis of models 2–4 (initial herding response, change in herding response, and capture outcome), we used a generalized linear mixed model (GLMM) with binomial error, with *tow* as a random factor. Analysis with GLMMs was carried out with the lme4 package (Bates et al., 2013) in R, vers. 3.0.2 (R Core Team, 2013). Explanatory variables with more than 2 categories (i.e., location) were automatically separated into binomials by R (i.e., port location versus starboard location; Table 3). Variables in the models were reduced by using backward stepwise deletion until only variables that explained a significant amount of variation (likelihood ratio test, $P<0.05$) in the data remained (Crawley, 2007).

Results

Catch composition of flatfishes varied with each tow, ranging from 84% to 92% for yellowtail and from 8% to 15% for American plaice. Witch flounder (*Glyptocephalus cynoglossus*) were present in only one tow (Table 1). The length of yellowtail in the catch ranged from

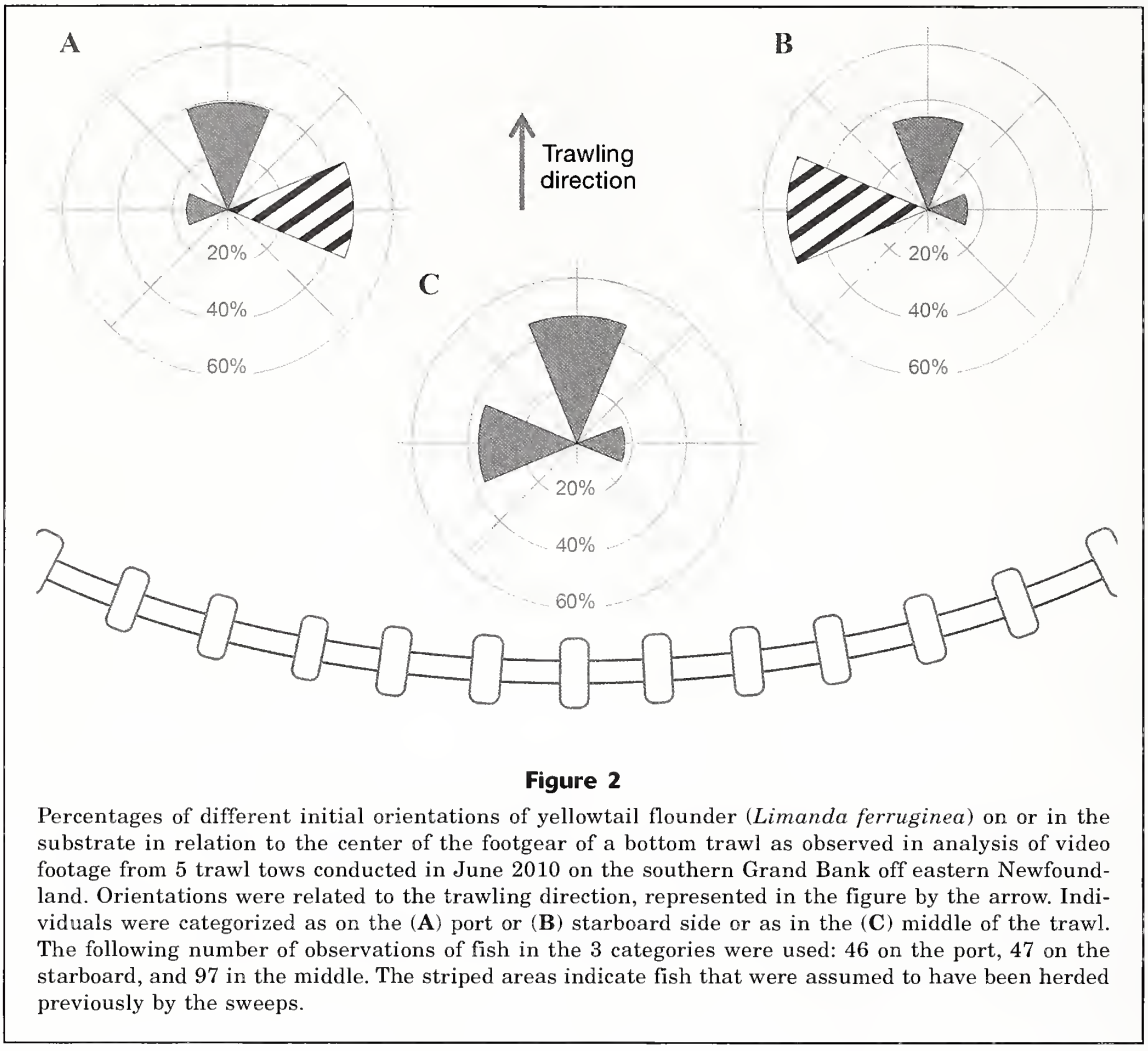

Figure 2

Percentages of different initial orientations of yellowtail flounder (*Limanda ferruginea*) on or in the substrate in relation to the center of the footgear of a bottom trawl as observed in analysis of video footage from 5 trawl tows conducted in June 2010 on the southern Grand Bank off eastern Newfoundland. Orientations were related to the trawling direction, represented in the figure by the arrow. Individuals were categorized as on the (**A**) port or (**B**) starboard side or as in the (**C**) middle of the trawl. The following number of observations of fish in the 3 categories were used: 46 on the port, 47 on the starboard, and 97 in the middle. The striped areas indicate fish that were assumed to have been herded previously by the sweeps.

20 to 52 cm. The majority of yellowtail (60–75%) were observed to be resting in or on the substrate in the video footage before they reacted to the footgear, while the remainder were observed swimming into the field of view. Yellowtail observed swimming into the frame rather than resting in or on the substrate in the video footage displayed behaviors (run, slope, and rise) similar to those of the fish recorded in this study.

Orientation

Orientation of yellowtail before their initial reaction to the central footgear varied, depending on where in the trawl mouth an individual originally was observed (Fig. 2), and orientation was found to be nonrandom, being significantly clustered, for run, slope, and rise behaviors (Rayleigh test, $P<0.001$). Most individuals in peripheral locations faced inward; 46% and 51% for individuals on the port and starboard sides (Fig. 2, A and B). Most individuals in the middle of the trawl mouth faced the vessel, away from the oncoming trawl (46%, Fig. 2C).

Initial response

None of the observed individuals displayed an initial behavior of pass under or hop. Most individuals (112 of 150 fish) had an initial response of run, and only 9 individuals were observed to initially rise. The majority of individuals (91%) swam in the direction in which they were oriented on the substrate. Location, fish length, gait, and start density alone did not have a significant influence on the initial herding responses of run and slope, but swimming direction significantly influenced each of those 2 responses (Table 3; Fig. 3). Most individuals that initially responded with slope behavior swam perpendicular to the trawling direction (79%), and individuals that exhibited a run response were twice as likely to swim in the trawling direction as fish that responded with slope behavior (42% versus 21%). Fish that initially responded with rise behavior did not have a 2-dimensional swimming direction; instead they propelled off the seabed vertically and past the height of the footgear. Individuals that were herded (with run and slope behavior) spent 3–4 times longer

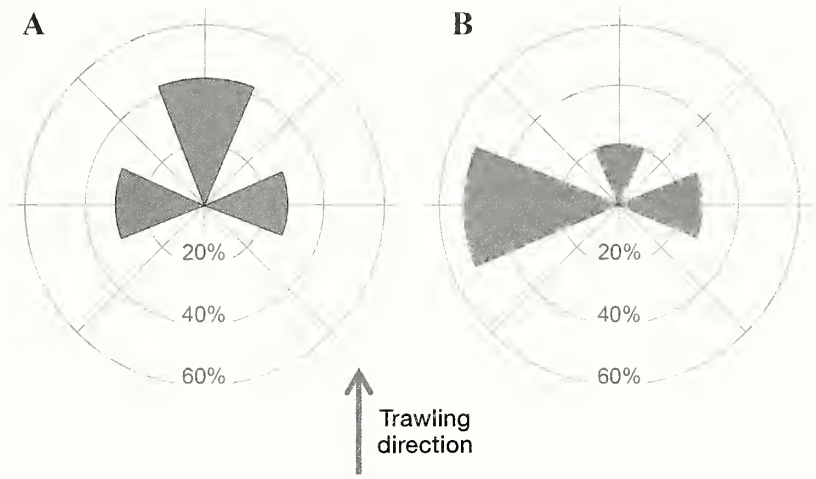

Figure 3

Percentages of different swimming directions of yellowtail flounder (*Limanda ferruginea*) after they left the substrate for each initial response of (**A**) run and (**B**) slope observed in analysis of video footage from 5 tows of a bottom trawl in June 2010 on the southern Grand Bank off eastern Newfoundland. Orientations were related to the trawling direction, represented in the figure by the arrow. There were 112 observations of fish with a run response and 29 observations of fish with a slope response. Observations from all 3 locations, port, starboard, or in the middle of the trawl, are combined together.

in the mouth of the trawl than the nonherded fish (run, 4.3 s, and slope, 3.0 s, versus rise, 1.1 s; Table 4) and maximum time spent in the mouth of the trawl was observed for individuals that had a run response (maximum time: run, 31.9 s, versus slope, 6.5 s).

Change in response

The majority of yellowtail continued their initial behavioral response to the footgear, but 40% of individual yellowtail showed a behavioral shift (Fig. 4). The change in response always resulted in the fish moving farther away from the substrate. Location, swimming direction, fish length, gait, residence time, and start density alone did not have a significant influence on change in herding response, but initial response significantly influenced the observed change in herding response (Table 3). Almost all changes occurred in individuals that initially exhibited run behavior (58 of 60 individuals); in contrast, all individuals that initially moved upward continued to do so.

Capture outcome

Of the fish that left the substrate, 37% escaped through or under the footgear. Most fish escaped by swimming across the mouth of the trawl toward the outer footgear and by finding gaps in the footgear (40 of 55 individuals; Table 4). The remainder collided with the gear or were passively overtaken by the footgear. Fish length, gait, residence time, and start density alone did not have a significant influence on capture, but initial orientation and response significantly influenced the probability of capture (Table 3). Individuals in the peripheral locations that were facing inward and were assumed to have been previously herded (indicated by the striped area in Fig. 2) were twice as likely as all other individuals to be caught (caught-to-escape ratio, 3.0:1 and 1.5:1, respectively). Nearly all yellowtail (≥ 97%) that had an initial response of slope or rise were caught; whereas, only half of the fish that exhibited a run response (52%) to the footgear were captured.

Discussion

This detailed analysis of the behavior of yellowtail in the central part of the mouth of an approaching bottom trawl revealed that individual fish responded in different ways and that the response of a fish had consequences for its probability of being caught. Some fish swam along the bottom in front of the moving trawl (run behavior), whereas other fish gradually left the bottom (slope behavior) and others swam directly upward (rise behavior). The behavioral decision of a fish was linked to its initial orientation. Fish that stayed in the middle location along the footgear tended to be oriented in the trawling direction and swam along the bottom, whereas fish at peripheral locations were usually oriented inward and swam upward. Leaving the bottom as a rule resulted in a fish being caught.

There are some limitations to our study. For instance, we assumed that only individuals that were in peripheral locations and facing inward were herded by the gear before our observation, but we recognize that some of the fish in the middle location may also have encountered the gear but were not categorized as previously herded. Likewise, some of the fish in peripheral locations could have maintained an inward orientation without having reacted to the gear. One solution to this conundrum may be the use of electronic tagging of individual fishes (Engås et al., 1998; Winger, 2004), an approach that could provide information about gear encounters by recording the position of an individual fish in relation to the sweeps before it enters the mouth of a trawl. Another potential bias in our analysis is the undercounting of fish that did not react to the footgear and were passed over by the trawl. These fish could not be distinguished from the substrate and, therefore, were not included in the database.

Table 4

Summary by categorical variables determined from yellowtail flounder (*Limanda ferruginea*) observed in analysis of video footage from 5 tows of a bottom trawl in June 2010 on the southern Grand Bank off eastern Newfoundland. Total numbers of individuals that escaped and those that were caught are in bold, with the total numbers broken down into trawl interactions (TI) in parentheses. Trawl interactions are actively escape/caught (A), over taken by the trawl (O), and collided with the gear (C). The start densities of flatfishes are provided below the categorical variables. The mean density at the start of an observation, as well as standard errors (SE), 95% confidence intervals (CI), and ranges, are calculated for all observations (Overall) and for escaped and caught fishes.

Category		Number	Escaped (TI)	Caught (TI)
Species	Yellowtail	150	**55** (A 40, O 12, C 3)	**95** (A70, O 21, C 4)
Length	Large	94	**33** (A 26, O 6, C 1)	**61** (A 548, O 10, C 3)
	Small	56	**22** (A 14, O 16, C 2)	**34** (A 22, O 11, C 1)
Gait	Kick-swim	73	**29** (A 20, O 8, C 1)	**44** (A 29, O 11, C4)
	Burst-and-coast	77	**26** (A 20, O 4, C 2)	**51** (A 41, O 10)
Initial herding response	Rise	9	**0**	**9** (A 8, C1)
	Run	112	**54** (A 39, O 12, C 3)	**58** (A 39, O 18, C 1)
	Slope	29	**1** (A 1)	**28** (A 23, O 3, C 2)
Previous gear experience	Herded	38	**9** (A 6, O 2, C 1)	**29** (A 23, O 5, C 1)
	Not herded	112	**46** (A 34, O 10, C 2)	**66** (A 47, O 16, C 3)
		Overall	Escaped	Caught
Start density	N	150	55	95
	Mean (SE)	13.0 (0.48)	13.0 (0.88)	13.0 (0.57)
	95% CI	0.95	1.76	1.13
	Range	2–30	4–30	2–27

In contrast to findings in earlier flatfish studies (Walsh, 1992; Godø et al., 1999; Gibson, 2005), results from our study indicate that neither fish size nor fish density in the trawl mouth influenced the response or capture of yellowtail. Walsh (1992) collected high numbers of small flatfishes (<31 cm) under the trawl with the use of bags. This outcome contrasts with our findings, but, as mentioned previously, we could not distinguish fish that were buried in the substrate, a circumstance that could explain the difference in these results. In Walsh's (1992) study, the small flatfishes may not have reacted to the footgear but could have reacted to the small bag itself after they passed under the footgear. The lack of a density effect in our study may be explained by density counts that were lower in our study than in the study by Godø et al. (1999). Furthermore, we modeled fish size and density along with other variables to establish which factors influenced herded individuals the most, and both fish size and density were not among those factors.

As predicted, peripherally located fish in the center of the footgear were mostly oriented inward, indicating that most of these fish had been previously herded. More than 90% of these fish also reacted by swimming in the direction in which they were initially oriented. In contrast, centrally positioned fish were generally oriented away from the oncoming trawl—a result that is similar to the findings of both Walsh and Hickey (1993) and Albert et al. (2003). The general orientation away from the trawl is a likely initial response to the impending trawl because the orientation of yellowtail was consistent despite the change in the direction of trawling for each haul. Vessel-radiating noise is expected to influence the orientation of flatfishes, and American plaice have been shown to react at considerable distances ahead of an approaching trawler (P. Winger and S. Walsh, unpubl. data). In comparison, fish in peripheral locations mainly were turned perpendicular to the trawl gear, indicating that earlier physical encounters with the sweeps and wings were the dominating influence for this type of movement.

The initial response and previous gear experience each had a strong influence on the capture of yellowtail in the central part of the trawl mouth. The observed rate of escapement (37%) was similar to that had been found for Greenland halibut (*Reinhardtius hippoglossoides*) (Albert et al., 2003), but the actual escapement rate for yellowtail is presumably much higher because of unobserved fish that pass under the footgear (Ryer and Barnett, 2006). Individuals that exhibited a run response had a 52% probability of escaping, but lifting from the bottom (slope and rise responses) resulted in all fish being caught. Flatfishes that leave the seabed can no longer see the threat of the footgear below (Ryer, 2008), and, although they avoid the immediate threat of the footgear, they do not avoid the net and are captured (Ryer et al., 2010). Because of the "ground effect," [term describing the change in performance of moving objects near a solid

surface] flatfishes that swim close to the seabed may also require less energy (Videler, 1993; Webb and Gerstner, 2000) to keep distance from the threat and, therefore, have more time to seek escapement. Finally, swimming at an angle to the seabed forces individuals to swim more rapidly, to use more energy (in order to maintain a distance over ground from the threat) and by contrast, to reduce their escapement time.

The initial response also could be affected by previous gear encounters and, therefore, also would influence the probability of capture. We observed that individuals assumed to be previously herded had only a 24% probability of avoiding capture and were twice as likely to be caught. These individuals were oriented toward the opposite wing of the trawl. Because most yellowtail generally swam in the direction in which they were oriented (also see Stickney et al. [1973]), these fish would hit the footgear and end by being captured.

The consistency of a fish's response depended on the initial behavioral decision. Fish that responded with a slope or rise behavior generally maintained this same behavior throughout the period of observation, but about 40% of the yellowtail that exhibited a run response shifted to a slope or rise response. Such a change in behavior was always one-way, that is, no individuals moved back toward the seabed after leaving it. If, however, the energetic cost of continuing a response increases to some threshold, presumably the point of fatigue, an animal would be expected to switch behavior (Ydenberg and Dill, 1986; Breen et al., 2004; Peake and Farrell, 2006; Winger et al., 2010). Although there was no influence of gait on change in response in our study, indicating that a fish did not reach the critical level of fatigue, the behavioral shifts that were observed indicate that there are cumulative energetic costs of swimming ahead of the footgear.

In light of the findings from previous behavioral studies and our study, the combined effects of trawl gear components need to be studied further in a manner that makes fishes initially have a run response then a rise or slope response during the capture process. Further experiments should include different combinations of vessel speed, sweep angle, and gear visibility to stimulate the run response in flatfishes before their approach to the mouth of a trawl. Once in the mouth of the trawl, lights in the central part of the footgear may cause a startled response (Walsh and Hickey, 1993) and trigger flatfishes to leave the seabed. Studying the effect of various light sources, like flashing or intermittent lights, on response to the footgear by different species of flatfishes would be worthwhile.

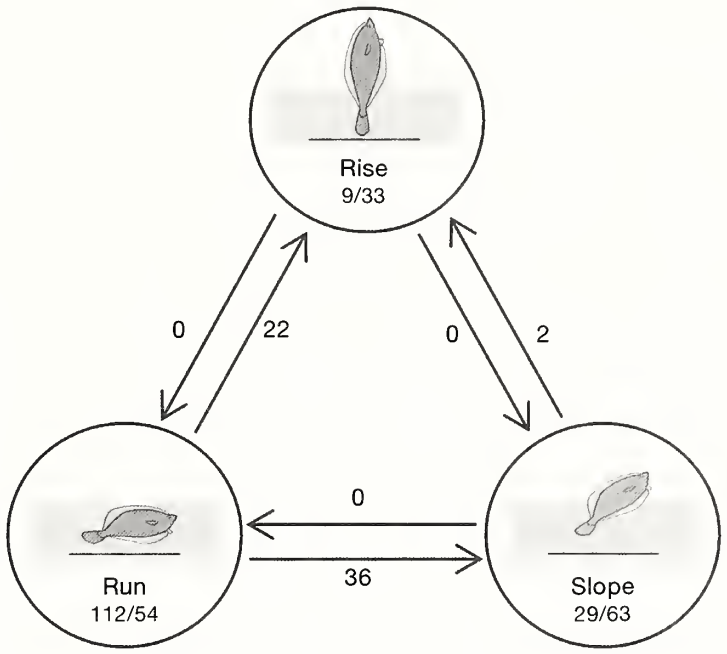

Figure 4

The behavioral responses of yellowtail flounder (*Limanda ferruginea*) from analysis of video footage collected during 5 tows of a bottom trawl in June 2010 on the southern Grand Bank off eastern Newfoundland. Each circle represents a single behavior with the initial and end counts of the number of individuals that exhibited that behavior. The arrows indicate the direction and count of individuals that changed their behavior. The fish drawings indicate the position of each behavior in relation to the substrate.

Acknowledgments

We thank the captains and crew of the FV *Aqviq* for their assistance and hospitality while out at sea, as well as to S. Mahlum, C. Batten, and J. White for their technical assistance. We also thank D. Schneider at Memorial University of Newfoundland, M. Pennington at Institute of Marine Research, and N. Cadigan at Fisheries and Oceans Canada for their statistical advice. Lastly, we, thank S. Grant and the anonymous reviewers for their comments on earlier versions.

Literature cited

Albert, O. T., A. Harbitz, and Å. S. Høines.
2003. Greenland halibut observed by video in front of survey trawl: behaviour, escapement, and spatial pattern. J. Sea Res. 50:117–127.

Bates, D., M. Maechler, B. Bolker, and S. Walker.
2013. lme4: Linear mixed-effects models using Eigen and S4. R package vers. 1.0-5. [Available at website.]

Beamish, F. W. H.
1966. Reactions of fish to otter trawls. Fish. Can. 19(5):19–21.
1969. Photographic observations on reactions of fish ahead of otter trawls. FAO Fish. Rep. 62:511–521.

Breen, M., J. Dyson, F. G. O'Neill, E. Jones, and M. Haigh.
2004. Swimming endurance of haddock (*Melanogrammus aeglefinus* L.) at prolonged and sustained swimming speeds, and its role in their capture by towed fishing gears. ICES J. Mar. Sci. 61:1071–1079.

Bryan, D. R., K. L. Bosley, A. C. Hicks, M. A. Haltuch, and W. W. Wakefield.
2014. Quantitative video analysis of flatfish herding behavior and impact on effective area swept of a survey trawl. Fish. Res. 154:120–126.

Bublitz, C. G.
1996. Quantitative evaluation of flatfish behavior during capture by trawl gear. Fish. Res. 25:293–304.

Chosid, D. M., M. Pol, M. Szymanski, F. Mirarchi, and A. Mirarchi.
2012. Development and observations of a spiny dogfish *Squalus acanthias* reduction device in a raised footrope silver hake *Merluccius bilinearis* trawl. Fish. Res. 114:66–75.

Collette, B. B., and G. Klein-MacPhee.
2002. Bigelow and Schroeder's fishes of the Gulf of Maine, 3rd ed., 748 p. Smithsonian Inst. Press, Washington, D.C.

Crawley, M. J.
2007. The R Book, 950 p. John Wiley & Sons, Ltd., Chichester, UK.

Engås, A., and O. R. Godø.
1989. Escape of fish under the fishing line of a Norwegian sampling trawl and its influence on survey results. ICES J. Mar. Sci. 45:269–276.

Engås, A., E. K. Haugland, and J. T. Øvredal.
1998. Reactions of cod (*Gadus morhua* L.) in the pre-vessel zone to an approaching trawler under different light conditions. Hydrobiologia 371–372:199–206.

Gibson, R. N.
2005. The behaviour of flatfishes. *In* Flatfishes: biology and exploitation (R. N. Gibson, ed.), p. 213–239. Blackwell Science, Ltd., Oxford, UK.

Godø, O. R., S. J. Walsh, and A. Engås.
1999. Investigating density-dependent catchability in bottom-trawl surveys. ICES J. Mar. Sci. 56: 292–298.

Kim, Y-H, and C. S. Wardle.
2003. Optomotor response and erratic response: quantitative analysis of fish reaction to towed fishing gears. Fish. Res. 60:455–470.

Main, J., and G. I. Sangster.
1981. A study of the fish capture process in a bottom trawl by direct observations from a towed underwater vehicle. Scott. Fish. Res. Rep. 23, 24 p. [Available at website.]

Millar, R. B., and M. J. Anderson.
2004. Remedies for pseudoreplication. Fish. Res. 70:397–4 07.

Peake, S. J., and A. P. Farrell.
2004. Locomotory behaviour and post-exercise physiology in relation to swimming speed, gait transition and metabolism in free-swimming smallmouth bass (*Micropterus dolomieu*). J. Exp. Biol. 207:1563–1575.
2006. Fatigue is a behavioural response in respirometer-confined smallmouth bass. J. Fish Biol. 68:1742–1755.

Piasente, M., I. A. Knuckey, S Eayrs, and P. E. McShane.
2004. *In situ* examination of the behaviour of fish in response to demersal trawl nets in an Australian trawl fishery. Mar. Freshw. Res. 55:825–835.

R Core Team.
2013. R: a language and environment for statistical computing. R Foundation for Statistical Computing, Vienna, Austria. [Available at website, accessed November 2013.]

Ryer, C. H.
2008. A review of flatfish behavior relative to trawls. Fish. Res. 90:138–146.

Ryer, C. H., and L. A. K. Barnett.
2006. Influence of illumination and temperature upon flatfish reactivity and herding behavior: potential implications for trawl capture efficiency. Fish. Res. 81:242–250.

Ryer, C. H., C. S. Rose, and P. J. Iseri.
2010. Flatfish herding behavior in response to trawl sweeps: a comparison of diel responses to conventional sweeps and elevated sweeps. Fish. Bull. 108:145–154.

Stickney, R. R., D. B. White, and D. Miller.
1973. Observations of fin use in relation to feeding and resting behavior in flatfishes (Pleuronectiformes). Copeia 1973:154–156. [Available at website.]

Underwood, M. J., P. D. Winger, and G. Legge.
2012. Development and evaluation of a new high definition self-contained underwater camera system to observe fish and fishing gears *in situ*. J. Ocean Technol. 7(1):60–70. [Available at website.]

Videler, J. J.
1993. Fish swimming, 260 p. Chapman & Hall, London, UK.

Walsh, S. J.
1992. Size-dependent selection at the footgear of a groundfish survey trawl. N. Am. J. Fish. Manage. 12:625–633.

Walsh, S. J., and W. M. Hickey.
1993. Behavioural reactions of demersal fish to bottom trawls at various light conditions. ICES Mar. Sci. Symp. 196:68–76.

Webb, P. W.
1994. Exercise performance of fish. *In* Comparative vertebrate exercise physiology: phyetic adaptations (J. H. Jones, ed.), p. 1–49. Academic Press, San Diego, CA.

Webb, P. W., and C. L. Gerstner.
2000. Fish swimming behaviour: predictions from physical principles. *In* Biomechanics in animal behaviour (P. Domenici and R. W. Blake, eds.), p. 59–77. BIOS Scientific Publishers, Ltd., Oxford, UK.

Weinberg, K. L., and P. T. Munro.
1999. The effect of artificial light on escapement beneath a survey trawl. ICES J. Mar. Sci. 56:266–274.

Winger, P. D.
2004. Effect of environmental conditions on the natural activity rhythms and bottom trawl catchability of Atlantic cod (*Gadus morhua*). Ph.D. diss., 151 p. Mem. Univ. Nfld., St. John's, Newfoundland, Canada.

2008. Fishing smarter: improving harvesting technology through the study of animal behaviour. J. Ocean Technol. 3(2):15–20.

Winger, P. D., S. Eayrs, and C. W. Glass.
2010. Fish behaviour near bottom trawls. *In* Behavior of marine fishes: capture processes and conservation challenges (P. He, ed.), p 67–102. Wiley-Blackwell, Arnes, IA.

Winger, P. D., P. He, and S. J. Walsh.
1999. Swimming endurance of American plaice (*Hippoglossoides platessoides*) and its role in fish capture. ICES J. Mar. Sci. 56:252–265.

Winger, P. D., S. J. Walsh, P. He, and J. A. Brown.
2004. Simulating trawl herding in flatfish: the role of fish length in behaviour and swimming characteristics. ICES J. Mar. Sci. 61:1179–1185.

Ydenberg, R. C., and L. M. Dill.
1986. The economics of fleeing from predators. Adv. Study Behav. 16:229–249.

NOAA
National Marine
Fisheries Service

Fishery Bulletin
established 1881

Spencer F. Baird
First U.S. Commissioner
of Fisheries and founder
of *Fishery Bulletin*

Genetically determined population structure of hogfish (Labridae: *Lachnolaimus maximus*) in the southeastern United States

Seifu Seyoum[1]
Angela B. Collins[1,3] **(contact author)**
Cecilia Puchulutegui[1]
Richard S. McBride[2]
Michael D. Tringali[1]

E-mail for contact author: angela.collins@myfwc.com

[1] Fish and Wildlife Research Institute
Florida Fish and Wildlife Conservation Commission
100 Eighth Avenue SE
St. Petersburg, Florida 33701

[2] Population Biology Branch
Fisheries and Ecosystems Monitoring Division
Northeast Fisheries Science Center
National Marine Fisheries Service, NOAA
166 Water Street
Woods Hole, Massachusetts 02543

[3] Florida Sea Grant
University of Florida
Institute of Food and Agricultural Sciences Extension
1303 17th Street West
Palmetto, Florida 34221

Abstract—Hogfish (Labridae: *Lachnolaimus maximus*) is distributed across several biogeographic regions, but its stock structure has been poorly documented, confounding stock assessment and management of this reef fishery species. In this study the genetic structure of hogfish over a portion of its southeastern U.S. range was examined by using a suite of 24 microsatellite DNA loci. Fin clips from 719 specimens were obtained from geographic locations ranging from northwest Florida through North Carolina. Genomic proportions of hogfish were partitioned into 3 distinct genetic clusters, geographically delineated as 1) the eastern Gulf of Mexico, 2) the Florida Keys and the southeast coast of Florida, and 3) the Carolinas. Clusters 1 and 2 converged along the coastal area west of the Florida Everglades, but the location of the genetic break between clusters 2 and 3 requires further study because of a discontinuity in specimen collection between southeast Florida and the Carolinas. The geographically limited reproductive exchange in this species indicates that future stock assessments should incorporate regionally partitioned analyses of life history and fishery data.

Manuscript submitted 6 May 2014
Manuscript accepted 13 August 2015.
Fish. Bull 113:442–455 (2015).
Online publication date: 2 September 2015.
doi: 10.7755/FB.113.7

A fundamental challenge for managing sustainable fisheries involves aligning biological evidence of stock structure with fishing and management sectors for the purpose of monitoring, assessment, and regulatory actions (Cadrin et al., 2014). This process is particularly challenging around the Florida peninsula, where several biogeographic regions overlap state and federal boundaries and fall under the jurisdiction of 2 federal fishery management councils (South Atlantic and Gulf of Mexico). In terms of biogeography, there is a strong environmental gradient both along (north–south) and between (east–west) coasts, resulting in distinctive faunal breaks at Cape Romano on the west coast of Florida and Cape Canaveral on the east coast (Briggs and Bowen, 2012). Subspecies are frequently recognized between the Gulf and Atlantic coasts of Florida (Bowen and Avise, 1990), and several coastal and marine species are considered to have distinct stocks on each coast (Tringali and Bert, 1996; Gold et al., 2002; McBride, 2014a).

Stock structure remains unclear for many marine fishery species, in part because of a lack of data (Cadrin et al., 2014; McBride, 2014a). One such example is the hogfish (Labridae: *Lachnolaimus maximus*), a long-lived reef fish that occurs in temperate to tropical waters of the western Atlantic Ocean (from Brazil to Bermuda) and throughout the Gulf of Mexico (Claro et al., 1989; McBride and Richardson, 2007; McBride et

al., 2008). This species supports a modest commercial fishery in the southeastern United States and is a highly valued target for recreational divers and spear fishermen (McBride and Murphy, 2003; FWC[1]; NMFS[2]). Hogfish occur in rocky and reef habitats, but those habitats are not continuous, and there are no studies that completely describe the continuity of their distribution along the Atlantic coast of the United States, let alone throughout their geographic range.

The available data pertinent to stock structure of hogfish are limited to general behavioral and life history patterns (e.g., Davis, 1976; McBride and Richardson, 2007; Collins and McBride, 2011) and to a preliminary genetic survey of this species in the eastern Gulf of Mexico (MERPDC, 2012). Hogfish are broadcast spawners, a characteristic that facilitates dispersal of the propagules away from the spawning site (Colin, 1982). The planktonic larval duration is 3–5 weeks (Colin, 1982; Victor, 1986), which is an average period among reef fishes (Victor, 1986; Leis et al., 2013) and does not imply extensive mixing of genotypes between ocean basins. Moreover, hogfish maintain site fidelity and spawn in stable, site-specific harems (i.e., they do not migrate long distances to form spawning aggregations; Colin, 1982; Muñoz et al., 2010), and there is evidence of reciprocal onshore larval dispersal and gradual offshore movement with growth (Collins and McBride, 2011). These behaviors have the potential to promote stock structure at a finer spatial scale than might be expected in an open marine ecosystem.

Life history differences (e.g., maximum age, maximum size, and fecundity) have been noted for hogfish in the eastern Gulf of Mexico and hogfish in south Florida (McBride et al., 2008), and variations also exist among fish within the same region (McBride and Richardson, 2007; Collins and McBride, 2011, 2015). Hogfish grow older and larger, and spawn more eggs per female, in areas with lower fishing rates or in less gear-accessible habitats. Although these patterns affect vital rates within each region, they have not been linked to underlying biological stock structure (Collins and McBride 2011; McBride and Richardson, 2007; McBride et al., 2008; MERPDC, 2012; McBride, 2014b). Questions regarding the underlying stock structure were raised most recently in a request to review hogfish stock structure and unit stock definitions as part of the most recent southeastern U.S. hogfish benchmark assessment (Cooper et al.[3]).

The goal of this research was to use genetic data to determine whether more than one stock of hogfish exists in the southeastern United States and, if so, where the genetic breaks occur. We used microsatellite DNA markers, which are preferred over other types of markers (e.g., allozymes and mitochondrial DNA) because of their ability to better detect the subtle genomic differences common among marine populations (Antoniou and Magoulas, 2014; Mariani and Bekkevold, 2014). Microsatellites are nuclear-encoded, codominant markers that have characteristically high mutation rates and, hence, a high degree of allelic variation. These loci are scattered throughout the genome and can be influenced independently by recombination, selection, and drift; therefore, each locus is expected to have its own genealogical history that is slightly different from that of others. Adding and combining many loci makes a genomic sampling increasingly representative of the history of the previously described genetic processes and provides a robust method for investigating gene flow and population connectivity (Hedrick, 1999; Kalinowski, 2002, 2005; Wilson and Rannala, 2003). Here we apply microsatellite loci previously isolated for hogfish and optimized for routine assay (MERPDC, 2012) to specimens collected in an area from the Big Bend region of northwest Florida through North Carolina.

Materials and methods

Specimen collection and DNA extraction

Specimens (N=719) were collected through intercepts of recreational and commercial spear fishermen or during directed research trips performed by biologists of the Fish and Wildlife Research Institute of the Florida Fish and Wildlife Conservation Commission. Specimens were identified according to Robins and Ray (1986) and were collected sporadically throughout the study area from November 2005 through August 2013. Fin clips were removed and preserved in 70% ethanol. Total DNA was isolated from approximately 500 mg of fin clip tissue with Gentra Puregene[4] DNA isolation kits (Qiagen, Valencia, CA) and rehydrated in 50 µL of deionized water.

Collection locations were subdivided into 9 geographic areas, referred to hereafter as *sampling areas* 1–9 (Fig. 1). These sampling areas were identified predominantly by latitude and coast (west [Gulf of Mexico] and east [Atlantic Ocean]) to delineate geographic regions corresponding to recognized faunal breaks, major estuaries, and (on a broader scale) management jurisdictions of hogfish. For example, faunal breaks are known to occur at Cape Romano (between sampling areas 5 and 6), at Cape Sable (between sampling areas 6 and 7), and at Cape Canaveral (between sampling areas 8 and 9) (Briggs and Bowen, 2012). Considerable estuarine flow onto the continental shelf occurs from

[1] FWC (Florida Fish and Wildlife Conservation Commission). 2013. Species account: Hogfish (*Lachnolaimus maximus*) in Florida, 4 p. [Available at website.]

[2] NMFS [National Marine Fisheries Service]. 2013. Commercial fisheries statistics. [Available at website.]

[3] Cooper, W., A. Collins, J. O'Hop, and D. Addis. 2014. The 2013 stock assessment report for hogfish in the South Atlantic and Gulf of Mexico, 569 p. Fish Wildl. Res. Inst., Florida Fish Wildl. Conserv. Comm., St. Petersburg, FL. [Available at website.]

[4] Mention of trade names of commercial companies is for identification purposes only and does not imply endorsement by the National Marine Fisheries Service, NOAA.

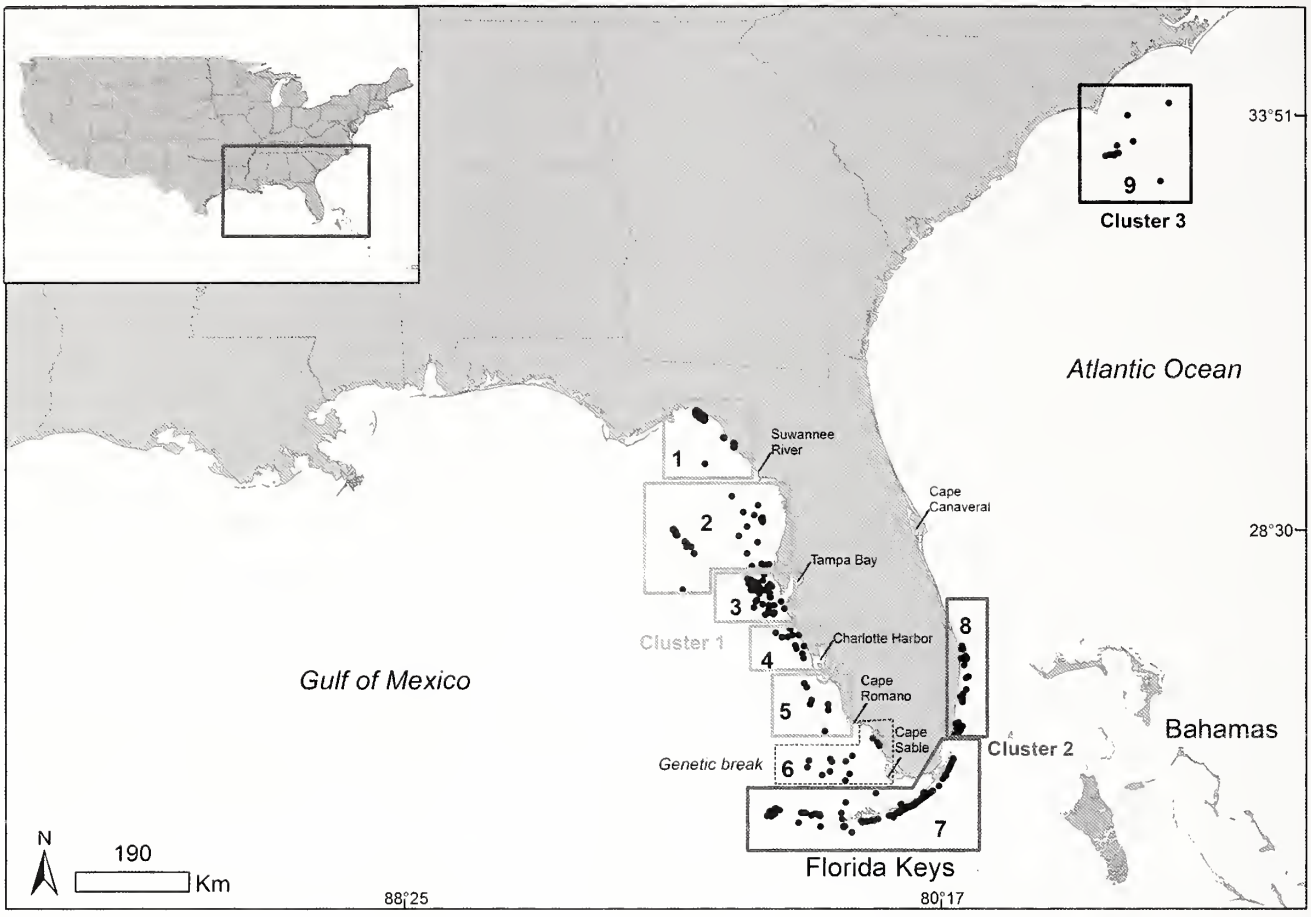

Figure 1

Capture locations for the specimens of hogfish (*Lachnolaimus maximus*) that were used to genetically determine the population structure within the southeastern United States. Specimens were collected sporadically between November 2005 and August 2013 and were grouped by collection location into sampling areas 1–9, where 1=Big Bend, 2=Nature Coast and Florida Middle Grounds, 3=Tampa Bay, 4=Sarasota, 5=Naples, 6=Everglades, 7=Florida Keys, 8=East Florida, 9=Carolinas. Three distinct clusters were identified as the 1) eastern Gulf of Mexico; 2) Florida Keys and southeast Florida; and 3) Carolinas, on the basis of the genetically determined population structure detected with 24 microsatellite loci. Sampling area 6 was identified as the region of gene flow restriction (genetic break) between clusters 1 and 2.

the Suwannee River (between sampling areas 1 and 2), Tampa Bay (in sampling area 3), and Charlotte Harbor (in sampling area 4). In terms of management jurisdictions, the Gulf of Mexico Fishery Management Council regulates federal waters throughout the Gulf of Mexico (which includes sampling areas 1–6), and the South Atlantic Fishery Management Council regulates federal waters from the Florida Keys through the Carolinas (an area that includes sampling areas 7–9). The state of Florida regulates state waters within 14.5 km (9 mi) from shore in the Gulf of Mexico and 4.9 km (3 mi) from shore in the Atlantic Ocean.

Microsatellite genotyping

Specimens were genotyped by using 24 of the 29 microsatellite markers identified in MERPDC (2012); markers Lmax11, Lmax14, Lmax15, Lmax24, and Lmax31 were not used. Multiplex polymerase chain reaction amplifications were carried out in a Mastercycler Pro thermal cycler (Eppendorf North America, Hauppauge, NY) containing 50–100 ng of total DNA, 10 µL of 50 µM dNTP mix, 0.25 µL of 0.1 mg/mL bovine serum albumin, a combination of 3 optimally selected primers of 3 loci with each forward primer labeled with a different fluorescent dye, 5 µL of Taq polymerase 10× buffer (Promega, Madison, WI) containing 15 mM $MgCl_2$ and 1.25 units of Taq polymerase (Promega). The reaction profile was 94°C for 2 min, 35 cycles of 94°C for 35 s, 55°C for 35 s, 72°C for 35 s, and final extension at 72°C for 30 min. Fragments were visualized on an Applied Biosystems 3130 XL genetic analyzer (Thermo Scientific Inc., Waltham, MA) and genotyped with GeneMapper software, vers. 4.0 (Thermo Scientific Inc.). For fragment assays, we used GeneScan 500 ROX Size Standard (Thermo Scientific Inc.).

Data analysis

Standard genetic measures and distances Data files for use in GENEPOP, vers. 4.3 (Rousset, 2008) were generated from fragment sizes recorded with the Microsatellite Toolkit add-on, vers. 3.1.1 (Park, 2001; available at website) for Microsoft Excel (Microsoft Corp., Redmond, WA); this GENEPOP data file was converted to other formats as needed with the conversion tool PGDspider, vers. 2.0.1.9 (Lischer and Excoffier, 2012). Pairwise genetic distances (F_{ST}) between sampling areas (Weir and Cockerham, 1984) were estimated with 10,000 permutations with the software program GENETIX (Belkhir et al., 2000). Departures from Hardy-Weinberg equilibrium were determined with GENEPOP. Sequential Bonferroni corrections were applied to multiple tests of hypotheses (Rice, 1989). Observed (H_o) and expected heterozygosity (H_e, with and without a bias correction), averaged over all loci, were obtained from GENETIX (Belkhir et al., 2000). Null allelism was investigated by using the randomization test of Guo and Thompson (1992) and the *U*-test statistic of Raymond and Rousset (1995), with the software program ML-NullFreq (available at website). For each locus, microsatellite variation was quantified in terms of genetic diversity, number of alleles, and allelic richness—a diversity measure that corrects for differences in sample size, with the program FSTAT, vers. 2.9.3.2 (Goudet, 2001). Chi-square tests were performed to determine whether sampling areas differed significantly from the previously described standard genetic measures.

Genetic structure Genetic data from specimens collected from the 9 sampling areas were examined with 3 analytical approaches. The first was based on principal coordinate analysis (PCA) to discriminate genetic clusters within the data by using the program GenAlEx, vers. 6.5 (Peakall and Smouse, 2006, 2012). The data were plotted at the first 2 primary coordinates on the basis of pairwise F_{ST} values for sampling areas (Latter, 1972) computed without sample size bias correction (uncorrected F_{ST}; Nei, 1973) and with sample size bias correction (corrected F_{ST}; Nei and Roychoudhury, 1974; Nei, 1987) with the software POPTREE2 (Takezaki et al., 2010).

The second method of examining the genetic structure was based on analysis of molecular variance (AMOVA) as implemented in the software program ARLEQUIN, vers. 3.5.1.3; 100,000 permutations (Excoffier and Lischer, 2010). Essentially a method to determine the strength of the PCA groupings, AMOVA assesses the best grouping of sampling areas into clusters. In the a priori hierarchical approach with AMOVA, correlations among genotypes at various levels are partitioned as *F*-statistics. Initially, the a priori hierarchical structure that was analyzed was based on the genetic groupings revealed by PCA. To find the greatest F_{ST} between groupings, we constructed 2 combinations of 3-clusters that placed sampling area 6 in either cluster 1 or cluster 2 on the basis of corrected or uncorrected F_{ST} values indicated by PCA. After this analysis, F_{ST} values for the 2-cluster combinations were also assessed by omitting one cluster at a time. The proportions of variation were computed among clusters (F_{CT}), within clusters (F_{SC}), and within sampling areas (F_{ST}), and the *F*-statistic was assessed by the permutation method of Excoffier et al. (1992).

The third analytical approach was based on the Bayesian population-assignment algorithm as implemented in the program STRUCTURE, vers. 2.3.4 (Pritchard et al., 2000). With this algorithm, individuals were probabilistically and proportionally assigned to one or more genetic clusters (K) in a manner that minimized Hardy-Weinberg and linkage disequilibria among their multilocus genotypes. For K=1 through K=9, 10 simulations were conducted by using 2 million Markov chain Monte Carlo replicates after a burn-in period of 1 million runs. We adopted the admixture model and the independent allele frequency option to minimize the chance of overestimating the number of clusters present in the data (Pritchard et al., 2009).

We used STRUCTURE HARVESTER, vers. 0.6.93 (Earl and vonHoldt, 2012) with each of the previously described replicate runs to compute the ad hoc statistics L(K) and ΔK so that we could determine the most plausible base value for K clusters (i.e., the upper-level hierarchy). L(K) denotes the log probability of the data at a given modeled K value; ΔK is based on the rate of change in L(K) between successively modeled K values. Simulation studies (Evanno et al., 2005) have shown that ΔK provides the most accurate indication of genetic structure under a variety of modeling conditions. We then used CLUMPP, vers. 1.1.2 (Jakobsson and Rosenberg, 2007) to determine the optimal alignment for replicate analyses and mean genomic membership coefficients across replicate runs for sampling areas and individuals. The coefficients of the CLUMPP output were plotted with Microsoft Excel.

Mantel test To determine whether genetic relationships among sampling areas conformed to a pattern of genetic isolation by distance (Wright, 1943; Malécot, 1955), we computed the Mantel correlation coefficient (r) between F_{ST} and geographic distance (measured in kilometers) with the program GenAlEx, vers. 6.5 (Peakall and Smouse, 2006, 2012). The significance of r was tested by using 9000 random permutations.

Effective population size The effective population size (N_e) of each cluster was estimated with the program NeEstimator, vers. 2 (Do et al., 2013) under the model option with the Burrows method to estimate linkage disequilibrium (Hill, 1981; Waples, 2006). This approach has been shown to give generally unbiased estimates of linkage disequilibrium from which estimates of N_e can be derived (Robinson and Moyer, 2012) with 95% confidence intervals on the basis of the parametric procedure of Waples (2006). Bias due to low-frequency alleles was avoided by estimating N_e from alleles with frequencies greater than 1% and 2% and also by omit-

Table 1

Total number of hogfish (*Lachnolaimus maximus*) collected, time span of specimen collection, total number of alleles sampled, and standard genetic indices for each sampling area in the southeastern United States (from northwest Florida to North Carolina). Sampling areas 1–9 are geographically defined in Figure 1. Genetic measurements were calculated over a suite of 24 microsatellite loci, and mean values of genetic diversity, number of alleles per locus, allelic richness, and observed and unbiased observed heterozygosity are presented for each sampling area as well as for all specimens combined. Numbers in parentheses in the last column indicate overall mean values for all specimens combined.

Sampling area	1	2	3	4	5	6	7	8	9	Total
Number of specimens	119	71	88	24	22	70	191	32	102	719
Time span of specimen collection (years)	2007–2012	2005–2012	2005–2012	2006–2012	2006–2012	2006–2012	2009–2013	2009–2013	2010–2012	2005–2013
Total number of alleles	246	223	237	165	161	238	296	203	174	350 (216)
Genetic diversity	0.63	0.65	0.65	0.63	0.64	0.67	0.67	0.68	0.61	0.65 (0.65)
Number of alleles per locus	10.3	9.3	9.9	6.9	6.7	9.9	12.3	8.5	7.3	14.6 (9.0)
Allelic richness	9.5	9.0	9.7	9.6	6.3	9.7	12.2	8.2	7.1	14.4 (9.0)
Observed heterozygosity	0.57	0.59	0.60	0.61	0.59	0.63	0.63	0.63	0.58	0.60 (0.60)
Unbiased observed heterozygosity	0.63	0.65	0.65	0.63	0.64	0.66	0.67	0.68	0.61	0.66 (0.65)
Expected heterozygosity	0.63	0.64	0.64	0.62	0.63	0.66	0.66	0.67	0.60	0.66 (0.64)

ting sampling area 6, which was a mixture of cluster 1 and cluster 2, to avoid interference with linkage disequilibrium.

Results

Standard genetic measures and distances

Significant heterozygote deficiencies were sporadically detected at 3 loci (Lmax4, Lmax29, and Lmax 35) in up to 5 sampling areas. Presumptive frequencies of null alleles at those loci that exhibited heterozygote deficits ranged from 0.17 to 0.24. There were no significant differences among sampling areas in the mean values of standard genetic measures (Table 1). For all loci, 350 alleles were identified (mean=216) over all 9 sampling areas. Over the 36 possible pairwise comparisons, 30 sampling area pairs had F_{ST} values that were significantly greater than zero (10,000 permutations; $P<0.05$).

Principal coordinate analysis

The PCA defined 3 genetic clusters, with the primary axis (coordinate 1) explaining 58.9% and the secondary axis (coordinate 2) explaining 38.9% of the genetic variability from the uncorrected F_{ST} values (Fig. 2A), compared with 68.0% and 32.0% on the basis of the corrected F_{ST} values (Fig. 2B). Cluster 1 included specimens collected in the eastern Gulf of Mexico from the Florida Panhandle to Naples (sampling areas 1–5). Cluster 2 included specimens collected from the Florida Keys and along the southeastern coast of Florida (sampling areas 7 and 8). Cluster 3 included specimens collected from the Carolinas (sampling area 9). The cluster identity of sampling area 6 (Everglades region) was unresolved, falling between cluster 1 and cluster 2 when analyzed on the basis of uncorrected F_{ST} (Fig. 2A).

Analysis of molecular variance

The AMOVA revealed that 98.2% of the variation occurred within sampling areas and 1.8% occurred among sampling areas. The overall F_{ST} value of 0.018 ($P<0.001$) indicated significant differentiation among sampling areas due to the presence of spatial structure at both regional and local scales. The greatest among-cluster variance in the AMOVA (Table 2) was observed when sampling areas were grouped according to the PCA results that were based on corrected F_{ST} (Fig. 2B)—an approach that placed sampling area 6 into cluster 1. Translocation of sampling area 6 from cluster 1 to cluster 2 only slightly reduced the among-cluster variance (Table 2).

Pairwise F_{CT} values between uncorrected (and corrected) F_{ST} values were 0.015 (0.016) between clusters 1 and 2, 0.027 (0.023) between clusters 1 and 3, and 0.030 (0.039) between clusters 2 and 3 (Table 2). All pairwise F_{CT} comparisons among the clusters were highly significant ($P<0.001$). Overall, the F_{ST} statistic and the AMOVA confirmed the presence of 3 geographically based clusters, but these clusters appeared to be hierarchically arranged; the least genetic differentiation was seen between clusters 1 and 2 and the differentiation between clusters 2 and 3 exceeded that observed between the geographically disjunctive clusters 1 and 3. Interestingly, the observed pattern of genetic differentiation did not conform with the expected greatest differentiation between clusters separated by the greatest geographic distances.

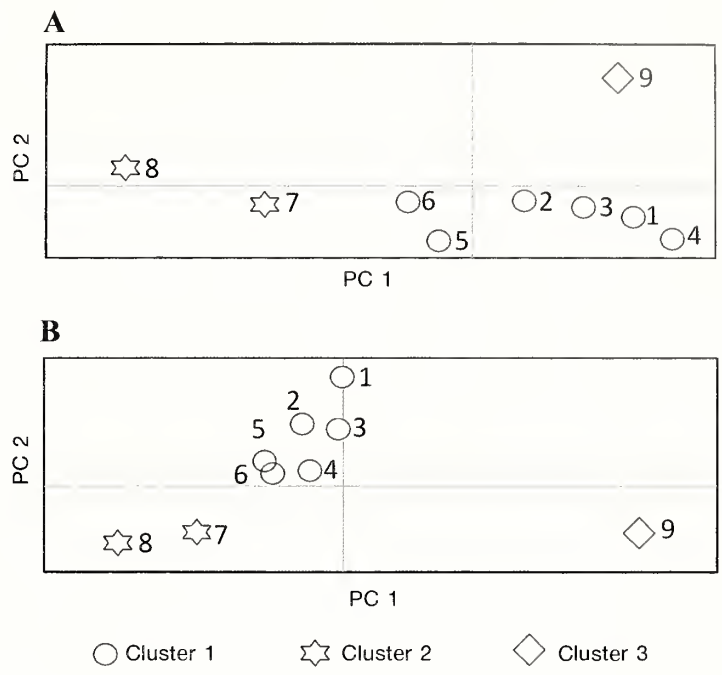

Figure 2

Principal coordinate analysis based on a nonstandardized distance method of a matrix of pairwise (**A**) uncorrected and (**B**) corrected genetic distances (F_{ST}) between sampling areas 1–9 for specimens of hogfish (*Lachnolaimus maximus*) collected from November 2005 through August 2013 in the southeastern United States (from northwest Florida to the Carolinas). Analysis separated the 9 sampling areas into 3 main genetic clusters, with principal coordinate 1 (PC1) and PC2 explaining 58.9% and 38.8% of the variability for uncorrected and 68% and 32% of the variability for corrected, respectively. Sampling areas 1–9 are labeled numerically by geographic region as defined in Figure 1 and are identified as cluster 1 (circles), cluster 2 (stars), or cluster 3 (diamond).

Bayesian population assignment

Lacking a method for determining whether values of L(K) statistically differed, we derived inferences herein by evaluating replicate likelihoods and resultant ΔK statistics for different values of K. L(K) increased quickly from K=1 to K=2 and somewhat less quickly from K=2 to K=3, reaching a plateau at successive values (L(K); Fig. 3). The largest value of ΔK occurred for K=2 (ΔK=281) and, secondarily, for K=3 (ΔK=118) (ΔK; Fig. 3). At the base hierarchical level of K=2, sampling areas of clusters 1 and 3 were predominantly conjoined within a single Bayesian cluster, whereas sampling areas of cluster 2 were predominantly assigned to a discrete Bayesian cluster (Fig. 4A). Virtually the same result was obtained under the model of no admixture analysis for K=2. At the next hierarchical level of K=3, sampling areas of clusters 1 and 3 were assigned to different Bayesian clusters (Fig. 4B). The CLUMPP analysis indicated that sampling areas 5 and 6, were admixtures of Bayesian clusters 1 and 2, respectively, exhibiting graduated mean genomic proportions (Fig. 4C).

Mantel test

The number of paired comparisons within cluster 1 (from Big Bend to the Everglades) was sufficient to allow only a within-cluster Mantel test. No significant correlation was observed between genetic and geographic distances (P=0.125, r=0.334). The F_{ST} value between sampling areas 7 and 8 was not significant (F_{ST}= −0.0007 P>0.9). However, when sampling areas 7 and 8 were included in the Mantel test with the sampling areas from cluster 1, there was a significant correlation between genetic and geographic distance (P=0.004, r=0.543). This correlation was attributed to the genetic break between cluster 1 and cluster 2 rather than to isolation by distance.

Effective population size

The 1% allele-frequency criterion was used to determine the following estimates of N_e for each of the 3 clusters: cluster 1=1368.2 (95% confidence interval [CI]=1022.6–2033.4; n=324); cluster 2=1035.7 (95% CI=833.5–1750.2; n=223); and cluster 3=285.6 (95% CI=216.2–411.2; n=102). The 2% allele-frequency criterion yielded the following: cluster 1=1478.4 (95% CI= 1022.6–2581.1); cluster 2=1075.5 (95% CI=748.3–1853.8); and cluster 3=327.5 (95% CI=231.9–537.23). The effective population size of cluster 3 (sampling area 9, from the Carolinas) was approximately 3 times smaller than that of the other 2 clusters.

Table 2

Analysis of molecular variance (AMOVA) based on 24 microsatellite loci genotypes of hogfish (*Lachnolaimus maximus*) (number of specimens=719) collected from the southeastern United States (from northwest Florida to the Carolinas) between November 2005 and August 2013. Numbers joined by hyphens indicate sampling areas (as geographically defined in Fig. 1) combined into clusters and analyzed on the basis of either the corrected or uncorrected genetic distances (F_{ST}), which were indicated by principal coordinate analysis. Only the proportions of variation computed among clusters (F_{CT}) for 3-cluster and 2-cluster combinations are given here. Probability of finding a more extreme variance by chance alone (1000 permutations) was <0.001 for all computed *F*CT values.

				Observed partition		
AMOVA results						
Among 3 clusters						
Cluster 1	Cluster 2	Cluster 3	Variance	Total (%)	F_{CT}	F_{ST}
1-2-3-4-5-6	7-8	9	0.14768	2.07	0.0208	Corrected
1-2-3-4-5	6-7-8	9	0.14331	2.02	0.0202	Uncorrected
Between 2 clusters						
Cluster 1	Cluster 2	Cluster 3	Variance	Total (%)	F_{CT}	F_{ST}
1-2-3-4-5-6	7-8	–	0.11203	1.56	0.0156	Corrected
1-2-3-4-5-6	–	9	0.16073	2.30	0.0230	Corrected
–	7-8	9	0.28595	3.93	0.0393	Corrected
1-2-3-4-5	6-7-8	–	0.10629	1.48	0.0149	Uncorrected
1-2-3-4-5	–	9	0.17683	2.56	0.0256	Uncorrected
–	6-7-8	9	0.22038	3.01	0.0301	Uncorrected

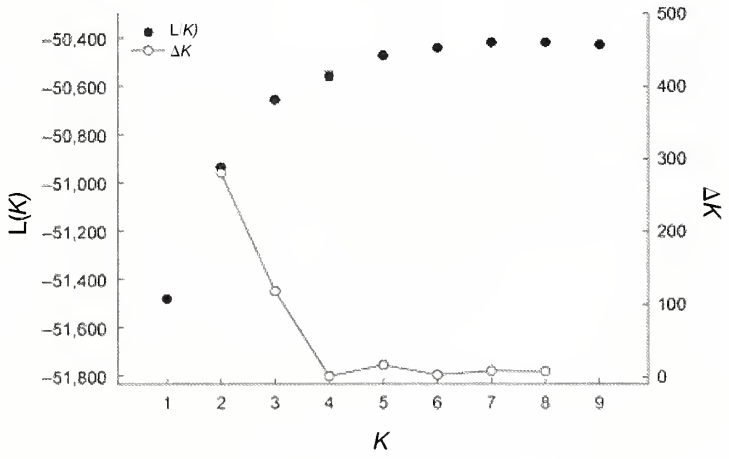

Figure 3

For K=1 through K=9, 10 simulations were conducted with 2 million Markov chain Monte Carlo replicates after a burn-in period of 1 million runs. L(K) denotes the log probability of the data at a given modeled K value; ΔK is based on the rate of change in L(K) between successively modeled K values. STRUCTURE HARVESTER was used to compute the ad hoc statistics L(K) and ΔK so that we could determine the most plausible base value of K (number of genetic clusters) within the 9 sampling areas where specimens of hogfish (*Lachnolaimus maximus*) were collected from November 2005 through August 2013 from the southeastern United States (from northwest Florida to the Carolinas).

Summary of genetic structure

The PCA, AMOVA, and Bayesian population-assignment analyses elucidated a concordant pattern of genetic structure within the studied geographical range. Three geographically based clusters were delineated as 1) the eastern Gulf of Mexico, 2) the Florida Keys and southeastern Florida, and (3) the Carolinas (Fig. 1). There was no indication of genetic isolation by distance in the eastern Gulf or over the geographic range of specimens collected. The area west of the Florida Everglades (sampling area 6) appeared to serve as a genetic break between clusters 1 and 2. The nature of the apparent genetic break between the Florida Keys and the Carolinas requires further study because of a discontinuity between sampling areas 8 and 9.

Discussion

The results of this study indicate the existence of at least 3 genetically distinct hogfish stocks in the southeastern United States: the eastern Gulf of Mexico, south Florida and the Florida Keys, and the Carolinas. Specimens were collected over a rela-

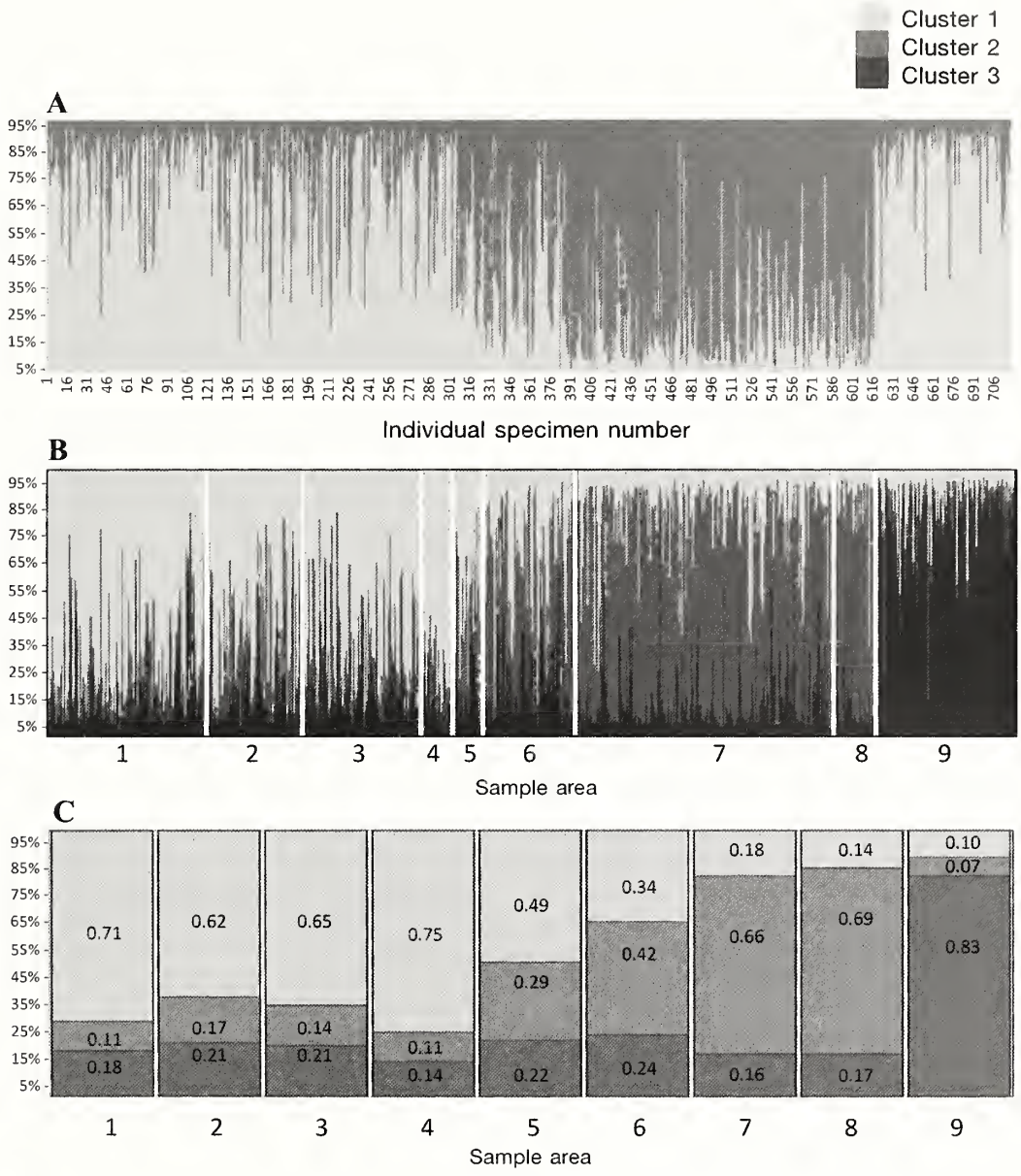

Figure 4

Genetically determined population structure among hogfish (*Lachnolaimus maximus*) (number of specimens=719) in the southeastern United States, according to posterior probability assignment produced by the analysis of 24 polymorphic microsatellite loci (4.5×10^6 burn-in, and 9.0×10^6 replications) with the program STRUCTURE. The output from 10 replicates from the program CLUMPP for 719 specimens and 9 sampling areas indicates (**A**) cluster percentage per individual for the highest modal value (number of genetic clusters) when K=2 (specimens were collected from the following sampling areas: 1–324 from sampling areas 1–5; 325–394 from sampling area 6; 395–616 from sampling areas 7 and 8; and 617–719 from sampling area 9); (**B**) cluster percentage for each individual, grouped by sampling areas for the best modal value of K=3 (hogfish population structure) by using the program DISTRUCT; and (**C**) proportional values represented by each cluster within sampling areas 1–9. Hogfish specimens were collected from November 2005 through August 2013 from northwest Florida to the Carolinas.

tively broad geographic distance and separated by the land mass of peninsular Florida; therefore, genetic differentiation across this scale was not necessarily surprising (Riginos et al., 2011). The factors that influence stock separation are not known but are explored here from 3 perspectives: in relation to other coastal and marine fishes; at a seascape level (particularly in regard to the descriptive hydrodynamics around Florida), and in terms of how these results affect stock assessment and management of this species.

In the western Atlantic Ocean, capes Romano and Canaveral have been identified previously as points of major shifts in marine animal community composition. Briggs and Bowen (2012) identified 1) Cape Romano as the point separating the marine community composition of the Gulf of Mexico from that of the Caribbean province and 2) Cape Canaveral as separating the marine community composition of the Caribbean province from that of the Carolinian province. Cape Romano was in fact the approximate point of the genetic break for hogfish in the eastern Gulf of Mexico in our study (cluster 1 versus cluster 2; Fig. 1). Unfortunately, the large geographic gap in hogfish collections between Cape Canaveral and South Carolina made it impossible to identify the point of the genetic break between clusters 2 and 3.

Strong genetic differences between the Gulf and Atlantic coasts of Florida are known for several estuarine and nearshore marine fishes, including common snook (*Centropomus undecimalis*) (Tringali and Bert, 1996), red drum (*Sciaenops ocellatus*) (Gold et al., 1999; Seyoum et al., 2000; Gold and Turner, 2002), and spotted seatrout (*Cynoscion nebulosus*) (Seyoum et al.[5]). Strong genetic and phenotypic differences between the Gulf and Atlantic coasts of Florida are recognized for the shelf-dwelling reef fish black sea bass (*Centropristis striata*) (Bowen and Avise, 1990; McCartney et al., 2013; McBride, 2014a). In contrast, only weak genetic differences have been found between the east and west coasts of Florida for other reef fishes, including red grouper (*Epinephelus morio*), scamp (*Mycteroperca phenax*) (Zatcoff et al., 2004), and vermilion snapper (*Rhomboplites aurorubens*) (Tringali and Higham, 2007). Similarly, there was little distinction between coasts for the pelagic king mackerel (*Scomberomorus cavalla*) (Gold et al., 2002). Curiously, at least in the southeastern United States, the stock structure of hogfish and black sea bass more closely resemble the stock structure of inshore and nearshore fishes (e.g., Seyoum et al.[5]) than that of offshore reef fishes or large coastal pelagic fishes (e.g., Zatcoff et al., 2004).

Hogfish reproduce in nearshore and offshore reef habitats on the continental shelf (depths of 10–70 m; Colin, 1982; Collins and McBride, 2011). They are broadcast spawners who release buoyant eggs (Colin, 1982), facilitating pelagic dispersal of propagules from the harem arenas. Early larvae raised in laboratory tanks formed bubbles around themselves while floating near the surface (Colin, 1982), a behavior that may also contribute to dispersal. The planktonic larval phase has been estimated to last for approximately 35 days, preceding strong benthic orientation (Colin, 1982; Victor, 1986). Larvae are transported inshore, and juveniles settle in shallow, nearshore grass beds (Davis, 1976; Colin, 1982). Therefore, cross-shelf (offshore–inshore) dispersal of hogfish larvae is evident, but little is known about along-shelf dispersal.

Hydrodynamic flow around Florida is complex (Liu and Weisberg, 2005), and dispersal of hogfish throughout this region is likely influenced by larval behavior and mortality (Cowen et al., 2000; Leis, 2006; Huebert et al., 2010). Although these are poorly understood for this species, a qualitative assessment indicates that northward and southward larval dispersal is likely along the western Florida shelf in particular. The peak spawning period for hogfish in the eastern Gulf of Mexico (March–May; McBride et al., 2008; Collins and McBride, 2015) occurs at a time when the currents are shifting from a predominantly southeasterly flow to a northwesterly flow (Liu and Weisberg, 2005, 2012). Hogfish spawning, however, occurs to some extent in most months (all except September) (Collins and McBride, 2015). Spawning throughout the year would subject larvae to a diverse (and difficult to predict) set of conditions, both physical (e.g., temperature and seasonal shifts in currents) and biological (e.g., prey availability through seasonal plankton blooms), that may affect dispersal vectors and survival rates (Cowen, 2002; Leis and McCormick, 2002).

The Loop Current in the Gulf of Mexico is an upstream portion of the Gulf Stream and affects different areas of the west Florida shelf to differing degrees throughout the year. Along the west Florida shelf, current flows are weakest near Cape Romano, and the low currents there may present a barrier to gene flow, as evident by the break between clusters 1 and 2; but current direction on the shelf also shifts seasonally from a southerly to northerly flow, and a strong looping current near the shelf break interacts periodically with local wind forces (He and Weisberg, 2003). The Loop Current presumably occurs beyond the range of hogfish spawning on the west Florida shelf (cluster 1; spawning occurs at <70 m; Collins and McBride, 2015), but the effects of this major current and its associated eddies are difficult to assess because many regional ichthyoplankton surveys report taxa only to the family level or collect too few hogfish larvae for analysis (Richards et al., 1993; Huebert et al., 2010).

Along the Atlantic side of the Florida Keys, the dominant current flow is to the east, fed by the Florida Current that flows through the Florida Strait and into the Gulf Stream. This current flow indicates that the

[5] Seyoum, S., M. D. Tringali, B. L. Barthel, V. Villanova, C. Puchulutegui, M. C. Davis, and A. C. C. Alvarez. 2014. Stock boundaries for spotted seatrout (*Cynoscion nebulosus*) in Florida based on population genetic structure. Technical Report TR-18, 27 p. [Available from Fish and Wildlife Research Institute, Florida Fish and Wildlife Conservation Commission, 100 Eighth Ave. SE, St. Petersburg, FL 33701-5020.]

majority of larvae produced south of the Everglades region would be transported into the Florida Keys or Atlantic Ocean and there would be very little larval transport north along the west Florida shelf. Models of regional hydrodynamics combined with the increased information available regarding hogfish distribution and spawning could simulate larval dispersal and settlement around Florida. Elsewhere, biological data are lacking; for example, courtship in hogfish has been observed off North Carolina (Parker, 2000), but the timing and extent of spawning in this region (cluster 3) have not been described.

Adult behavior may also play an important role in determining connectivity and population structure (Frisk et al., 2014). Hogfish are protogynous hermaphrodites (McBride and Johnson, 2007). Sex change does not occur until fish are at least 305 mm in total length (TL) (Davis 1976), and most fish remain female until they are at least 350 mm TL (McBride and Johnson, 2007; Collins and McBride, 2011). A single, dominant male will spawn daily with multiple females in harems of up to 15 individuals (Colin, 1982; McBride and Johnson, 2007; Muñoz et al., 2010; Collins and McBride, 2011). For hogfish, stable harems and a strong association with reef habitats promote relatively strong site fidelity to specific locations for months or even years (Colin, 1982; Lindholm et al., 2006; Muñoz et al., 2010). However, gradual ontogenetic movement offshore with growth is evident.

Juveniles settle in shallow, inshore habitats (Davis, 1976; Collins and McBride, 2011), and hogfish <2 years old have rarely been collected from habitats deeper than 30 m (similarly, it is rare to collect individuals >8 years old from nearshore habitats). For those reasons, it is assumed that hogfish gradually move to deeper water farther from shore as they grow. Hogfish may live for 23 years (McBride and Richardson, 2007), and females mature as early as an age of 1–2 years (McBride and Johnson, 2007). Therefore, gradual movement of individuals across the shelf through time would increase the exposure of larvae to different environmental conditions and current regimes that may, as a result, affect larval distribution and gene flow. Finally, although there is no evidence of natal homing by hogfish, it has been documented for other reef fish (Paris et al., 2013) and should be considered a possibility.

Demographic differences in hogfish between or within regions of Florida have been noted (McBride and Richardson, 2007; McBride et al., 2008; Collins and McBride, 2011). In the central–eastern Gulf of Mexico, adult size, longevity, and fecundity differed between deepwater and shallow-water fish across the shelf (Collins and McBride, 2011; Collins and McBride, 2015), but these life history traits were unrelated to the genetic structure of hogfish (MERPDC, 2012). Similar demographic differences for hogfish have also been observed between the Gulf of Mexico and south Florida (Florida Keys) (McBride and Richardson, 2007; McBride et al., 2008). Although hogfish within these regions are now known to be genetically different, it seems unlikely that life history differences are solely the result of genetic differences. The effects of ontogenetic behaviors, as well as the effects of fishing on size at age, maturity, fecundity, and harem stability, likely play a significant role in the demographics of hogfish throughout the range of this species (McBride et al., 2008; Muñoz et al., 2010).

The close relationship between clusters 1 and 3 was surprising because both are geographically separated, and the genetic forces responsible for such a relationship are not readily apparent. The geographic isolation and modest sample size of cluster 3 may have led to a sample-specific association between clusters 1 and 3, one that may not hold up once more samples from the Carolinas are examined and compared. Still, some specific genetic mechanisms could be operating and deserve consideration. Drift may be important within cluster 3, which had the smallest N_e, and thereby led to a coincidental similarity between clusters 1 and 3. It is also possible that some environmental correlate along a latitudinal cline could be driving selection for particular genotypes, and the microsatellites, while neutral markers, could be linked in some way to adaptive markers. A possible driver for selection is temperature, which is high (>25C°) and relatively homogeneous around Florida during the summer (June–September), but, during the rest of the year, temperature is high only around south Florida (cluster 2) (He and Weisberg, 2003).

Drift and selection are possible, but the most testable hypothesis is based on gene flow. Suppose that hogfish in each cluster are disproportionally connected by hydrodynamically driven gene flow with a more southerly stock (McBride and Horodysky, 2004); in such a case, the most likely scenario is that cluster 2 alone is affected by introgression from the south, and the effect of such gene flow does not reach farther up along either the east or the west coast of Florida. The result would be as we report here: a disruption of the genetic continuity of hogfish around the Florida peninsula. Such a disruptive pattern has been reported for European anchovy (*Engraulis encrasicolus*), explained by introgression of an African population with populations around the Iberian peninsula (Zarraonaindia et al. 2012; Antoniou and Magoulas, 2014). This last hypothesis is particularly interesting because it would expand the currently understood sources of recruitment to the Florida Keys, but proving it would require examination of new collections from the Bahamas and Caribbean Sea.

Application of the findings in this study to monitoring, assessment, and regulatory actions regarding hogfish are relatively straight forward. Landings and fishing effort data in Florida are already collected at the county level (FWC[1]), and the Florida Keys are contained within one county (Monroe). Federal fisheries data can also be separated by coast (e.g., NMFS[2]), and it is likely that regional stock assessments will reveal further differences in fishing effort between regions.

Fishing effort within the region of cluster 1 is significant (NMFS[2]), but pressure is less concentrated there

than in cluster 2 because of the nature of the habitat and the expansiveness of the west Florida shelf. Fishing effort in cluster 2 is also high, but the effort is condensed into a much smaller area than that of cluster 1 and is highly accessible to divers throughout the year. In both clusters 1 and 2, hogfish in shallow waters are harvested from the population relatively soon after reaching legal size, particularly near areas of high human density (McBride and Richardson, 2007). Although commercial and recreational fisheries do exist within the region of cluster 3, that area presumably has lower fishing pressure for hogfish because of the distance from shore required to reach hogfish habitat, as well as inclement weather patterns during the winter months and lower densities of humans in coastal areas.

Previous stock assessments designed to quantify regional fishing effort and landings have been challenging (Kingsley[6]). As an alternative, Ault et al. (2005) promoted a size-based approach to addressing the data-poor nature of hogfish assessment, and Collins and McBride (2011, 2015) underscored the importance of considering spatial demographic structure. The genetic data presented herein strongly indicate that regional assessments are warranted for at least the eastern Gulf of Mexico and south Florida, and a separate assessment should be considered for the broad (but still undefined) region of habitat that stretches from northeast Florida to North Carolina.

Acknowledgments

We thank all the members of the Saint Petersburg Underwater Club (SPUC) for their involvement in this project, as well as J. Atack, B. Bateman, L. Borden, E. Burge, C. Collier, K. Fex, T. Grogan, J. Haag, J. Herrera, J. Shepard, A. Solana, M. Stokley and the contributing participants of the St. Pete Open, Spearboard Open, Key West Open, and Wrightsville Beach Spearfishing Tournaments. The Marine Fisheries-Independent and Marine Fisheries-Dependent Monitoring programs of the Fish and Wildlife Research Institute, Florida Fish and Wildlife Conservation Commission, also provided specimens. E. Schotsman went above and beyond to collect data in south Florida. We are grateful to W. Cooper, D. Richardson, and 3 anonymous reviewers for their insightful comments. The majority of the work described herein was funded by grant NA05NMF4540040 to the Florida Fish and Wildlife Conservation Commission from NOAA's Cooperative Research Program, as well as through the U.S. Department of the Interior, U.S. Fish and Wildlife Service, under the Federal Aid in Sport Fish Restoration Program, Grant F-69.

[6] Kingsley, M. C. S (ed.). 2004. The hogfish in Florida: assessment review and advisory report. Report prepared for the South Atlantic Fishery Management Council, the Gulf of Mexico Fishery Management Council, and the National Marine Fisheries Service. Southeast Data, Assessment, and Review, Charleston, SC. [Available at website.]

Literature cited

Antoniou, A., and A. Magoulas.
2014. Application of mitochondrial DNA in stock identification. *In* Stock identification methods: applications in fishery science, 2nd ed. (S. X. Cadrin, L. A. Kerr, and S. Mariani, eds.), p. 257–295. Academic Press, London.

Ault, J. S., S. G. Smith, and J. A. Bohnsack.
2005. Evaluation of average length as an estimator of exploitation status for the Florida coral-reef fish community. ICES J. Mar. Sci. 62:417–423.

Belkhir, K, P. Borsa, L. Chikhi, N. Raufaste, and F. Bonhomme.
2000. GENETIX 4.05, logiciel sous Windows™ pour la génétique des populations. Laboratoire Génome, Populations, Interactions CNRS UMR 5000, Université de Montpellier II, Montpellier, France.

Bowen, B. W., and J. C. Avise.
1990. Genetic structure of Atlantic and Gulf of Mexico populations of sea bass, menhaden, and sturgeon: influence of zoogeographic factors and life-history patterns. Mar. Biol. 107:371–381.

Briggs, J. C., and B. W. Bowen.
2012. A realignment of marine biogeographic provinces with particular reference to fish distributions. J. Biogeogr. 39:12–30.

Cadrin, S. X., L. A. Kerr, and S. Mariani.
2014. Stock identification methods, 2nd ed., 566 p. Academic Press, San Diego, CA.

Claro, R., A. Garcia-Cagide, and R. Fernández de Alaiza.
1989. Caracteristicas biológicas del pez perro, *Lachnolaimus maximus* (Walbaum), en el golfo de Batabanó, Cuba. Rev. Invest. Mar. 10:239–252.

Colin, P. L.
1982. Spawning and larval development of the hogfish, *Lachnolaimus maximus* (Pisces: Labridae). Fish. Bull. 80:853–862.

Collins, A. B., and R. S. McBride.
2011. Demographics by depth: spatially explicit life-history dynamics of a protogynous reef fish. Fish. Bull. 109:232–242.
2015. Variations in reproductive potential between nearshore and offshore spawning contingents of hogfish in the eastern Gulf of Mexico. Fish. Manage. Ecol. 22:113–124.

Cowen, R. K., K. M. M. Lwiza, S. Sponaugle, C. B. Paris, and D. B. Olson.
2000. Connectivity of marine populations: Open or closed? Science 287:857–859.

Cowen, R. K.
2002. Larval dispersal and retention and consequences for population connectivity. *In* Coral reef fishes: dynamics and diversity in a complex ecosystem (P. F. Sale, ed.), p. 149–170. Academic Press, Amsterdam.

Davis, J. C.
1976. Biology of the hogfish, *Lachnolaimus maximus* (Walbaum), in the Florida Keys. M.S. thesis, 86 p. Univ. Miami, Coral Gables, FL.

Do, C., R. S. Waples, G. M. Macbeth, B. J. Tillet, and J. R. Ovenden.
2014. NeEstimator v2: re-implementation of software for the estimation of contemporary effective population size (N_e) from genetic data. Mol. Ecol. Resour. 14:209–214.

Earl, D. A., and B. M. vonHoldt.
2012. STRUCTURE HARVESTER: a website and program for visualizing STRUCTURE output and implementing the Evanno method. Conserv. Genet. Resour. 4:359–361.

Evanno, G., S. Regnaut, and J. Goudet.
2005. Detecting the number of clusters of individuals using the software STRUCTURE: a simulation study. Mol. Ecol. 14:2611–2620.

Excoffier, L., and H. E. L. Lischer.
2010. Arlequin suite vers 3.5: a new series of programs to perform population genetics analyses under Linux and Windows. Mol. Ecol. Resour. 10:564–567.

Excoffier, L., P. E. Smouse, and J. M. Quattro.
1992. Analysis of molecular variance inferred from metric distances among DNA haplotypes: application to human mitochondrial DNA restriction data. Genetics 131:479–491.

Frisk, M. G., A. Jordaan, and T. J. Miller.
2014. Moving beyond the current paradigm in marine population connectivity: Are adults the missing link? Fish Fish. 15:242–254.

Gold, J. R., E. Pak, and D. A. DeVries.
2002. Population structure of king mackerel (*Scomberomorus cavalla*) around peninsular Florida, as revealed by microsatellite DNA. Fish. Bull. 100:491–509.

Gold, J. R., L. R. Richardson, and T. F. Turner.
1999. Temporal stability and spatial divergence of mitochondrial DNA haplotype frequencies in red drum (*Sciaenops ocellatus*) from coastal regions of the western Atlantic Ocean and Gulf of Mexico. Mar. Biol. 133:593–602.

Gold, J. R., and T. Turner.
2002. Population structure of red drum (*Sciaenops ocellatus*) in the northern Gulf of Mexico, as inferred from variation in nuclear-encoded microsatellites. Mar. Biol. 140:249–265.

Goudet, J.
2001. FSTAT, a program to estimate and test gene diversities and fixation indices (vers. 2.9.3.2). [Available at website.]

Guo, S. W., and E. A. Thompson.
1992. Performing exact test of Hardy-Weinberg proportions for multiple alleles. Biometrics 48:361–372.

He, R. Y., and R. H. Weisberg.
2003. A loop current intrusion case study on the west Florida shelf. J. Phys. Oceanogr. 33:465–477.

Hedrick, P. W.
1999. Perspective: highly variable loci and their interpretation in evolution and conservation. Evolution 53:313–318.

Hill, W. G.
1981. Estimation of effective population size from data on linkage disequilibrium. Genet. Res. 38:209–216.

Huebert, K. B., S. Sponaugle, and R. K. Cowen.
2010. Predicting the vertical distributions of reef fish larvae in the Straits of Florida from environmental factors. Can. J. Fish. Aquat. Sci. 67:1755–1767.

Jakobsson, M., and N. A. Rosenberg.
2007. CLUMPP: a cluster matching and permutation program for dealing with label switching and multimodality in analysis of population structure. Bioinformatics 23:1801–1806.

Kalinowski, S. T.
2002. How many alleles per locus should be used to estimate genetic distances? Heredity 88:62–65.
2005. Do polymorphic loci require large sample sizes to estimate genetic distances? Heredity 94:33–36.

Latter, B. D. H.
1972. Selection in finite populations with multiple alleles. III. Genetic divergence with centripetal selection and mutation. Genetics 70:475–490.

Leis, J. M.
2006. Are larvae of demersal fishes plankton or nekton? Adv. Mar. Biol. 51:57–141.

Leis, J. M., J. E. Caselle, I. R. Bradbury, T. Kristiansen, J. K. Llopiz, M. J. Miller, M. I. O'Connor, C. B. Paris, A. L. Shanks, S. M. Sogard, S. E. Swearer, E. A. Treml, R. D. Vetter, and R. R. Warner.
2013. Does fish larval dispersal differ between high and low latitudes? Proc. R. Soc., B 280:20130327.

Leis, J. M., and M. I. McCormick.
2002. The biology, behavior, and ecology of the pelagic, larval stage of coral reef fishes. *In* Coral reef fishes: dynamics and diversity in a complex ecosystem (P. F. Sale, ed.), p. 171–199. Academic Press, Amsterdam.

Lindholm, J., A. Knight, L. Kaufman, and S. Miller.
2006. A pilot study of hogfish (*Lachnolaimus maximus* Walbaum 1792) movement in the Conch Reef Research Only Area (northern Florida Keys). NOAA Mar. Sanctuaries Conserv. Ser. NMSP–06–06, 14 p.

Lischer H. E. L., and L. Excoffier.
2012. PGDSpider: an automated data conversion tool for connecting population genetics and genomics programs. Bioinformatics 28:298–299.

Liu, Y., and R. H. Weisberg.
2005. Patterns of ocean current variability on the west Florida shelf using the self-organizing map. J. Geophys. Res. 110:C06003.
2012. Seasonal variability on the west Florida shelf. Prog. Oceanogr. 104:80–98.

Mariani, S., and D. Bekkevold.
2014. The nuclear genome: netural and adaptive markers in fisheries science. *In* Stock identification methods, 2nd ed. (S. X. Cadrin, L. A. Kerr, and S. Mariani, eds.), p. 297–327. Academic Press, San Diego.

Malécot, G.
1955. Decrease of relationship with distance. Cold Spring Harbor Symp. Quant. Biol. 20:52–53.

McBride, R. S.
2014a. Managing a marine stock portfolio: stock identification, structure, and management of 25 fishery species along the Atlantic coast of the United States. N. Am. J. Fish. Manage. 34:710–734.
2014b. The continuing role of life history parameters to identify stock structure. *In* Stock identification methods, 2nd ed. (S. X. Cadrin, L. A. Kerr, and S. Mariani, eds.), p. 77–107. Academic Press, San Diego, CA.

McBride, R. S., and A. Z. Horodysky.
2004. Mechanisms maintaining sympatric distributions of two ladyfish (Elopidae: *Elops*) morphs in the Gulf of Mexico and western North Atlantic Ocean. Limnol. Oceanogr. 49:1173–1181. [Available at website.]

McBride, R. S., and M. R. Johnson.
2007. Sexual development and reproductive seasonality of hogfish (Labridae: *Lachnolaimus maximus*), an hermaphroditic reef fish. J. Fish Biol. 71:1270–1292.

McBride, R. S., and M. D. Murphy.
2003. Current and potential yield per recruit of hogfish, *Lachnolaimus maximus*, in Florida. Proc. Gulf Caribb. Fish. Inst. 54:513–525.

McBride, R. S., and A. K. Richardson.
2007. Evidence of size-selective fishing mortality from an age and growth study of hogfish (Labridae: *Lachnolaimus maximus*), a hermaphroditic reef fish. Bull. Mar. Sci. 80:401–417.

McBride, R. S., P. E. Thurman, and L. H. Bullock.
2008. Regional variations of hogfish (*Lachnolaimus maximus*) life history: consequences for spawning biomass and egg production models. J. Northwest Atl. Fish. Sci. 41:1–12.

McCartney, M. A., M. L. Burton, and T. G. Lima.
2013. Mitochondrial DNA differentiation between populations of black sea bass (*Centropristis striata*) across Cape Hatteras, North Carolina (USA). J. Biogeogr. 40:1368–1398.

MERPDC (Molecular Ecology Resources Primer Development Consortium), M. Andris, M. C. Arias, B. L. Barthel, B. H. Bluhm, J. Bried, D. Canal, X. M. Chen, P. Cheng, M. B. Chiappero, M. M. Coelho, A. B. Collins, M. Dash, M. C. Davis, M. Duarte, M.-P. Dubois, E. Françoso, M. A. Galmes, K. Gopal, P. Jarne, M. Kalbe, L. Karczmarksi, H. Kim, M. B. Martella, R. S. McBride, V. Negri, J. J. Negro, A. D. Newell, A. F. Piedade, C. Puchulutegui, L. Raggi, I. E. Samonte, J. H. Sarasola, D. R. See, S. Seyoum, M. C. Silva, C. Solaro, K. A. Tolley, M. D. Tringali, A. Vasemägi, L. S. Xu, and J. I. Zanón-Martínez.
2012. Permanent genetic resources added to Molecular Ecology Resources Database 1 February 2012–31 March 2012. Mol. Ecol. Resour. 12:779–781.

Muñoz, R. C., M. L. Burton, K. J. Brennan, and R. O. Parker.
2010. Reproduction, habitat utilization, and movements of hogfish (*Lachnolaimus maximus*) in the Florida Keys, U.S.A.: comparisons from fished versus unfished habitats. Bull. Mar. Sci. 86:93–116.

Nei, M.
1973. Analysis of gene diversity in subdivided populations. Proc. Natl. Acad. Sci. U.S.A. 70:3321–3323.
1987. Molecular evolutionary genetics, 513 p. Columbia Univ. Press, New York.

Nei, M. and A. K. Roychoudhury.
1974. Sampling variances of heterozygosity and genetic distance. Genetics 76:379–390.

Paris, C. B., J. Atema, J.-O. Irisson, M. Kingsford, G. Gerlach, and C. M. Guigand.
2013. Reef odor: a wake up call for navigation in reef fish larvae. PLoS ONE 8(8):e72808.

Park, S. D. E.
2001. Trypanotolerance in West African cattle and the population genetic effects of selection. Ph.D. diss, 241 p. Univ. Dublin, Dublin, Ireland.

Parker, R. O, Jr.
2000. Courtship in hogfish, *Lachnolaimus maximus*, and other behavior of reef fishes off Beaufort, North Carolina. J. Elisha Mitchell Sci. Soc. 116:260–261.

Peakall, R., and P. E. Smouse.
2006. GENALEX 6: genetic analysis in Excel. Population genetic software for teaching and research. Mol. Ecol. Notes 6:288–295.
2012. GenAlEx 6.5: genetic analysis in Excel. Population genetic software for teaching and research—an update. Bioinformatics 28:2537–2539.

Pritchard, J. K., M. Stephens, and P. Donnelly.
2000. Inference of population structure using multilocus genotype data. Genetics 155:945–959.

Pritchard, J. K., X. Wen, and D. Falush.
2009. Documentation for *structure* software: vers. 2.2. Univ. Chicago, Chicago, IL.

Raymond, M., and F. Rousset.
1995. An exact test for population differentiation. Evolution 49:1280–1283. [Available at website.]

Rice, W. R.
1989. Analyzing tables of statistical tests. Evolution 43:223–225.

Richards, W. J., M. F. McGowan, T. Leming, J. T. Lamkin, and S. Kelley.
1993. Larval fish assemblages at the loop current boundary in the Gulf of Mexico. Bull. Mar. Sci. 53:475–537.

Riginos, C., K. E. Douglas, Y. Jin, D. F. Shanahan, and E. A. Treml.
2011. Effects of geography and life history traits on genetic differentiation in benthic marine fishes. Ecography 34:566–575.

Robins, C. R., G. C. Ray, J. Douglass, and R. Freund.
1986. A field guide to Atlantic Coast fishes, 354 p. Houghton Mifflin Co., Boston.

Robinson, J. D., and G. R. Moyer.
2012. Linkage disequilibrium and effective population size when generations overlap. Evol. Appl. 6:290–302.

Rousset, F.
2008. GENEPOP'007: a complete reimplementation of the GENEPOP software for Windows and Linux. Mol. Ecol. Resour. 8:103–106.

Seyoum, S., M. D. Tringali, T. M. Bert, D. McElroy, and R. Stokes.
2000. An analysis of genetic population structure in red drum, *Sciaenops ocellatus*, based on mtDNA control region sequences. Fish. Bull. 98:127–138.

Takezaki, N., M. Nei, and K. Tamura.
2010. POPTREE2: software for constructing population trees from allele frequency data and computing other population statistics with Windows-interface. Mol. Biol. Evol. 27:747–752.

Tringali, M. D., and T. M. Bert.
1996. The genetic stock structure of common snook (*Centropomus undecimalis*). Can. J. Fish. Aquat. Sci. 53:974–984.

Tringali, M. D., and M. Higham.
2007. Isolation-by-distance gene flow among vermilion snapper (*Rhomboplites aurorubens* Cuvier, 1892) from the Gulf of Mexico and southeastern United States. Gulf Mex. Sci. 2007:2–14.

Victor, B. C.
1986. Duration of the planktonic larval stage of one hundred species of Pacific and Atlantic wrasses (family Labridae). Mar. Biol. 90:317–326.

Waples, R. S.
2006. A bias correction for estimates of effective population size based on linkage disequilibrium at unlinked gene loci. Conserv. Genet. 7:167–184.

Weir, B. S., and C. C. Cockerham.
1984. Estimating F-statistics for the analysis of population structure. Evolution 38:1358–1370.

Wilson, G. A., and B. Rannala.
2003. Bayesian inference of recent migration rates using multilocus genotypes. Genetics 163:1177–1191.

Wright, S.
1943. Isolation by distance. Genetics 28:114–138.

Zarraonaindia, I., M. Iriondo, A. Albaina, M. A. Pardo, C. Manzano, W. S. Grant, X. Irigoien, and A. Estonba.
2012. Multiple SNP markers reveal fine-scale population and deep phylogeographic structure in European anchovy (*Engraulis encrasicolus* L.). PLoS ONE 7(7):e42201.

Zatcoff, M. S., A. O. Ball, and G. R. Sedberry.
2004. Population genetic analysis of red grouper, *Epinephelus morio*, and scamp, *Mycteroperca phenax*, from the southeastern U.S. Atlantic and Gulf of Mexico. Mar. Biol. 144:769–777.

NOAA
National Marine
Fisheries Service

Fishery Bulletin
established 1881

Spencer F. Baird
First U.S. Commissioner
of Fisheries and founder
of *Fishery Bulletin*

Early life history of the Argentine sea bass (*Acanthistius patachonicus*) (Pisces: Serranidae)

Lujan Villanueva Gomila (contact author)[1]
Martín D. Ehrlich[2,3]
Leonardo A. Venerus[1]

Email address for contact author: gomila@cenpat-conicet.gob.ar

[1] Centro Nacional Patagónico (CENPAT)
Consejo Nacional de Investigaciones Científicas y Técnicas (CONICET)
Boulevard Brown 2915
Puerto Madryn
Chubut, U9120ACD Argentina

[2] Instituto Nacional de Investigación y Desarrollo Pesquero (INIDEP)
P.O. Box 175
Mar del Plata
Buenos Aires, B7602HSA Argentina

[3] Instituto de Ecología, Genética y Evolución de Buenos Aires (IEGEBA)
CONICET
Facultad de Ciencias Exactas y Naturales
Universidad de Buenos Aires (UBA)
Intendente Güiraldes 2160
Ciudad Universitaria
Ciudad Autónoma de Buenos Aires, C1428EGA Argentina

Abstract—The Argentine sea bass (*Acanthistius patachonicus*) is one of the most conspicuous and abundant species in the rocky-reef fish assemblage of Northern Patagonia, which sustains important recreational and commercial activities, such as scuba diving, hook-and-line fishing, and spear fishing. We describe the morphological features of eggs, larvae, and posttransition juveniles of *A. patachonicus* and summarize abundance and distribution data for larvae collected on the Argentine shelf (between ~40°S and 44°S). Eggs and yolk-sac larvae came from an in vitro fertilization experiment. Larger larvae were distinguished by relevant morphological features, including the development of the opercular complex and head spination, meristics, and pigmentation pattern. The early stages of *A. patachonicus* are similar to those of the koester (*A. sebastoides*) and of the western wirrah (*A. serratus*), the other 2 species of *Acanthistius* whose larval development has been described. The body and head in *A. patachonicus* were moderate in size, but its preanal length was long. The particular head spination pattern of larvae of *A. patachonicus*, namely a few conspicuous smooth spines (mainly on the preopercle and opercle), and 2 posttemporal spines, was useful for differentiating this species from others and, therefore, made it possible to describe the whole developmental series and to link the early stage morphological features to those of adults.

Manuscript submitted 5 November 2014.
Manuscript accepted 18 August 2015.
Fish. Bull. 113:456–467 (2015).
Online publication date: 10 September 2015.
doi: 10.7755/FB.113.8

The genus *Acanthistius*, included in the speciose family Serranidae (Nelson, 2006; but see Smith and Craig, 2007), is represented by 2 species in the Southwest Atlantic Ocean: *Acanthistius brasilianus*, which ranges from 15°S (Brazil) to 36°S (Uruguay) (Irigoyen et al., 2008) and *Acanthistius patachonicus*, which ranges from 23°S in Brazil to 48°S on the Argentine shelf (Irigoyen et al., 2008), at depths of 0–100 m (Cousseau and Perrotta, 2000). Until recently, *A. patachonicus* was misclassified as *A. brasilianus*, giving rise to a nomenclatural confusion in the ichthyological literature from Argentina. Irigoyen et al. (2008) clarified the taxonomic status of the species of *Acanthistius* in the Southwest Atlantic Ocean and developed a new diagnostic key to discriminate between these taxa.

Acanthistius patachonicus is the most abundant rocky-reef fish in Northern Patagonia (Galván et al., 2009), where it sustains commercial, recreational, and sport activities like scuba diving and hook-and-line and spear fishing. In offshore waters, it is caught by coastal and high-seas fleets, partly as bycatch in fisheries that target Argentine hake (*Merluccius hubbsi*) and Argentine red shrimp (*Pleoticus muelleri*). Commercial annual landings of *A. patachonicus* decreased between 1989 (14,509 metric tons) and 2013 (2462 metric tons) (MAGYP[1]).

Despite the large economic and recreational values of this species, there is little information about its reproductive ecology and behavior.

[1] MAGYP (Ministerio de Agricultura, Ganadería y Pesca). 2013. Total landings of marine catch by species and month. Ministerio de Agricultura, Ganadería y Pesca, Argentina. [Available at website, accessed November 2014.]

What we know is that *A. patachonicus* is a long-lived (maximum age recorded for fish ~47 cm in total length was 40–41 years, see Rubinich, 2001), slow-growing fish that reaches 65 cm in total length and 4 kg in weight (Irigoyen et al., 2008). It is a dioecious partial spawner and fertilization is external. The spawning season of this species extends between September and December off the coast of Buenos Aires province and in Northern Patagonia (Ciechomski and Cassia, 1976; Dell'Arciprete et al., 1987), where at least a fraction of its populations congregate in massive spawning aggregations (Irigoyen[2]). No data about its early life stages are available in the scientific literature.

In this study, the development of *A. patachonicus* from the egg stage to the posttransition juvenile stage (sensu Vigliola and Harmelin-Vivien, 2001) is described, and the distinctive features of its early life stages are compared with those of other species of *Acanthistius*. In addition, abundance and distribution patterns of larvae in the San Matías Gulf (SMG) and San José Gulf (SJG), in Northern Patagonia, and in adjacent waters are presented. Beyond a purely scientific interest, identification of the early stages of *A. patachonicus* will help to identify spatial and temporal patterns in reproduction and, in turn, will shed light on the location of spawning and nursery grounds for this species.

Materials and methods

Collection of samples

Eggs and yolk-sac larvae came from in vitro fertilization. Ripe adults were caught by trawling near the mouth of SMG (41°45′S 63°28′W) on 11 November 1978, on board the RV *Walther Herwig*. Hydrated oocytes and sperm were mixed in a bucket with saltwater. Later, the fertilized eggs were washed and transferred to 2-L buckets containing seawater at 18°C. At approximately every 2 h over the course of a week, a variable number of eggs (between 16 and 39 eggs) and yolk-sac larvae (between 1 and 47 larvae) in different developmental stages were taken from the buckets and fixed in 5% formalin.

Aboard the RV *Puerto Deseado* on the Argentine shelf in November 2009, 41 ichthyoplankton samples were collected during the research cruise CONCACEN 2009, which was conducted by the Consejo Nacional de Investigaciones Científicas y Técnicas (CONICET) and the Servicio de Hidrografía Naval and also involved the Centro Austral de Investigaciones Científicas (CADIC) and Centro Nacional Patagónico (CENPAT) (Table 1; Fig. 1). Another 212 ichthyoplankton samples were collected monthly during a 2-year survey that we conducted) aboard outboard motorboats in the SJG, covering a regular grid of 25 stations, from October 2011 through March 2012 and from September 2012 through April 2013 (Table 1; Fig. 1). No samples were available for January and November 2012 within the SJG. In addition, 105 ichthyoplankton samples were collected during 2 surveys, CC-01/08 and EH-05/11, conducted by the Instituto Nacional de Investigación y Desarrollo Pesquero (INIDEP, based in Mar del Plata, Argentina) in December 2008 and November 2011 aboard the RV *Capitán Canepa* and RV *Eduardo Holmberg*, respectively.

Ichthyoplankton tows were made with Hensen nets with mouth diameters of 70 cm (CONCACEN, SJG), multinets (CC-01/08) with square mouths (50×50 cm), and bongo nets (EH-05/11) with mouth diameters of 60 cm, all fitted with 300-µm mesh. General Oceanics[3] (Miami), Hydro-Bios (Altenholz, Germany), and T.S.K. (Tsurumi-Seiki Co., Ltd., Yokohama, Kanagawa, Japan) flowmeters were mounted in the mouths of the nets to estimate the volume of filtered water. Towing speed ranged between 77 and 154 cm/s. During the research cruise CONCACEN 2009, 2 plankton tows (1 oblique tow (depths sampled: 5–172 m) and 1 horizontal tow (depths sampled: 1–20 m), were made at each station. During the 2 surveys in the SJG, tows were oblique tows (depths sampled: 7–52 m) or horizontal tows (depths sampled: 3–28 m), depending on bottom depth, to increase the volume of water sampled. Horizontal tows were made a few meters below the surface when conducted aboard the RV *Puerto Deseado* and close to the bottom of the seafloor when conducted aboard motorboats within the SJG. Tows were horizontal during the survey CC-01/08 (depths sampled: 0–57 m) and oblique during the survey EH-05/11 (depths sampled: 9–60 m). Maximum depth for each ichthyoplankton tow was recorded by depth sensors attached to the nets (Table 1). Water temperature was recorded with sensors coupled to the nets or with conductivity, temperature, and depth (CTD) sensors (during surveys CC-01/08 and EH-05/11, water temperature was recorded with a SBE 25 Sealogger CTD and SBE 19 SeaCAT Profiler CTD [Sea-Bird Electronics, Bellevue, WA], respectively).

Samples were fixed immediately after collection and preserved in 5% formalin. Larval abundance was expressed as the number of larvae/1000 m^3.

Only one posttransition juvenile was available, and it was used for the description of that stage. This specimen was caught near Mar del Plata, Argentina, in December 1963 in a bottom shrimp net at a depth of less than 30 m. No further details were found on the label to identify the collection lot (ichthyoplankton collection, INIDEP, uncataloged).

[2] Irigoyen, A. J. 2014. Personal commun. Centro Nacional Patagónico (CENPAT), Consejo Nacional de Investigaciones Científicas y Técnicas (CONICET), Puerto Madryn, Chubut, U9120ACD Argentina.

[3] Mention of trade names or commercial companies is for identification purposes only and does not imply endorsement by the National Marine Fisheries Service, NOAA.

Table 1

Data from stations where larvae of *Acanthistius patachonicus* were caught in the Argentine Sea during ichthyoplankton tows conducted by Consejo Nacional de Investigaciones Científicas y Técnicas (CONICET) as part of the CONCACEN (CONICET-CADIC [Centro Austral de Investigaciones Científicas]-CENPAT [Centro Nacional Patagónico]) research cruise in 2009, during a survey that we conducted in the San José Gulf (SJG), 2011–2013, and during 2 surveys (CC-01/08 and EH-05/11) conducted by the Instituto Nacional de Investigación y Desarrollo Pesquero in 2008 and 2011. Three types of tows were used: horizontal subsurface tow (HSS), horizontal deep tow (HD), or oblique tow (O). For stratified stations, indicated with a plus sign (+), mean temperatures above and below the thermocline are provided in parentheses. w/d=missing data.

Research cruise	Station	Tow type	Date	Local hour	Lat. S	Long. W	Mean water temperature (°C)	Maximum Bottom depth (m)	Maximum depth sampled (m)	Number of larvae	Abundance (larvae /1000 m^3)
CC-01/08	20	HD	17 Dec 2008	1120	42°28′	63°17′	10.5	62	52	10	56.98
CONCACEN	7	HSS	16 Nov 2009	0106	40°45′	60°49′	12.7	54	8	1	5.37
	7	O	16 Nov 2009	0135	40°45′	60°50′	12.7	55	20	3	25.52
	8	HSS	16 Nov 2009	1234	41°11′	62°25′	13.9	52	w/d	1	2.85
	8	O	16 Nov 2009	1308	41°10′	62°27′	14.1	23	5	1	2.16
	9	O	16 Nov 2009	1900	41°20′	63°00′	13.3	33	17	12	25.12
	10	HSS	17 Nov 2009	0014	41°25′	63°19′	13.0	33	4	1	4.93
	17	O	20 Nov 2009	1120	41°38′	63°40′	12.7	50	26	2	5.35
EH-05/11	583	O	26 Nov 2011	1849	40°51′	61°48′	17.0	35	28	111	750.62
	591	O	28 Nov 2011	0935	40°31′	61°04′	14.3	44	41	19	174.82
SJG survey	11	O	30 Nov 2011	1550	42°17′	64°21′	14.5	72	w/d	2	16.88
	15	HD	19 Dec 2011	1657	42°15′	64°15′	16.0	31	w/d	1	15.44
	5	O	20 Dec 2011	1707	42°17′	64°27′	16.0	34	w/d	1	Present
	1	HD	12 Mar 2012	1326	42°19′	64°33′	16.7	19	13	1	9.26
	23+	O	14 Mar 2012	1124	42°21′	64°09′	(17.1–16.2)	58	50	1	4.80
	21+	O	14 Mar 2012	1244	42°17′	64°09′	(17.0–16.6)	55	44	1	5.39
	20	HD	23 Dec 2012	1243	42°15′	64°15′	14.0	24	w/d	2	16.53
	17+	O	14 Feb 2013	1453	42°19′	64°15′	(15.9–15.4)	65	43	1	32.46

Description of early stages

In all, 170 eggs, 48 yolk-sac larvae 1.1–2.9 mm in body length (BL), 31 preflexion larvae (2.2–6.1 mm BL), 16 flexion larvae (4.9–7.6 mm BL), 4 postflexion larvae (7.2–8.4 mm BL), and 1 posttransition juvenile (13.1 mm BL), were used to describe morphometrics, meristics, pigmentation (melanophores), and head spination according to the series method of Neira et al. (1998). Description of eggs was based on the typical identification characters: egg shape and size, presence and number of oil globules, perivitelline space width, and distinctive features of the yolk and oil droplet. The measurements of larvae, categories for body proportions, and the terminology for morphometrics followed Neira et al. (1998): body length (BL), distance from the tip of the snout to the notochord tip (in preflexion and flexion larvae), and to the posterior margin of the hypural bones (postflexion larvae and posttransition juvenile); eye diameter (ED), longest diameter of the eye; snout length (SnL), distance from the tip of the snout to the anterior margin of the eye; head length, distance from the tip of the snout to the posterior margin of the opercle; body depth, vertical distance on pectoral fin base; preanal length, distance from the tip of the snout to the anus.

In the following descriptions, larval length always refers to BL, and morphometric measurement was calculated as a proportion of BL, with the exception of ED and SnL, which were calculated as a proportion of head length. Specimens were measured to the nearest 0.1 mm from digital images that were taken with a Cybershot DSC-W200 camera (Sony Corp., Tokyo) coupled to a Wild M3 stereomicroscope (Leica Geosystems AG, St. Gallen, Switzerland) and processed with the AxioVision LE software, vers. 4.1 (Zeiss, Oberkochen, Germany). Possible shrinkage effects were not considered in the measurements. Whenever possible, the number of myomeres, spines, and rays of dorsal, anal, caudal, pectoral, and pelvic fins were recorded. All measures and meristic counts were made on the left side of the body. To describe head spination and the sequence of opercular development, as well as other osteological features, 21 preflexion, 11 flexion, and 3 postflexion larvae and

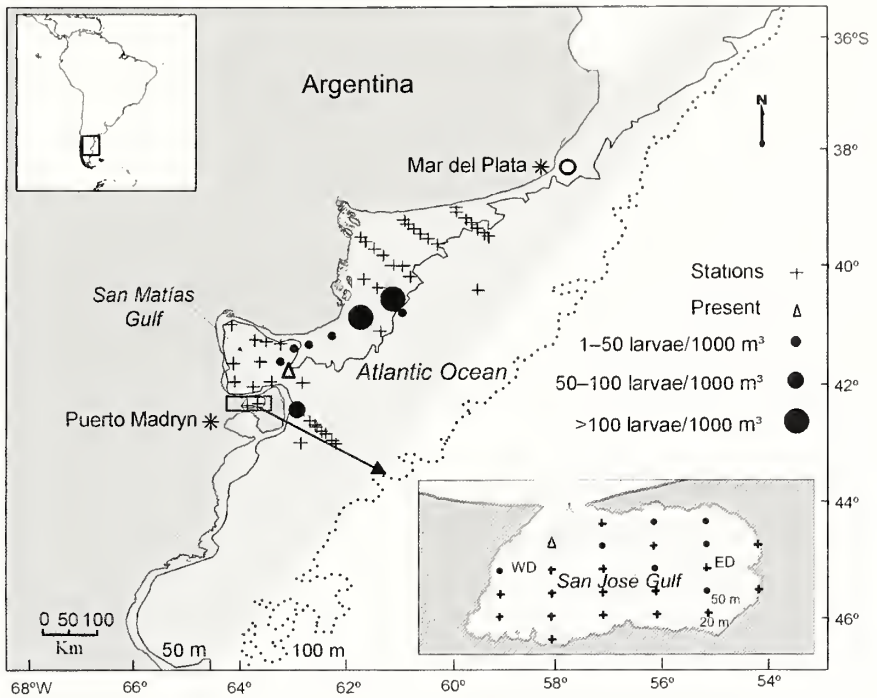

Figure 1

Distribution of larvae of *Acanthistius patachonicus* collected on the Argentine shelf, 2008–2013. The shaded area of water indicates the approximate distributional range for this species determined by Cousseau and Perrotta (2000). Only the oceanographic stations within the area of this range were plotted. The diameters of dots, classified into 3 categories, are proportional to larval abundance at each station. The open triangle indicates the position where ripe adults were caught for the fertilization experiment. The open circle indicates the area where the posttransition juvenile was caught. WD and ED indicate the western and eastern domains within the San José Gulf (sensu Amoroso and Gagliardini [2010]).

the posttransition juvenile were cleared and double stained with alcian blue and alizarin, according to Potthoff (1984) and Taylor and Van Dyke (1985). Different development stages were illustrated according to the guidelines of Trnski and Leis (1991).

Results

Eggs and yolk-sac larvae

The pelagic eggs in *A. patachonicus* were spherical, with a mean diameter of 1.1 mm (standard deviation [SD] 0.1), lacked pigmentation, and had a single, pale yellow oil globule (mean diameter: 0.2 mm [SD 0.1]) and a clear, segmented yolk (Fig. 2). The thin perivitelline space (mean: 0.2 mm [SD 0.1]) had no pigmentation, and the chorion was translucent.

Recently hatched larvae had a small, ovoid yolk sac that represented ~17% of BL, with 1 oil globule located anteriorly. The eyes were unpigmented and the mouth was not yet formed at this stage (Fig. 3A).

Morphology and development of larvae and posttransition juveniles

Four larvae were deposited as vouchers in the ichthyological collection of the Centro Nacional Patagónico: CNPICT 2009/21, flexion, broken larva, 41°25′S, 63°19′W; CNPICT 2009/22-1, postflexion, 7.6 mm, 41°20′S, 63°00′W; CNPICT 2009/22-2, flexion, 7.5 mm, 41°20′S, 63°00′W; CNPICT 2011/7, preflexion, 5.0 mm, 42°17′S, 64°21′W.

Body shape The smallest preflexion larva collected (2.2 mm) had round and incipiently pigmented eyes; the yolk was completely absorbed, and the mouth was terminal and open (Fig. 3B). Notochord flexion began at about 4.9 mm and was completed by 7.6 mm. The coiled digestive tract was already evident at preflexion.

Larval development was a gradual process. However, some discontinuities in body proportions were evident between larvae of 2.2–3.0 mm and larger individuals (Fig. 4). Head length was moderate, averaging 23% BL in larvae <4.2 mm, and was 28%–35% in larvae

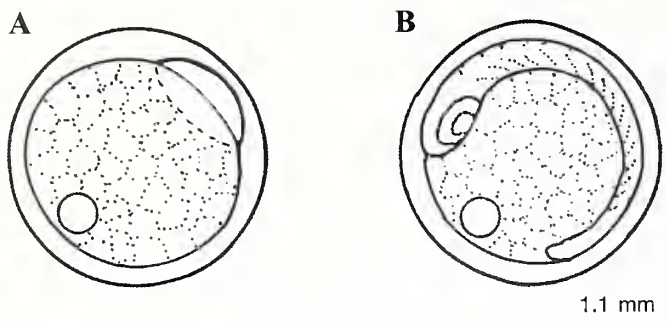

Figure 2

Illustrations of stages of eggs of *Acanthistius patachonicus*: (**A**) early stage with blastodermal cup, 12 h after fertilization, and (**B**) late stage with embryo surrounding the yolk (approximately 270°), 60 h after fertilization. The diameter of the eggs is 1.1 mm.

4.2–8.4 mm; it was 34% in the posttransition juvenile and reached 39% in adults (reference values for adults from Nakamura et al., 1986) (Fig. 4A). Body depth was moderate, with means of 22–26% BL in larvae <4.2 mm and of 27–33% in larvae 4.2–8.4 mm; it was 35% in the posttransition juvenile and 28% in adults (Fig. 4B). The preanal length was moderate in larvae <4.2 mm (44–46% BL) and long in larger larvae (54–62%), posttransition juveniles (62%), and adults (57%) (Fig. 4C).

In the head, SnL increased between 30% and 40% and remained rather stable in larger larvae and in the posttransition juvenile (Fig. 5A), and ED decreased markedly (between 41% and 24% [Fig. 5B]). The mouth size increased slightly with development. By ~6 mm, the larvae had conic teeth in the upper jaw.

The posttransition juvenile stage was identified by its morphological similarities with the morphological features of adults (Fig. 3G). The snout was short and rounded. The mouth was terminal and reached the anterior edge of the eye. Both jaws showed only caniniform teeth.

Development of meristic characters Most of the meristic features of larvae of *A. patachonicus* developed between ~6 and 8.4 mm (flexion and postflexion stages) (Table 2). Larvae had 23–26 myomeres (mode: 25 myomeres), 7–12 preanal and 13–18 postanal; the myomere formula did not change with development. Preflexion larvae had only an undifferentiated finfold and paired pectoral-fin buds (Fig. 3, B–D). Fin-ray formation started with the development of dorsal, pectoral, caudal, and pelvic fins during flexion and was completed between 8.4 and 13.1 mm; fin elements reached their full complement in the posttransition juvenile. All fin spines were smooth.

Three branchiostegal rays were present at 4.4 mm; by 6.8 mm, 6 rays were formed, and, by 7.7 mm, the full complement of 7 rays was present (Table 2).

Fin formation The finfold in yolk-sac and preflexion larvae was symmetrical around the tip of the notochord (Fig. 3, A–C). By 5.5 mm, the first ray ventral to the notochord appeared, and in larger larvae the number of rays were added nearly symmetrically in the upper and lower lobes (Fig. 3D). In postflexion larvae, the caudal fin had a rounded, homocercal outline with about 8 rays in each of the upper and lower lobes. The adult complement of 9 branched rays in the upper lobe and 8 branched rays in the lower lobe developed by 13.1 mm (Table 2; Fig. 3G).

Pectoral fin buds were present in the smallest preflexion larvae (Fig. 3B). By ~6 mm, the upper 2–5 pectoral-fin rays, 1 pelvic-fin spine, and 3 pelvic-fin rays were present (Fig. 3E). Rays in the pectoral fin developed ventrally (Fig. 3F).

The undifferentiated dorsal finfold extended from the nape to the caudal region in larvae <6.1 mm. The dorsal-fin spines and rays started to appear during flexion and were added in an anterior to posterior sequence. Between 6.1–6.9 mm, 2 spines had already formed, and between 7.0–7.6 mm the 3 first rays had formed. Anal-fin rays were not yet developed in larvae <8.4 mm (Table 2; Fig. 3F).

Nearly full complements of fin spines and rays were present as early as the posttransition juvenile stage: the pelvic fin had 1 spine and 4 rays; the pectoral fin had 17 rays; the dorsal fin had 12 spines and 16 rays; and the anal fin had 2 spines and 9 rays (Table 2; Fig. 3G). The first and second dorsal spines were shorter than the third and fourth spines. The first 2 dorsal interneurals were separate and supported the first 2 spines. The first anal spine was shorter than the second spine (Fig. 3G). The spines in the anal fin were supported by 2 separate interhaemals.

Axial skeleton Ossification of the vertebral column proceeded posteriorly from the first vertebra. This process began at 6.1 mm; by 7.0 mm, 11 vertebrae were ossified, and by 7.7 mm all except for the last 8 vertebrae and the urostyle were ossified. Each neural spine and arch ossified first, followed by the centrum and then by the haemal arch and spine. Ossification of the pleural ribs was not evident in the posttransition juvenile studied.

The caudal complex in the posttransition juvenile was the typical perciform type (Fig. 6). The caudal skeleton had 3 epurals, the urostyle, a small uroneural dorsal to the urostyle, 4 hypurals, and 2 autogenous haemal arches on the antepenultimate and penultimate vertebrae. There were 15 branched, segmented rays supported by the hypurals: 6 ventrally on hypurals 1 and 2 and 9 dorsally on hypurals 3 and 4. Four dorsal and 7 ventral raylets were adjacent to the segmented rays.

Head spination and opercular complex development The number and location of head spines in *A. patachonicus* were of great taxonomic value and helpful in the construction of the larval developmental series. All head spines were smooth.

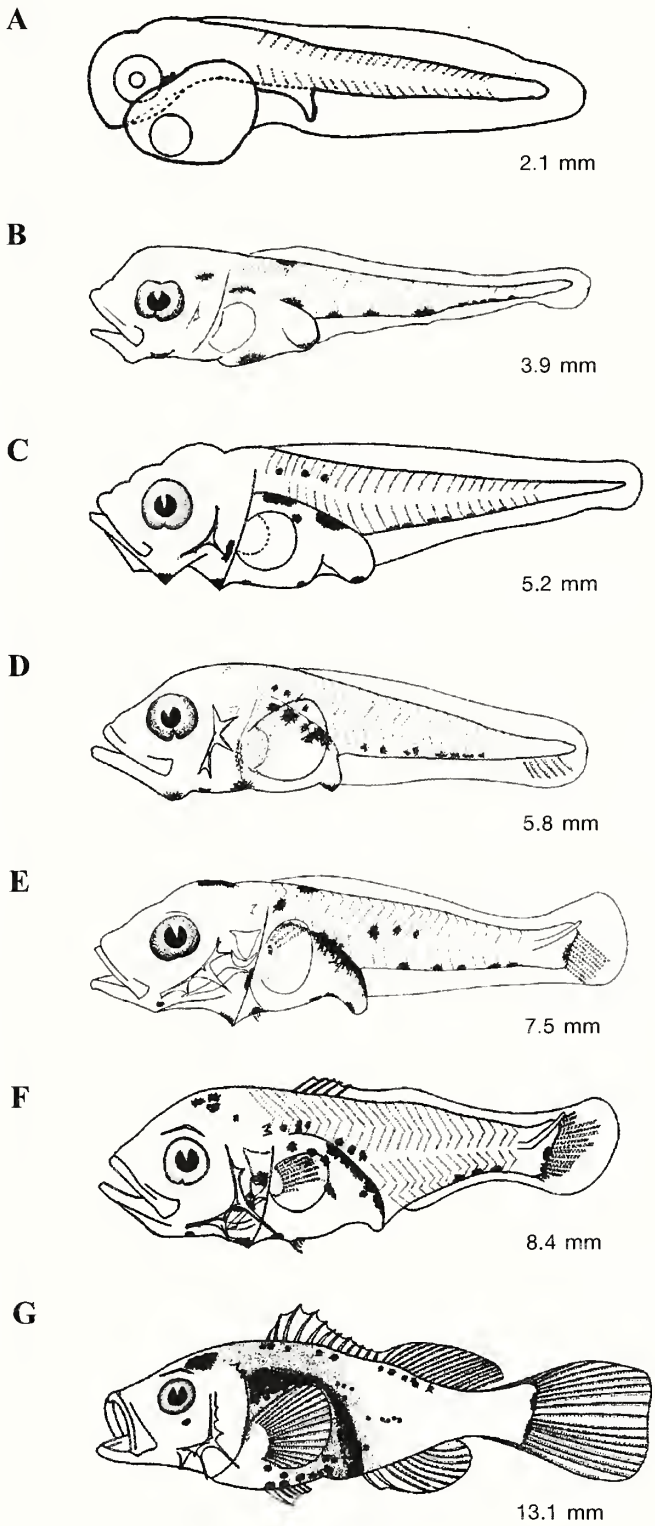

Figure 3

Illustrations of early stages of *Acanthistius patachonicus*: (**A**) yolk-sac larva (2.1 mm body length [BL]); preflexion at (**B**) 3.9 mm BL, (**C**) 5.2 mm BL, and (**D**) 5.8 mm BL; (**E**) flexion (7.5 mm BL); (**F**) postflexion (8.4 mm BL); and (**G**) posttransition juvenile (13.1 mm BL).

In early preflexion larvae, the preopercle was a partially ossified triangular plate with a sharp point where a spine would develop later. Its anterior margin was slightly thickened (Fig. 7A). In advanced preflexion larvae, the larger preopercle ossified completely, and its anterior margin became thicker. Two minute foramina and a well-defined posteroventral-oriented spine developed on the posterior margin of the preopercle (Fig. 7B). The opercle ossified partially and had a thickened margin.

In early flexion larvae, 2 anterior and 3 posterior preopercular spines were present (Fig. 7C). The middle spine was the largest, followed in size by the dorsal spine. The ventral spine was minute. The triangular-shaped opercle ossified completely and articulated with the hyomandibular at this stage. The subopercle was incipient and located below the opercle; the interopercle was situated below the middle preopercular spine.

In advanced flexion, the preopercle maintained its overall shape and increased in size (Fig. 7D). The opercle developed an anterior projection and a posterior spine. The U-shaped subopercle ossified, occupying the whole space between the opercle and the interopercle. The supracleithrum, bearing 1 spine, was already evident at this stage. By late flexion, all elements were completely ossified (Fig. 7E). The anterior preopercular margin had 3 spines; the middle one was the largest. The long, mid-posterior preopercular spine extended beyond the cleithrum. The interopercle reached the ventral posterior preopercular spine.

In postflexion (Fig. 7F, the posttransition juvenile), the preopercle formed an approximate right angle with 3 small, anterior spines and 6 posterior spines; the 4 lower posterior spines were larger (the spine at the angle was largest) and 3 of these spines were ventrally oriented. The supracleithrum had 3 spines, and the interopercle had 2 spines. The opercle had 3 spines—the one in the middle forming a middle opercular ridge. The V-shaped subopercle had 4 acute vertices.

In larvae >7.5 mm, there was a supraocular crest and 2 posttemporal spines (Fig. 3, E–G).

Pigmentation pattern Pigmentation pattern in formalin-preserved larvae of *A. patachonicus* consisted of a few melanophores in specific positions. Yolk-sac larvae were unpigmented (Fig. 3A). In 3.9-mm preflexion larvae, pigmentation on the head consisted of one external spot at the angle of the lower jaw and another posterior and dorsal to the eye (Fig. 3B). A small internal spot also appeared at the base of the pectoral buds anterior to the cleithrum (Fig. 3C). In flexion and postflexion

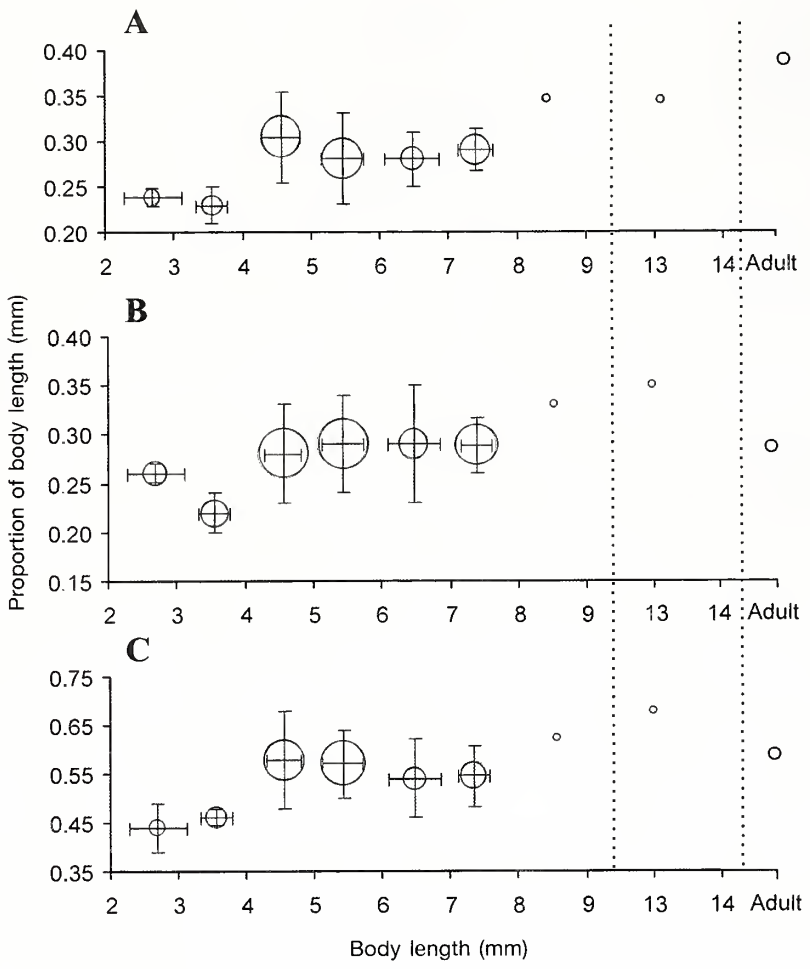

Figure 4

Body proportions of *Acanthistius patachonicus* (trunk region) examined for this study and collected on the Argentine shelf, 2008–2013: (**A**) head length, (**B**) body depth, and (**C**) preanal length. Bubble size in each plot is proportional to the number of larvae in each size range (from 1 to 14 larvae). Solid bars on bubbles indicate standard deviations for mean body lengths (BLs) and for the proportions of BL. Adult proportions were taken from Nakamura et al. (1986). Vertical dotted lines indicate discontinuities along the *x*-axis.

larvae (Fig. 3, E and F), a group of stellate external melanophores was located in the parietal region, and another internal group was located beneath the longest preopercular spine. The parietal patch of melanophores increased in size in the posttransition juvenile (Fig. 3F). A large internal melanophore was present at the base of the cleithrum in advanced preflexion larvae (Fig. 3, C–F).

Considerable internal pigmentation developed in the dorsal area of the gut cavity and gas bladder, primarily on the surface of the viscera. The number of melanophores over the gut increased with development. A few internal melanophores also were present at the ventral margin of the gut (Fig. 3, B–F).

A few, small isolated spots on the anterolateral side of the trunk were present in larvae ranging between ~5 and 7.5 mm (Fig. 3, C–E). Pigmentation along the midventral line consisted of a short series of 3–4 small spots (Fig. 3, B–F). As the caudal rays developed, less prominent spots appeared in the middle of the hypural margin (Fig. 3, E and F).

Abundance and distribution of larvae

Larvae of *A. patachonicus* were collected from mid-November to mid-March (during the years described previously in this section), between 40°31′S and 42°28′S, somewhere above the bottom in water up to 52 m deep (Table 1; Fig. 1). At stations where larvae were captured, mean water temperature ranged broadly between 10.5°C and 17.9°C. Overall, both the frequency of occurrence and larval density were low at stations where larvae were caught: between 1 (2.16 larvae/1000 m^3) and 111 larvae (750.62 larvae/1000 m^3) were collected in shallow tows to the east of the mouth of the SMG and within the SJG, predominantly in the eastern domain (sensu Amoroso and Gagliardini, 2010) (Table 1). The distribution pattern of small preflexion larvae matched the overall distribution of larvae of *A. patachonicus* in the study area.

Discussion

In this study, the eggs and yolk-sac larvae came from a fertilization experiment, and that origin confirmed their species identity. Morphological features, including the development of the opercular complex and head spination, the sequence of development of meristic characters, and the position and relative size of the melanophores in preflexion, flexion, and postflexion larvae, allowed reconstruction of a developmental series and identification of the remaining individuals studied as *A. patachonicus*.

At present, the larval development has been described for only 2 of the 11 species of *Acanthistius*. Baldwin and Neira (1998) studied the larvae of the western wirrah (*A. serratus*) from Western Australia, and Brownell (1979) described the eggs and larvae of the koester (*A. sebastoides*) from the southern coast of Africa. For our study, we considered that the

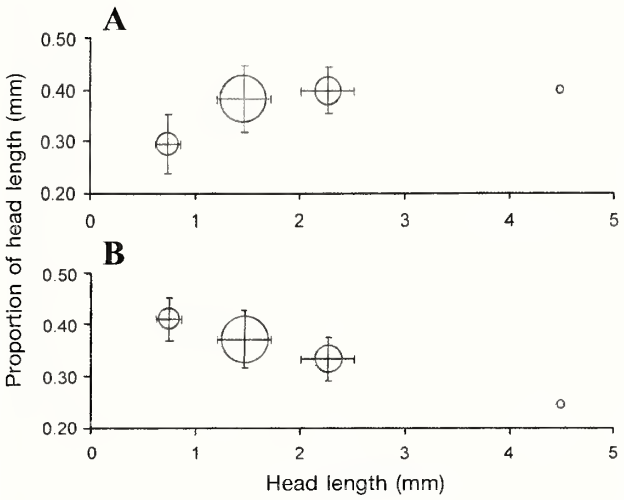

Figure 5

Body proportions of *Acanthistius patachonicus* (head region) examined for this study and collected on the Argentine shelf, 2008–2013: (**A**) snout length and (**B**) eye diameter. Bubble size in each plot is proportional to the number of larvae in each size range (from 1 to 30 larvae. Solid bars on bubbles indicate standard deviations for mean head lengths (HLs) and for the proportions of HL.

"Perciform Species 1" in Brownell (1979) was *A. sebastoides* (Brownell[4]; Baldwin and Neira, 1998; Heemstra, 2010).

Some morphological characteristics of the early stages of *A. patachonicus* were similar to those of other species in this genus. The eggs, for example, resembled those of koester, which has pelagic eggs about 0.9 mm in diameter, with a single 0.2-mm oil globule (Brownell, 1979). The number of myomeres, spines and rays in *A. patachonicus* were in the same range as those from larvae of other *Acanthistius* species (Brownell, 1979; Baldwin and Neira, 1998). The preopercular spines in *A. patachonicus* were as conspicuous as those found in western wirrah and koester, and the preopercular spine at the posterior angle was the largest one among all 3 species. Two posttemporal spines were present in western wirrah and *A. patachonicus*.

However, other characteristics, including pigmentation and the sequence of formation of the fin elements, differed among the species. The number of pigmentation spots in the head and trunk of *A. patachonicus* was lower than the number observed in larvae of both the western wirrah and koester (Brownell, 1979; Baldwin and Neira, 1998). Notochord flexion in *A. patachonicus* and western wirrah began at a similar size but ended at a larger size in *A. patachonicus* (4.9–7.5 mm; western wirrah, 4.1–5.3 mm: Baldwin and Neira, 1998). In *A. patachonicus*, the anal-fin rays began to form after notochord flexion, but in western wirrah the dorsal- and anal-fin soft rays began to form simultaneously during flexion (Baldwin and Neira, 1998), although anal-fin development was not complete until the postflexion stage (by 7.5 mm).

Undoubtedly, the most relevant feature that allowed reconstruction of the developmental series and linkage from the posttransitional stage to the adult stage in *A. patachonicus* was the opercular complex. It was possible to track the morphological changes observed in the preopercle, opercle, subopercle, interopercle, and supracleithrum and to track the development of spination in those structures, from the initial development

[4] Brownell, C. L. 1979. Personal commun. Oceanic Institute, Waimanalo, HI 96795.

Table 2

Development of meristic characters in *Acanthistius patachonicus*. Data for adults were obtained from Nakamura et al. (1986) and Irigoyen et al. (2008). Asterisks indicate the size ranges at which notochord flexion occurs. w/d=missing data. *N*=number of specimens.

Body length range (mm)	*N*	Dorsal fin		Pelvic fin		Pectoral-fin rays	Anal fin		Branchiostegal rays	Total myomeres	Vertebrae	Caudal-fin rays	
		Spines	Rays	Spines	Rays		Spines	Rays				Upper	Lower
2.0–2.9	3	–	–	–	–	–	–	–	–	25	–	–	–
3.0–3.9	4	–	–	–	–	–	–	–	–	25	–	–	–
4.0–4.9	14	–	–	–	–	–	–	–	3–4	22–25	–	–	–
5.0–5.9*	16	–	–	–	–	–	–	–	3–4	23–26	–	–	–
6.0–6.9*	5	II	–	–	3	2–5	I	–	2–6	24–25	5–13	3–6	3–9
7.0–7.9*	8	II–V	3	–	3	3–7	I	–	4–7	23–26	10–16	3–8	3–8
8.0–8.9	1	VI	–	–	–	–	–	–	–	–	–	8	7
13.0–13.9	1	XII	16	I	4	17	II	9	7	–	25	9	8
Adults	w/d	XII–XIII	15–16	I	5	17	II–III	8–10	7	–	25	9	8

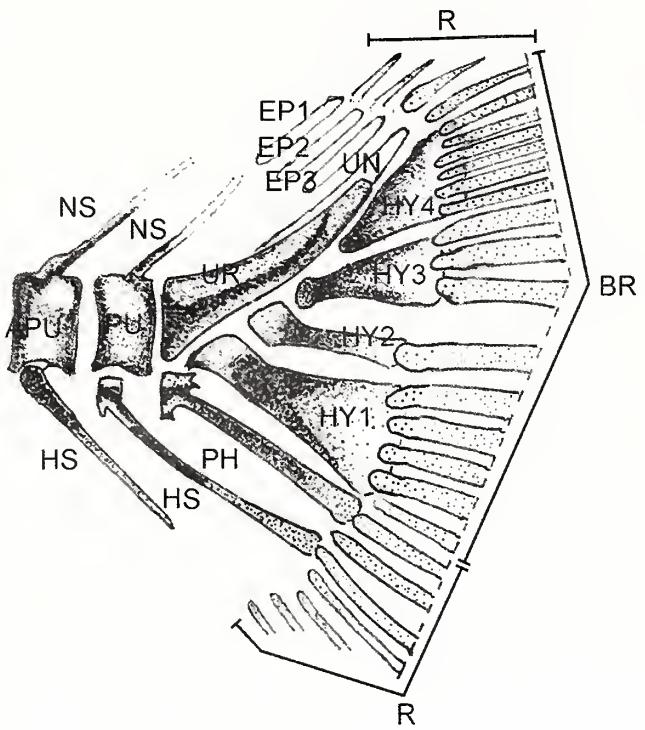

Figure 6

Illustration of the caudal skeleton of the single posttransition juvenile (13.1 mm in body length) of *Acanthistius patachonicus* that was examined for this study; this specimen was caught near Mar del Plata, Argentina, in December 1963: raylets (R), epurals 1–3 (EP), uroneural (UN), neural spines (NS), hypurals 1–4 (HY), branched rays (BR), antepenultimate vertebra (APU), penultimate vertebra (PU), urostyle (UR), haemal spines (HS), and parahypural (PH).

of the preopercle in preflexion larvae <3.1 mm BL. In the larger posttransition juvenile (13.1 mm BL), the preopercle and the opercle allowed linkage from the postflexion stage to the adult stage, because both bones in this juvenile matched the osteological description for adult fish (Gosztonyi and Kuba[5]; Irigoyen et al., 2008).

Head spination and pigmentation were useful for distinguishing larvae of *A. patachonicus* from other, morphologically somewhat similar species described for the Argentine Sea (Sánchez, 1991). Rough scad (*Trachurus lathami*) has a higher number of spines on the preopercular margin (Sánchez-Ramírez and Flores-Coto, 1993), and larvae of cabrilla (*Sebastes oculatus*) have visible parietal spines by 5.3 mm BL (Sánchez and Acha, 1988). The pigmentation pattern of larvae of *A. patachonicus* also differed from those of rough scad, cabrilla, and wreckfish (*Polyprion americanus*). Rough scad has numerous melanophores on the head and along the dorsal and ventral midlines (Sánchez-Ramírez and Flores-Coto, 1993), cabrilla has heavy pectoral-fin pigmentation throughout larval development (Sánchez and Acha, 1988), and wreckfish has strongly pigmented larvae with stellate melanophores all over the body (Sparta, 1939). The wreckfish also has a large, oblique mouth that reaches the posterior margin of the eye, another difference from *A. patachonicus* (Fig. 3). Finally, larvae of dusky grouper (*Epinephelus marginatus*) have serrate and pigmented dorsal and pelvic spines that distinguish this species from *A. patachonicus* (Cunha et al., 2013).

The spawning season of *A. patachonicus* lasts for about 4 months (September–December) during the austral spring, between ~36°S and 43°S. The presence of its planktonic larvae, which were collected from November through March, 2008–2013, was slightly delayed in relation to the spawning season. Because the surveys conducted were not specifically designed to study the spatial or temporal distribution of this species outside of the SJG where a 2-year systematic survey was conducted, only limited inference about their distribution and abundance patterns can be derived from the data available. Analyzing an extensive database of fisheries surveys, Irigoyen (2006) reported high concentrations of *A. patachonicus* in shelf areas (depths: <90 m) during the reproductive season. The occurrence of larvae in coastal areas, to the east and north of the mouth of the SMG, was coincident with the reported distribution patterns of ripe adults (Irigoyen[2]).

Although *A. patachonicus* is the most abundant rocky-reef fish in Northern Patagonia, between ~40°S and 45°S (Irigoyen et al., 2008), its larvae have been scarce: overall, they were present in only 17% of the tows conducted between November and March in 2009–2013. Only a single individual was captured in most of the tows, with few exceptions (Table 1, Fig. 1). This patchy distribution is consistent with the occurrence of spawning aggregations of adults of this species (Irigoyen[2]). However, the small size of the larvae collected may also indicate a short pelagic life. Indeed, larvae longer than 8.4 mm BL were not found (see also Acha et al., 2012), and the juvenile fish that was 13.1 mm BL had already metamorphosed, indicating that individuals of this species could adopt a demersal habit at around 13 mm BL.

Similarly, the mean planktonic larval duration of some serranid fishes of the genera *Paralabrax*, *Epinephelus*, and *Serranus*, for example, ranges between 18 and 33 days (McClean, 1999; Macpherson and Raventos, 2006; Allen and Block, 2012), and 3 species of *Paralabrax* settle to the bottom as larvae between 9.1 and 10.2 mm BL (Allen and Block, 2012). Further, Baldwin and Neira (1998) stated that western wirrah would settle between 10.5 and 23.0 mm BL, and Brownell (1979) registered one koester taking up a

[5]Gosztonyi, A. E., and L. Kuba. 1996. Atlas de huesos craneales y de la cintura escapular de peces costeros patagónicos. Inf. Tec. 4, 29 p. Fundacion Patagonia Natural, Chubut, Patagonia, Argentina. [Available at website.]

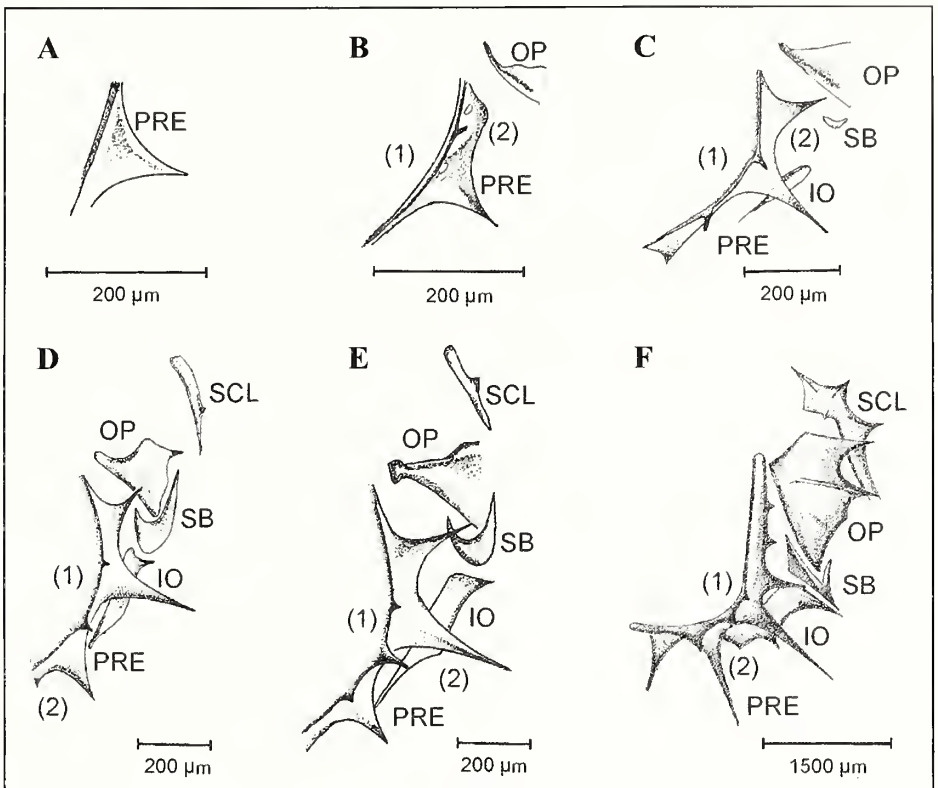

Figure 7

Illustrations of left lateral view of opercular complex development in *Acanthistius patachonicus* at the following body lengths (BLs): (**A**) 3.0 mm BL; **B**) 4.5 mm BL; (**C**) 5.4 mm BL; (**D**) 6.8 mm BL; (**E**) 7.0 mm BL, and (**F**) 13.1 mm BL. PRE=preopercle, OP=opercle: (1) anterior and (2) posterior margins; SB=subopercle; IO=interopercle; and SCL=supracleithrum.

benthic lifestyle and changing its coloration by a standard length of 9.0 mm.

Alternatively, another explanation may be avoidance of the plankton nets by larger larvae, especially during daylight hours. Hence, other sampling techniques (e.g., the use of light traps, trawl nets, or video stations; Harasti et al., 2014) and survey designs specific to collection of larger fish (e.g., between 8.4 and 13.1 mm BL) should be used to sample fish and determine more precisely the size at settlement.

The identification of the early stages of *A. patachonicus* is a first step toward a better understanding of its reproductive behaviour and ecology, connectivity patterns, and dispersal capabilities, all of which in turn will serve as fundamental pieces of knowledge for the proper management of its populations in the Argentine Sea.

Acknowledgments

We want to thank M. López, P. Fiorda, R. Hernández Moresino, L. Getino, G. Trobbiani, N. Ortíz, D. Remenar, I. D'ercole, and the crews of the RV *Puerto Deseado*, RV *Capitán Cánepa*, and RV *Eduardo Holmberg* for their help during surveys. L. Machinandiarena and M. R. Marín collaborated on laboratory work and data analysis, respectively. J. Dignani designed and calibrated depth and temperature sensors. C. Pipitone provided useful literature. C. Guerrero helped with revisions of figures. A. Gosztonyi and 2 anonymous reviewers made useful comments on an earlier version of this article, and N. Glembocki helped with the English language. CONICET partially funded the research cruise CONCACEN 2009. This study was funded by projects from the Agencia Nacional de Promoción Científica y Tecnológica (PICT 2010–2461) (granted to L. Venerus) and the Conservation, Research and Education Opportunities International (granted to the senior author). Field work was partially conducted within a World Natural Heritage Site and was authorized by the Secretaría de Turismo y Áreas Protegidas del Chubut.

Literature cited

Acha, E. M., M. Orduna, K. Rodrigues, M. I. Militelli, and M. Braverman.

2012. Caracterización de la zona de "El Rincón" (Provin-

cia de Buenos Aires) como área de reproducción de peces costeros. Rev. Invest. Desarr. Pesq. 21:31–43.

Allen, L. G., and H. E. Block.
2012. Planktonic larval duration, settlement, and growth rates of the young-of-the-year of two sand basses (*Paralabrax nebulifer* and *P. maculatofasciatus*: fam. Serranidae) from Southern California. Bull. South. Calif. Acad. Sci. 111:15–21.

Amoroso, R. O., and D. A. Gagliardini.
2010. Inferring complex hydrographic processes using remote-sensed images: turbulent fluxes in the Patagonian gulfs and implication for scallop metapopulation dynamics. J. Coast. Res. 26:320–332.

Baldwin, C. C., and F. J. Neira.
1998. Serranidae (Anthiinae): sea basses, sea perches, wirrahs. *In* Larvae of temperate Australian fishes: laboratory guide for larval fish identification (F. J. Neira, A. G. Miskiewicz, and T. Trnski, eds.), p. 288–291. Univ. Western Australia Press, Nedlands, Australia.

Brownell, C. L.
1979. Stages in the early development of 40 marine fish species with pelagic eggs from the Cape of Good Hope. Ichthyol. Bull. J.L.B. Smith Inst. Ichthyol. 40, 84 p.

Ciechomski, J. D., and M. C. Cassia.
1976. Características de la reproducción y fecundidad del mero, *Acanthistius brasilianus*, en el Mar Argentino (Pisces; Serranidae). Physis 35:27–36.

Cousseau, M. B., and R. G. Perrotta.
2000. Peces marinos de Argentina: biología, distribución, pesca, 2nd ed., 167 p. Instituto Nacional de Investigación y Desarrollo Pesquero, Mar del Plata, Buenos Aires, Argentina.

Cunha, M. E., P. Ré, H. Quental-Ferrerira, P. J. Gavaia, and P. Pousao-Ferreira.
2013. Larval and juvenile development of dusky grouper *Epinephelus marginatus* reared in mesocosms. J. Fish Biol. 83:448–465.

Dell'Arciprete, O. P., H. E. Christiansen, and J. M. Díaz de Astarloa.
1987. Observaciones sobre el ciclo reproductivo del mero, *Acanthistius brasilianus* (Serranidae, Pisces). Rev. Invest. Desarr. Pesq. 7:67–84.

Galván, D. E., L. A. Venerus, and A. J. Irigoyen.
2009. The reef-fish fauna of the Northern Patagonian gulfs, Argentina, South-western Atlantic. Open Fish Sci. J. 2:90–98.

Harasti, D., C. Gallen, H. Malcolm, P. Tegart, and B. Hughes.
2014. Where are the little ones: distribution and abundance of the threatened serranid *Epinephelus daemelii* (Günther, 1876) in intertidal habitats in New South Wales, Australia. J. Appl. Ichthyol. 30:1007–1015.

Heemstra, P. C.
2010. Taxonomic review of the perciform fish genus *Acanthistius* from the east coast of southern Africa, with description of a new species and designation of a neotype for *Serranus sebastoides* Castelnau, 1861. Zootaxa 2352:59–68.

Irigoyen, A. J.
2006. Distribución espacial y temporal del mero (*Acanthistius brasilianus*) en la plataforma Argentina. B.Sc. thesis, 54 p. Universidad Nacional de la Patagonia San Juan Bosco, Puerto Madryn, Chubut, Argentina.

Irigoyen, A. J., L. Cavaleri Gerhardinger, and A. Carvalho-Filho.
2008. On the status of the species of *Acanthistius* (Gill, 1862) (Percoidei) in the South-West Atlantic Ocean. Zootaxa 1813:51–59.

Macpherson, E., and N. Raventos.
2006. Relationship between pelagic larval duration and geographic distribution of Mediterranean littoral fishes. Mar. Ecol. Prog. Ser. 327:257–265.

McClean, A. M.
1999. Patterns of settlement of juvenile kelp bass (*Paralabrax clathratus*) at Catalina Island during the summers of 1997 and 1998. M.Sc. thesis, 70 p. Calif. State Univ., Northridge, CA.

Nakamura, I., T. Inada, M. Takeda, and H. Hatanaka.
1986. Important fishes trawled off Patagonia, 369 p. Japan Marine Fishery Resource Research Center, Tokyo, Japan.

Neira, F. J., A. G. Miskiewicz, and T. Trnski.
1998. Methods. *In* Larvae of temperate Australian fishes: laboratory guide for larval fish identification (F. J. Neira, A. G. Miskiewicz, and T. Trnski, eds.), p. 11–19. Univ. Western Australia Press, Nedlands, Australia.

Nelson, J. S.
2006. Fishes of the world, 4th ed., 601 p. John Wiley & Sons Inc., Hoboken, NJ.

Potthoff, T.
1984. Clearing and staining techniques. *In* Ontogeny and systematics of fishes: based on an international symposium dedicated to the memory of Elbort Halvor Ahlstrom. Spec. Publ. 1 (G. Moser, W. J. Richards, D. M. Cohen, M. P. Fahay, A.W. Kendall, and S. L. Richardson, eds.), p. 35–37. Am. Soc. Ichthyologists and Herpetologists, Lawrence, KS.

Rubinich, J. P.
2001. Edad y crecimiento del mero *Acanthistius brasilianus* (Pisces, Serranidae) en el golfo San Matías, Argentina. B.Sc. thesis, 44 p. Universidad Nacional de la Patagonia San Juan Bosco, Puerto Madryn, Chubut, Argentina.

Sánchez, R. P.
1991. Current state of marine ichthyoplankton research in Argentina and Uruguay. Atlantica 13:215–231.

Sánchez, R. P., and M. Acha.
1988. Development and occurrence of embryos, larvae and juveniles of *Sebastes oculatus* with reference to two Southwest Atlantic Scorpaenids: *Helicolenus dactylopterus lahillei* and *Pontinus rathbuni*. Meeresforschungen 32:107–133.

Sánchez-Ramírez, M., and C. Flores-Coto.
1993. Desarrollo larvario y clave de identificación de algunas especies de la familia Carangidae del sur del Golfo de México. An. Inst. Cienc. Mar Limnol. Univ. Nac. Auton. Mex. 20:1–38.

Smith, W. L., and T. M. Craig.
2007. Casting the percomorph net widely: the importance of broad taxonomic sampling in the search for the placement of serranid and percid fishes. Copeia 2007:35–55.

Sparta, A.
1939. Contributo alla conoscenza dello sviluppo nei percidi. Uova, stadi embrionali e post-embrionali di *Polyprion cernium*. Consiglio Nazionale delle Ricerche. R. Comitato talassografico italiano. Memoria CCLIX.

Taylor, W. R., and G. C. Van Dyke.
1985. Revised procedures for staining and clearing small fishes and other vertebrates for bone and cartilage study. Cybium 9:107–119.
Trnski, T., and T. M. Leis.
1991. A beginner's guide to illustrating fish larvae. *In* Larval biology (D.A. Hancock, ed.), p. 198–202. Australian Government Publishing Service. Bureau of Rural Resources Proceedings, Canberra, Australia.
Vigliola, L., and M. Harmelin-Vivien.
2001. Post-settlement ontogeny in three Mediterranean reef fishes of the genus *Diplodus*. Bull. Mar. Sci. 68:271–286.

NOAA
National Marine
Fisheries Service

Fishery Bulletin
established 1881

Spencer F. Baird
First U.S. Commissioner
of Fisheries and founder
of *Fishery Bulletin*

Modeling age and growth of the bigeye thresher (*Alopias superciliosus*) in the Atlantic Ocean

Joana Fernandez-Carvalho[1,2]
Rui Coelho (contact author)[1,2]
Karim Erzini[2]
Miguel N. Santos[1]

Email address for contact author: rpcoelho@ipma.pt

[1] Instituto Português do Mar e da Atmosfera (IPMA)
Avenida 5 de Outubro s/n
8700-305 Olhão, Portugal

[2] Centro de Ciências do Mar (CCMAR)
Universidade do Algarve, FCT Ed. 7
Campus de Gambelas
8005-139 Faro, Portugal

Abstract—The bigeye thresher (*Alopias superciliosus*) is a pelagic shark captured as bycatch in pelagic longline fisheries. Important information on its biology is still missing, especially from the Atlantic Ocean. In all, 546 vertebrae collected by fishery observers between 2007 and 2009 were used to estimate age and growth parameters for this species in the Atlantic Ocean. The size composition was 102–265 cm fork length (FL) for females and 94–260 cm FL for males. The estimated ages ranged from 0 to 25 years for both sexes. From the 5 growth models used, the 3-parameter von Bertalanffy growth model, reparameterized to estimate length at birth (L_0), produced the best results. The estimated parameters were asymptotic maximum length (L_{inf})=284 cm FL, growth coefficient (k)=0.06/year, and L_0=109 cm FL for females and L_{inf}=246 cm FL, k=0.09/year, and L_0=108 cm FL for males. Although differences between hemispheres indicate slower growth rates in the South Atlantic Ocean, these differences may also have been caused by the lower sample size and larger specimen sizes for the Southern Hemisphere. The estimated growth coefficients are among the lowest found for the Alopiidae, highlighting the bigeye thresher's slow growth and consequent low resilience to fishing pressure.

Manuscript submitted 5 September 2014.
Manuscript accepted 1 September 2015.
Fish. Bull. 113:468–481 (2015).
Online publication date: 22 September 2015.
doi: 10.7755/FB.113.9

The bigeye thresher (*Alopias superciliosus*) is a pelagic shark distinguished by its long, whiplike upper caudal lobe, large eyes, and deep horizontal grooves above the gills (Bigelow and Schroeder, 1948). It has a worldwide distribution in the Atlantic, Pacific, and Indian oceans and Mediterranean Sea, ranging from tropical to temperate regions in primarily oceanic epipelagic waters, but it sometimes approaches coastal waters (Stillwell and Casey, 1976; Compagno, 2001; Nakano et al., 2003; Weng and Block, 2004; Smith et al., 2008; Cao et al., 2011).

Like other members of the order Lamniformes, the bigeye thresher is an aplacental, viviparous species with intrauterine oophagy, bearing 2–4 pups per litter, resulting in an extremely low fecundity (Moreno and Morón, 1992; Gilmore, 1993; Chen et al., 1997; Compagno, 2001). This species has been described as having one of the lowest intrinsic rates of population increase among elasmobranchs, highlighting its high vulnerability to exploitation (Smith et al., 1998; Chen and Yuan, 2006; Cortés, 2008). According to the International Union for the Conservation of Nature (IUCN) Red List Criteria, this species is classified as "vulnerable" globally and "endangered" in the northwestern and western central Atlantic Ocean (Amorim et al., 2009). Furthermore, this species was classified as being at high risk in an ecological risk assessment of pelagic sharks caught in pelagic longlines in the Atlantic Ocean, highlighting the urgent need for better basic biological information on this shark (Cortés et al., 2010).

In the Atlantic Ocean, the pelagic longline fisheries that target swordfish (*Xiphias gladius*) also capture several species of pelagic sharks as bycatch (Moreno and Morón, 1992; Buencuerpo et al., 1998; Megalofonou et al., 2005; Coelho et al., 2012). Bycatch of bigeye thresher by these fisheries has been estimated at around 0.2% of the total shark bycatch for the entire Atlantic Ocean (Mejuto et al., 2009). The International Commission for the Conservation of Atlantic Tunas (ICCAT), responsible for the management of

bigeye thresher in the Atlantic Ocean, recently prohibited the retention and commercialization of bigeye thresher caught in tuna fisheries, recommending the release of live specimens when they are accidentally captured and requiring that both incidental catches and live releases be recorded in accordance with ICCAT data reporting requirements (ICCAT[1]). However, simply releasing caught specimens may not be enough to protect this species because 51% of bigeye thresher that are caught in the pelagic swordfish longline fishery have been estimated to have been released dead (Coelho et al., 2012).

Although pelagic sharks are affected by fishing, they remain among the least studied elasmobranchs because of their highly migratory nature and because the lack of information on these species poses particular difficulties for their management and conservation (Pikitch et al., 2008). Knowledge of the life history of a species is essential for successful management of that species. In particular, age and growth studies provide information for estimating important biological variables, such as growth rates, natural mortality, productivity, and longevity of a species (Campana, 2001; Goldman, 2004, Goldman et al., 2012). Understanding these biological parameters is important for assessment of the current status of shark populations and for prediction of how their population size and structure may change over time (Goldman et al., 2012). In fact, it is crucial that age determinations be precise and accurate because an erroneous understanding of the population dynamics of a species may lead to serious bias in stock assessment, bias that frequently results in overexploitation (Goldman et al., 2012).

Because elasmobranch species are characterized by slow growth rates (e.g., Coelho and Erzini, 2002) and a low reproductive potential (e.g., Coelho and Erzini, 2006), they are extremely vulnerable to fishing pressure, and overexploitation occurs with even relatively low levels of fishing-induced mortality (Smith et al., 1998). Therefore, study of their life history, including age and growth, is more critical than it is for more resilient species (Goldman et al., 2012).

In most age and growth studies of teleost fishes, otoliths or scales are used; however, vertebrae are the most widely used structures for age determination in elasmobranch fishes, but dorsal spines (usually in Squalidae) and caudal thorns (in skates) have also been used (Campana, 2001; Caillet and Goldman, 2004, Goldman, 2004; Coelho and Erzini, 2007; Moura et al., 2007; Coelho and Erzini, 2008). In general, an annual vertebral growth ring is composed of one opaque band (representing faster summer growth) and one translucent band (representing winter growth), although the periodicity of deposition may be different for some elasmobranchs (Cailliet and Goldman, 2004; Caillet et al., 2006). It should be noted that the opacity and translucency of these bands varies depending on the light source used (transmitted versus reflected) and method of preparation of the vertebrae (Goldman et al., 2012). Because the pattern of calcification can vary greatly within and among taxonomic groups of elasmobranchs, a species-specific approach is necessary for studies of their age and growth; it cannot be assumed that the banding pattern of one species is representative of another (Ridewood, 1921; Goldman, 2004).

In the case of bigeye thresher, little biological information is currently available, especially for this species in the Atlantic Ocean, probably because of its low prevalence numbers in longline catches (Mejuto and Garcés[2]; Mejuto[3]; Castro et al., 2000; Berrondo et al., 2007; Mejuto et al., 2009). Gruber and Compagno (1981) explored the age and growth of this species on the basis of a limited data set of mostly museum specimens captured in the Pacific and Atlantic oceans. Fernandez-Carvalho et al. (2011) estimated growth parameters for a specific region of the tropical northeastern Atlantic Ocean. Mancini (2005) studied the age and growth of bigeye thresher caught by longliners in the southwestern coast of Brazil. In the Pacific Ocean, an extensive age and growth study was carried out by Liu et al. (1998) in the western central Pacific region (Taiwan). In addition, some reproductive parameters have been reported for the Pacific Ocean (Gruber and Compagno, 1981; Gilmore, 1993; Chen et al., 1997) and Atlantic Ocean (Moreno and Morón, 1992; Mancini, 2005). The objective of this study was to improve the biological information for bigeye thresher by providing new knowledge about the age and growth parameters for this species throughout the Atlantic Ocean.

Materials and methods

Sampling and processing

All samples were collected by fishery observers, from the Portuguese Institute for the Ocean and Atmosphere onboard Portuguese commercial longline vessels that targeted swordfish in the Atlantic Ocean. Vertebral samples were collected only from bigeye thresher specimens that were retrieved already dead when the longline was hauled aboard. From September 2007 to December 2009, vertebral samples from 546 shark were collected throughout the Atlantic Ocean, between latitudes 38°N and 35°S (Fig. 1). Some of these samples

[1] ICCAT (International Commission for the Conservation of Atlantic Tunas). 2009. Recommendation by ICCAT on the conservation of thresher sharks caught in association with fisheries in the ICCAT convention area. ICCAT Recommandation 09-07, 1 p. [Available at website.]

[2] Mejuto, J., and A. G. Garcés. 1984. Shortfin mako, *Isurus oxyrinchus*, and porbeagle, *Lamna nasus*, associated with longline swordfish fishery in NW and N Spain. ICES Council Meeting (C.M.) Documents 1984/G:72, 10 p.

[3] Mejuto, J. 1985. Associated catches of sharks, *Prionace glauca*, *Isurus oxyrinchus*, and *Lamna nasus*, with NW and N Spanish swordfish fishery, in 1984. ICES Council Meeting (C.M.) Documents 1985/H:42, 16 p.

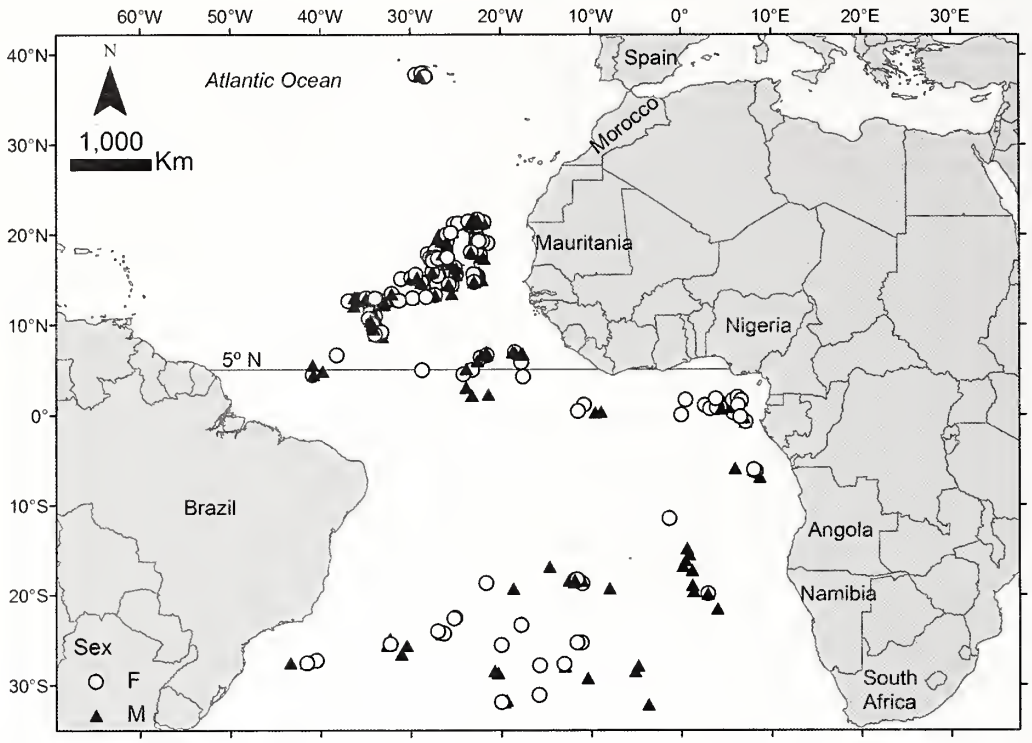

Figure 1

Locations where the vertebrae of bigeye thresher (*Alopias superciliosus*) were collected between September 2007 and December 2009 for use in estimation of the age and growth of this species in the Atlantic Ocean. Open circles represent females and black triangles indicate males. The horizontal line at 5°N represents the parallel used by the International Commission for the Conservation of Atlantic Tunas (ICCAT) to separate the stocks in the Southern and Northern Hemispheres and was, therefore, also used in this study as the boundary between samples of the North and South Atlantic Ocean.

(n=117) were used by Fernandez-Carvalho et al. (2011) to estimate initial growth curves, and a relationship between size of specimen and size of vertebrae, for the region of the Cape Verde Archipelago in the tropical northeastern Atlantic Ocean. These samples from the Cape Verde Archipelago were also included in this study (and used as a reference set to model the growth of this species for a wider area in the Atlantic Ocean) because the readers were the same, our sample size was small, and because it was desirable to increase our sample area.

The sexes of specimens were determined and fork lengths (FLs) measured in a straight line (in centimeters) onboard ship. A section of vertebrae was removed from the area below the anterior part of the first dorsal fin. Each of these samples was kept frozen on the vessel and during land transport until it was processed in the laboratory. One vertebra was removed from each sample and processed by following the method described in detail in Fernandez-Carvalho et al. (2011). First, scalpels were used to remove the soft tissue, and then the vertebrae were immersed in a solution of 4–6% sodium hypochlorite (commercial bleach) for 10–20 min, depending on the size of the vertebrae. The vertebrae were mounted on a microscopic slide with either thermoplastic cement or a synthetic polymer glue and sectioned sagittally with a Buehler[4] (Lake Bluff, IL) low-speed saw, with 2 blades spaced approximately 0.5 mm apart. For a better visualization of the growth band pairs, the sections were stained with crystal violet solution (Sigma-Aldrich Co., St. Louis, MO) for 5–15 min depending on the size of the vertebrae (Fig. 2). Once dried, the sections were mounted onto microscope slides with Cytoseal 60 (Thermo Fisher Scientific Inc., Waltham, MA). Finally, growth bands were examined under a dissecting microscope with transmitted white light.

Age estimation and comparison of age readings

A preliminary reading of a reference set (n=117) of vertebrae (from the full set of 546 vertebrae) was completed to familiarize the readers with the banding pattern of this species. Then, this reference set was independently read by 2 readers 3 times to maintain quality control and precision of the readings (see Fernandez-

[4] Mention of trade names or commercial companies is for identification purposes only and does not imply endorsement by the authors or the National Marine Fisheries Service, NOAA.

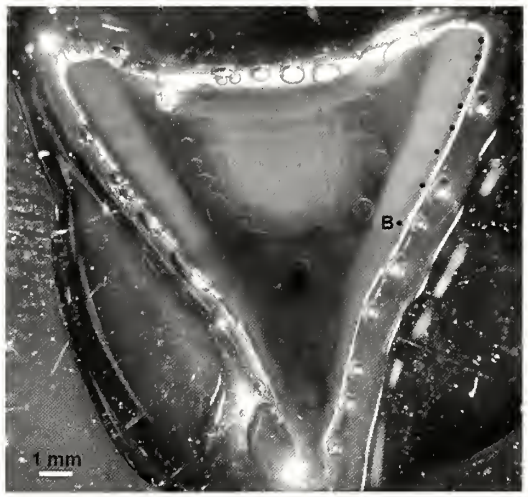

Figure 2

Image of a vertebral section of a vertebra from a female bigeye thresher (*Alopias superciliosus*) with a fork length of 170 cm and with 8 visible growth bands (B=birth mark). The specimen was collected in 2008 as part of this study to estimate the age and growth of this species in the Atlantic Ocean.

Carvalho et al., 2011). To prevent bias in counting bands, the 2 readers had no knowledge of the length or sex of each shark. After that step, the remaining samples (n=429) were then read 3 times by the primary reader (J. Fernandez-Carvalho), and only those vertebrae with band counts that were the same for at least 2 of the 3 readings were accepted for the age and growth analysis. To prevent reader familiarity with any particular vertebrae, each reader completed the first or second readings of each set of vertebrae (n=117 or 429 before starting the second or third readings. The temporal periodicity of band formation was assumed to be annual, although this notion was not validated (see the *Discussion* section).

To compare the aging precision between the 3 readings, both the coefficient of variation (CV) (Chang, 1982) and the average percent error (APE) (Beamish and Fournier, 1981) were calculated and compared. The percentage of agreement (PA) and percentage of agreement within one growth band (PA ±1 year) among the readings were also calculated. Age-bias plots, where the mean (with 95% confidence interval [CI]) of the reading thought to be less accurate is plotted for each distinct age from the reading thought to be more accurate (reading 3), were used to graphically assess the precision of aging between the 3 readings (Campana, 2001).

Furthermore, contingency tables and 2 chi-square tests of symmetry (McNemar and Evans and Hoenig tests) were used to test the null hypothesis that the readings are interchangeable versus the alternative that there are systematic differences between the readings (Hoening et al., 1995; Evans and Hoenig, 1998). The McNemar test is a "maximally pooled" test of symmetry where all squared differences of the values of the contingency table on each size of the diagonal are added and that result is divided by the sum of the values on each size of the diagonal; the Evans and Hoenig method is a diagonally projected test of symmetry, in which the values are summed along a series of diagonal cells that project outward from the central diagonal (Hoening et al., 1995; Evans and Hoenig, 1998). In addition, the symmetry of all 3 readings was tested simultaneously by plotting triplets of readings on a hexagon plot (Evans and Hoenig, 1998). All symmetry analysis was carried out by using R statistical software, vers. 3.0.1 (R Core Team, 2013), with the package "fishmethods" (Nelson, 2013). The hexagon plots for the triplets of readings were created and interpreted with R code provided by J. Hoenig (Hoenig[5]).

Growth modeling

Five growth models were used and compared in order to describe the growth of this species: 3 variations of the von Bertalanffy growth function (VBGF) and 2 versions of the Gompertz growth function (GGF). The VBGF variations were 1) a reparameterisation of the 3-parameter VBGF to estimate size at birth (L_0) instead of theoretical length at age 0 (t_0) as suggested by Cailliet et al. (2006), 2) a modified 2-parameter VBGF that used a known and fixed L_0, and 3) a generalized VBGF with 4 parameters.

For the 3-parameter VBGF model derived to estimate L_0, the following equation was used:

$$L_t = L_{\text{inf}} - (L_{\text{inf}} - L_0)e^{-kt}, \quad (1)$$

where L_t = mean length at age t;
L_{inf} = asymptotic maximum length;
k = the growth coefficient; and
L_0 = length at birth.

For the modified 2-parameter VBGF model with a fixed L_0, the following equation was used:

$$L_t = L_{\text{inf}}(1 - be^{-kt}), \quad (2)$$

where b was calculated with the equation immediately below:

$$b = (L_{\text{inf}} - L_0)/L_{\text{inf}}, \quad (3)$$

For the latter model, a fixed value of 84 cm FL was used for L_0. This value was chosen to be equivalent to a range of total lengths (TL) of 135–140 cm, the size estimated for this species at birth by Chen et al. (1997). This value is comparable with the smallest sizes of free-swimming bigeye thresher reported to date (130 cm TL, Bigelow and Shroeder, 1948; 155 cm TL, Still-

[5] Hoenig, J. M. 2014. Personal commun. Dep. Fish. Sci., Virginia Inst. Mar. Sci., Gloucester Point, VA 23062

well and Casey, 1976; 159 cm TL, Gruber and Compagno, 1981; 156 cm TL, Moreno and Morón, 1992). The mean value of this range (135 to 140 cm TL) was converted to FL (84 cm FL) by using this equation (n=390; coefficient of multiple determination [R^2]=0.92; standard error of the intercept=2.41; standard error of the slope=0.01; regression analysis of variance: F=4675; P<0.01) (see Fernandez-Carvalho et al., 2011):

$$FL = 0.58\ TL + 4.83. \quad (4)$$

The generalized VBGF with 4 parameters was defined by Richards (1959) with the following equation:

$$L_t = L_{\inf}((1-e(-k(1-m)(t-t_0)))^{(1/1-m)}, \quad (5)$$

where t_0 = the theoretical age at zero length; and
m is the fitted fourth function parameter.

Two versions of the GGF (Ricker, 1975) were fitted, one with 3 parameters and the other with 2 parameters and a fixed L_0. The same value of L_0 that was used in the 2-parameter VBGF model (84 cm FL) was used in the second GGF model:

$$L_t = L_0 e^{G[1-e(-kt)]}, \quad (6)$$

where G = the instantaneous rate of growth at time t;
L_t = the mean length at age t;
k = the rate of decrease in G; and
L_0 = length at birth.

The size distribution of the sample was plotted and analyzed in R with ggplot2 (Wickham, 2009). All but 1 of the 5 growth models were fitted in R, by using nonlinear least squares with the Gauss-Newton algorithm (nls function in R). The generalized VBGF model was fitted through the use of nonlinear least squares with a grid-search technique (package nls2; Grothendieck, 2013). For each model, the mean values of parameters were estimated, and the standard errors and 95% CIs of those estimates were calculated. Furthermore, model goodness-of-fit was assessed with the Akaike information criterion (AIC) and the Bayesian information criterion values. A likelihood ratio test (LRT), as defined by Kimura (1980) and recommended by Cerrato (1990), was used to test the null hypothesis that there is no difference in growth parameters between males and females for the bigeye thresher. The growth parameters of the samples from the North and South Atlantic Ocean were also compared. For the purposes of this analysis, the samples from the 2 hemispheres were separated on the basis of the 5°N parallel, as recommended in the ICCAT manual for shark species (ICCAT[6]).

[6] ICCAT (International Commission for the Conservation of Atlantic Tunas). 2013. ICCAT Manual. [Online publication under development]. [Available at website, accessed January 2014.]

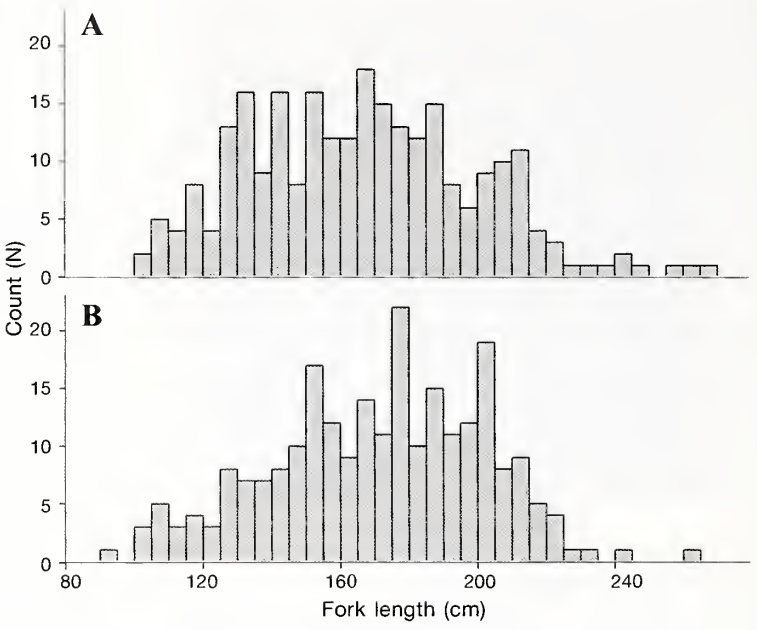

Figure 3

Length-frequency distributions of the (**A**) female and (**B**) male bigeye thresher (*Alopias superciliosus*) collected between 2007 and 2009 and used to estimate the age and growth of this species in the Atlantic Ocean. These histograms show size classes by increments of 5 cm in fork length.

Results

Samples

Of the 546 vertebrae of bigeye thresher, 501 were used for the age and growth analysis because they had at least 2 identical readings. From these samples, 258 vertebrae were from females (52%) and 241 vertebrae were from males (48%); the sex of 2 specimens could not be determined. The size distribution used in this study ranged from 102 to 265 cm FL for females (mean: 165.7 cm FL [standard deviation (SD)] 32.8) and from 94 to 260 cm FL for males (mean: 170.2 cm FL [SD 30.9]) (Fig. 3).

The sample size for vertebrae of bigeye thresher that were collected in the North Atlantic Ocean was 358 (200 from females and 158 from males), and the size distribution ranged from 94 to 242 cm FL (mean: 159.3 cm FL [SD 29.9]). The sample size for vertebrae that were collected in the South Atlantic Ocean was 141 (58 from females and 83 from males), and size distribution ranged from 128 to 260 cm FL (mean: 189.5 cm FL [SD 26.2]).

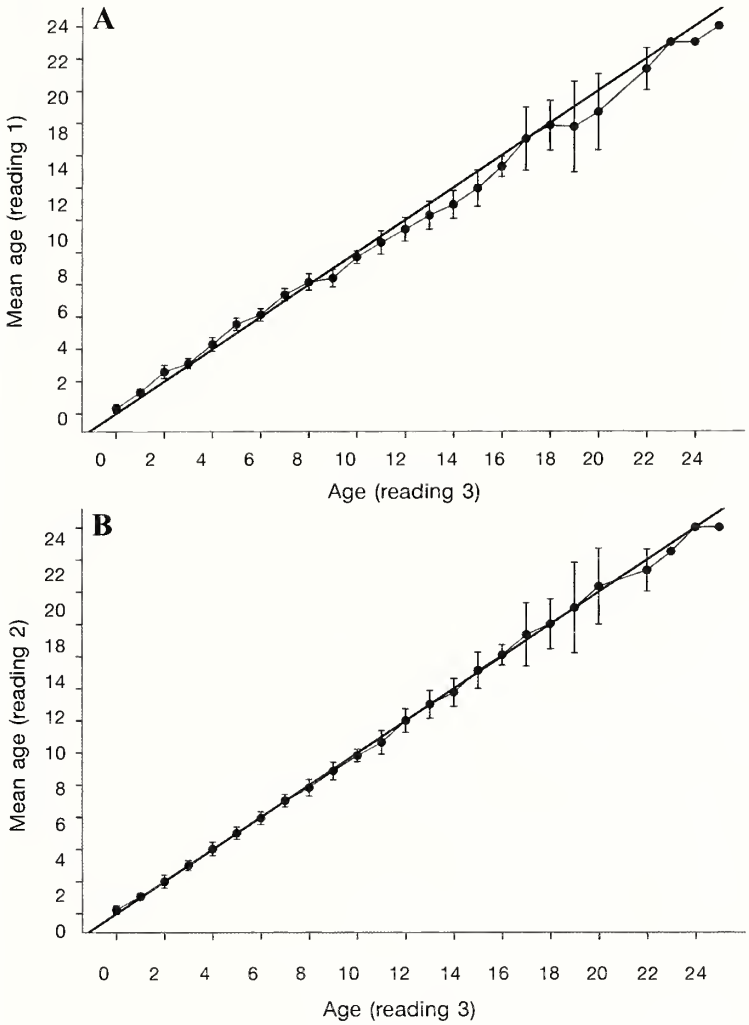

Figure 4

Age-bias plots of pairwise comparisons of mean ages for the 3 readings by the primary reader: (**A**) reading 1 versus reading 2 and (**B**) reading 2 versus reading 3. The readings were based on an examination of vertebrae taken from bigeye thresher (*Alopias superciliosus*) collected between 2007 and 2009 and used to estimate the age and growth of this species in the Atlantic Ocean.

Age estimation and comparison of age readings

Although the vertebrae of bigeye thresher were in general difficult to read, the birth band was easily identifiable because it coincides with an angle change in the *corpus calcareum* of vertebrae (Goldman and Musick, 2005). A high degree of agreement over time was observed between the 3 readings of the primary reader, with the PA between the first and second, first and third, and second and third readings being 46%, 43% and 87%, respectively. Of the vertebrae examined, 91.8% had at least 2 identical readings (94.4% within one growth band) and, therefore, were accepted for growth modeling. The CV between the 3 readings of the primary reader was 10%, and the APE was 7.7%. In a graphical comparison with age-bias plots, a high agreement with no systematic bias was observed between the first 2 readings and the last reading of the primary reader (Fig. 4). The chi-square tests of symmetry showed little evidence of systematic differences between these readings, and only one test indicated marginally significant differences (McNemar test of readings 2 and 3: χ^2=4, df=1, P=0.046) (Table 1).

In the hexagon plot (Fig. 5), 3 axes correspond with readings 1, 2, and 3. If all 3 readings are the same, the triplet is plotted in the center, regardless of the reading values (e.g., 1,1,1 or 3,3,3). If 2 of the readings agree, the observation will fall along one of the axis lines; for example, a reading of 3,3,5 will fall along the line where readings 1 and 2 agree, and the point will be 2 units away from the center (because the observation that disagrees is 2 values higher than the readings that agree). Similarly, a reading of 6,6,8 will fall on top of the reading of 3,3,5. If all 3 readings are equivalent (i.e., interchangeable), then there would be an overall symmetry. That is, each triangle would have the same number of observations, and the 6 rays from the center outward would have the same number of observations (except for discrepancies solely due to sampling error).

The hexagon plot developed in this study shows that most of the observations fell on the A axis (the horizontal line) (Fig. 5). This placement of observations in the plot corresponds with the second reading (B) equaling the third reading (C) and with the first reading (A) being more variable than the other 2 readings. However, the tests of symmetry did not reveal significant differences that would have supported systematic changes in the readings over time toward higher or lower values (i.e., the aging criteria remained stable). As time passed, the primary reader's readings showed less variability but did not change systematically because there was little evidence of differences between the readings from causes other than random error.

Growth modeling

The ages estimated in this study ranged from 0 (young of the year) to 25 years for both sexes. Of the 5 growth models used, the generalized VBGF with 4 parameters was the only model that did not converge, even when the grid-search technique (with the starting values

Table 1

Results from the 2 forms of chi-square (χ^2) tests of symmetry used to compare and detect nonrandom differences between the 3 sets of age readings of bigeye thresher (*Alopias superciliosus*), the McNemar maximally pooled method and the Evans and Hoenig method that pools along diagonals (Hoening et al., 1995; Evans and Hoenig, 1998). The vertebrae were collected in the Atlantic Ocean between September 2007 and December 2009.

	McNemar		Evans and Hoenig		
Readings	χ^2	P	χ^2	df	P
Reading 1 vs. reading 2	0.03	0.85	3.18	7	0.87
Reading 1 vs. reading 3	0.51	0.47	3.98	7	0.78
Reading 2 vs. reading 3	4.00	0.05	8.49	5	0.13

varying between a range of possible values) was used. The growth parameters obtained from the regular 3-parameter VBGF model were considered best for describing the growth of this species for both sexes. This designation was decided on the basis of both the statistical goodness-of-fit of this model and because the estimated biological parameters obtained seemed realistic. When this VBGF model was used, the estimated L_{inf} values were always higher and the k values were lower than those values obtained from the VBGF model with a fixed L_0, for both females (L_{inf}=284.2 cm FL, k=0.06/year) and males (L_{inf}=245.6 cm FL, k= 0.09/year) (Table 2; Fig. 6). When the GGF models were used, a similar pattern was found, with the GGF producing lower k values for both sexes than the values obtained from the GGF model with a fixed L_0.

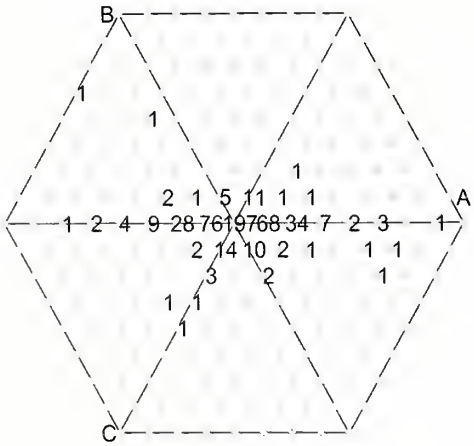

Figure 5

Hexagon plot used to test the symmetry of the 3 readings of growth bands in vertebrae taken from bigeye thresher (*Alopias superciliosus*) collected between 2007 and 2009 and used to estimate the age and growth of this species in the Atlantic Ocean. The 3 axes correspond to the first reading (A), second reading (B), and third reading (C). The numbers refer to the number of triplets at each location on the plot, and all possible locations are represented as gray circles.

With the LRT tests (Kimura, 1980), significant differences were found between sexes in all the estimated VBGF parameters, except for the L_0 (L_{inf} LRT: χ^2=6.08, df=1, P<0.05; k LRT: χ^2=4.13, df=1, P<0.05; L_0 LRT: χ^2=1.66, df=1, P>0.05; combined parameters LRT: χ^2=9.69, df=3, P<0.05). For all models, k values were lower and L_{inf} values were higher for females than for males.

When we compared the growth of bigeye thresher between the 2 hemispheres (North and South Atlantic Ocean), only the 2-parameter VBGF model with a fixed L_0 converged for the separate sexes in each hemisphere and the traditional VBGF model converged for the North Atlantic Ocean but not for the South Atlantic Ocean. Therefore, the VBGF model with a fixed L_0 was used to obtain and compare the growth parameters for the 2 hemispheres (Table 3). The overlaps in the 95% CIs of the parameters were used for this comparison. There was no overlapping of the 95% CIs between the North and South Atlantic Ocean, with the exception of a slight overlap in the L_{inf} for males. For both sexes, the L_{inf} was higher for the South Atlantic Ocean than for the North Atlantic Ocean and the estimated k values were higher for the North Atlantic Ocean ($k_{females}$=0.16 [95% CI 0.14, 0.18]; k_{males}=0.18 [CI 0.15, 0.21]) than for the South Atlantic Ocean ($k_{females}$=0.09 [CI 0.07, 0.11]; k_{males}=0.13 [CI 0.11, 0.15]).

Discussion

Several approaches were used in this study to evaluate the precision of age estimates and to test for bias in the age determinations of bigeye thresher, as suggested by Goldman et al. (2012): PA, PA ±1 year, APE, CV, age-bias plots, and tests of symmetry. To our knowledge, this study is the first to test the symmetry of 3

Table 2

Estimated means for growth parameters of bigeye thresher (*Alopias superciliosus*) collected from the Atlantic Ocean between 2007 and 2009, obtained with the regular 3-parameter von Bertalanffy growth function (VBGF) model, the VBGF model with a fixed size at birth (L_0), the 3-parameter Gompertz growth function (GGF) model, and the GGF model with a fixed L_0 (L_0=84 cm in fork length). For each model, the estimated means for parameters, including asymptotic maximum length (L_{inf}), growth coefficient (k), size at birth (L_0), and instantaneous rate of growth (G), are given with their respective standard errors (SE) and 95% confidence intervals (CIs). The Akaike information criterion (AIC) and Bayesian information criterion (BIC) values are given for a comparison of models within each sex group.

							95% CI	
Sex	Model	AIC	BIC	Parameter	Mean	SE	Lower	Upper
Sexes combined				L_{inf}	263.50	7.516	248.75	278.28
	VBGF	3827.1	3843.9	k	0.07	0.006	0.06	0.08
				L_0	108.80	1.623	105.63	112.01
	VBGF fixed L_0	3984.0	3996.6	L_{inf}	224.70	2.513	219.72	229.59
				k	0.14	0.005	0.13	0.15
				G	0.80	0.016	0.77	0.83
	GGF	3837.1	3854.0	k	0.11	0.007	0.09	0.12
				L_0	110.90	1.494	107.91	113.79
	GGF fixed L_0	4042.2	4054.8	G	0.94	0.009	0.92	0.96
				k	0.22	0.006	0.20	0.23
Males				L_{inf}	245.60	7.535	230.73	260.42
	VBGF	1831.0	1845	K	0.09	0.009	0.07	0.10
				L_0	108.50	2.306	103.91	113.00
	VBGF Fixed L_0	1908.8	1919.2	L_{inf}	218.10	3.077	211.99	224.11
				K	0.16	0.008	0.14	0.18
				G	0.75	0.020	0.71	0.79
	GGF	1835.4	1849.4	K	0.12	0.010	0.10	0.14
				L_0	110.30	2.143	106.10	114.55
	GGF fixed L_0	1936.2	1946.6	G	0.92	0.011	0.90	0.94
				K	0.23	0.009	0.21	0.25
Females				L_{inf}	284.20	14.430	255.76	312.60
	VBGF	1993.3	2007.5	k	0.06	0.008	0.04	0.08
				L_0	109.00	2.249	104.61	113.47
	VBGF fixed L_0	2073.7	2084.3	L_{inf}	231.90	4.037	223.99	239.89
				k	0.13	0.007	0.12	0.15
				G	0.86	0.027	0.80	0.91
	GGF	1998.5	2012.8	k	0.10	0.009	0.08	0.11
				L_0	111.20	47.000	107.20	115.27
	GGF fixed L_0	2105.9	2116.5	G	0.96	0.014	0.94	0.99
				k	0.20	0.008	0.19	0.22

age counts by using a hexagon plot, as described by Evans and Hoenig (1998). The values obtained in this study, together with the results of the age-bias and symmetry plots, indicate that our age estimates are consistent and adequate for this species.

It was not possible to objectively determine marginal growth increments because of the morphological structure of the vertebrae of bigeye thresher; these vertebrae were very difficult to read as a result of the narrow and faint bands at their edges. Few studies on the age and growth of alopiid sharks exist, and of these the majority of studies have focused on the Pacific Ocean (bigeye thresher: Liu et al., 1998; common thresher shark (*A. vulpinus*): Cailliet and Bedford, 1983; Smith et al., 2008; and pelagic thresher (*A. pelagicus*): Liu et al., 1999), only 2 studies have been conducted within the North Atlantic Ocean (bigeye thresher: Fernandez-Carvalho et al., 2011; common thresher shark: Gervelis and Natanson, 2013), and 1 study in the South Atlantic Ocean (bigeye thresher: Mancini, 2005).

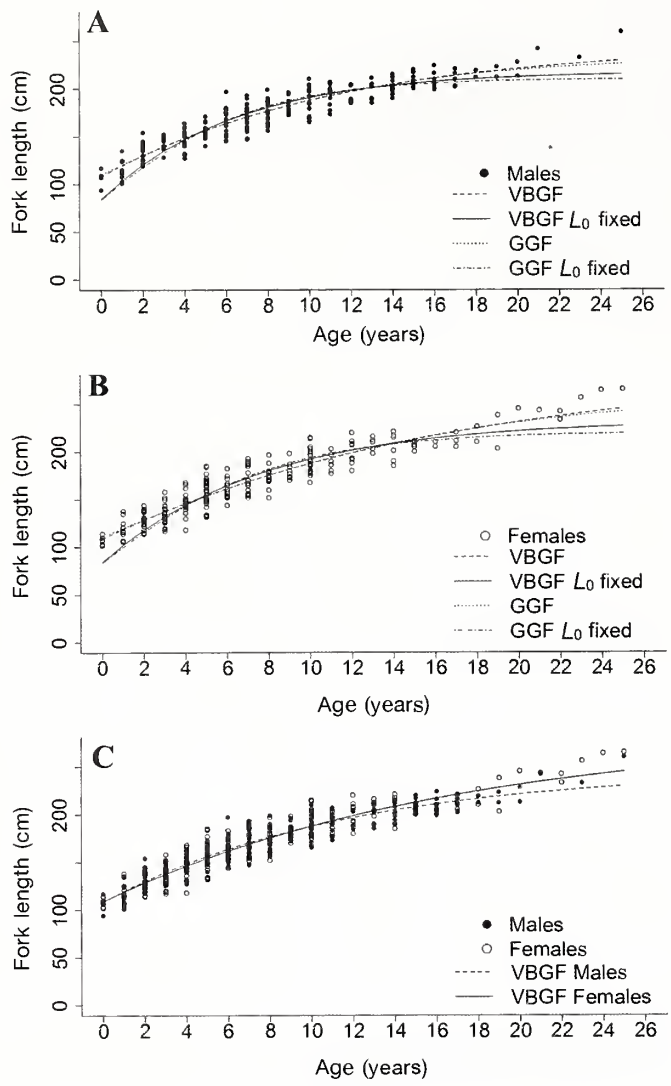

Figure 6

Growth curves estimated for (**A**) male and (**B**) female bigeye thresher (*Alopias superciliosus*), collected between 2007 and 2009 in the Atlantic Ocean by using models fitted with data from readings of vertebrae. Results are presented for the regular 3-parameter von Bertalanffy growth function (VBGF) model reparameterized to estimate size at birth (L_0), the VBGF model with a fixed L_0, the 3-parameter Gompertz growth function (GGF) model, and the GGF model with a fixed L_0 (L_0=84 cm in fork length). The bottom panel (**C**) shows the growth curve estimated with the regular VBGF model, which was selected on the basis of the statistical goodness-of-fit as the best model for describing the growth of this species for both males and females and highlighting the differences in growth between the sexes.

Of these studies, only in 3 of them was age verification attempted and in none of them was age validation attempted. Liu et al. (1998) verified a periodicity of one band (composed of one opaque ring and one hyaline ring) per year in bigeye thresher, and Liu et al. (1999) verified the same pattern for the pelagic thresher, in both cases using marginal increment analysis for populations of the northwestern Pacific Ocean. In the Atlantic Ocean, Mancini (2005) attempted marginal increment analysis and centrum edge analysis that weakly supported annual growth-band formation. Also in the Atlantic Ocean, preliminary centrum edge analysis (with limited samples from 6 months of each year) was conducted for bigeye thresher, also indicating a seasonal pattern in band formation (Fernandez-Carvalho et al., 2011). Therefore, although no age verification or validation was carried out in the study presented here, the assumption of a one-band-per-year periodicity for this species is reasonable in light of the few available studies.

Furthermore, in age and growth studies of other species of lamniform sharks an annual band deposition has been validated. Natanson et al. (2002), who used vertebrae from recaptured oxytetracycline-injected porbeagle (*Lamna nasus*), proposed that vertebral band pairs are deposited annually. On the other hand, Francis et al. (2007), when performing bomb radiocarbon assays, found that the ages of older porbeagle (>20 years) were underestimated from vertebral band counts, indicating that in some long-lived shark species, after a certain age, either growth bands are deposited on vertebrae in extremely narrow increments (and are impossible to recognize) or vertebrae cease to grow altogether. Nevertheless, Campana et al. (2002) and Francis et al. (2007) found that it was possible to validate that the visible growth bands were formed annually, with no gaps, for the first 20 years of life in porbeagle.

The same periodicity of one band per year was validated for the shortfin mako (*Isurus oxyrinchus*), both by bomb carbon chronology and by oxytetracycline marking (Ardizzone et al., 2006; Natanson et al., 2006). Finally, Wintner and Cliff (1999) stated that, although they could not determine band periodicity by using marginal increment analysis in the white shark (*Carcharodon carcharias*) off the coast of South Africa, annual deposition was indicated for one specimen that had been tagged with oxytetracycline and recaptured. More recently, Hamady et al. (2014), using bomb radiocarbon, also observed deposition of one band pair per year for white shark from the northwestern Atlantic Ocean up to 44 years old. On the other hand, Hamady et al. (2014) and Andrews and Kerr (2015) suggested that some age underestimation for older white shark resulted from change in the rate of deposition of vertebral material or from the narrowing of the growth bands to the point of becoming unreadable.

Therefore, there is a growing body of evidence that annual banding counts of growth bands in shark vertebrae may not provide an accurate estimate of maximum age, given that long-lived sharks can become con-

Table 3

Estimated means of growth parameters for bigeye thresher (*Alopias superciliosus*) collected from the North and South Atlantic Ocean between 2007 and 2009, obtained with the VBGF model with a fixed size at birth (L_0=84 cm in fork length [FL]). For the models for each sex and region, the parameter means are given with their respective standard errors (SE) and 95% confidence intervals (CIs). L_{inf}=asymptotic maximum length, given in FL; k=growth coefficient per year.

					95% CI	
Sex	Atlantic	Parameter	Estimate	SE	Lower	Upper
Males	North	L_{inf}	211.77	4.64	202.62	220.93
		k	0.18	0.01	0.15	0.21
	South	L_{inf}	229.00	5.10	218.85	239.15
		k	0.13	0.01	0.11	0.15
Females	North	L_{inf}	219.20	4.34	210.64	227.77
		k	0.16	0.01	0.14	0.18
	South	L_{inf}	265.70	11.34	243.01	288.43
		k	0.09	0.01	0.07	0.11

siderably older than the age at which band counting is no longer possible for aging (Francis et al., 2007; Andrews et al., 2011; Hamady et al., 2014; Passerotti et al., 2014; Andrews and Kerr, 2015). Underestimation of longevity may cause little change in the estimation of growth parameters, but the life-time reproductive productivity of long-lived sharks would be greater (Passerotti et al., 2014). Despite the lack of validation for bigeye thresher in this study, the growth data presented are the most comprehensive age estimates for this species for the North and South Atlantic Ocean and, as such, are an important contribution to our understanding of the biology of this species. Nonetheless, it should be noted that these estimates should be used with caution for stock assessment and management decisions until a definitive age validation is accomplished.

In this study, all growth parameters estimated with the 4 growth models that converged had biologically reasonable values. The differences between the AIC values of the VBGF model with the lowest AIC (3-parameter VBGF model) and the 3-parameter GGF for both sexes were small ($\Delta_{AIC\ males}$=4.4; $\Delta_{AIC\ females}$=5.2), but the differences between the VBGF model with the lowest AIC and both the VBGF and GGF models with a fixed L_0 were high (>10); therefore, these models with a fixed L_0 should be discarded, as suggested by Katsanevakis (2006). Nevertheless, it should be noted that when considering VBGF and GGF models with a fixed L_0, different authors give different values for size at birth (e.g., Bass et al., 1975; Moreno and Morón, 1992; Gilmore, 1993) and that changing this value will affect the estimation of the other parameters (Pardo et al., 2013). On the other hand, although the GGF models also produced realistic growth parameters, this growth function has been described as better suited for batoids (or elasmobranchs that hatch from eggs), for which volume increases more with age than with length (e.g., Myliobatiformes) (Goldman et al., 2012). Because the growth parameters obtained by the 3-parameter VBGF model had the best statistical fit and seemed to be biologically realistic, we recommend its use for describing the growth of bigeye thresher.

To our knowledge, this study is the first comprehensive one for the age and growth of bigeye thresher, covering both the North and South Atlantic Ocean. Initial growth curves have been produced by Fernandez-Carvalho et al. (2011) for the region of the Cape Verde Archipelago in the tropical northeastern Atlantic Ocean. Because the sample size and coverage area in that study were relatively small, these samples collected in Cape Verde Archipelago have been included in the study described in this article. In comparisons of the parameters from our most recent study with our previous estimates for the Cape Verde region, the main differences were observed among Males; among females, the growth parameters were similar (Table 4). The k value obtained in this study for males (k=0.09/year) was lower than our first estimate (k=0.18/year), and the L_{inf} of 245.6 cm FL for this study was higher than the L_{inf} of 206.0 cm FL for just the Cape Verde region.

The growth parameters obtained in this study are comparable with those parameters generated by Liu et al. (1998) for the population in the northwestern Pacific Ocean and by Mancini (2005) for the southwestern Atlantic Ocean—with some differences. Females in our study grew to a larger size (L_{inf}=284.2 cm FL) but did so at a slower rate (k=0.06/year) than did the females in the study in the northwestern Pacific Ocean (L_{inf}=241.7 cm FL, k=0.09/year) (Table 4). On the other hand, males sampled in our study grew to a slightly larger size (L_{inf}=245.6 cm FL) but did so at a rate similar to that of males described for the northwestern Pacific Ocean (L_{inf}=235.5 cm FL, k=0.09/year) (Table 4). Mancini (2005) presented L_{inf} values higher than those of

Table 4

Comparison of von Bertalanffy growth function (VBGF) parameters from studies (carried out worldwide) of age and growth of species of *Alopias* : bigeye thresher (*A. superciliosus*), common thresher shark (*A. vulpinus*), and pelagic thresher (*A. pelagicus*). The parameters presented in this table are asymptotic maximum length (L_{inf}) and growth coefficient per year (k). An asterisk (*) indicates data for sexes combined, and 2 asterisks (**) indicate sizes in precaudal length. NA=values not available.

Study	Sex	Size range (FL, cm)	Sample size (n)	VBGF parameters		Max. obs age (y)	Region	Species
				L_{inf}	k			
This study	Males	94–260	241	245.6	0.09	25	Atlantic wide	*A. superciliosus*
	Females	102–265	258	284.2	0.06	25		
Fernandez-Carvalho et al. (2011)[1]	Males	101–210	42	206.0	0.18	17	NE Tropical Atlantic	*A. superciliosus*
	Females	115–242	73	293.0	0.06	22		
Liu et al. (1998)[2]	Males	NA–213.5	214	235.5	0.09	20	NW Pacific (Taiwan)	*A. superciliosus*
	Females	NA–256.5	107	241.7	0.09	21		
Mancini (2005)[3]	Males	162–232	73	272	0.073	18	SW Atlantic	*A. superciliosus*
	Females	164–245	87	296	0.06	19		
Cailliet and Bedford (1983)[4]	Males	35.1–312.7*	143*	271.1	0.22	15*	NE Pacific (California/Oregon)	*A. vulpinus*
	Females			345.2	0.16			
Smith et al. (2008)[5]	Males	NA	83	229.7	0.19	19	NE Pacific (California/Oregon)	*A. vulpinus*
	Females	NA	129	253.9	0.12	22		
Gervelis and Natanson (2013)[6]	Males	56.3–264.4*	135	227.9	0.16	22	NW Atlantic (NE USA)	*A. vulpinus*
	Females		173	274.5	0.09	24		
Liu et al. (1999)[7]	Males	NA	323	182.2**	0.12	14	NW Pacific (Taiwan)	*A. pelagicus*
	Females	NA	508	197.2**	0.09	16		

[1] Fernandez-Carvalho, J., R. Coelho, K. Erzini, and M. N. Santos. 2011. Age and growth of the bigeye thresher shark, *Alopias superciliosus*, from the pelagic longline fisheries in the tropical northeastern Atlantic Ocean, determined by vertebral band counts. Aquat. Living Resour. 24:359–368.

[2] Liu, K.-M., P.-J. Chiang, and C.-T. Chen. 1998. Age and growth estimates of the bigeye thresher shark, *Alopias superciliosus*, in northeastern Taiwan waters. Fish. Bull. 96: 482–491.

[3] Mancini, P. L. 2005. Estudo Biológico-pesqueiro do tubarão-raposa, *Alopias superciliosus* (Lamniformes, Alopiidae) capturado no sudeste-sul do Brasil. M.S. thesis, 195 p. São Paulo State Univ., São Paulo, Brazil.

[4] Cailliet, G. M., and D. W. Bedford. 1983. The biology of three pelagic sharks from california waters, and their emerging fisheries: a review. CalCOFI Rep. 24:57–69.

[5] Smith, S. E., R. C. Rasmussen, D. A. Ramon, and G. M. Cailliet. 2008. The biology and ecology of thresher sharks (Alopiidae). *In* Sharks of the open ocean: biology, fisheries and conservation (M. D. Camhi, E. K. Pikitch, and E. A. Babcock, eds.), p. 60–68. Blackwell Publ., Oxford, UK.

[6] Gervelis, B. J., and L. J. Natanson. 2013. Age and growth of the common thresher shark in the western North Atlantic Ocean. Trans. Am. Fish. Soc. 142:1535–1545.

[7] Liu, K.-M., C.-T. Chen, T.-H. Liao, and S.-J. Joung. 1999. Age, growth, and reproduction of the pelagic thresher shark, *Alopias pelagicus* in the northwestern Pacific. Copeia 1999:68–74.

our estimates for both males and females (L_{inf}=272 and 296 cm FL) and similar k values for females (k=0.06/year) and slightly lower values for males (k=0.07/year). In age and growth studies, there is a high potential for bias in specimen sampling; therefore, these differences could be explained by the fact that our sample contained both female and male bigeye thresher of larger sizes and consequently of older ages than the males and females in the study in the northwestern Pacific Ocean (Liu et al., 1998).

The values of L_{inf} obtained in our study were close to the maximum sizes of bigeye thresher reported in the literature (Gruber and Compagno, 1981; Moreno and Morón, 1992; Liu et al., 1998; Mancini 2005). The k values obtained in our study (and by Mancini, 2005) for bigeye thresher are the lowest growth coefficients ever presented for this species and within the Alopiidae (Table 4), highlighting the slow growth pattern of this species and its consequent vulnerability to fishing pressure and mortality.

As has been described for other shark species, the growth of bigeye thresher was statistically different for males and females, with a lower k value and higher L_{inf} value observed for females than for males (e.g.,

Piercy et al., 2007; Coelho et al., 2011; Gervelis and Natanson, 2013). Therefore, it is advisable to use the growth parameters obtained specifically for each sex, instead of the parameters obtained for the sexes combined. The growth curves of both sexes were similar until age 10, after which males exhibited a considerable reduction in growth rate, and females showed a straighter growth curve.

Future studies of this species should include more samples from the South Atlantic Ocean, and especially of the smaller and larger length classes, because some difficulties occurred when comparing results for samples from the 2 hemispheres. These difficulties were due to not only the relatively smaller sample size for the Southern Hemisphere but also the fact that most samples from the North Atlantic Ocean were collected around the Cape Verde Archipelago, where the majority of the specimens tended to be small (size distribution: North Atlantic Ocean, 102–242 cm FL; South Atlantic Ocean, 128–265 cm FL). The differences observed in the growth of bigeye thresher samples from the North and South Atlantic Ocean, especially for females, indicate slower growth rates for the southern population. However, because this species seems to be segregated by size and sex, the differences in the VBGF parameters may also be caused by the possibility that we modeled 2 parts of the same population. The differences do not necessarily indicate the existence of 2 distinct populations. Future studies of this species should address the genetic structure and population delimitation in the Atlantic Ocean.

Accurate age information is vital for obtaining quality estimates of growth, which in turn are essential for successful and sustainable fisheries management. The growth parameters determined in this study and presented here are the first estimates for bigeye thresher that cover an extensive area in the Atlantic Ocean, and they now can be incorporated into stock assessment models to improve science-based fishery management and conservation initiatives. The slow growth rates determined in our study indicate a high susceptibility to fishery-induced mortality for this species and, therefore, the importance of protecting it. Although the bigeye thresher is managed currently and some conservation measures are already in place (ICCAT[1] prohibits onboard retention), its slow growth rates, together with its high mortality at haulback, indicate the need for further studies to help implement additional conservation measures designed to prevent increased fishing mortality and population declines.

Acknowledgments

This study was funded by projects THRESHER (Portuguese Foundation for Science and Technology [FCT] proj. PTDC/MAR/109915/2009), SELECT-PAL (PROMar proj. 31-03-05-FEP-1), and the EU Data Collection Framework. We thank the skippers and crews of several Portuguese longliners, as well as the technicians (S. Amorim, M. Cerqueira, S. Góis, I. Ribeiro, J.R. Táta, and C. Barbosa) for collecting samples. We are grateful to G. Burgess and A. Piercy (Florida Museum of Natural History) for their help with processing vertebrae and to J. Hoenig (Virginia Institute of Marine Science) for providing the R code and helping with the interpretation of the hexagon plots. J. Fernandez-Carvalho was supported with a doctoral grant from FCT (grant ref: SFRH/BD/60624/2009), and R. Coelho was supported by an Investigador-FCT contract funded by the EU European Social Fund and Programa Operacional Potencial Humano (ref: IF/00253/2014). We also thank A. Andrews (NOAA Fisheries) and 2 anonymous reviewers for their comments and suggestions that greatly improved this manuscript.

Literature cited

Amorim, A., J. Baum, G. M. Cailliet, S. Clò, S. C. Clarke, I. Fergusson, M. Gonzalez, D. Macias, P. Mancini, C. Mancusi, R. Myers, M. Reardon, T. Trejo, M. Vacchi, and S. V. Valenti. 2009. *Alopias superciliosus*. *In* IUCN Red List of Threatened Species, vers. 2013.2. [Available at website, accessed June 2014.]

Andrews, A. H, and L. A. Kerr.
2015. Validated age estimates for large white sharks of the northeastern Pacific Ocean: altered perceptions of vertebral growth shed light on complicated bomb ^{14}C results. Environ. Biol. Fish. 98:971–978.

Andrews, A. H., L. J. Natanson, L. A. Kerr, G. H. Burgess, and G. M. Caillet.
2011. Bomb radiocarbon and tag-recpture dating of sandbar shark (*Carcharhinus plumbeus*). Fish. Bull. 109:454–465.

Ardizzone, D., G. M. Cailliet, L. J. Natanson, A. H. Andrews, L. A. Kerr, and T. A. Brown.
2006. Application of bomb radiocarbon chronologies to shortfin mako (*Isurus oxyrinchus*) age validation. Environ. Biol. Fish. 77:355–366.

Bass, A. J., J. D. D'Aubrey, and N. Kistnasamy.
1975. Sharks of the east coast of southern Africa. IV. The families Odontaspididae, Scapanorhynchidae, Isuridae, Cetorhinidae, Alopiidae, Orectolobidae and Rhiniodontidae. Invest. Rep. 39, 99 p. Oceanogr. Res. Inst., Durban, South Africa.

Beamish, R. J., and D. A. Fournier.
1981. A method for comparing the precision of a set of age determinations. Can. J. Fish. Aquat. Sci. 38:982–983.

Berrondo, L., M. Pons, R. Forselledo, P. Miller, and A. Domingo.
2007. Distribución espaciotemporal y composición de tallas de *Alopias superciliosus* y *A. vulpinus* observados en la flota palangrera Uruguaya en el océano Atlántico (2001–2005). Collect. Vol. Sci. Pap. ICCAT 60:566–576.

Bigelow, H. B., and W. C. Shroeder.
1948. Sharks. *In* Fishes of the Western North Atlantic, part one. Lancelets, cyclostomes, sharks (A. E. Parr and Y. H. Olsen, eds.), p. 59–564. Sears Found. Mar. Res., Yale Univ., New Haven, CT.

Buencuerpo, V., S. Rios, and J. Morón.
1998. Pelagic sharks associated with the swordfish, *Xiphias gladius*, fishery in the eastern North Atlantic Ocean and the Strait of Gibraltar. Fish. Bull. 96:667–685.

Cailliet, G. M., and D. W. Bedford.
1983. The biology of three pelagic sharks from california waters, and their emerging fisheries: a review. CalCOFI Rep. 24:57–69.

Cailliet, G. M., and K. J. Goldman.
2004. Age determination and validation in chondrichthyan fishes. *In* Biology of sharks and their relatives (J. Carrier, J. A. Musick, and M. R. Heithaus, eds.), p. 399–447. CRC Press, Boca Raton, FL.

Cailliet, G. M., W. D. Smith, H. F. Mollet, and K. J. Goldman.
2006. Age and growth studies of chondrichthyan fishes: the need for consistency in terminology, verification, validation, and growth function fitting. Environ. Biol. Fish. 77:211–228.

Campana, S. E.
2001. Accuracy, precision and quality control in age determination, including a review of the use and abuse of age validation methods. J. Fish Biol. 59:197–242.

Campana, S. E., L. J. Natanson, and S. Myklevoll.
2002. Bomb dating and age determination of large pelagic sharks. Can. J. Fish. Aquat. Sci. 59:450–455.

Cao, D.-M., L.-M. Song, Y. Zhang, K.-K. Lv, and Z. X. Hu.
2011. Environmental preferences of *Alopias superciliosus* and *Alopias vulpinus* in waters near Marshall Islands. N.Z. J. Mar. Freshw. Res. 45:103–119.

Castro, J., J. M. Serna, D. Mácias, and J. Mejuto.
2000. Estimaciones científicas de los desembarcos de especies asociadas realizados por la flota española de palangre de superficie en 1997 y 1998. Collect. Vol. Sci. Pap. ICCAT 51:1882–1893.

Cerrato, R. M.
1990. Interpretable statistical tests for growth comparisons using parameters in the von Bertalanffy equation. Can. J. Fish. Aquat. Sci. 47:1416–1426.

Chang, W. Y. B.
1982. A statistical method for evaluating the reproducibility of age determination. Can. J. Fish. Aquat. Sci. 39:1208–1210.

Chen, P., and W. Yuan.
2006. Demographic analysis based on the growth parameter of sharks. Fish. Res. 78:374–379.

Chen, C.-T., K.-M. Liu, and Y.-C. Chang.
1997. Reproductive biology of the bigeye thresher shark, *Alopias superciliosus* (Lowe, 1839) (Chondrichthyes: Alopiidae), in the northwestern Pacific. Ichthyol. Res. 44:227–235.

Coelho, R., and K. Erzini.
2002. Age and growth of the undulate ray, *Raja undulata*, in the Algarve (Southern Portugal). J. Mar. Biol. Assoc. U.K. 82:987–990.
2006. Reproductive aspects of the undulate ray, *Raja undulata*, from the south coast of Portugal. Fish. Res. 81:80–85.
2007. Population parameters of the smooth lantern shark, *Etmopterus pusillus*, in southern Portugal (NE Atlantic). Fish. Res. 86:42-57.e
2008. Life history of a wide-ranging deepwater lantern shark in the north-east Atlantic, *Etmopterus spinax* (Chondrichthyes: Etmopteridae), with implications for conservation. J. Fish Biol. 73: 1419–1443.

Coelho, R., J. Fernandez-Carvalho, S. Amorim, and M. N. Santos.
2011. Age and growth of the smooth hammerhead shark, *Sphyrna zygaena*, in the Eastern Equatorial Atlantic Ocean, using vertebral sections. Aquat. Living Resour.24:351–357.e

Coelho, R., J. Fernandez-Carvalho, P. G. Lino, and M. N. Santos.
2012. An overview of the hooking mortality of elasmobranchs caught in a swordfish pelagic longline fishery in the Atlantic Ocean. Aquat. Living Resour. 25:311–319.

Compagno, L. J. V.
2001. Sharks of the world. An annotated and illustrated catalogue of shark species known to date. Vol. 2. bullhead, mackerel and carpet sharks (Heterodontiformes, Lamniformes and Orectolobiformes). FAO Species Catalogue for Fishery Purposes 1, 269 p. FAO, Rome.

Cortés, E.
2008. Comparative life history and demography of pelagic sharks. *In* Sharks of the open ocean: biology, fisheries and conservation (M. D. Camhi, E. K. Pikitch, and E. A. Babcock, eds.), p. 309–322. Blackwell Publ., Oxford, UK.

Cortés, E., F. Arocha, L. Beerkircher, F. Carvalho, A. Domingo, M. Heupel, H. Holtzhausen, M. N. Santos, M. Ribera, and C. Simpfendorfer.
2010. Ecological risk assessment of pelagic sharks caught in Atlantic pelagic longline fisheries. Aquat. Living Resour. 23:25–34.e

Evans, G. T., and J. M. Hoenig.
1998. Testing and viewing symmetry in contingency tables, with application to readers of fish ages. Biometrics 54:620–629.

Fernandez-Carvalho, J., R. Coelho, K. Erzini, and M. N. Santos.
2011. Age and growth of the bigeye thresher shark, *Alopias superciliosus*, from the pelagic longline fisheries in the tropical northeastern Atlantic Ocean, determined by vertebral band counts. Aquat. Living Resour. 24:359–368.e

Francis, M. P., S. E. Campana, , and C. M. Jones.
2007. Age under-estimation in New Zealand porbeagle sharks (*Lamna nasus*): is there an upper limit to ages that can be determined from shark vertebrae? Mar. Freshw. Res. 58:10–23.

Gervelis, B. J., and L. J. Natanson.
2013. Age and growth of the common thresher shark in the western North Atlantic Ocean. Trans. Am. Fish. Soc. 142:1535–1545.

Gilmore, R. G.
1993. Reproductive biology of lamnoid sharks. Environ. Biol. Fish. 38:95–114.e

Goldman, K. J.
2004. Age and growth of elasmobranch fishes. *In* Elasmobranch fisheries management techniques (J. A. Musick and R. Bonfil, eds.), p. 97–132. APEC Secretariat, Singapore.

Goldman, K. J., G. M. Cailliet, A. H. Andrews, and L. J. Natanson.
2012. Assessing the age and growth of Chondrichthyan fishes. *In* Biology of sharks and their relatives, 2nd ed. (J. C. Carrier, J. A. Musick, and M. R. Heithaus, eds.), p. 423–451. CRC Press, Boca Raton, FL.

Goldman, K. J., and J. A. Musick.
2005. Growth and maturity of salmon sharks (*Lamna ditropis*) in the eastern and western North Pacific, and comments on back-calculation methods. Fish. Bull. 104:278–292.

Grothendieck, G.
2013. nls2: non-linear regression with brute force. R package, vers. 0.2. [Available at website, accessed May 2013.]

Gruber, S. H., and L. J. V. Compagno.
1981. Taxonomic status and biology of the bigeye thresher, *Alopias superciliosus*. Fish. Bull. 79:617–640.

Hamady, L. L., L. J. Natanson, G. B. Skomal, and S. R. Thorrold.
2014. Vertebral bomb radiocarbon suggests extreme longevity in white sharks. PLoS ONE 9(1):e84006.

Hoening, J. M., M. J. Morgan, and C. A. Brown.
1995. Analysing differences between two age determination methods by tests of symmetry. Can. J. Fish. Aquat. Sci. 52:364–368.e

Katsanevakis, S.
2006. Modelling fish growth: model selection, multi-model inference and model selection uncertainty. Fish. Res. 81:229–235.

Kimura, D. K.
1980. Likelihood methods for the von Bertalanffy growth curve. Fish. Bull. 77:765–773.

Liu, K.-M., P.-J. Chiang, and C.-T. Chen.
1998. Age and growth estimates of the bigeye thresher shark, *Alopias superciliosus*, in northeastern Taiwan waters. Fish. Bull. 96: 482–491.

Liu, K.-M., C.-T. Chen, T.-H. Liao, and S.-J. Joung.
1999. Age, growth, and reproduction of the pelagic thresher shark, *Alopias pelagicus* in the northwestern Pacific. Copeia 1999:68–74.

Mancini, P. L.
2005. Estudo Biológico-pesqueiro do tubarão-raposa, *Alopias superciliosus* (Lamniformes, Alopiidae) capturado no sudeste-sul do Brasil. M.S. thesis, 195 p., São Paulo State Univ., São Paulo, Brazil.

Megalofonou, P., C. Yannopoulos, D. Damalas, G. De Metrio, M. Deflorio, J. M. de la Serna, and D. Macias.
2005. Incidental catch and estimated discards of pelagic sharks from the swordfish and tuna fisheries in the Mediterranean Sea. Fish. Bull. 103:620–634.

Mejuto, J., B. García-Cortés, A. Ramos-Cartelle, and J. M. Serna.
2009. Scientific estimations of by-catch landed by the Spanish surface longline fleet targeting swordfish (*Xiphias gladius*) in the Atlantic Ocean with special reference to the years 2005 and 2006. Collect. Vol. Sci. Pap. ICCAT 64:2455–2468.

Moreno, J. A., and J. Morón.
1992. Reproductive biology of the bigeye thresher shark, *Alopias superciliosus* (Lowe, 1839). Aust. J. Mar. Freshw. Res. 43:77–86.

Moura, T., I. Figueiredo, I. Farias, B. Serra-Pereira, R. Coelho, K. Erzini, A. Neves, and L. S. Gordo.
2007. The use of caudal thorns for ageing *Raja undulata* from the Portuguese continental shelf, with comments on its reproductive cycle. Mar. Freshw. Res. 58:983–992.

Nakano, H., H. Matsunaga, H. Okamoto, and M. Okazaki.
2003. Acoustic tracking of bigeye thresher shark *Alopias superciliosus* in the eastern Pacific Ocean. Mar. Ecol. Prog. Ser. 265:255–261.

Natanson, L. J., J. J. Mello, and S. E. Campana.
2002. Validated age and growth of the porbeagle shark *(Lamna nasus)* in the western North Atlantic Ocean. Fish. Bull. 100:266–278.

Natanson, L. J., N. E. Kohler, D. Ardizzone, G. M. Cailliet, S. P. Wintner, and H. F. Mollet.
2006. Validated age and growth estimates for the shortfin mako, *Isurus oxyrinchus*, in the North Atlantic Ocean. Environ. Biol. Fish. 77:367–383.

Nelson ,G. A.
2013. fishmethods: fishery science methods and models in R. R package, vers. 1.5-0. [Available at website, accessed February 2014.]

Pardo, S. A., A. B. Cooper, and N. K. Dulvy.
2013. Avoiding fishy growth curves. Methods Ecol. Evol. 4:353–360.

Passerotti, M. S., A. H. Andrews, J. K. Carlson, S. P. Wintner, K. J. Goldman, and L. J. Natanson.
2014. Maximum age and missing time in the vertebrae of sand tiger shark (*Carcharias taurus*): validated lifespan from bomb radiocarbon dating in the western North Atlantic and southwestern Indian Ocean. Mar. Freshw. Res. 65:674–687.

Piercy, A. N., J. K. Carlson, J. A. Sulikowski, and G. H. Burgess.
2007. Age and growth of the scalloped hammerhead shark, *Sphyrna lewini*, in the north-west Atlantic Ocean and Gulf of Mexico. Mar. Freshw. Res 58:34–40.

Pikitch, E. K., M. D. Camhi, and E. A. Babcock.
2008. Introduction to sharks of the open ocean. *In* Sharks of the open ocean: biology, fisheries and conservation (M. D. Camhi, E. K. Pikitch, and E. A. Babcock, eds.), p. 3–13. Blackwell Publ., Oxford, UK.

R Core Team.
2013. R: a language and environment for statistical computing. R Foundation for Statistical Computing, Vienna, Austria. [Available at website, accessed May 2013.]

Richards, F. J.
1959. A flexible growth function for empirical use. J. Exp. Bot. 10:290–301.

Ricker, W. E.
1975. Computation and interpretation of biological statistics of fish populations. Fish. Res. Board Can., Bull. 191, 382 p.

Ridewood, W. G.
1921. On the calcification of the vertebral centra in sharks and rays. Philos. Trans. R. Soc. Lond., B, 210:311–407.

Smith, S. E., D. W. Au, and C. Show.
1998. Intrinsic rebound potentials of 26 species of Pacific sharks. Mar. Freshw. Res. 49:663–678.

Smith, S. E., R. C. Rasmussen, D. A. Ramon, and G. M. Cailliet.
2008. The biology and ecology of thresher sharks (Alopiidae). *In* Sharks of the open ocean: biology, fisheries and conservation (M. D. Camhi, E. K. Pikitch, and E. A. Babcock, eds.), p. 60–68. Blackwell Publ., Oxford, UK.

Stillwell, C. E., and J. G. Casey.
1976. Observations on the bigeye thresher shark, *Alopias superciliosus*, in the western North Atlantic. Fish. Bull. 74:221–225.

Weng, K. C., and B. A. Block.
2004. Diel vertical migration of the bigeye thresher shark (*Alopias superciliosus*), a species possessing orbital retia mirabilia. Fish. Bull. 102:221–229.

Wickham, H.
2009. ggplot2: elegant graphics for data analysis, 213 p. Springer-Verlag, New York.

Wintner, S. P., and G. Cliff.
1999. Age and growth determination of the white shark, *Carcharodon carcharias*, from the east coast of South Africa. Fish. Bull. 97:153–169.

Fishery Bulletin

Guidelines for authors

Contributions published in *Fishery Bulletin* describe original research in marine fishery science, fishery engineering and economics, as well as the areas of marine environmental and ecological sciences (including modeling). Preference will be given to manuscripts that examine processes and underlying patterns. Descriptive reports, surveys, and observational papers may occasionally be published but should appeal to an audience outside the locale in which the study was conducted.

Although all contributions are subject to peer review, responsibility for the contents of papers rests upon the authors and not on the editor or publisher. *Submission of an article implies that the article is original and is not being considered for publication elsewhere.*

Plagiarism and double publication are considered serious breaches of publication ethics. To verify the originality of the research in papers and to identify possible previous publication, manuscripts may be screened with plagiarism-detection software.

Manuscripts must be written in English; authors whose native language is not English are strongly advised to have their manuscripts checked by English-speaking colleagues before submission.

Once a paper has been accepted for publication, online publication takes approximately 3 weeks.

Types of manuscripts accepted by the journal

Articles

Articles generally range from 20 to 30 double-spaced typed pages (12-point font) and describe an original contribution to fisheries science, engineering, or economics. Tables and figures are not included in this page count, but the number of figures should not exceed one figure for every four pages of text. Articles contain the following divisions: **abstract, introduction, methods, results, and discussion.**

Short communications

Short communications are generally less than 20 double spaced typed pages (12-point font) and, like articles, describe an original contribution to fisheries science. They follow the same format as that for articles: **abstract, introduction, results and discussion, but the results and discussion sections may be combined**. Short communications are distinguished from full articles in that they report a noteworthy new observation or discovery—such as the first report of a new species, a unique finding, condition, or event that expands our knowledge of fisheries science, engineering or economics—and do not require a lengthy discussion.

Companion articles

Companion articles are presented together and published together as a scientific contribution. Both articles address a closely related topic and may be articles that result from a workshop or conference. They must be submitted to the journal at the same time.

Review articles

Review articles generally range from 40 to 60 double-spaced typed pages (12-point font) and address a timely topic that is relevant to all aspects of fisheries science. They should be forward thinking and address novel views or interpretations of information that encourage new avenues of research. They can be reviews based on the outcome from thematic workshops, or contributions by groups of authors who want to focus on a particular topic, or a contribution by an individual who chooses to review a research theme of broad interest to the fisheries science community. A review article will include an **abstract, but the format of the article *per se* will be up to the authors.** Please contact the Scientific Editor to discuss your ideas regarding a review article before embarking on such a project.

Preparation of manuscript

Title page should include authors' full names, mailing addresses, and the senior author's e-mail address.

Abstract should be limited to 200 words (one-half typed page), state the main scope of the research, and emphasize the authors conclusions and relevant findings. Do not review the methods of the study or list the contents of the paper. Because abstracts are circulated by abstracting agencies, it is important that they represent the research clearly and concisely.

General text must be typed in 12-point Times New Roman font throughout. A brief introduction should convey the broad significance of the paper; the remainder of the paper should be divided into the following sections: Materials and methods, Results, Discussion, and Acknowledgments. Headings within each section must be short, reflect a logical sequence, and follow the rules of subdivision (i.e., there can be no subdivision without at least two subheadings). The entire text should be intelligible to interdisciplinary readers; therefore, all acronyms, abbreviations, and technical terms should be written out in full the first time they are mentioned. Abbreviations should be used sparingly because they are not carried over to indexing databases and slow readability for those readers outside a discipline. They should never be used for the main subject (species, method) of a paper.

For general style, follow the U.S. *Government Printing Office Style Manual* (2008) [available at website] and *Scientific Style and Format: the CSE Manual for Authors, Editors, and Publishers* (2014, 8th ed.) published by the Council of Science Editors. For scientific nomenclature, use the current edition of the American Fisheries Society's *Common and Scientific Names of Fishes from the United States, Canada, and Mexico* and its companion volumes (*Decapod Crustaceans, Mollusks, Cnidaria and Ctenophora*, and *World Fishes Important to North Americans*). For species not found in the above mentioned AFS publications and for more recent changes in nomenclature, use the Integrated Taxonomic Information System (ITIS) (available at website), or, secondarily, the California Academy of Sciences *Catalog* of *Fishes* (available at website) for species names not included in ITIS. Common (vernacular) names of species should be lowercase. Citations must be given of taxonomic references used for the identification of specimens. For example, "Fishes were identified according to Collette and Klein-MacPhee (2002); sponges were identified according to Stone et al. (2011)."

Dates should be written as follows: 11 November 2000. Measurements should be expressed in metric units, e.g., 58 metric tons (t); if other units of measurement are used, please make this fact explicit to the reader. Use numerals, not words, to express whole and decimal numbers in the general text, tables, and figure captions (except at the beginning of a sentence). For example: We considered 3 hypotheses. We collected 7 samples in this location. Use American spelling. Refrain from using the shorthand slash (/), an ambiguous symbol, in the general text.

Word usage and grammar that may be useful are the following:

- *Aging* For our journal the word *aging* is used to mean both age determination and the aging process (senescence). The author should make clear which meaning is intended where ambiguity may arise.

- *Fish and fishes* For papers on taxonomy and biodiversity, the plural of *fish* is *fishes,* by convention. In all other instances, the plural is *fish.*
  Examples:
  The fishes of Puget Sound [biodiversity is indicated];
  The number of fish caught that season [no emphasis on biodiversity];
  The fish were caught in trawl nets [no emphasis on biodiversity].
  The same logic applies to the use of the words *crab* and *crabs, squid* and *squids,* etc.

- *Sex* For the meaning of male and female, use the word *sex*, not *gender.*

- *Participles* As adjectives, participles must modify a specific noun or pronoun and make sense with that noun or pronoun.
  Incorrect:
  Using the recruitment model, estimates of age-1 recruitment were determined. [Estimates did not use the recruitment model.]
  Correct:
  Using the recruitment model, we determined age-1 estimates of recruitment. [The participle now modifies the word *we,* i.e., those who were using the model.]
  Incorrect:
  Based on the collected data, we concluded that the mortality rate for these fish had increased. [*We* were not based on the collected data.]
  Correct:
  We concluded on the basis of the collected data that the mortality rate for these fish had increased. [Eliminate the participle and replace it with an adverbial phrase.]

Equations and mathematical symbols should be set from a standard mathematical program (MathType) and tool (Equation Editor in MS Word). LaTex is acceptable for more advanced computations. For mathematical symbols in the general text (α, χ^2, π, $\pm$, etc.), use the symbols provided by the MS Word program and italicize all variables, except those variables represented by Greek letters. Do not use photo mode when creating these symbols in the general text.

Number equations (if there are more than 1) for future reference by scientists; place the number within parentheses at the end of the first line of the equation.

Literature cited section comprises published works and those accepted for publication in peer-reviewed journals (in press). Follow the name and year system for citation format in the "Literature cited" section (that is to say, citations should be listed alphabetically by the authors' last names, and then by year if there is more than one citation with the same authorship. A list of abbreviations for citing journal names can be found at website.

Authors are responsible for the accuracy and completeness of all citations. Literature citation format: Author (last name, followed by first-name initials). Year. Title of article. Abbreviated title of the journal in which it was published. Always include number of pages. For a sequence of citations in the general text, list chronologically: (Smith, 1932: Green. 1947; Smith and Jones, 1985).

Digital object identifier (doi) code ensures that a publication has a permanent location online. Doi code should be included at the end of citations of published literature. Authors are responsible for submitting accurate doi codes. Faulty codes will be deleted at the page-proof stage.

Cite all software, special equipment, and chemical solutions used in the study within parentheses in the general text: e.g., SAS, vers. 6.03 (SAS Inst., Inc., Cary, NC).

Footnotes are used for all documents that have not been formally peer reviewed and for observations and personal communications. These types of references should be cited sparingly in manuscripts submitted to the journal.

All reference documents, administrative reports, internal reports, progress reports, project reports, contract reports, personal observations, personal communications, unpublished data, manuscripts in review, and council meeting notes are footnoted in 9 pt font and placed at the bottom of the page on which they are first cited. Footnote format is the same as that for formal literature citations. A link to the online source (e.g., [http://www/..... , accessed July 2007.]), or the mailing address of the agency or department holding the document, should be provided so that readers may obtain a copy of the document.

Tables are often overused in scientific papers; it is seldom necessary to present all the data associated with a study. Tables should not be excessive in size and must be cited in numerical order in the text. Headings should be short but ample enough to allow the table to be intelligible on its own.

All abbreviations and unusual symbols must be explained in the table legend. Other incidental comments may be footnoted with italic numeral footnote markers. Use asterisks only to indicate significance in statistical data. Do not type table legends on a separate page; place them above the table data. *Do not submit tables in photo mode.*

- Notate probability with a capital, italic *P*.
- Provide a zero before all decimal points for values less than one (e.g., 0.07).
- Round all values to 2 decimal points.
- Use a comma in numbers of five digits or more (e.g., 13,000 but 3000).

Figures must be cited in numerical order in the text. Graphics should aid in the comprehension of the text, but they should be limited to presenting patterns rather than raw data. Figures should not exceed one figure for every four pages of text and must be labeled with the number of the figure. Place labels **A, B, C,** etc. within the upper left area of graphs and photos. Avoid placing labels vertically (except for the y axis).

Figure legends should explain all symbols and abbreviations seen in the figure and should be double-spaced on a separate page at the end of the manuscript.

Line art and halftone figures should be submitted as pdf files with >800 dpi and >300 dpi, respectively. Color is allowed in figures to show morphological differences among species (for species identification), to show stain reactions, and to show gradations in temperature contours within maps. Color is discouraged in graphs, and for the few instances where color may be allowed, the use of color will be determined by the Managing Editor. Approved color figures should be submitted as EPS files in CMYK format.

- Capitalize the first letter of the first word in all labels within figures.
- Do not use overly large font sizes in maps and for units of measurements along axes in graphs.
- Do not use bold fonts or bold lines in figures.
- Do not place outline rules around graphs.
- Place a North arrow and label degrees latitude and longitude (e.g., 170°E) in all maps.
- Use symbols, shadings, or patterns (not clip art) in maps and graphs.

Failure to follow these guidelines and failure to correspond with editors in a timely manner will delay publication of a manuscript.

Copyright law does not apply to *Fishery Bulletin,* which falls within the public domain. However, if an author reproduces any part of an article from *Fishery Bulletin*, reference to source is considered correct form (e.g., Source: Fish. Bull. 97:105).

Submission of manuscript

Submit manuscript online at the ScholarOne website. Commerce Department authors should submit papers under a completed NOAA Form 25-700. For further details on electronic submission, please contact the Associate Editor, Kathryn Dennis, at

kathryn.dennis@noaa.gov

When requested, the text and tables should be submitted in Word format. Figures should be sent as separate PDF files (preferred), TIFF files, or EPS files. Send a copy of figures in the original software if conversion to any of these formats yields a degraded version of the figure.

Questions? If you have questions regarding these guidelines, please contact the Managing Editor, Sharyn Matriotti, at

sharyn.matriotti@noaa.gov

Questions regarding manuscripts under review should be addressed to Kathryn Dennis, Associate Editor.

Fishery Bulletin

Subscription form

Superintendent of Documents **Publications** Order Form

*5178

☐ YES, please send me the following publications:

____ Subscriptions to *Fishery Bulletin*
for $32.00 per year ($44.80 foreign)

The total cost of my order is $ _____ . Prices include regular domestic postage and handling and are subject to change.

_____
(Company or Personal Name) (Please type or print)

_____
(Additional address/attention line)

_____
(Street address)

_____
(City, State, ZIP Code)

_____
(Daytime phone including area code)

_____
(Purchase Order No.)

Charge your order. IT'S EASY!

VISA

MasterCard

Please Choose Method of Payment:

☐ Check payable to the Superintendent of Documents
☐ GPO Deposit Account ☐☐☐☐☐☐☐–☐
☐ VISA or MasterCard Account
☐☐☐☐☐☐☐☐☐☐☐☐☐☐☐☐
☐☐☐☐ (Credit card expiration date)

To fax your orders (202) 512-2104

_____
(Authorizing Signature)

Mail to: Superintendent of Documents
P.O. Box 979050, St. Louis, Missouri 63197
Tel. no. (U.S. callers): 866-512-1800
Tel. no. (International callers): 1-202-512-1800

Thank you for your order!

Also available online at
http://bookstore.gpo.gov/actions/GetPublication.do?stocknumber=703-023-00000-2
email: ContactCenter@gpo.gov